

INTERCOH 2017
Montevideo - Uruguay
November 13 - 17

14th International Conference on Cohesive Sediment Transport Processes

Book of abstracts

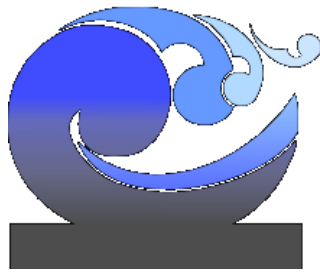
13 to 17 November 2017
Montevideo URUGUAY

Courtesy of the U.S. Geological Survey



UNIVERSIDAD
DE LA REPÚBLICA
URUGUAY





INTERCOH 2017

Montevideo - Uruguay

November 13 - 17

**14th International Conference on Cohesive
Sediment Transport Processes**

Book of abstracts



UNIVERSIDAD
DE LA REPÚBLICA
URUGUAY



INTERCOH 2017 - 14th International Conference on Cohesive Sediment Transport Processes is organized by the Instituto de Mecánica de los Fluidos e Ingeniería Ambiental (IMFIA), Facultad de Ingeniería, Universidad de la República.

Steering Committee

Carl Friedrichs, Virginia Institute of Marine Science, USA
Joe Gailani, ERDC, US Army Corps of Engineers, USA
Qing He, East China Normal University, China
Guan-Hong Lee, Inha University, Korea
Yasuyuki Nakagawa, PARI, Japan
Francisco Pedocchi, Universidad de la República, Uruguay
Larry Sanford, University of Maryland Center for Environmental Science, USA (chair)
Mohsen Soltanpour, K. N. Toosi University of Technology, Iran
Jez Spearman, HR Wallingford, UK
Erik Toorman, KU Leuven, Belgium
Bram van Prooijen, TU Delft, The Netherlands
Susana Vinzon, Federal University of Rio de Janeiro, Brazil
Romaric Verney, IFREMER, France

Organizing Committee

Mónica Fossati
Fernanda Maciel
Rodrigo Mosquera
Francisco Pedocchi (chair)
Ismael Piedra-Cueva
Pablo Santoro

Editors:

Francisco Pedocchi, Universidad de la República, Uruguay
Susana Vinzon, Federal University of Rio de Janeiro, Brazil
Carl Friedrichs, Virginia Institute of Marine Science, USA

With the support of:



<https://www.saltogrande.org/>
<http://www.montevideo.gub.uy/>
<http://www.hidrovia-sa.com.ar/>
<http://www.comisionriodelaplata.org/>
<https://www.ancap.com.uy/>
<http://www.saceem.com/>

Available online at:

<https://www.fing.edu.uy/imfia/intercoh/>

Preface

INTERCOH2017 is the 14th edition of the biannual meeting that gathers the international community of scientists and engineers, who have chosen to embrace the challenge of study, work, and find engineering solutions in fluvial, estuarine, and marine environments where cohesive sediments dominate the sediment dynamics in a close relation with the hydrodynamics, chemistry, and biology. More information on the past and future meetings and the activities of the cohesive sediment research community can be found on www.intercoh.org.

When I had just graduated as an hydraulic and environmental engineer, and was starting to look at flocculation dynamics, an officemate told me the following story: a well know engineer that was visiting Uruguay was asked if, having worked and researched extensively on sediment transport, he had not considered studding cohesive sediments, to what he replied “I like to see the result of my research during my lifetime”. I kept that phrase in my mind and recall it every time I feel that the progress we are making is not successful or fast enough. For some of us that live in front of one of the largest estuaries of the world staying clean was not an option and we happily decided to dive ourselves into the “mud” and the study of the wonderful complexity of cohesive sediment dynamics.

This is the second time that the INTERCOH Meeting comes to South America; the previous time was in 2009 in the cities of Rio de Janeiro and Paraty, Brazil. The need of engineering solutions in the Rio de la Plata and the Montevideo Bay made that the study of cohesive sediments started early. The Montevideo Port is literally build on mud and dredging and building in the area required the study of the cohesive sediments in the area as early as 1871. The “recent” study of cohesive sediments in the Universidad de la República, started with the experiences of Oscar Maggiolo in the late 60s and early 70s. The research on cohesive sediments stopped, as most of the research in the country, during the 11 years of dictatorship, during which most of the research team that worked with Maggiolo was expelled from the University and several had to leave the country. You can still see the gap for those years in the Journal of Fluid Mechanics collection at our library. With the return of the democracy, the cohesive sediment research at the University also returned in the newly created Instituto de Mecánica de los Fluidos e Ingeniería Ambiental (IMFIA), and the work on cohesive sediments has continued for the last 30 years.

The abstracts on this book summarize the current activity of research groups across the globe, covering the topics of: Mud rheology and fluid mud; Suspended matter and flocculation; Bed shear, erosion and bed exchange; Sediment characterization; Siltation, Dredging and plumes; Biological and ecological controls; Coastal and estuarine hydrodynamics; Coastal and estuarine morphodynamics; and Wetlands dynamics. The review of the abstracts was in charge of the INTERCOH Steering Committee, while the Local Committee was in charge of the editorial duties, with the help of Susana Vinzón and Carl Friedrichs. We expect that the complete works will be submitted to an Special Issue in the Topical Collection of the Ocean Dynamics journal.

This current edition of INTECOH is possible thanks to the work and help of several people. First, thanks to the Steering Committee, Ashish Mehta and Han Winterwerp for trusting us the organization of the meeting. Also thanks to Susana Vinzón and Carl Friedrichs for their help during the review process, to Erik Toorman and Larry Sanford for their advice and tips for the organization of the meeting. Thanks to the Local Committee; Dominique who was in charge of the secretary; Gonzalo Rodriguez, who was in charge of the webpage and the informatics; the School of Engineering Accountant Office, which managed the founds; the School of Engineering Dean, María Simon, and the School Board for their support and allowing us to use the school facilities for the meeting. Finally, thanks to my Colleagues: Christian Chreties, Sebastián Solari, and Rodrigo Alonso; and the Students: Michael Jackson, Daniela Martinez, Guillermo Echavarría, Manuel Teixeira, and María Ballesteros; for their support and help during the event.

Finally thanks for the support of the Sponsors: Delegación Uruguaya a la Comisión Técnico Mixta de Salto Grande, Intendencia de Montevideo, Hidrovía S.A., Delegación Uruguaya a la Comisión Administradora del Río de la Plata, ANCAP, Saceem S.A. Your support is truly appreciated.

Welcome to Montevideo.

Prof. Francisco Pedocchi
Chairman INTERCOH2017

Table of Contents

1. Numerical modelling of Montevideo Bay hydrodynamics and cohesive sediment dynamics. Pablo Santoro, Mónica Fossati, Pablo Tassi, Nicolas Huybrechts, Damien Pham Van Bang and Ismael Piedra-Cueva	1
2. An efficient consolidation model for morphodynamic simulations in low SPM-environments. Johan C Winterwerp, Zeng Zhou, Guilia Battista, Thijs van Kessel, Bert Jagers, Bas van Maren and Mick van der Wegen	3
3. Experimental Investigations of Vertical Turbulence in Concentrated Mud Suspensions. Oliver Chmiel and Andreas Malcherek	5
4. Modelling river hydro-sedimentaries fluxes during a high flood event. Jérémy Lepesqueur, Renaud Hostache and Christophe Hissler	7
5. Using rheological measurements to predict the flow behaviour of cohesive sediment gravity flows. Megan Baker, Jaco H. Baas and Ricardo Silva Jacinto	9
6. Characterization of fluid mud layers for navigational purposes. Alex Kirichek, Claire Chassagne, Han Winterwerp, Ronald Rutgers, Arie Noordijk, Karoune Nipius and Tiedo Velinga	11
7. Monitoring of the rapid variation of the suspended sediment concentration in an estuary with large tidal rage. Dong-Young Lee, Jin-Soon Park, Guoxiang Wu, Kwang-Soo Lee and Jun Seok Park	13
8. Laboratory and numerical studies on the sediment transport processes for the sand-mud mixed bed. Bingchen Liang, Jun Wang, Zhaoyan Xu, Zhipeng Qu, Dongyoung Lee and Earl Hayter	15
9. Reduction in Sediment Accumulation at a Coastal Marina by Entrance Modifications. Ashish Mehta, Neelamani Subramaniam and Earl Hayter	17
10. Flocculation Behavior of Sediments from a Mining Dam Collapse: Before and After Rio Doce Disaster. Caroline Grilo, Gabriella Amorim and Valéria Quaresma	19
11. The effect of initial conditions on the consolidation of mud. Maria Barciela Rial, Barend A.P. van den Bosch, Johan C. Winterwerp, Leon A. van Paassen, Jasper Griffioen and Thijs van Kessel	21
12. Modelling unsteady flow and sediment deposition in large lowlands rivers: An application to the Paraná River. Marina Laura Garcia, Pedro Abel Basile and Gerardo Adrián Riccardi	23
13. Assessing rheological properties of fluid mud samples through tuning fork data. Diego Fonseca, Juliane Carneiro, Patrícia Marroig, Marcos Gallo and Susana Vinzon	25
14. Characterization of bottom sediments in the Río de la Plata estuary. Diego Moreira and Claudia Simionato	27
15. On the processes that determine the fine sediments transport in the Rio de la Plata estuary. Diego Moreira and Claudia Simionato	29
16. Estuarine morphodynamic adaptation to sediment supply and human activities: a case study of turbidity maximum. Chunyan Zhu, Leicheng Guo, Bo Tian, Qing He and Zheng Bing Wang	31
17. Turbulence and flocculation in an estuarine tidal channel. Steven Figueroa, Guan-Hong Lee and Ho Kyung Ha	33
18. Disturbance of cohesive sediment dynamics in the world's largest tidal power plant: Lake Sihwa, South Korea. Ho Kyung Ha, Jong-Wook Kim and Seung-Buhm Woo	35
19. Wave attenuation by brushwood dams in a mud-mangrove coast. Alejandra Gijón Mancheño, S.A.J. Tas, P.M.J. Herman, A.J.H.M. Reniers, W.S.J. Uijttewaal and J.C. Winterwerp	37
20. Wave transformation on the mangrove-mud coast of Demak, Indonesia. S.A.J. Tas, A. Gijón Mancheño, P.M.J. Herman, A.J.H.M. Reniers, W.S.J. Uijttewaal and J.C. Winterwerp	39

21. Sediment trapping in the Zeebrugge Coastal Turbidity Maximum. Bas van Maren and Julia Vroom.....	41
22. Flume experiment of fluid mud dynamics around navigation channel. Yasuyuki Nakagawa and Futoshi Murayama	43
23. SPM dynamics in a mud bank area crossing an estuary mouth. The case of Kaw mud bank in the Mahury Estuary (French Guiana). Noelia Abascal Zorrilla, Nicolas Huybrechts, Vincent Vantrepotte, Antoine Gardel, Sylvain Orseau, Sylvain Morvan and Sandric Lesourd	45
24. Plume measurements in the AMORAS underwater cell. Bart De Maerschalck, Styn Claeys, Erwin De Backer and Stefaan Ides	47
25. Local study of erosion with a transparent model cohesive sediment. Zaynab Tarhini, Sebastien Jarny and Alain Texier	49
26. A tri-modal flocculation model coupled with TELEMAC for suspended cohesive sediments in the Belgian coastal zone. Xiaoteng Shen, Erik Toorman and Michael Fettweis	51
27. The Importance of Wind-induced Sediment Fluxes on Tidal Flats. Irene Colosimo, Bram C. van Prooijen, Dirk S. van Maren, Johan C. Winterwerp and Ad J.H.M. Reniers	53
28. Space - and time-varying bed roughness at Mixed Continental Shelves. Kyssyanne Oliveira and Valéria Quaresma.....	55
29. Reoccurrence of high-energy events: how is a shallow coastal lagoon impacted? A study based on in situ and numerical investigations. Pernille L. Forsberg, Verner B. Ernsten, Ulrik Lumborg, Nils Drønen, Thorbjørn J. Andersen and Aart Kroon	57
30. Diachronic numerical modelling of the turbidity maximum dynamics in the macrotidal Seine estuary (France) from 1960 to 2010. Florent Grasso, Pierre Le Hir and Nicolas Chini	59
31. Quantitative clay mineralogy as provenance indicator for the recent muds in the southern North. Rieko Adriaens, Edwin Zeelmaekers, Michael Fettweis, Elin Vanlierde, Joris Vanlede, Peter Stassen, Jan Elsen, Jan Środoń and Noël Vandenberghe.....	61
32. Seasonal variation of sediment flocculation and the modeling thereof as function of biochemical factors. Zhirui Deng, Qing He, Claire Chassagne and Han Winterwerp.....	63
33. Revealing suspended sediments variability in highly-turbid estuaries through spectral methods: a comparison of observations and model predictions. Isabel Jalón-Rojas, Sabine Schmidt, Aldo Sottolichio and Katixa Lajaunie-Salla.....	65
34. Mud dynamics in the harbor of Zeebrugge. Joris Vanlede, Arvid Dujardin and Michael Fettweis	67
35. On best practice for in situ high-frequency long-term observations of suspended particulate matter concentration using optical and acoustic systems. Michael Fettweis, Rolf Riethmüller, Romaric Verney, Marius Becker, Joan Backers, Matthias Baeye, Marion Chapalain, Stijn Claeys, Jan Claus, Tom Cox, Julien Deloffre, Davy Depreiter, Flavie Druine, Götz Flöser, Steffen Grünler, Frederic Jourdin, Robert Lafite, Janine Nauw, Bouchra Nechad, Rüdiger Röttgers, Aldo Sottolichio, Wim Vanhaverbeke, Thomas Van Hoestenbergh and Hans Vereecken.....	69
36. Response of SPM concentrations to storms in the North Sea: investigating the water-bed exchange of fine sediments. Erik Hendriks, Bram van Prooijen, Han Winterwerp, Stefan Aarninkhof, Carola van der Hout and Rob Witbaard.....	71
37. Regime shifts in a D3D schematized Scheldt model: recent progress. M A de Lucas Pardo, Y Dijkstra, B van Maren, J Vroom, T van Kessel, J C Winterwerp	73
38. How important is mud transport on large scale estuarine and deltaic morphodynamics? Leicheng Guo, Chunyan Zhu and Qing He	76

39. On the homogeneity of suspended matter concentration data in an integrated coastal ocean observing system. Goetz Floeser, Rolf Riethmueller and Wolfgang Schoenfeld.....	78
40. Evaporation reduces the erodibility of mudflats in Plum Island Sound, Massachusetts, USA. Sergio Fagherazzi, Giulio Mariotti, Amanda Vieillard, Robinson Fullweiler and Tammy Viggato	80
41. The influence of turbulence on suspended sediment concentrations within a rapidly prograding mangrove forest. Julia Mullarney, Erik Horstman and Karin Bryan	82
42. Biophysical controls on sediment deposition in mangroves. Erik Horstman, Julia Mullarney and Karin Bryan	84
43. Mixing tank experiments on floc size distributions of suspended cohesive sediment in Yangtze River Estuary. Yuyang Shao and Xiaoteng Shen.....	86
44. A three dimensional coupled wave-current model for mud transport simulations in the Persian Gulf. Afshan Khaleghi and S. Abbas Haghshenas.....	88
45. Mud rheology in the North-Western Persian Gulf by contrast with sediment constituents. Farzin Samsami, Samane Ahmadi, S. Abbas Haghshenas, Abbasali Aliakbari Bidokhti and Michael John Risk	90
46. An application of Artificial Neural Network for analyzing sediment erodibility data. Ebrahim Hamidian J., S. Abbas Haghshenas, Lawrence P. Sanford and Farhang Ahmadi Givi.....	92
47. Field investigations of effects of macro flora on fine-grained sediment transport. Ulrik Lumborg.....	94
48. Modelling net-deposition of cohesive sediments within the ETM. Roland Hesse.....	96
49. Numerical modelling of flow and sediment transport under the impact of vegetation. Sina Saremi and Nils Dronen.....	98
50. Influence of Salinity on the Coastal Turbidity Maximum in the Southern Bight of the North Sea. Diem Nguyen, Joris Vanlede and Bart De Maerschalck.....	100
52. Dynamics of the suspended particle matter transport in an estuary with morphology strongly modified by human activities. Beatriz M. Marino, Luis P. Thomas, Ricardo N. Szupiany and Manuel A. Gutierrez	102
53. Dynamics of the settling of the flocculated suspended particle matter in specific places of a modified estuary. Luis P. Thomas, Beatriz M. Marino, Ricardo N. Szupiany and Manuel A. Gutierrez.....	104
54. Study of dimensionless wave attenuation rate on fluid mud beds. Sima Ghobadi and Mohsen Soltanpour.....	106
55. How settling velocity impacts modeled intratidal ssc patterns and residual sediment fluxes. Anna Zorndt, Steffen Grünler, Frank Kösters and Marius Becker	108
56. Impacts of maintenance dredging on suspended sediment dynamics in the Seine estuary. Jean-Philippe Lemoine, Pierre Le Hir and Florent Grasso	110
57. Mud-induced periodic stratification in the hyperturbid Ems estuary. Marius Becker and Christian Winter.....	112
58. Experimental study on continuous turbulence effects on sediment adsorption of heavy metals. Jingjing Zhou, Xian Zu and Naiyu Zhang	114
59. Assessment of the spatio-temporal variability of sediment fluxes on the French continental shelf under the influence of natural and anthropogenic forcings. Baptiste Mengual, Pierre Le Hir, Florence Cayocca and Thierry Garlan	116
60. Fractal flocs: “primary particles” variability and consequences on floc characteristics. Romaric Verney, Aurelien Gangloff, Marion Chapalain, Flavie Druine, David Le Berre and Matthias Jacquet.....	118
61. Using real time monitoring networks for investigating sediment dynamics in estuaries: a step beyond turbidity time series analysis. Romaric Verney, Florent Grasso, Flavie Druine, Julien Deloffre and Jean Philippe Lemoine	120

62. Equilibria and Evolution of Estuarine Fringing Intertidal Mudflats. Bram van Prooijen, Florent Grasso, Pierre Le Hir, Lodewijk de Vet, Zheng Bing Wang, Brenda Walles and Tom Ysebaert.....	122
63. Size and settling velocity of suspended mud in the Mississippi River mouth estuary. Jarrell Smith, Kelsey Fall and Michael Ramirez.....	124
64. Dynamics of suspended particulate matter in coastal waters (Seine Bay). Marion Chapalain, Romaric Verney, Michael Fettweis, Pascal Claquin, Matthias Jacquet, David Le Berre and Pierre Le Hir	126
65. In situ response of optical turbidity sensors to suspended sediment characteristics in turbid estuarine system. Flavie Druine, Romaric Verney, Julien Deloffre, Jean-Philippe Lemoine and Robert Lafite	128
66. Modelling morphodynamics in the sand/mud context of the Seine estuary mouth: methodology, validation and questions. Pierre Le Hir, Jean Philippe Lemoine, Florent Grasso and Bénédicte Thouvenin	130
67. Modelling the dispersal of microplastic particles: anthropogenic cohesive particles and their fate in coastal waters. Erik Toorman, Qilong Bi, Xiaoteng Shen, Annika Jahnke and Jaak Monbaliu	132
68. Validation of satellite remote sensing for coastal turbidity monitoring by sediment transport modelling. Qilong Bi, Jonas Royakkers, Nitin Bhatia, Sindy Sterckx, Els Knaeps, Erik Toorman and Jaak Monbaliu	134
69. Wave effects on hydrodynamics and sediment transport in a deep channel of the Changjiang Estuary. Jie Jiang, Qing He and Chao Guo	136
70. Fine-sediment transfer and accumulation in the Amazon dispersal system: from the beginning of tides to the edge of the shelf. Charles Nittrouer, Andrea Ogston, Aaron Fricke, Daniel Nowacki, Nils Asp, Pedro Souza Filha, Alberto Figueiredo, Steven Kuehl and Odete Silveira	139
71. The controls on flocculation and suspended sediment concentrations in a muddy subtropical mangrove forest. Iain MacDonald, Nicola Lovett and Julia Mullarney	141
72. Numerical modeling of cohesive sediment transport along a mud dominated coast. Samor Wongsoredjo, Gerben Ruessink, Sieuwnath Naipal, Jaak Monbaliu and Erik Toorman.....	143
73. Investigating Rhone river plume dynamics using innovative metrics: ocean color satellite data Vs 3D sediment transport model results. Aurélien Gangloff, Romaric Verney and Claude Estournel.....	145
74. Mississippi River salt wedge estuary: observations of fluid shear and its effect on sedimentary processes. Michael Ramirez and Jarrell Smith	147
75. Fine-sediment exchange between fluvial source and Amazon mangrove coastlines. Andrea Ogston, Nils Asp, Robin McLachlin, Charles Nittrouer, Pedro Walfir Souza Filho and Aaron Fricke.....	148
76. Evidence of muddy aggregates as resilient pellets in suspension throughout the water column using traps and a Particle Image Camera System (PICS) in a tidal estuary. Grace Massey, Kelsey Fall, Carl Friedrichs and S. Jarrel Smith	150
77. Fractal floc properties in the surface waters of a partially-mixed estuary: insights from video settling, LISST, and pump sampling. Kelsey Fall, Carl Friedrichs, Grace Cartwright, David Bowers and Jarrell Smith	152
78. Trapping and bypassing of SPM, and particulate biogeochemical components, in the river estuary transition zone (RETZ) of a shallow macrotidal estuary. Colin Jago, Eleanor Howlett, Francis Hassard, Suzanna Jackson, Shelagh Malham, Paulina Rajko-Neno and Peter Robins.....	154
79. Multiple Turbidity Maxima in a Short River Estuary – Why? David Jay, Joseph Jurisa, Saeed Moghimi and Stefan Talke	157
80. Laminar, intermittent and turbulent fluid mud flow. Erik Toorman.....	159
81. Sediment measures during dredging operations near Montevideo’s coast. Rodrigo Mosquera, Teresa Sastre, Juliane Castro, Pablo Santoro and Francisco Pedocchi.....	161

82. Observations of the settling velocity of fine sediment associated with deep sea mining of Fe-Mn crusts. Jeremy Spearman, Andrew Manning, Neil Crossouard and Jon Taylor.....	163
83. Implementation of a high resolution 3D wave-current-sediment transport model for the Río de la Plata and Montevideo Bay. Pablo Santoro, Monica Fossati, Pablo Tassi, Nicolas Huybrechts, Damien Pham Van Bang and Ismael Piedra-Cueva.....	165
84. Temporal and spatial changes in floc fraction on a macro-tidal channel-flat complex: Results from Kingsport, Nova Scotia, Bay of Fundy. Brent Law, Paul Hill, Timothy Milligan and Vanessa Zions.....	167
85. Biological-Physical Interactions In Fine Sediment Environments. Lawrence Sanford.....	169
86. Analytical model for the prediction of sedimentation rates in Montevideo navigation channels. Francisco Pedocchi, Sebastián Solari and Monica Fossati.....	171
87. Fine Sediment Dynamics in the 'Río de la Plata' river-estuarine-ocean system. Monica Fossati, Pablo Santoro, Rodrigo Mosquera, Francisco Pedocchi and Ismael Piedra-Cueva.....	173
88. Temporal and Spatial variability of the La Plata and Patos Lagoon Coastal Plumes. Paulo Lisboa and Elisa Fernandes.....	175
89. Multi-vegetation feedbacks affecting flow routing and sediment distributions in Everglades wetland. William Nardin and Laurel Larsen.....	177
90. Sediment resuspension and flocculation processes in a transverse mudflat-channel. Guan-Hong Lee, Steven Figueroa, Hyun-Jung Shin, Jongwi Chang and Adonis Gallentes.....	179
91. Detection of fluid mud layers using tuning fork and acoustic measurements. Juliane Carneiro, Marcos Gallo and Susana Vinzon.....	180
92. Modelling Patos Lagoon dredging suspended sediment plume dispersion. Elisa Helena Fernandes, Caio Stringari, Roberto Valente, Pablo Silva and Paulo Victor Lisboa.....	182
94. Fluidization in consolidated mud beds under water waves. Mohsen Soltanpour, Mohammad Hadi Jabbari, Tomoya Shibayama, Kourosh Hejazi, Shinsaku Nishizaki and Tomoyuki Takabatake.....	184
95. Comparative rheological characterization of fluid mud from different regions in Brazil. Caio Manganeli, Diego Fonseca and Susana Vinzon.....	186
96. Impact of tidal variation in vertical mixing and SPM concentrations on primary production and oxygen concentrations. Tom Cox and Thijs van Kessel.....	188
97. Evaluation of the artificial intelligence techniques for estimating suspended sediment concentration in a regularized river. Marcelo Di Lello Jordão, Susana Beatriz Vinzon and Marcos Nicolas Gallo.....	190

Numerical modelling of Montevideo Bay hydrodynamics and cohesive sediment dynamics

Santoro Pablo¹, Fossati Mónica¹, Tassi Pablo², Huybrechts Nicolas³, Pham Van Bang Damien², Piedra-Cueva Ismael¹

¹ Instituto de Mecánica de los Fluidos e Ingeniería Ambiental, Universidad de la República, Herrera y Reissig 565, CP 11300 Montevideo, Uruguay
E-mail: psantoro@fing.edu

² Saint Venant Laboratory for Hydraulics, EDF R&D, 6 Quai Watier, 78400 Chatou, France

³ Sorbonne Universités, Université de Technologie de Compiègne, CNRS, UMR 7337 Roberval, LHN (joint research unit UTC-CEREMA EMF) Compiègne, France.

Introduction

The hydrodynamics and fine sediment dynamics modelling in estuarine environments is important for coastal engineering design and environmental assessment. The objective of this work is to characterize the hydrodynamics and fine sediment dynamics of the Montevideo Bay area based on a numerical modelling approach. The work is based on the analysis of numerical results from a circulation, wave, sediment transport and bed evolution model implemented for the Río de la Plata focusing on the Montevideo coastal area. Continuous dredging is needed to maintain the navigation channels and harbor area at the operational depth. A reliable characterization of the hydrodynamics and sediment dynamics is needed in order to optimize dredging tasks and design new projects.

Methodology

The methodology is based on the implementation of a set of numerical models, able to represent the circulation, waves and fine sediment transport in complex geometries under the effect of several forcings. Based on the open source TELEMAC-MASCARET Modelling System (TMS), it was possible to address the simulation of both the tidal and wave hydrodynamics, fine sediment transport and bed evolution with a single code. For the calibration and validation of the models we utilized field data of sea surface elevation (SSE), currents, waves, salinity and suspended sediment concentration (SSC) especially including recent field data measurements in the Montevideo Bay area.

It was performed an analysis of the sedimentation patterns in the bay based on the bottom evolution results after a one year simulation using realistic forcings. A sediment budget analysis focused on the water and sediment exchange between the bay and the adjacent coastal area was made by analyzing the fluxes through the bay mouths.

The influence of the consolidation process on the sediment transport module was explored using a multi-layer iso-pycnal Gibson's model available in the TMS. The closure equations for the permeability and effective stress were calibrated based on settling column experiments (Fossati et al., 2015). A two years simulations was made in order to initialize the bed. Without specific information about the dependence among the erosion parameters and the bed concentration for the Río de la Plata, laws taken from the bibliography were tested. It was analyzed the impact of this process on the suspended sediment dynamics. The simulated vertical bed density profiles at the navigation channels and harbor area were compared against measured profiles using a tuning fork densimeter DensiTune (Groposo et al., 2015).

Results

The obtained results with all the modules show good agreement with the measured data, demonstrating to represent satisfactorily the main features of the Río de la Plata dynamics and specifically of the Montevideo coastal area. Fig. 1d shows a comparison between the observed and simulated suspended sediment concentration (SSC) at the station PR during January- April 2015.

The west mouth plays a major role in the sediment exchange between the bay and coastal area during the storm events, which is coherent with the water circulation and its relationship with the wind conditions. The highest sediment fluxes take place during strong storm conditions. Wind blowing from the SE and SW quadrants are mainly responsible for these severe wave conditions. Under SW winds conditions water with high SSC goes inwards the bay through the west mouth. Wind from NE direction enhances the opposite water circulation, but do not have fetch to generate waves and induce important sediment resuspension. Inside the bay the navigation channel "La Teja" plays an important role in the circulation patterns, and depending on the flow configuration inside the bay some of the main resuspension events observed outside the bay reaches the inner zone of the bay or not.

The consolidation model results showed to be very sensitive to the calibration parameters of the permeability and effective stress closure equations. Once calibrated, it was performed a simulation including it in the Río de la Plata model with realistic forcings. Good agreement was found between the model results and measured vertical density profiles in the Montevideo Bay access channel (Fig. 1e). Including the consolidation model allowed us to have spatial variability on the erosion parameters. The simulated suspended sediment dynamics behavior in the Montevideo Bay area does not show significant differences compared to the results without consolidation. A possible explanation is that in contrast with other estuaries, at the Río de la Plata only a few centimeters of the bed are eroded (maximum SSC in general do not exceed 1 kg/m^3) even during the storm events. So in our simulations the bed-water column sediment exchange usually is not enough to involve more than one layer of the bed.

Conclusions

At the larger scale of the estuary the currents induced stress is relevant to represent the permanent suspended sediment concentrations, while the wave induced stress is essential to reproduce the main re-suspension events. Inside the Montevideo Bay the wave forcing plays a relevant role especially on the west area. However, the advection of sediment coming from the near coastal area and the circulation conditions are determinant, and can for example change the bed evolution tendency for similar wave conditions. We found a connection between this behavior and the dominant circulation conditions at the inner areas.

The reproduction of the measured vertical density profiles in the Montevideo Bay access channel is an interesting result, and the consolidation process will be necessary to address other important process like the fluid mud modelling.

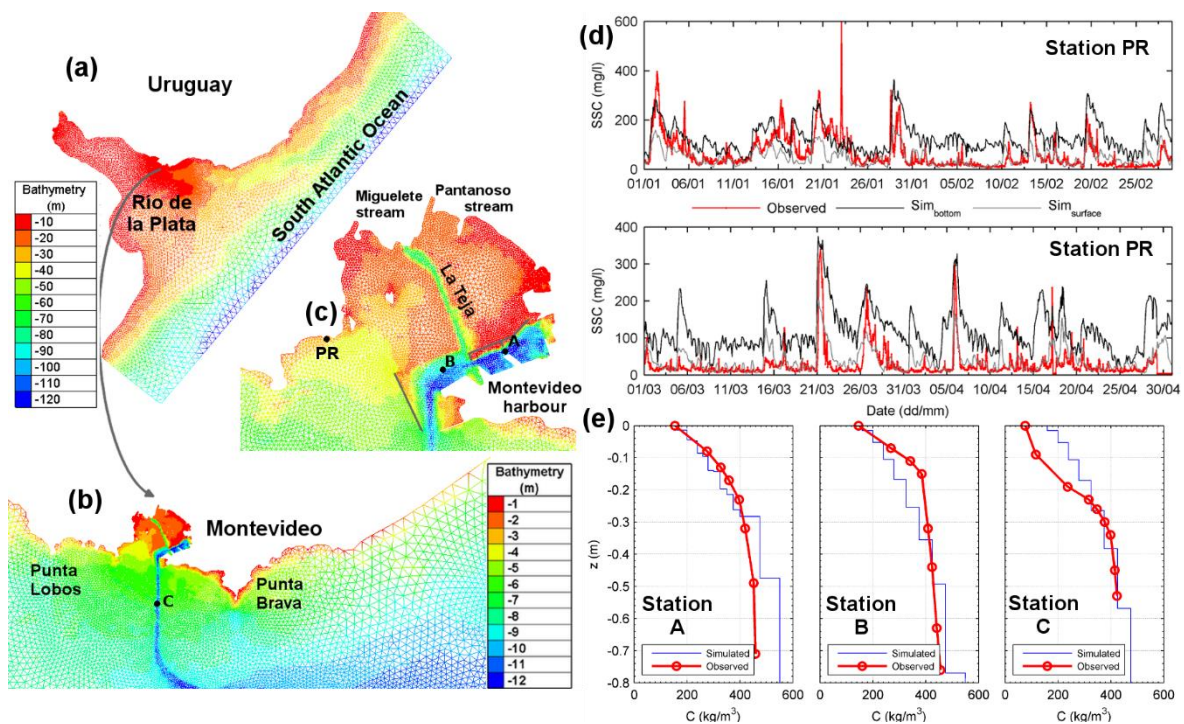


Fig. 1 (a) Río de la Plata mesh and bathymetry, (b) Montevideo coastal area and (c) Montevideo Bay. (d) Observed and simulated suspended sediment concentration (SSC) at station PR during January-April 2015. (e) Observed and simulated vertical bed concentration profiles at stations A, B and C.

References

- Groposo V., Mosquera R., Pedocchi F., Vinzón S. and Gallo M. (2015). Mud density prospection using a Turnin Fork, *Journal of Waterway, Port, Coastal, and Ocean Engineering*, ASCE, 141(5) 1-7.
- Fossati, M., Mosquera, R., Pedocchi, F. & Piedra-Cueva, I. (2015). Self-weight consolidation tests of the Río de la Plata sediments. In *Proceeding of the 13th International Conference on Cohesive Sediment Transport Processes (INTERCOH2015)*, Leuven, Belgium, September 2015. Edts.: Toorman E., Mertens, T., Fettweis, M. & Vanlede J. Flanders Marine Institute (VLIZ) Special Publication 74.
- Fossati M., Cayocca F. and Piedra-Cueva I. (2014). Fine sediment dynamics in the Río de la Plata. *Advances in Geosciences*, 39, 75-80.

An efficient consolidation model for morphodynamic simulations in low SPM-environments

Johan C Winterwerp^{1,2}, Zeng Zhou³, Guilia Battista¹, Thijs van Kessel¹, Bert Jagers¹, Bas van Maren¹ and Mick van der Wegen⁴

¹ Deltares

PO Box 177, 2600 MH, Delft, The Netherlands

E-mail: han.winterwerp@deltares.nl

² also: Civil Engineering and Geosciences, Section of Env. Fluid Mechanics

Delft University of Technology, PO Box 5048, 2628CN Delft, The Netherlands

³ College of Harbour, Coastal and Offshore Engineering

Hohai University, Nanjing, China

⁴ UNESCO-IHE

Westvest 7, 2611 AX, Delft, The Netherlands

Abstract

This paper presents a fast consolidation model suitable for long-term morphodynamic simulations. This model is applicable for muddy systems where sedimentation rates are smaller than consolidation rates, assuming quasi-equilibrium of the consolidating bed. It compares to the consolidation model developed by Sanford (2008). However, in that model, a heuristic, exponential density profile was used. Instead, the current model is derived from the full consolidation (Gibson) equation. The model's material parameters (hydraulic conductivity, consolidation coefficient and strength) can therefore be derived from soil mechanical experiments in the laboratory.

This consolidation model has been implemented in Deltares' generic bed model (GBM), which contains a mixed Eulerian-Lagrangian discretization of the bed in multiple layers (Van Kessel et al., 2011). The choice for this approach was based on numerical considerations, guaranteeing stable and non-negative solutions, while numeric diffusion remains small. The most upper layer represents the so-called Fluffy Layer, which thickness is undefined. This layer communicates with the water column above. Below the Fluffy Layer, we find the Active Layer (AL) of variable thickness and variable dry density. This Lagrangian Active Layer is sub-divided into six (or more) sub-layers for the new consolidation model proposed. Below the (Lagrangian) Active Layers, a number of Eulerian Bed Layers are defined (maximum thickness and dry density of different sediment fractions are user-defined). However, thickness and sediment composition may vary over time. The sediment composition in the Active and Bed Layers may vary in response to mixing/bioturbation. If a Eulerian layer becomes too thick, it is split, creating a new Eulerian bed layer above that thickening layer. Similarly, bed layers may disappear when depleted through erosion. The model's density distribution is updated at a user-defined time step, which may differ from the time step of the sediment-hydrodynamic simulations. The total mass in the bed model is updated at this latter time step, accounting for erosion and deposition. The bed model is coupled to the Delft3D software of Deltares, but may be run in stand-alone mode as well.

The new consolidation model has been favorably tested against the results of one-dimensional consolidation experiments, and for virtual test cases in a straight tidal flume and a two-dimensional tidal basin. Fig. 1 shows the computed vertical density profile with the profile measured in a settling column. The model's material parameters were obtained from the measured settling curve of that consolidation experiment. The large peak in the measured density profile is attributed to a gas bubble in the bed, affecting the response of the acoustic measuring sensor. These material properties were also used in our other test cases.

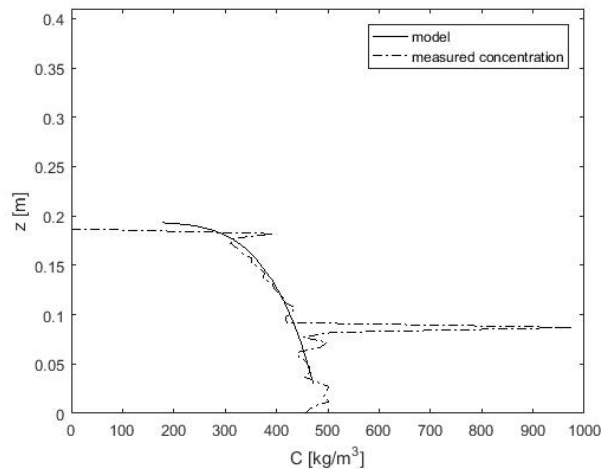


Fig. 1: Comparison computed and measured density profile at equilibrium for mud from Lake Markermeer. The large peak in measured concentration is caused by gas in the sample.

Next, we applied the model in a morphodynamic simulation of a hypothetical tidal inlet. An initial bathymetry was established by running Delft3D in morphodynamic mode for 100 years, with sand alone. Then the model is run another 25 years with mud alone (by prescribing a constant SPM value at the open model boundary), filling in the sandy channels and intertidal areas determined by the sandy morphology. An example of the computational results is given in Fig. 2, presenting the bathymetry for the cases with and without consolidation, showing that in the latter case, tidal channels fill in, whereas sediments do not reach the head of the basin.

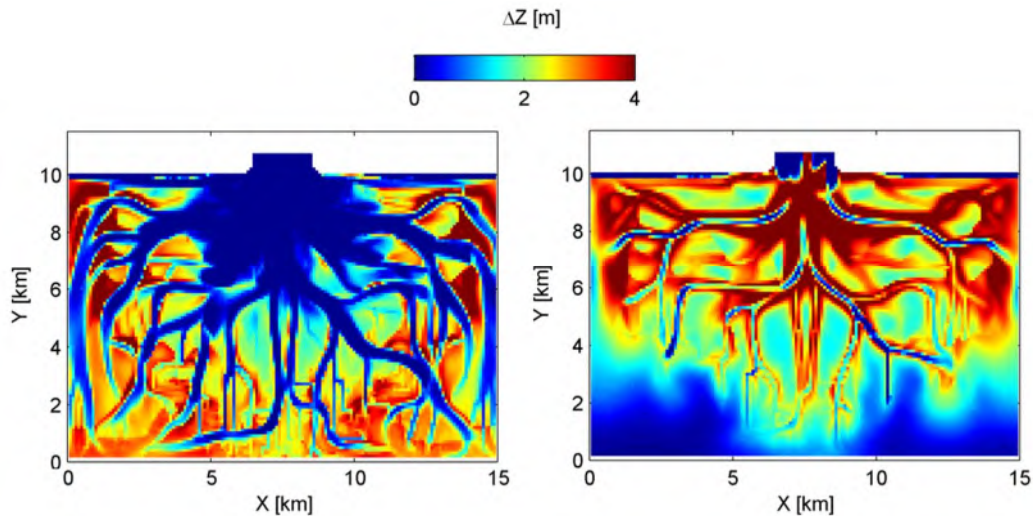


Fig. 2: Computed bed evolution after 25 years by mud w.r.t. to original sand bathymetry with (left panel) and without (right panel) consolidation.

The computational overhead of the new consolidation model is a few 100% (for the tidal inlet simulations above a factor two in case waves are included, and a factor five when waves are not included). However, because of its off-line coupling, the model can easily be vectorized.

References

- Sanford, L. (2008). Modeling a dynamically varying mixed sediment bed with erosion, deposition, bioturbation, consolidation, and armoring. *Computational Geosciences*, 34(10): 1263–1283, doi:10.1016/j.cageo.2008.02.011
- Van Kessel, T., J.C. Winterwerp, B. Van Prooijen, M. Van Ledden and W. Borst (2011). Modelling the seasonal dynamics of SPM with a simple algorithm for the buffering of fines in a sandy seabed. *Continental Shelf Research*, 31 (10-suppl): S124–S134, doi:10.1016/j.csr.2010.04.008.

Experimental Investigations of Vertical Turbulence in Concentrated Mud Suspensions

Oliver Chmiel¹ and Andreas Malcherek¹

¹ Institute of Hydro Sciences, Chair of Hydromechanics and Hydraulic Engineering, University of the German Armed Forces Munich, 85577 Neubiberg, Germany
E-mail: Oliver.Chmiel@unibw.de, Andreas.Malcherek@unibw.de

Introduction

The numerical simulation of vertical turbulent processes can be performed with the $k-\varepsilon$ turbulence model, for instance. This turbulence model is well investigated and provides reasonable results for most engineering applications (Toorman, 2000). In case of stratified and highly concentrated mud layers, like they appear in the Ems Estuary, the suspension's flow behaviour changes. Turbulence is damped, the flow becomes laminar and is driven by the complex rheological viscosity ν_{rh} , which depends on the solid content ϕ , the shear rate $\dot{\gamma}$ and flocculation parameters.

In order to simulate the vertical flow structure within a continuous modelling approach, the effective viscosity $\nu_{eff} = \nu_t + \nu_{rh}$ is introduced, being the sum of the turbulent and the rheological viscosity. Combining the continuous approach with the standard $k-\varepsilon$ turbulence model will fail in a vertical 1D model and high suspended solid concentrations at the bottom. The turbulence production due to shear will increase inside the mud layers, though a decrease of turbulence is expected.

To investigate the application of a continuous modelling of turbulence and rheology, experimental data is needed about turbulent properties in the transition from turbulent to rheological flow behaviour. Therefore an experimental set up was developed to measure the turbulent quantities in suspensions of different concentrations.

Methods and Results

Different experimental studies with concentrated mud suspensions were conducted. Cellino (1998) was measuring velocity and concentration fluctuations of sand suspensions in a longitudinal channel. Further investigations in longitudinal channels were based on steep slopes and underwater mudflows (van Kessel and Kranenburg, 1996). When it comes to highly concentrated mud suspensions, many experiments were conducted in annular flumes or other closed facilities (Ockenden and Delo, 1991; Winterwerp *et al.*, 2002; Bruens, 2003). Here, secondary currents and non-stationary conditions complicate the measuring procedure, as well as the installation of measurement devices.

Based on experimental investigations for stratified flows with salt water, which was presented by Toorman *et al.* (2002), a new experiment was created in a longitudinal channel. The measuring section is covered with quartz powder, which has similar granular properties than mud from the Ems Estuary. Fig. 1 shows a conceptual sketch of the experimental facility at the UniBw in Munich.

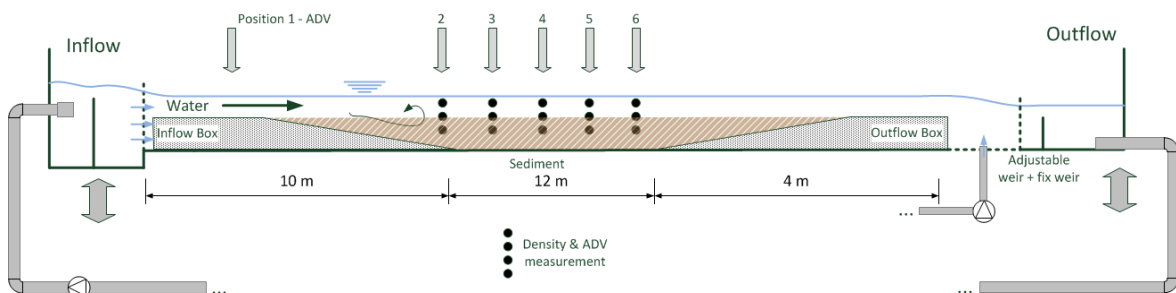


Fig. 1. Conceptual sketch of the experimental facility at the UniBw Munich (not to scale).

Different flow and concentration conditions could be produced, whereby measurements were conducted with ADV probes in vertical and horizontal direction. Additionally the Signal-to-Noise Ratio of the ADV probe was calibrated for quartz powder suspensions, so that fluctuations and vertical profiles of velocity, turbulent kinetic energy and concentration can be measured simultaneously (Fig. 2).

The results of the measurements of vertical velocity, turbulent kinetic energy and concentration will be presented and discussed for different experimental setups and concentrations. Effects of granular suspensions towards the vertical and horizontal production and evolution of turbulence will be analysed and compared with numerical results based on the continuous modelling approach.

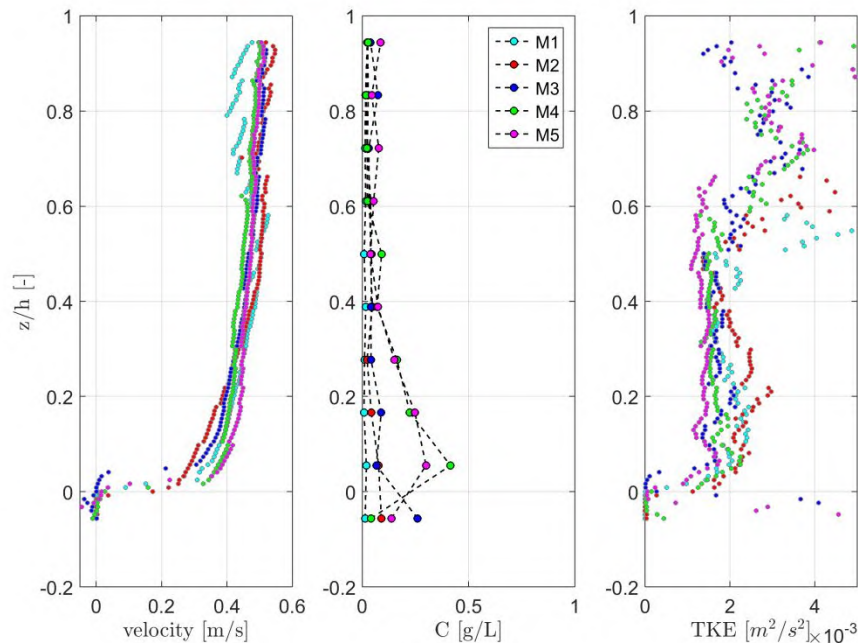


Fig. 2. Measured horizontal evolution (M1 - M5) of averaged velocity, concentration and turbulent kinetic energy profiles along the quartz powder section. M1 indicates the beginning and M5 the end of the measurement section.

References

- Bruens, A. (2003). *Communications on Hydraulic and Geotechnical Engineering – Entraining Mud Suspensions*. Report No. 03-01, Delft University of Technology.
- Cellino, M. (1998). *Experimental Study of Suspension Flow in Open Channels*. PhD thesis, Ecole Polytechnique Federale de Lausanne.
- Ockenden, M. and Delo, E. (1991). Laboratory Testing of Muds. *Geo-Marine letters*, 11(4-4):138-142.
- Toorman, E. A., Bruens, A., Kranenburg, C. and Winterwerp, J. (2002). Interaction of Suspended Cohesive Sediment and Turbulence. In: *Fine Sediment Dynamics in the Marine Environment – Proceedings in Marine Science*, 5:7-23.
- Toorman, E. A. (2000). Parameterization of Turbulence Damping in Sediment-laden Flow. Technical Report. Report No. HYD/ET/00/COSINUS/3, Hydraulics Laboratory – Katholieke Universiteit Leuven.
- van Kessel, T. and Kranenburg, C. (1996). Gravity current of fluid mud on sloping bed. *Journal of Hydraulic Engineering*, 122(12):710-717.
- Winterwerp, J., Bruens, A., Gratiot, N., Kranenburg, C., Mory, M. and Toorman, E. A. (2002). Dynamics of Concentrated Benthic Suspension Layers. *Proceedings in Marine Science*, 5:41-55.

Modelling river hydro-sedimentaries fluxes during a high flood event

Jeremy Lepesqueur¹, Renaud Hostache¹ and Christophe Hissler¹

¹ ERIN/LIST, 41, rue du Brill, 4422 Belvaux, Luxembourg

E-mail: jeremy.lepesqueur@list.lu

Extensive Metallurgical activities nearby river systems in Europe have been responsible over the two past centuries for river system contaminations. In this context River Orne located in eastern France is suffering from sediment contamination due to the past metallurgical activities. Although recent water policies are more conservative past contaminations due to industrial wastewater still represent an issue. As a matter of fact, there is a need for monitoring and predicting the potential resuspension of persistent pollutants in rivers like Orne. In this framework one objective of the project MOBISED (Modelling the reMObilization of SEDiments and the release of associated contaminants <https://www.list.lu/fr/projet/mobised/>) is to implement a 3D hydrodynamic model coupled with a morphodynamic model in order to evaluate the sediment transport and remobilization in a 4km long reach of river Orne during flood events.

In this area of interest, the riverbed has an average width of 30 m and the river basin is draining 1268 km². Since 2014 maximum instantaneous discharges higher than 200 m³/s have been recorded. The modelled reach is composed of two large meanders. Its downstream boundary is equipped with a dam that contributes to the formation of mud banks due the deposition of the suspended load as a result of reduced streamflow velocities. The stream bed is mainly composed of pebbles, coarse gravels and sand and of a small silt portion. The river banks are mainly composed of a sandy mud mixture with a varying content of mud covered by dense vegetation. More locally the river banks are made of concrete or silted up rockfill. Over the last two years monitoring efforts have been concentrated on continuously recording the flow and the solid discharge, and more episodically measuring the bathymetry and the deposition of the sediment on the selected banks.

In this study the hydrodynamic code TELEMAC 3D (Hervouet et al., 2007) fully coupled with the sediment transport module SISYPHE (Villaret, 2011) is forced by the flow at the upstream boundary of the domain and by the water level at the downstream one. The unstructured mesh has been generated using the POLYMESH@ software (developed by A. Roland T.U. Darmstadt) and is composed of 16492 nodes separated by distances in a range of 7m up to 25m.

The standard version of SISYPHE does not allow for running simulations while mixing stratum type, i.e. the user has to choose between three kinds of bed composed of non cohesive sediment (up to 10 classes), purely cohesive sediment (1 classe), or a mixture sand and mud (two classes). However this kind of representation does not fit for river Orne as the non cohesive sediment is characterized by a large range of particle size and as the cohesive sediment represents a significant part of the sediment. Consequently, for the sake of an accurate representation of sediment transport over the domain SISYPHE has been further developed to allow for taking ten classes of sediment into account regardless their type of stratum (cohesive sediments or non-cohesive). Indeed, through sediment mobility criterium and the sediment particle fall velocity, the erosion fluxes and the suspended load are related to the sediment diameter. This explains also why it is important to take into account a realistic granulometric distribution. The development of SYSIPHE allows then to simulate solid discharges for the 10 classes of sediments. The parameterization of SISYPHE is similar to the one used in Lepesqueur et al (2009) except that the slope effect and the mud consolidation have been taken into account in the present study. The bottom friction is calculated using the Nikuradse law with a roughness depending on the median grain size (in absence of bedforms) except on the riverbanks where the apparent roughness is fixed to 4cm to take account of the presence of dense vegetation. The formulation of Soulsby (1997) is used to calculate the shield parameter. In presence of mixed sediment, the formulation of Van Ledden (2001) is used. It distinguishes two behaviours: the cohesive one and the non-cohesive one depending on the fraction of mud. It is assumed that in the cohesive behaviour sand is eroded based on mud erosion law. The non-cohesive sediment or in the non cohesive behaviour sediment are transported through suspended and bed loads. The formulation of Celik and Rodi (1988) for the deposition and erosion for the suspended transport is used with an equilibrium concentration calculated according Smith and Mc Lean (1997). Cohesive sediment is transported only in suspension based on the formulation of Krone and Partheniades. A masking effect is imposed to the erosion flux on the river banks to reduce surface potentially erodible where the vegetation is dense and consequently reduce the surface of the interface water sediment. This mask coefficient consists in a factor corresponding to the portion of sediment exposed to erosion and is used to compute the net erosion flux. In absence of vegetation, the surface is totally exposed so the mask coefficient is setted to 1.

The proposed SYSIPHE developments are discussed and evaluated based on the comparison with the standard

version of SISYPHE. The necessity of including new development to take into account the process of flocculation is also argued due to the impossibility to correctly represent the signal of turbidity in absence of sufficient current velocity for suspended load advection.

Celik I., Rodi W. (1988). Modelling suspended sediment transport in nonequilibrium situations. *Journal of Hydraulic Engineering*, 10, 114, 1157-1119.

Hervouet J.M. (2007). *Hydrodynamics of Free Surface Flows*, John Wiley and sons.

Lepesqueur J., Chapalain G., Guillou N. , et Villaret C. (2009). Quantification des flux sédimentaires dans la rade de brest et ses abords, 31 émes Journées de l'Hydraulique de la SHF: Morphodynamique et gestion des sédiments dans les estuaires, les baies et les deltas.

Mitchener H. and Torfs H. (1996). Erosion of sand/mud mixtures, *Journal of Coastal Engineering*, 29: 1-25.

Partheniades E. (1965). Erosion and deposition of cohesive soils, *ASCE Journal of the Hydraulic Division*, 91:105-139.

Smith J. and McLean S. (1977). Spatially averaged flow over a wavy surface, *Journal of Geophysical Research*, 82:1735-1746.

Soulsby R. (1997). *Dynamics of marine sands*. Thomas Telford, H.R. Wallingford, 249 pages.

Van Ledden M. (2001). Modelling of sand-mud mixtures. Part II: A process-based sandmud model. WL | DELFT HYDRAULICS (Z2840).

Villaret C., Hervouet J.M., Kopmann R., Merkel U. and Davies A.G. (2011). Morphodynamic modelling using the Telemac finite-element system, *Computers and Geosciences*, 53: 105-113.

Using rheological measurements to predict the flow behaviour of cohesive sediment gravity flows

Megan Baker¹, Jaco H. Baas¹ and Ricardo Silva Jacinto²

¹ School of Ocean Sciences, Bangor University, Menai Bridge, Isle of Anglesey, United Kingdom
E-mail: m.baker@bangor.ac.uk

² IFREMER, Laboratoire Géodynamique et Enregistrement Sédimentaire (LGS), BP70, 29280 Plouzané, France

Abstract

Lock-exchange experiments show that the flow velocity and run-out distance of cohesive sediment gravity flows change with clay type and concentration. Complimentary rheological data allow the starting conditions of the flow material to be represented by the yield stress rather than clay type and concentration. This is the first step in linking cohesive sediment gravity flow properties to rheological, rather than compositional, measurements.

Introduction

In the marine environment, the transportation of sediment into deep water often occurs via bottom-hugging sediment gravity flows (SGFs), *i.e.* flows of suspended sediment that move downslope, driven by the density difference between the flow and seawater. Knowledge of cohesive clay-laden sediment gravity flows is limited, despite clay being one of the most abundant sediment types on earth and subaqueous SGFs transporting the greatest volumes of sediment on our planet (Kneller and Buckee, 2000; Healy *et al.*, 2002). Cohesive SGFs are complex owing to the dynamic interplay between turbulent forces, generated at the boundaries of the flow, and cohesive forces (Baas *et al.*, 2009). The cohesive forces are controlled by the clay concentration and the cohesive strength of the clay within the flow, which may differ between types of clay minerals. The cohesive forces can be correlated to the rheological properties of the material, such as the yield stress.

Methods

Laboratory experiments using a lock-exchange tank have been conducted to isolate the effect of clay mineral type and concentration on the flow dynamics of cohesive SGFs in natural seawater. The experiments contrasted SGFs composed of kaolinite clay (weakly cohesive) and bentonite clay (strongly cohesive) at a range of volumetric concentrations. For each experiment the distance the flow travelled for (run-out distance), the velocity of the front of the flow (head velocity) and the thickness distribution of the deposit were measured. In addition, rheological tests were conducted on samples of the same composition as the experimental flows, to obtain rheological values, *i.e.* yield stress, on the initial flow material in the laboratory experiments.

Results

Initially, increasing the volumetric concentration of kaolinite and bentonite within the flows led to a progressive increase in the maximum head velocity and flows that reflected off the end of the 5-m long tank (Figs 1a, b). However, increasing the volume concentration of kaolinite and bentonite above 22% and 17%, respectively, reduced both the maximum head velocity and the run-out distances of the SGFs. The kaolinite rheology results showed an exponential increase in yield stress with increasing volume concentration (Fig. 1c). The yield stress of the bentonite samples increased gently with increasing concentrations up to 18%, where after the yield stress rose rapidly for greater concentrations (Fig. 1c).

Moving from flows carrying bentonite to kaolinite, a progressively larger volumetric suspended sediment concentration was needed to produce similar run-out distances and maximum head velocities (Figs 1a, b). Bentonite suspensions produced a higher yield stress compared to kaolinite suspensions of the same volume concentration, at concentrations above 10% (Fig. 1c).

Discussion

The initial increase in head velocity with volume concentration suggests that suspended sediment concentration intensifies the density difference between the turbulent suspension and the ambient water, which drives the flow. As the clay concentration increases so does the potential for the clay particles to collide and flocculate, this results in an increasing yield stress of the starting material with concentration. Above 17% bentonite and 22% kaolinite, the yield stress of the flows is high enough to limit shear-induced turbulence, and reduce the forward momentum of the flows.

The rheology and flume experiments suggest that above circa 10% volume concentration the strongly cohesive bentonite suspensions were able to create a stronger network of particle bonds than weakly cohesive kaolinite suspensions of a similar concentration, thus producing the higher yield stresses and lower maximum head velocities and run-out distances observed. The flume data results are significant when interpreting the deposits of fine-grained SGFs in the geological record. We suggest that natural high-density SGFs that carry weakly cohesive clays may reach a greater distance from their origin than flows that contain strongly cohesive clays.

The next step of this work is to link the flow and deposits properties with the rheological data, and remove the need for data on the clay type and concentration, as this may not be known for natural flows. Initial results show that yield stress is a major control on the run-out distance, independent of clay type and concentration (Fig. 1d).

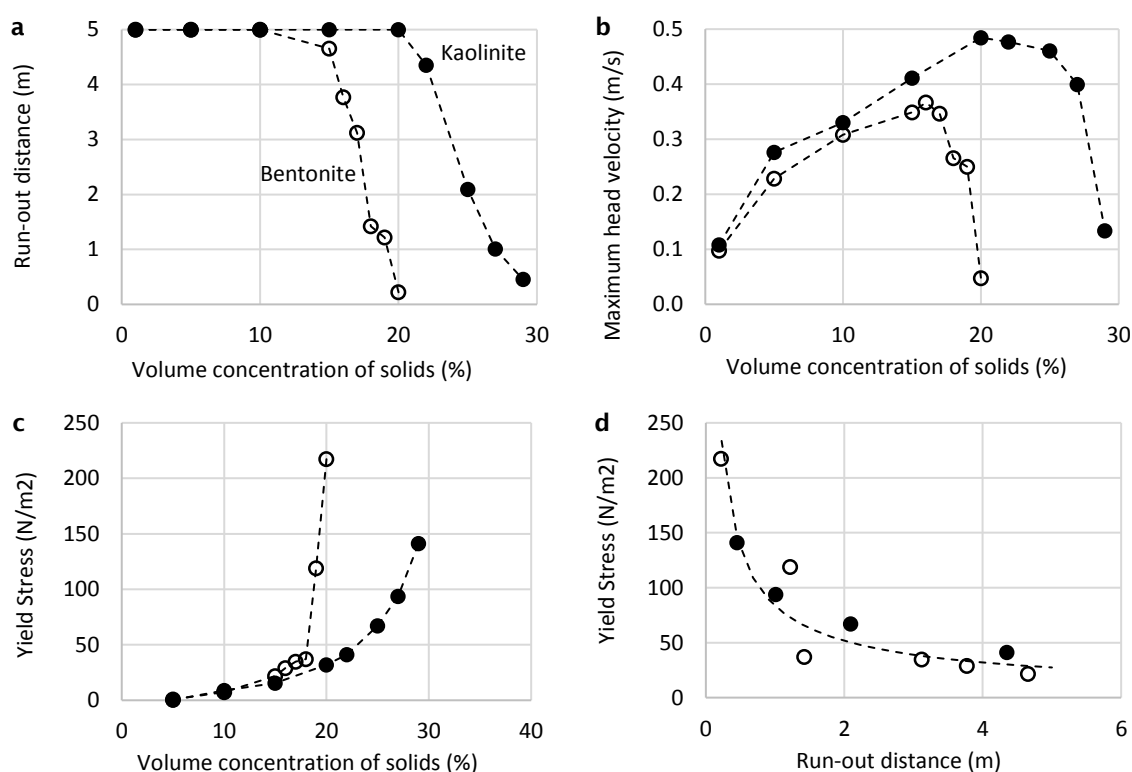


Fig. 1. a) changes in the distance the flows travel along the tank with volume concentration; b) maximum head velocity of each flow against volume concentration; c) relationship between concentration and yield stress for the two clay types; d) flow run-out distance against yield stress, with best fit curve. Black circles = kaolinite, open circles = bentonite.

Conclusions

These results demonstrate that clay concentration and clay mineral type are important controls on the mobility of cohesive SGFs, and should be considered when looking at natural flows. We hope to improve the link between the flume and rheology results and use measurable rheological parameters as predictive tools for flow behaviour.

References

Baas, J. H., Best, J. L., Peakall, J., & Wang, M. (2009). A phase diagram for turbulent, transitional, and laminar clay suspension flows. *Journal of Sedimentary Research*, 79(4), 162-183.

Healy, T., Wang, Y., & Healy, J.A. (2002). *Muddy Coasts of the World: Processes, Deposits and Function*. Elsevier. Amsterdam. 556 p.

Kneller, B., & Buckee, C. (2000). The structure and fluid mechanics of turbidity currents: A review of some recent studies and their geological implications. *Sedimentology*, 47, 62-94.

Characterization of fluid mud layers for navigational purposes

Alex Kirichek¹, Claire Chassagne¹, Han Winterwerp¹, Ronald Rutgers², Arie Noordijk², Karoune Nipius³ and Tiedo Velinga^{1,4}

¹ Department of Hydraulic Engineering, Faculty of Civil Engineering and Geosciences, TU Delft, Stevinweg 1, 2628 CN Delft, the Netherlands
E-mail: o.kirichek@tudelft.nl

² Department of Asset Management, Port of Rotterdam, Wilhelminakade 909, 3072 AP Rotterdam, the Netherlands

³ Rijkswaterstaat PPO, Boompjes 200, 3011 XD Rotterdam, The Netherlands

⁴ Department of Environmental Management, Port of Rotterdam, Wilhelminakade 909, 3072 AP Rotterdam, the Netherlands

Abstract

The objective of this study is to get a new insight into in-situ characterization of fluid mud layers. Water Injection Dredging has been performed to create a fluid mud layer in the 8th Petroleumhaven at the Port of Rotterdam. Four measuring tools, conventional multi-beam echo-sounder, DensX, Graviprobe and Rheocable have been used to monitor the fluid mud layer properties over the time. The results suggest that the currently employed density-based nautical depth criterion has to be revised to ensure more efficient navigation in the vicinity of fluid mud layers.

Introduction

The detection of fluid mud layers at ports and waterways is of primary importance to safeguard navigation. For practical reasons, the nautical depth (ND) is defined within the fluid mud layer as the depth where the mud density does not exceeds a density of 1.2 kg/l (PIANC, 2014). This layer typically consists of water-sediment mixture and has weak shear strengths.

Echo-sounding measurements have been successfully used to assess the ND (Hamilton and Bachman, 1982). As the acoustic impedance along can be correlated to density. Currently, multi-beam echo-sounders are utilized to determine fluid mud deposits. Two frequencies of the emitted acoustic signal, 200 kHz and 38 kHz, are used to detect the approximate size of the fluid mud layer. However, the low-frequency (18-45kHz) signal has to be calibrated using the SILAS system, which correlates the measured acoustic impedance to in-situ density measurements. Typically, the density measurements are done with penetrometer-type tools or mud samplers. The acoustic impedance of the mud of density 1.2 kg/l is then correlated to the low-frequency echo-sounder signal and corresponding depth is used as a nautical depth. This method is currently employed the Port of Rotterdam and Rijkswaterstaat.

In our experiments we would like to estimate which of the density or the rheological properties of the mud are the most effective criteria for navigation in the vicinity of fluid mud layers. For this purpose, we compare two penetrometers, DensX and Graviprobe, which provide vertical profiles of the density and cone penetration resistance, respectively. DensX is an X-ray based direct measurement density profiler. It measures the densities of a water-mud column between 1.0 kg/l and 1.5 kg/l with an accuracy of 0.25 %. Graviprobe measures the cone penetration resistance and pressures while falling free in a water-mud column. The cone penetration resistance is then correlated to the undrained shear strength of the fluid mud layer.

The Rheocable method (Druyts and Brabers, 2012) is based on the physics of a towing body. Towed within a certain velocity window the position of the Rheocable is then related to the interface between fluid and consolidated mud. The depth of the cable is recorded by measuring the hydrostatic pressure. An electrode array is positioned along the length of the cable. The electrical resistivity of mud is linked to the density of mud using the calibration performed in the laboratory. During the Rheocable survey the resistivity is monitored and the velocity of the towing is adapted in or order to always keep the cable within the fluid mud layer at the ND.

Field experiment

The 8th Petroleumhaven has been selected for this study. The water depth in this harbour is varies from 23m to 27m. Initially, the Water Injection Dredging method was employed to mobilize the mud from the bottom and create a fluid mud layer up to 1.5m. The total area of 500×200 m² has been monitored on a weekly basis. The Rheocable measurements are compared to the results of conventionally used low-frequency acoustic sounding technique. The rheological properties in terms

of undrained shear strength is shown in the Graviprobe figure. The DensX measurements have been used to calibrate the echo-sounding data.

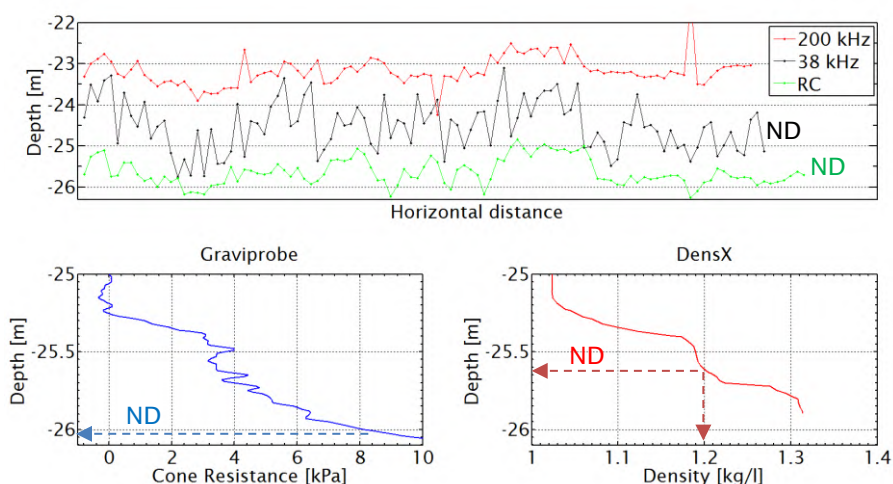


Fig. 1. Characterization of the fluid mud layer by means of the echo-sounder, Rheocable, Graviprobe and DensX. 'ND' stands for the nautical depth.

Discussion

Figure 1 clearly indicates the differences between the ND's found by conventional echo-sounder and the Rheocable method, which can be attributed to inaccuracies of the measuring techniques or calibration limitations.

The output of penetrometers DensX and Graviprobe also give a different ND estimate. The analysis of the complete dataset of the Graviprobe and DensX depth profiles confirm the non-linearity between density and shear strength of mud. Density measurements do not reflect the thixotropic effect of mud. Therefore, a more complete definition of the ND should be derived that includes the rheological properties as key criteria for safe and cost-efficient navigation.

The non-linear relationship between density and rheological properties is investigated further by means of laboratory consolidation and rheological experiments. We found that the undrained shear strength of mud develops slower with time than the density which confirms the experiments of Staelens *et al.* (2013). A remaining open question is whether the output of the Graviprobe technique is correctly related to the rheological properties of mud.

Conclusion

This study provides a new insight into the non-linear relationship between density and rheological properties. Rheological properties are sought to be the relevant parameters for defining the nautical depth to safeguard navigation in the vicinity of the fluid mud layer.

In order to get detailed bathymetry mapping, acoustic signal of echo-sounders could then be related to rheological properties of mud instead of density.

References

- Druyts, M. and P. Brabers (2012). Nautical depth sounding - the Rheocable survey method. *International Hydrographic Review*, 7: 64-98.
- Hamilton, E.L. and R.T. Bachman (1982). Sound velocity and related properties of marine sediments. *Journal of Acoustic Society of America*, 72: 1891-1904.
- PIANC (2014). Harbour Approach Channels - Design Guidelines. Report 121.
- Staelens P., Geirnaert K., Deprez S., Noordijk A. and A. Van Hassent (2013). Monitoring the consolidation process of mud from different European ports in a full scale test facility. *Conference Proceedings, WODCON XX: The Art of Dredging, Brussels, Belgium*

Monitoring of the rapid variation of the suspended sediment concentration in an estuary with large tidal range

Dong-Young Lee¹, Jin Soon Park², Guoxiang Wu¹, Jun Seok Park² and Kwang-Soo Lee²

1 Ocean University of China, Qingdao, China

2 Korea Institute of Ocean Science and Technology, Ansan, Korea

1. INTRODUCTION

Various regional and coastal models have been developed and are used operationally in predicting hydro-dynamic parameters of the coastal sea such as water level, circulation and waves. However, the environmental parameters including suspended sediment concentration are still not adequately predicted. The prediction of the 3-D features of rapidly varying suspended sediment concentration(SSC) at an estuary with large tidal range and river flow like Gyeonggi Bay, Korea is a challenge.

Gyeonggi Bay is characterized with large tidal range of 8-9 meters, inflow of Han River, mud and sand mixed sediment environment, which make the sediment transport processes complicated and the coastal environmental parameters vary rapidly with time and space. The space and time variation of the SSC at the Gyeonggi Bay have been investigated from the combination of modern technologies of in situ, un-manned monitoring of vertical profiles, Geostationary satellite remote sensing and 3D numerical model by means of solving the problem in obtaining the bottom boundary condition for fine sediment transport model.

2. REAL-TIME MONITORING OF THE VERTICAL PROFILES OF SSC

Korea institute of Ocean Science and Technology (KIOST) had developed an Intelligent Buoy System (INBUS) that automatically measures the vertical profiles of more than 10 parameters including temperature, salinity, suspended sediment concentration, Chlorophyll every half an hour. The data are transmitted using the CDMA network and saved at computer for on-line distribution to the users. The observed marine environment data, especially the SSC are analyzed and presented. The time variations of the vertical profile of the SSC are analyzed for different environment of tide phase, winter monsoon and passage of typhoon.

3. HOURLY MONITORING OF SSC FROM GEOSTATIONARY SATELLITE REMOTE SENSING

Korea's Communication, Ocean and Meteorological Satellite(COMS) was launched in June 2010 and has been operating successfully to accumulate

considerable amount of data. The sampling interval of GOCI is 1 hour during daytime with a spatial resolution of 500m x 500m and an eight-band spectral resolution. The COMS is the first satellite to observe the ocean color at a specific location eight times a day. Such high temporal resolution makes it possible to investigate the spatial and time variation of the SSC for successive tidal cycles in the bay and estuary.

The surface layer SSC data of the INBUS System are used in the calibration of the GOCI satellite remote sensing data. The vertical profile of the *in situ*. SSC data of the INBUS system and surface SSC data from the GOCI geostationary satellite remote sensing have been analyzed together with the detailed wave and tide simulation data to see the time and space variation characteristics of SSC at the Gyeonggi Bay.

4. INTEGRATION OF IN SITU. MONITORING, SATELLITE REMOTE SENSING AND 3D NUMERICAL MODEL

The initial condition of the SSC prediction model, Delft3D model in this study, have been prepared from the combination of the *in situ*. and the satellite remote sensing data. The sedimentation parameters of the bed materials needed in estimating the erosion and deposition rate at the bottom interface needed for the SSC prediction model are prepared from the information of the bed materials first. The parameter have been adjusted repeatedly to provide the best results of the SSC prediction by comparing with the hourly SSC data from the GOCI satellite remote sensing.

The bed material properties estimated by this method is used in building operational SSC prediction system. The established SSC prediction system is evaluated from the *in situ*. observation and hourly satellite remote sensing data.

5. DISCUSSION AND CONCLUSION

Method of producing SSC information at the Gyeonggi Bay with large tidal range such as *in situ*. monitoring using smart buoy system, geostationary satellite remote sensing and 3D numerical model have been demonstrated. Through integration of these three methods, SSC observation system can be established to provide time and space variation of the SSC efficiently. Further extension of this system to cover the entire area of the Yellow Sea will be discussed to include high SSC area along the coast of China through proper calibration of the GOCI data.

Laboratory and numerical studies on the sediment transport processes for the sand-mud mixed bed

B.C. Liang¹, J. Wang¹, Z. Xu¹, Z. Qu¹, D. Y. Lee¹, and E. Hayter²

¹*College of Engineering, Ocean University of China*

Qingdao, Shandong, China

²*ERDC, USACE, Vicksburg, Mississippi, USA*

Bed materials of the estuaries and semi-enclosed waters in the Yellow Sea mostly consist of mixtures of sand and mud sediment. The sediment transport processes for the sand-mud mixed bed at coastal waters is poorly understood because of the difficulties in measurement of the fundamental parameters such as bed load and suspended load transport rate, erosion rate and deposition rate, especially at oscillatory flow induced by wave motion. To be able to predict the sediment and contaminant transport and morphology change for various engineering applications for the coastal waters, the sediment transport processes for the sand-mud bed need to be well understood through well-organized laboratory or field experiments. In developing process based sediment transport model, the proper estimation of the vertical sediment flux at the bed surface, erosion rate and deposition rate, is essential together with hydro-dynamics.

A series of flume experiment are conducted first to investigate sediment transport of sand, silt and mud independently and then those of their mixtures in various wave conditions by measuring the precise time and space evolution of bottom profile together with detailed suspended sediment concentration(SSC). Laboratory experiments and data analysis and their applications are done as follows:

1). Precise measurement of SSC at constant water depth for different wave conditions

Utilizing recent technologies of precise measurement of SSC based on optical and electric properties, SSC is measured continuously at 2D wave flume with constant water depth for various regular wave conditions. The space and time evolution of the SSC are monitored precisely using side-looking video. The spectral reflectance measurement method is developed for the precise measurement of the SSC without disturbing the flow condition. A light source with parallel and uniform light intensity is placed at one side of the wave flume and the light intensities at both sides of the wave flume are obtained using side looking video cameras with proper filters.

Conductivity concentration profiler(CCP) manufactured and provided by Korea Institute of Science and technology(KIOST) is used in the measurement of the high concentration vertical SSC profile near the bed with space resolution of 2 mm. By correlating the transmitted and reflected light intensities with the SSC obtained by CCP through calibration processes, the SSC is estimated by detecting the transmitted and reflected light intensities using video camera.

Adv anemometers and staff wave gages are used to measure wave and wave orbital flow velocity. Linear wave theory is used to estimate orbital flow velocity at the point of interest.

2). Data analysis and applications of the precise measurement of SS

Following studies are carried out through the analysis of the detailed time and space evolution of the

SSC together with hydro-dynamics estimated by linear wave theory at 2D wave flume:

- i). The studies on the basic sediment transport processes for different sediment types and their mixtures in the coastal waters
- ii) Empirical formulation of the erosion rate and deposition rates for different wave conditions for bottom boundary condition of the process based morphology prediction model
- iii). Studies on the effects of the fine sediment fraction on the sand transport processes including bed armoring processes.
- iv). Validation and calibration of the process based sediment transport model for sand-silt-mud mixture

3). Precise measurement of beach profile and SSC at sloping bed for different wave conditions

The laboratory experiments are conducted at 2D wave flume for two different bed slopes and various incident wave conditions. The time variations of surface elevation and bed profile are observed precisely every 0.1 second time interval with space resolution of 2 mm using video cameras mounted aside the glass wall of 2D wave flume through geometric compensation. The precise measurement of SSC is done using above mentioned CCP and light spectral reflectance measurement using filtered video camera.

Adv anemometers are used to measure flow velocity at surf-zone. After showing good agreement of the numerical simulation result of the wave resolving model such as SWASH, CFD model with the observation data in the surf-zone, the hydro-dynamics simulated by the wave resolving model are used for the swash-zone where in situ. measurement using anemometer is not feasible.

4). Data analysis and application of the precise measurement of beach profile together with SSC at sloping bed with different sediment types

Following studies are carried out through the analysis of the detailed time and space evolution of the bed profile and SSC together with hydro-dynamics estimated by wave resolving models at 2D wave flume:

- i). Estimation of sediment transport rate from the time and space evolution of the bed profile using conservation of sediment, Exner Equation, and also by estimation of movement of sand ripples.
- ii). Formulation of the sediment transport rates to be used for the process based morphology prediction model
- iii). Evaluation and improvement of the existing sediment transport and morphology prediction model at surf-zone and swash-zone.
- iv). Studies on the impacts of fine sediment on the sediment transport processes of the sand at surf-zone and swash-zone

5). Validation of numerical model for sand-mud mixture and discussion on further research

The existing sediment transport models for the sand-mud mixture bed including SEDZLJ sediment bed model will be evaluated using the laboratory experiment data and development of more realistic model will be discussed together with the method used for the precise measurement of the bed profile and SSC, and the data analysis will be discussed in detail at the Conference.

Further research on the sediment transport and morphology change for the sand and mud mixed bed at coastal waters with various wave conditions will be also discussed.

Reduction in Sediment Accumulation at a Coastal Marina by Entrance Modifications

Ashish J. Mehta¹, Neelamani Subramaniam² and Earl J. Hayter³

¹ Department of Civil and Coastal Engineering, University of Florida, Gainesville, FL 32611, USA

² Kuwait Institute of Scientific Research, Safat 13109, Kuwait

³ U.S. Army Engineer Research and Development Center, Vicksburg, MS, 39180, USA

Abstract

Predicting a reduction in the frequency of dredging in coastal marinas by modifications at the basin entrance is predicated on the properties of the sediment and the hydrodynamic driving forces. When the heterogeneous sediment includes sand, silt as well as cohesive material, and forcing is due to astronomical tide combined with wind-induced water level variation, the temporal and spatial patterns of sediment accumulation rate tend to exhibit significant sensitivity to these properties. The case of Failaka Marina with a basin area of 0.62 km² and a single entrance to the Gulf of Kuwait subject to semidiurnal meso-tidal range and wind-waves is summarized to illustrate these trends in a somewhat qualitative sense. A fairly comprehensive field investigation was carried out at the site in 2015 to characterize the physical property parameters and resorting to a combination of analytic and numerical modeling. In recognition of hiatuses inherent in the hydrodynamic and sediment transport data, simplifications were introduced in modeling with the aim to derive a rough estimate of the sedimentation rate and locations of significant accumulation as functions of tide and waves.

Two notable requirements of the analysis were found to be: (1) the need to include water waves, as tide alone was shown to be insufficient to drive sediment into the basin, and (2) the need to include a 0.05 m thick layer of fluid mud with a solids volume fraction of 0.45 as the source and sink of bottom sediment outside the basin. Modeling results were generally found to corroborate known rates and sites of accumulation of sand as well as mud. This made it possible to test reoriented entrance jetties and a sediment trap between the jetties as alternatives for reducing the annual sediment influx. It was found that lengthening the jetties would have a beneficial effect, and the sediment trap was shown to serve as an efficient means to trap sand but not mud (Figs. 1a,b).

An important lesson learnt was the need for a greater emphasis on field data collection to evaluate critical parameters for modeling sediment influx. *A priori* analytic calculations can be very useful both to design the field experiment and to guide the numerical modeling of transport.

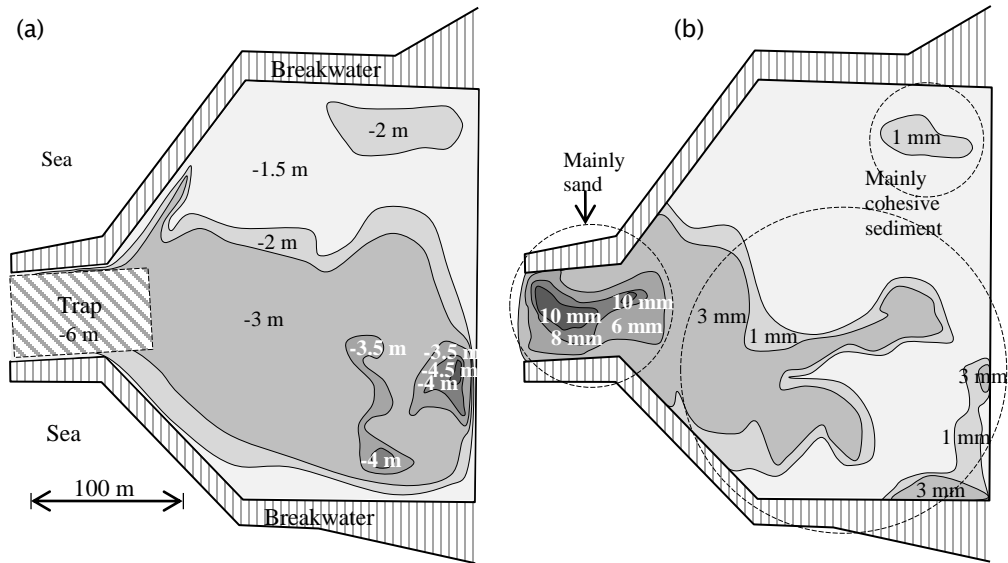


Fig. 1 Sediment accumulation in the Failaka Marina basin (shown with a slightly modified planview geometry): (a) Depths in the basin relative to mean sea level, (b) simulated sediment influx over 30 days.

FLOCCULATION BEHAVIOR OF SEDIMENTS FROM A MINING DAM COLLAPSE: BEFORE AND AFTER RIO DOCE DISASTER

Caroline Fiório Grilo¹, Gabriella Fávaro Lima Amorim¹ and Valéria da Silva Quaresma¹

¹ Department of Oceanography and Ecology, University of Espírito Santo, 514 Avenue Fernando Ferrari, Goiabeiras, Vitória, Espírito Santo, 29075-910, Brazil.

E-mail: carolinegrilo@gmail.com

Introduction

The Doce River watershed is one of the most important in Brazil, providing a large sediment input to the continental shelf adjacent to the Espírito Santo state (Quaresma et al., 2015). In November 2015, a mining dam failure at Minas Gerais state changed the role of this relevant hydrographic network, as about 60 million m³ of tailings sludge were dumped in the Doce River, later reaching the sea as a high suspended particulate matter (SPM) concentration plume. The SPM showed to be peculiar after its arrival in the ocean, presenting coloration and behavior in the water column in an unnatural way. One part of the material appeared to be non-flocculating, while another behaved like a hyperpycnal flow near the bottom. Such finer material, depending on hydrodynamic conditions, can be continued resuspended, altering the characteristics of habitats (chemical, biological and geological ways) and act as a pool of pollutants to the water column (Bastos et al., 2016).

Methods

Four samples were chosen to describe different scenarios and properties of the sediment before and after the mining dam collapse: 1) bed sediment from continental shelf in front of the river's mouth before the disaster (CS A); 2) bed sediment from continental shelf in front of the river's mouth after the disaster (CS B); 3) bed sediment from inside the river (no tide influence) after the disaster (RV); 4) sediment near the mining dam after the disaster (MD). Sandy fraction was removed and after complete disaggregation, the concentrated suspension was transferred to the sedimentation column, which was filled with the same Artificial Saline Water (controlled temperature and salinity; Furukawa et al., 2014). An acrylic cylinder with dimensions of 70mm of diameter and 50cm in height was used as a sedimentation column for floc area and settling velocity measurements. Concentrations along the tests were acquired by a previous calibrated Optical Backscatter Sensor (one calibration for each sample; $R^2 \geq 90$) positioned at 40 and 10cm depth. Floc parameters were acquired by a high resolution video camera (50 to 500x of zoom).

Discussion and Conclusions

Different properties and behavior of flocs could be identified. Almost all sediment deposited at the first 30min of experiment for CS A and B samples, while RV and MD did not deposited. Natural coastal suspended particulate matter typically exhibits a multimodal granulometry distribution that can be partitioned into multiple groups of particles consisting of macroflocs (>200 μ m), microflocs (30 - 200 μ m) and single grain populations (10-30 μ m) (Eisma, 1986), and can be further divided into primary particles (0.25-7 μ m) (van Leussen, 1994). The smallest measured particles were those from MD, falling into microflocs group, while larger particles were those found at the base of the column during CS A experiments, fitting into macroflocs group. Sediment from MD was the only one to not generate macroflocs, even at the base tests. Despite particles from RV had been able to produce macroflocs during base measurements, they were close to the upper limit of microflocs group. The higher velocities occurred at the column top for all samples, due to hindering settling at the base, with higher speeds for MD followed by RV. The lower settling velocity were observed for CS A and B, indicating that besides larger, the flocs were lighter than the others.

Sediment from RV had a group of particles with higher settling velocity than sediments from CS A, resulting in an almost steady curve, while all others presented a clear positive tendency, indicating a progressive settling. Even for column base measurements, this increased speed pattern occurs for other samples, although less visible, while a slightly negative curve was acquired from RV at the column base. Such pattern may indicate a pronounced hindering settling, where flocs are lighter and more susceptible to turbulence (like counter flux). This differentiated samples behavior clearly indicates the presence of two groups of particles, which can also be seen more smoothly on the CS B sample at the column top. MD sediment presented a settling velocity increase through time, as showed by a positive tendency curve. At the column base, most of sediment had already settled, so flocs with very low speeds must have same characteristics as those very lighter flocs from RV.

Experiments indicate that the particles from inside the river and mine dam have peculiar characteristics and yet, that not all kind of particles present in the river settled on the continental shelf. The absence of some part of this material on the continental shelf can be explained by its inability to generate denser and larger flocs, remaining in the water column with greater dispersion than natural fine sediment of the local environment. Another interesting feature is that MD sample presented different behavior from RV sample, containing denser particles, as although having smallest diameters, most of them had a fast settlement. Because they are denser, these particles must have been trapped in the vicinity of the dam, while lighter particles had been carried by the flow. This differentiated settlement was intensified by the drought in which Doce River was passing through, but some of these denser particles could be carried, as observed in the behavior of CS B sediment.

So the dam failure changed sediment properties and caused an impact on its behaviour through the river and at the continental shelf, as clearly shown by the settling and flocculation sediment behaviour from samples before and after the disaster. We can jump on some conclusion about the consequences of this disaster mainly for the local continental shelf and coastline, once the settling process has been more difficult the probability of fluid mud formation increase and its interaction with the wave pattern as well. Besides it this sort of sediment that continuum reach the continental shelf can be transported for longer distances, disseminating pollutants and turbidity at unusual places.

References

- Yoko Furukawa, Allen H Reed, Guoping Zhang. (2014). Effect of organic matter on estuarine flocculation: a laboratory study using montmorillonite, humic acid, xanthan gum, guar gum and natural estuarine flocs. *Geochemical Transactions*, 15:1–9.
- Eisma, D. (1986). Flocculation and de-flocculation of suspended matter in estuaries, *Netherlands Journal of Sea Research*, 20 (2–3), 183–199.
- van Leussen, W. (1994), *Estuarine Macroflocs and Their Role in Fine-Grained Sediment Transport*, Fac. Aardwetenschappen, Univ. Utrecht, Utrecht, Netherlands.
- Quaresma, V.S.; G.M. Catabriga; Bourguignon, S.C.; Godinho, E.; Bastos, A.C. (2015). Modern sedimentary processes along the Doce river adjacent continental shelf. *Brazilian Journal of Geology*, 45, 635–644.
- Bastos, A. C, Dias Jr, C., Loureiro, L. F. F., Ghisolfi, R. D., Neto, R. R., Quaresma, V. Da S., Grilo, C. F., Rodrigues, D., Costa, E. S., Sá, F., Perassoli, F., Boni, G. C., Lázaro, G., Lemos, K., Leite, M. D., Bandeira, M., Cagnin, R. C., Bisi Jr., R., Servino, R., Rossi, R., Martins, T. (2016). Resultados Parciais das Análises Realizadas em Amostras Coletadas na Plataforma Adjacente a Foz do Rio Doce: Embarque NOc. Vital de Oliveira. Vitória: Universidade Federal do Espírito Santo, 1–17.

The effect of initial conditions on the consolidation of mud

Maria Barciela Rial¹, Barend A.P. van den Bosch¹, Johan C. Winterwerp¹, Leon A. van Paassen², Jasper Griffioen^{3,4} and Thijs van Kessel⁵

¹ Delft University of Technology, Faculty of Civil Engineering and Geosciences, The Netherlands
E-mail m.barcielarial@tudelft.nl

² Arizona State University, School of Sustainable Engineering and the Built Environment, Arizona

³ Utrecht University, Copernicus Institute of Sustainable Development, The Netherlands

⁴ TNO Geological Survey of the Netherlands, The Netherlands

⁵ Deltares, The Netherlands

Introduction

Sediment is becoming scarce. Therefore, soft sediments are progressively being used for nature building. The MarkerWadden is an example of an ongoing *Building with Nature* (BwN) project which aims to improve the ecology of Lake Markermeer (The Netherlands) by creating a wetland with the cohesive sediments from the bed of the lake. It represents one of the first projects using fresh unconsolidated mud as a filling material. However, building with these fine sediments represents a great challenge, because of their complex properties.

Various authors have studied the settling and consolidation behaviour of mud at initial concentrations below the gelling point, e. g. Merckelbach (2000), Dankers (2006). However, slurries at much higher initial sediment concentrations are used for BwN, and the consolidation behaviour of such mixtures has been less studied.

In this research, the influence of the initial concentration c_0 on the consolidation behaviour of mud was studied for mud mixtures with an initial concentration above the gelling point.

Methods

The material parameters of Markermeer mud were obtained with two different experimental methods: settling columns and the Seepage Induced Consolidation test (SIC). The two sets of parameters were used as input for a 1DV model to compute density profiles. To account for over-consolidated initial conditions, the effect of swelling was implemented in the 1DV-model. These computed profiles were then compared with the profiles measured with an Ultrasonic High Concentration Meter (UHCM). Further, the sensitivity of the model results was evaluated by interchanging the coefficients of the material properties.

Results and discussion

In our analysis, we presume self-similar sediment properties, and apply a fractal material model. The fractal dimension n_f and the effective stress coefficient K_b obtained with the settling columns and the SIC tests appeared to be of the same order of magnitude. However, the permeability coefficient K_k differed by a factor of 20, suggesting dependency on the initial concentration and/or sample preparation and/or accuracy problems with the methods deployed. Consequently, the final bed heights are predicted correctly when using the different sets of material parameters to model a hypothetical settling column of arbitrary height. However, the consolidation time may vary considerably due to the high variability of K_k .

Both sets of material parameters predict the density profile and bed height well for equilibrium conditions. The differences are minor, but the SIC material parameters provide a better agreement with respect to final bed height and shape of the density profile (Fig. 1).

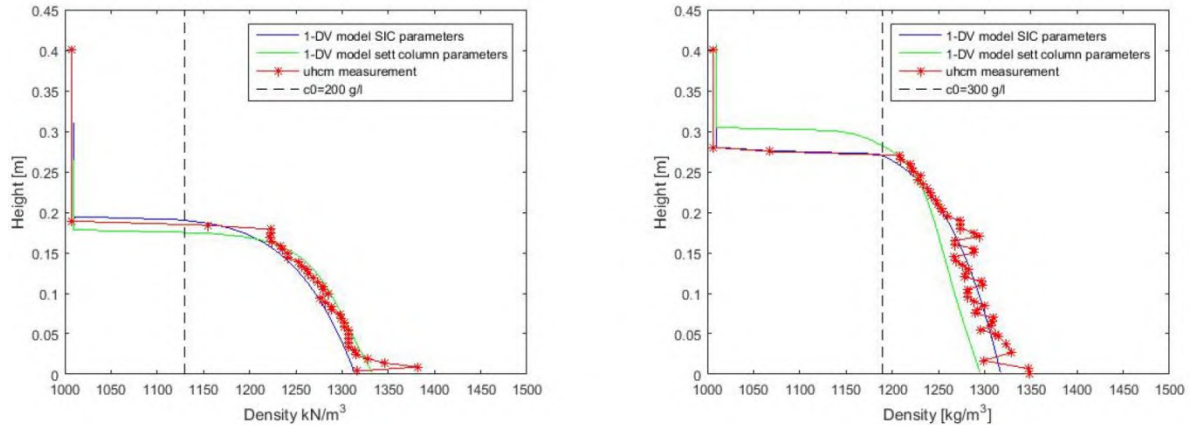


Fig. 1. Left panel: density profiles for $c_0 = 200$ g/l computed with material parameters obtained from the settling column experiment and SIC test. Both profiles are compared with UHCM measurement at $t = 67$ days. Right panel: density profiles for $c_0 = 300$ g/l computed with material parameters obtained from the settling column experiment and SIC test. Both profiles are compared with UHCM measurement at $t = 67$ days.

When the material parameters from columns with different c_0 were interchanged, the bed height and density profile agree less to the measurement (see Table I).

Table I. Offsets of the computed density profiles with respect to the measured ones.

$C_0=200$ g/l. Parameters:	Offset Profile [%]	Offset Bed height [%]	$C_0=300$ g/l. Parameters:	Offset Profile [%]	Offset Bed height [%]
SCE	2	7	SCE	8	9
SIC300	2	2	SIC300	4	0
SIC200	9	7	SIC200	5	6

Discussion and conclusions

This research presented two different experimental procedures, the settling columns and the SIC tests, which showed consistent results.

The results showed to be highly sensitive to the experimental procedure, notably to the sample preparation. The mixing method, together with the room temperature and light conditions, seem to be the most critical factors. The mixing procedure likely affects the size of flocs and the environmental conditions may induce gas production and the development of biofilms. Our results suggest that these factors affect in particular the consolidation time. We are carrying out further research on these effects.

The initial concentration of sediment was also found to play an important role in the consolidation behaviour. In the case that part of the initial column is over-consolidated, the consolidation curves showed an initial linear phase caused by a higher density than at equilibrium in the uppermost part of the mud layer. This excess of density acts like an overburden inducing what we defined as “piston effect”. Further, under over-consolidated conditions, swelling needs to be taken into account and be included in the model.

Thus, our study gives insight in the effect of the initial conditions on the consolidation of high concentrated mud mixtures. These initial conditions are particularly important for land reclamation and wetland construction, where the initial density may be high but the flocs may have been broken due to the mixing during the dredging process.

References

- Dankers, P. (2006). On the hindered settling of suspensions of mud and mud-sand mixtures. PhD-thesis, Delft University of Technology.
- Merckelbach, L. M. (2000). Consolidation and strength evolution of soft mud layers. PhD-thesis, Delft University of Technology.

Modelling unsteady flow and sediment deposition in large lowlands rivers: An application to the Paraná River

Garcia Marina Laura¹, Pedro Abel Basile¹ and Gerardo Adrián Riccardi¹

¹ Centre for Hydro- Environmental Research - Department of Hydraulic, Faculty of Exact Sciences, Engineering and Surveying, National University of Rosario. Rosario 2000, Argentina
E- mail: mgarcia@fceia.unr.edu.ar

Abstract

In this work a quasi- 2D model suitable for the simulation of time-dependent water flow and fine sediment transport processes in large lowland river-floodplain systems is presented. These rivers formed by main channel-floodplain involve large exchanges of water and sediments within the system, as well as nutrients and biota. Floodplains play an important role in river flood attenuation, it is important to understand floodplain inundation dynamics in order to make decisions on flood risk management. The deposit of fine sediments is the process responsible for the long- term modification of the floodplain. Moreover, it can become a reservoir of contaminated sediments. Large lowland river-floodplain systems have very complex morphology with a network of permanent channels, interconnected lagoons, natural levees. The sediments are transported mainly as wash load. These systems have flooding duration on the order of several months, with a gradual and fairly slow floodplain filling due to overbank flows from the main stream and secondary floodplain channels. Quasi- 2D models can capture the fundamental characteristics of water flow and sediment dynamics in these areas. These slow dynamics are compatible with the hypothesis on which quasi- 2D models are based allowing for an effective compromise between computational costs and process representation. In this contribution, the application of a quasi- 2D unsteady flow and sediment transport model in a large lowland river system is presented. The study area comprises a reach 208 km long of the Paraná River (between Diamante- Ramallo, Argentina) representing total a river-floodplain area of 8,100km². The model was already calibrated and validated in previous work. In this paper, the model results corresponding to simulations of water and sediment dynamics during a recent five-year period are presented.

CTSS8- FLUSED model

Water flow is simulated with the CTSS8 hydrodynamic model (Riccardi, 2000). The governing equations for the quasi two- dimensional horizontal time- depending flow field are represented by the well- known approach of interconnected cells (Cunge, 1975). Water continuity for each link between cells is used. Different discharge laws between cells can be used. Fluvial type links can be specified by means of kinematic, diffusive, quasi- dynamic and dynamic discharge laws derived from the Saint Venant momentum equation. In order to deal with special features of fluvial systems, weir- like discharge laws representing natural sills, levees, road embankments, etc., are included in the model. The spatial distribution of model parameters and hydrodynamic variables is done through the subdivision of model domain in irregular cells.

The sediment module FLUSED (Basile *et al.*, 2007) incorporated into the CTSS8 model simulates transport of fine sediments and deposition processes by solving the quasi- 2D continuity equation of suspended sediment, which for the j- th cell reads (neglecting horizontal diffusion):

$$A_{s,j} \frac{\partial(hC_s)_j}{\partial t} = (A_s \phi_s)_j + \sum_{k=1}^N (QC_s)_{j,k} \quad (1)$$

where h is the water depth in the cell, C_s is the volumetric sediment concentration and ϕ_s is the downward vertical flux of fine sediments (deposition rate), expressed as: $\phi_s = P_d w_s C_s$, where P_d is the probability of deposition; w_s is the fall velocity of suspended sediment particle. The probability P_d of particle remaining deposited is given by:

$$P_d = 1 - (U/U_{cd})^2, \text{ if } U < U_{cd} \quad (2)$$

where U is the mean flow velocity and U_{cd} is the critical mean flow velocity for deposition. Water flow and sediment equations are solved using a finite difference numerical scheme. Water levels in each computational cell are determined by an implicit algorithm and water discharges are successively obtained by applying the discharge laws between cells. Using an implicit algorithm, suspended sediment concentration, horizontal and vertical sediment fluxes are determined. Additionally, mean and total cumulative daily, monthly and annual sediment deposition (volume and weight) as well as bed level changes are computed for each cell. The initial conditions are represented by the water levels, discharges and sediment concentrations at each computational cell of the simulated domain. Boundary conditions for water flow are represented by the hydrographs at the upstream end of the reach and by water depth-discharge relations at the downstream boundary. The incoming suspended sediment transport at the upstream end is specified.

Study area

The model was implemented along a 208-km reach of the Paraná River, Argentina, between Diamante and Ramallo and involving a river-floodplain area of 8,100 km². The floodplain is morphologically complex, due to past episodes of sea-level rise and climate change. A well developed network of surface-floodplain channels, oxbow lakes, lagoons, permanent pond areas, and different types of vegetation can be observed. The floodplain width in the study area varies between 30 and 60 km, while the width of the main channel varies from 0.5 to 3 km. The mean annual water discharge at station Rosario is 17,000 m³/s, while during the extraordinary floods of 1983 the maximum water discharge was approximately 60,000 m³/s with almost 30,000 m³/s flowing in the main stream, and the floodplain was completely inundated. The minimum water discharge observed at Rosario was 6,700 m³/s, in 1970. The ratio between maximum and minimum water discharges is 9, a rather low value as in other large rivers of the world. A 56-km long road embankment connecting Rosario and Victoria (RV) crosses the entire floodplain.

The annual average total sediment transport entering the system is approximately 150 × 10⁶ t/yr, of which 83% is composed of silt and clay transported in suspension as wash load. Sediment load entering the system is the main driver of changes in floodplain levels over long time periods. In general, suspended sediment concentrations vary seasonally, from 50 to 60 mg/l up to 500 or 600 mg/l (that occurs between March and April) in the main stream. Annual mean values are approximately within the range of 150 to 250 mg/l. The few available measurements in the floodplain indicate lower values, typically below 100 mg/l.

Application of the model

The topological discretisation was carried out by selecting river cells and valley cells, and by defining the different type of links between cells to represent special topographic features (natural levees, road embankments, bridges, etc.). Currently, the model has 1413 stream cells that represent the main stream, secondary surface-floodplain channels and the Coronda river tributary and 140 floodplain cells representing the alluvial valley and islands, with 4248 links between the different cells. Calibration (for low, medium, and high water stages) and validation results were very satisfactory, with the average error in calibration lower than 10% at all stations and most Nash-Sutcliffe coefficients were above 0.8 (Garcia *et al.*, 2015). The different water stages (specially medium and high) are well reproduced by the model. In this work a recent hydrological five-year were simulated (Sep 2010- Ago 2015), with incoming discharges derived from available records in upstream stations.

Sediment transport and deposition simulations were performed by using synthetic sedigraphs (determined from available historic suspended sediment concentrations and water discharges) and sedimentological parameters (sediment fall velocity for a range between coarse clay (3.35 m/s) to medium silt (21.2 m/s), critical mean flow velocity for deposition of the 0.15 m/s, sediment porosity 0.42).

Model results

The obtained results of hydrodynamic simulations of observed floods are very satisfactory, with an average error between calculated and observed daily water levels and discharges lower than of 15% in all stations. Moreover, the Nash-Sutcliffe coefficients obtained (0.86 to 0.92 in the principal registration stations, and 0.56 to 0.61 in others stations) indicate an adequate model performance. From the results of the analyzed periods, it can be indicated that the higher deposits were observed in cells corresponding to lagoon areas in which the flow velocity was very low, and also in cells where the floodplain widened. Practically no deposition occurred in the main stream. The simulation results for all observed floods show that average annual incoming sediment load were 76.7 × 10⁶ t/yr. The annual average deposition over the entire domain (floodplain-channel system) varied from 10.2 × 10⁶ to 17.5 × 10⁶ t/yr and, thus, the entire domain retained between 13% and 23% of the incoming sediments. The amount of sediment deposited on the floodplain varied from 3.4 × 10⁶ to 4.4 × 10⁶ t/yr, representing a retention of 4.5% to 5.7%. Such deposits induces an increase in floodplain bed levels of the order of 0.3 to 0.4 mm/yr. The present results constitute an important advance in the knowledge of sedimentation processes in the reach.

References

- Basile, P.A., Riccardi, G.A., Garcia, M.L., and Stenta, H.R. (2007). Quasi-2D modeling of hydro-sedimentological processes in large lowland river-floodplain systems. Workshop on Morphodynamics Processes in Large Lowland Rivers, National Center for Earth-Surface Dynamics (USA) and National University of Litoral, Cayastá, 3 p. Santa Fe, Argentina.
- Garcia, M.L., Basile, P.A. and Riccardi, G.A. (2015). Modelling extraordinary floods and sedimentological processes in a large channel-floodplain system of the Lower Paraná River (Argentina). *International Journal of Sediment Research*, 30 (2): 150-159.
- Riccardi, G.A. (2000). A quasi-2D hydrologic-hydraulic multilayer simulation system for rural and urban environments. Doctoral thesis, Faculty of Exact, Physical and Natural Sciences, National University of Córdoba, Argentina (in Spanish).

Assessing rheological properties of fluid mud samples through tuning fork data

Fonseca Diego¹, Juliane Carneiro¹, Patrícia Marroig¹, Marcos Gallo¹ and Susana Vinzon¹

¹ Cohesive Sediments Dynamics Laboratory
Federal University of Rio de Janeiro, CT 203 PO Box 68508 Rio de Janeiro, Brazil
E-mail: diegoluz@poli.ufrj.br

Muddy bottoms in ports and navigation channels are usually associated with draft restrictions. However, part of the muddy layers can be used for navigation, following the concept of nautical bottom. At this approach, “the level where physical characteristics of the bottom reach a critical limit beyond which contact with a ship's keel causes effects on controllability and manoeuvrability” is stated as the depth reference (McBride et al., 2014). This critical limit is associated with changes in the rheological properties of the mud and is typically referred to as the rheological transition of the mud. Although suitable rheological tests can be performed in the laboratory, it is still difficult to generate rheological profiles in situ. Thus, these properties are usually correlated with more easily measured properties, e.g., density (Carneiro et al., 2017).

One widespread method for in situ density determination is the use of a vibrating-fork density probe (densitometer). It consists of a drop probe with a depth sensor and a tuning fork on its far end which is forced to vibrate at a particular frequency that leads to a phase shift between input and output signals applied and received by piezoelectric elements (Groposo et al., 2014). From amplitude and frequency data, the equipment can calculate the density of the fluid it is in contact with. However, the relationship between frequency and amplitude data and density values is not unique for every mud sample, as it depends on the elasticity and viscosity of the mud and also its strain state (Groposo et al., 2014). Thus, a calibration is required for a correct calculation of the mud density at a given location. Nevertheless, once a calibration is performed with a local representative sample, viscosity and elasticity become only functions of the density of the mud (and not of its composition – e.g. grain size, organic matter etc).

Therefore, the shape of the calibration domain (frequency, amplitude, density) will necessarily be conditioned by the rheology of the mud and it will be as different as the flow properties are. In order to understand these relations between rheological properties and the densitometer calibration domain, this study tested and compared mud samples from different locations in Brazil. Each sample was employed at the densitometer calibration procedure and also submitted to rheological tests.

For the densitometer calibration, the frequency & amplitude clusters of each measurement were processed, following the procedure proposed by Fonseca et al. (2016). The authors established an algorithm for density calculation based on a calibration procedure and the resulting density profiles were compared to the ones obtained with the standard equipment software. For the rheological tests, a Rheolab-QC rheometer was employed and tests followed an adaptation of the protocol proposed by Claeys et al. (2015) as explained in Carneiro et al. (2017).

Figure 1 presents two domains obtained with the densitometer calibration procedure for the Port of Santos (left) and for the Amazon South Bar (right). The mud from Santos was so hard to stir after 1300kg/m³ that tests could not be performed far beyond this value whereas values up to 1500kg/m³ could be tested for the Amazon samples. The shapes of these domains are highly different, suggesting great differences at the rheological properties of each sample. The Amazon's domain presents a thinner shape for densities from 1200 until 1000kg/m³ (upper part of the domain). This suggests that the mud from the Amazon behaves more like water (low viscosity and yield stress) at this whole range of density.

As the amplitude signal decreases for increasing thickness of the mud (Groposo et al., 2014), it can be inferred that the mud from Santos will present higher viscosities at a given density, as its viscous amplitude values are smaller than those for the Amazon's domain. Figure 2 presents Bingham yield stress versus density curves assessed with the rheometer for these two locations. Indeed, these curves are in agreement to the observations based only in the shape of the domains (Figure 1). Similar yield stresses are obtained once densities of similar viscous amplitude values (the left edge of the domains (Fonseca et al., 2016)) are compared for both locations (e.g. around 500Pa yield stress for 1300kg/m³ at the Port of Santos while for 1510kg/m³ at the Amazon South Bar both at a 2V amplitude value).

Therefore, it can be concluded that there is a relationship between rheology and the densitometer calibration domains, which can allow a quick rheological assessment even if a rheometer is not available. For this, a numerical relation between yield stress and amplitude based in a wider range of locations was also investigated.

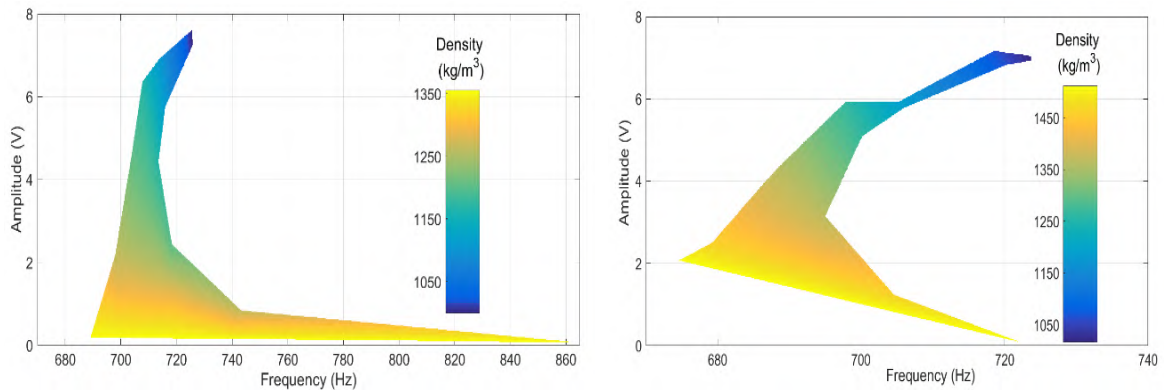


Fig. 1. Representation of the domains of calibration generated at this study for mud collected in Brazil. Colour bars indicating the density at a given frequency and amplitude point for the range tested: until 1350kg/m³ for the Port of Santos (left) while until 1510kg/m³ for the Amazon South Bar (right).

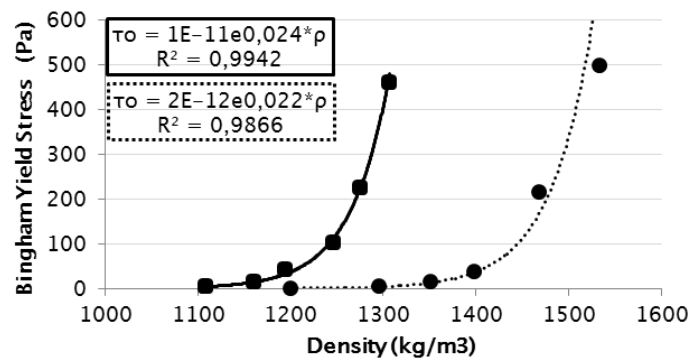


Fig. 2. Bingham yield stress versus density for the sample from the Port of Santos (straight line with ■ markers) and for that from the Amazon South Bar (dashed line with ● markers). Equations for the exponential trend adjustments are stated in the legend at boxes following the line pattern of the data.

References

- Carneiro, J. C., Fonseca, D. L., Vinzon, S., B., Gallo, M. N (2017). Strategies for Measuring Fluid Mud Layers and Their Rheological Properties in Ports. *Journal of Waterway, Port, Coastal and Ocean Engineering*. 10.1061/(ASCE)WW.1943-5460.
- Claeys, S., Staelens, P., Vanlede, J., Heredia, M., Van Hoestenbergh, T., Van Oyen T. and Toorman, E. (2015). A rheological lab measurement protocol for cohesive sediment. Proc., 13th International Conference on Cohesive Sediments (INTERCOH), Leuven, Belgium, 20–21.
- Fonseca, D.; Marroig, P.; Carneiro, J.; Vieira, F.; Molinas, E. and Vinzon, S. (2016). Assessing density profiles for nautical bottom approach. Proc., IX PIANC-COPEDEC, 2016, Rio de Janeiro, Brazil.
- Groposo, V.; Mosquera, R.; Pedocchi, F.; Vinzón, S. and Gallo, M. (2014). Mud density prospection using a tuning fork. *Journal of Waterway, Port, Coastal, Ocean Engineering*, 10.1061/(ASCE)WW.1943-5460.0000289, 04014047.
- McBride, M. et al. (2014). Harbour approach channels –Design guidelines. PIANC Report N°. 121. World Association for Waterborne Transport Infrastructure, Brussels, Belgium.

Characterization of bottom sediments in the Río de la Plata estuary

Moreira Diego and Claudia Simionato¹

¹ Centro de Investigaciones del Mar y la Atmósfera (CONICET-UBA); Instituto Franco-Argentino para el Estudio del Clima y sus Impactos (UMI IFAECI/CNRS-CONICET-UBA); Departamento de Ciencias de la Atmósfera y los Océanos (FCEN-UBA). Intendente Güiraldes 2160 - Ciudad Universitaria - Pabellón II - 2do. piso, (C1428EGA) Buenos Aires - Argentina. E-mail: moreira@cima.fcen.uba.ar

Abstract

Draining the second largest basin of South America, the Río de la Plata (RdP) is one of the largest and most turbid estuaries of the world. Its fresh water plume impacts the properties of the shelf for more than 500 km. The sediments' load that reach the system mainly come from the Paraná river (in its two main branches, Paraná de las Palmas and Paraná Guazú), and has been between 80 and 160 Mtons^y¹ (Urien 1972, Menéndez and Sarubbi, 2007). From that total, 10% correspond to bed load (sand and silt) and 90% to suspended matter (fine silt and clay). The deposits go from sand on the upper estuary and silts in the intermediate estuary, to clay and silts in its exterior part. In the area of the salt wedge, where the river waters meet the sea waters, the flocculation of suspended sediments occurs and, therefore, a zone of maximum turbidity occurs. Turbulence over the bottom, due to tidal currents, waves or winds, can be strong enough to mix and homogenize the water column, and resuspend the sediments. The aim of this work is to characterize the bottom surficial sediments mean distribution and to study their composition including the organic matter and water contents, to obtain a qualitative description of the mean transports.

Introduction

The RdP (Figure 1) is one of the most turbid estuaries in the world, with extreme concentrations more than 400mg^l⁻¹. The amount of sediments transported by the RdP represent more than 1% of the global input of suspended sediments that reach the oceans in the entire world, between 15,000 and 20,000 Mtony¹. It has been estimated that 90% of the sediments that reach the RdP as suspended sediments are silts and clays; the rest correspond to very fine sands. Besides its geographical extension, the RdP has large social, ecological and economic importance for the countries along its shores, Argentina and Uruguay. Parker *et al.* (1987) made an interpretation of the grain size observations available at that time and a synthesis of various geological and oceanographic arguments to develop a first hypothesis for the processes associated to the sediments transport and dispersion in the estuary.

Study area

The RdP is located on the eastern coast of southern South America at approximately 35°S, is one of the largest estuaries in the world. It has a northwest to southeast oriented funnel shape approximately 300km long, which narrows from 220km at its mouth to 40km at its upper end. The estuarine area is 35,000km² and the fluvial drainage area is 3.1×10⁶ km².

Data and methods

The bottom sediments samples analyzed in this work were collected between 2009 and 2010, in the frame of the FREPLATA/FFEM Experiment, funded by the French Fund for the Global Environment (FFEM). Six oceanographic synoptic cruises every approximately 2 months were made during the Experiment. Cruises lasted 2 to 3 days and visited the 26 sites shown as black dots in Figure 1. We analyze the grain size distribution, water and organic matter contents from the bottom sediments.

Statistical methods applied

For every sample, the mean grain size, μ , standard deviation, σ , and skewness, Sk , were calculated using the statistic moment method. We also computed the degree of sorting, defined as the ratio between the standard deviation and mean grain size (Skene *et al.*, 2005). The sediments were classified according to Shepard (1954). We applied the Principal Components Analysis (PCA, Preisendorfer, 1988) to analyze the large number (5×26=130) of different CILAS grain size histograms obtained from the 5 different samples (cruises 2 to 6) collected at each stations.

Results

Mean distribution of bottom sediments and water and organic matter contents

The mean percentage and standard deviation between samples of sand (grain sizes between 62.5 and 250 μ m), silt (grain sizes between 3.9 and 62.5 μ m) and clay (grain sizes less than 3.9 μ m, in the Wentworth scale classification), are shown in the upper left and central panels, upper right and lower right panels, and lower left and central panel of Figure 1, respectively. The mean percentage concentration and standard deviation between samples of the water contents and organic matter contents resemble those of the clay, suggesting that they could reflect in some extent the effective porosity, related in turn to the degree of compaction, of bottom sediments.

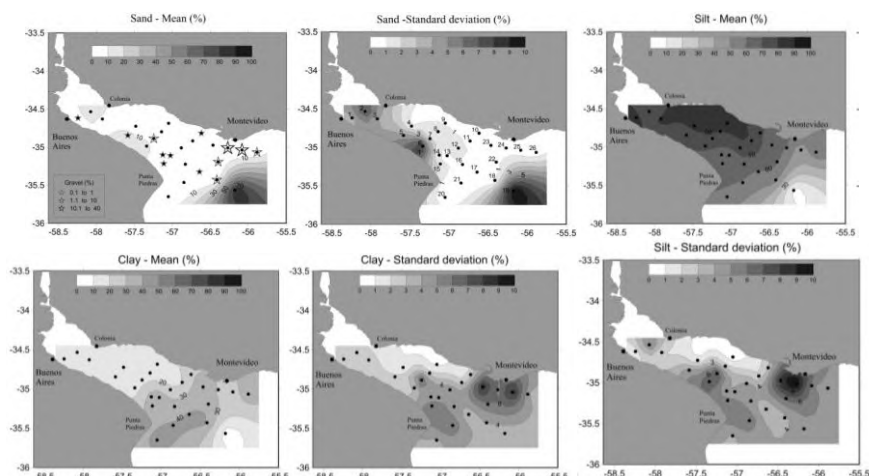


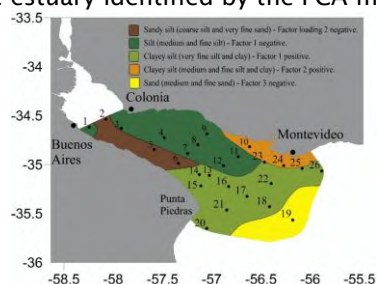
Figure 1. Mean and standard deviation between samples of the percentage concentration of sand (upper left and centre panel), silt (right upper and lower panel) and clay (lower left and centre panel). Stars in the upper left panel represent the mean percentage of gravel.

Sediment's distribution according to Shepard's classification

The Shepard scheme shows that sediments classified as "sand" are only present in the site located at the exterior RdP, and does not seem to have the same origin than the sediments observed in the rest of the estuary. "Sandy silt" is observed in the Argentinean coast of the upper and intermediate estuary. Sediments classified as "silt" are observed in the northern intermediate estuary, over and downstream the Ortiz Bank and close to Buenos Aires harbor. Sediments classified as "clayey silt" are present over and seawards Barra del Indio shoal.

Principal components analysis of the bottom sediments distribution

Results have been summarized in Figure, which schematically displays the five different regions of the estuary identified by the PCA method.



Conclusion

Results show that the bottom sediments have a gradational arrangement of textures as they are transported seawards, from dominant sand at the head, silt in the intermediate estuary and clayey silt and clay at its mouth. The distributions of water and organic matter contents resemble those of the clay, suggesting that they could reflect in some extent the degree of compaction of bottom sediments. Coarse deposits (carbonated shell) are more abundant in the northern sector of the exterior estuary, close to Montevideo, and a lower percentage is observed to the northwest of Punta Piedras. Along the Northern coast of the intermediate RdP, medium and fine silt predominates, whereas in the Southern coast, coarser sand and silt prevails. This could be due to differences in tidal currents and/or to differences in the riverine water pathways along both coasts depending on their source. Around Barra del Indio shoal, clay prevails over silt and sand, and the water and organic matter contents reach a maximum. Physicochemical flocculation processes probably become important there, and the width and the depth of the estuary also largely increase, producing a significant reduction of the currents. Immediately seawards the salt wedge, coarser sand dominates. This sand is much coarser than the sediment transported by the RdP tributaries, suggesting that it comes from the adjacent shelf. Between the Santa Lucía River mouth and Montevideo, a different type of sediment is observed consisting fine silt and clay; they seem to be relict sediments.

Reference

- Menéndez, A.N. and Sarubbi, A. (2007). A Model to Predict the Paraná Delta Front Advancement, Workshop on Morphodynamic Processes in Large Lowland Rivers, (Santa Fe, Argentina), pp. 25.
- Parker, G.; Cavalloto, J.L.; Marcolini, S., and Violante, R. (1986b). Transporte y dispersión de los sedimentos actuales del Río de la Plata (análisis de texturas). Proceedings of the 1er Reunión de Sedimentología (La Plata, Argentina), pp. 38-41.
- Preisendorfer, R.W. (1988). Principal Component Analysis in Meteorology and Oceanography. Amsterdam: Elsevier, 425p.
- Skene, D.; Ryan, D.; Brooke, B.; Smith, J., and Radke, L. (2005). The Geomorphology and Sediments of Cockburn Sound. Geoscience Australia, Record 2005/10, pp. 90.
- Urien, C.M. (1972). Río de la Plata Estuary environments. Geological Society of America Memoirs, 133, 213-234.

On the processes that determine the fine sediments transport in the Rio de la Plata estuary

Moreira Diego and Claudia Simionato¹

¹ Departamento de Ciencias de la Atmósfera y los Océanos (FCEN-UBA); Centro de Investigaciones del Mar y la Atmósfera (CONICET-UBA); Instituto Franco-Argentino para el Estudio del Clima y sus Impactos (UMI IFAECI/CNRS-CONICET-UBA). Intendente Güiraldes 2160 - Ciudad Universitaria - Pabellón II - 2do. piso, (C1428EGA) Buenos Aires - Argentina. e-mail: moreira@cima.fcen.uba.ar

Abstract

Numerical models are excellent tools for conducting process studies and testing hypotheses based on observations. They constitute a 'laboratory' in which the forcing can be set 'on' or 'off', or even the environmental conditions can be modified. The Rio de la Plata (RdP, Figure 1) is one of the most turbid estuaries in the world and the one most important in terms of continental discharge and drainage area. Observations of suspended fine sediments, particularly those remote and *in situ* collected on recent studies, have driven to the statement of several hypotheses about the processes that would determine the concentration of suspended sediments in the different parts of the estuary. Nevertheless, the relative scarcity of data do not allow to demonstrate the validity of those hypothesis and the role of several physical processes and of the morphology remain unknown. The objective of this work is, therefore, to analyze the role of the different forcings and the environmental conditions in the determination of the distribution of suspended fine sediments in the RdP applying processes oriented numerical simulations.

Introduction

The RdP is one of the most turbid estuaries in the world, with extreme concentrations of more than 400mg l⁻¹. The amount of sediments transported has been estimated between 80 and 160 Mtons y⁻¹ (Urien 1972, Menéndez and Sarubbi, 2007), representing more than 1% of the global input of suspended sediments that reach the oceans in the entire world. It has been estimated that 90% of the suspended sediments that reach the RdP are silts and clays, the rest correspond to fine sands.

Study area

The RdP, located on the eastern coast of southern South America at approximately 35°S, is one of the largest estuaries in the world. It has a northwest to southeast oriented funnel shape approximately 300km long, which narrows from 220km at its mouth to 40km at its upper end. The estuarine area is 35,000km² and the fluvial drainage area is 3.1×10⁶ km². The RdP displays a complex geometry and bathymetry, and drains the waters of the Paraná and Uruguay rivers, which constitute the second largest basin of South America, after the Amazon. It exhibits a very high discharge of 22,500m³s⁻¹ on average, and extremes peak from 90,000m³s⁻¹ to 8,000m³s⁻¹. The Paraná River converges to the estuary in two main branches (Paraná Guazú-Bravo and Paraná de las Palmas) after forming the large Paraná Delta. Considering the orientation and the relative low depth (less than 10 m), only the continental waves from the southeast can reach the interior, and they are dampen and break as they propagate inward (Dragani and Romero, 2004).

Model and simulations description

MARS (Model for Applications at Regional Scale, Lazure and Dumas, 2008) is a hydrodynamic model for coastal regions, bays, estuaries, adjacent shelf and open ocean, applied for modelling processes at time scales that range from hours to decades. MARS code solves the primitive equations of an incompressible fluid, with the assumption of hydrostatic balance and the Boussinesq approximation. It is based on traditional finite differences on an Arakawa C grid (vertical and horizontal). The vertical coordinate used is of generalized sigma-type. The sediment dynamics module includes processes of erosion, transport in suspension and simultaneous deposition of different types of sedimentological particles: gravel, sand and mud. The sediment settling velocity is expressed as a function of sediment concentration to take into account the flocculation processes (Le Hir *et al.*, 2000). Wind waves are considered and generated locally from wind data.

Results

Sensitivity studies to the different forcings

A set of process oriented numerical simulations was performed to analyze the effect of the different forcings (runoff, tides, winds and wind waves) on the sedimentological process in the RdP. The bottom erosion parameter E_0 was set to 0.0001kgm⁻²s⁻¹. Simulations were run for an equivalent to two years. To favour the inter-comparison between the different cases, results are presented for the average of the hourly numerical solutions obtained over the last year.

Case 1: Simulation forced by continental discharge alone

Results show that after the period of simulation, silts are almost entirely deposited in the upper region of the estuary, close to the tributaries, where they are discharged. The surface concentration

maximizes at the mouth of the Paraná de las Palmas and Parana Guazú-Bravo tributary rivers. In the upper estuary, suspended sediments in the bottom layer display a distribution similar to that of the surface layer, but with higher concentrations at the mouth of the tributaries. The plumes extend more over the intermediate and exterior estuary, along the southern coast.

Cases 2: Simulations forced with continental discharge and tide

Tides play an important role in the distribution of suspended sediment in the RdP due the relatively high associated currents. Both clays and silts are transported by a much larger distance during the same period than in the case without tides, reaching the exterior estuary. This is due to both the increment in the currents, which inhibits the deposition of sediments and re-suspend them, and to the lateral mixing (or stirring) associated with the tide. Concentrations decrease towards the exterior estuary and over the Barra del Indio region a large gradient is observed. A relative maximum is observed in the proximity of Punta Rasa. Sediments at the bottom layer show a distribution similar to those at the surface.

Cases 3: Simulations forced with continental discharge, tides and winds

The distribution of the concentration of suspended silts at the surface layer is similar to that of the case without winds. Over the entire estuary, the wind increases the dynamics of the system, maintaining the sediments suspended for a longer period of time and exporting them, in part, to the Continental Shelf.

Case 4: Simulation forced with continental discharge, tides, winds and waves

Results of the simulation in which wind waves are included, are shown in Figure 1. The upper left (right) panel shows the distribution of the concentration of suspended silts (clays) averaged over one year of simulation. The maximum concentration of suspended sediments at the surface layer occurs to the south of Punta Piedras. At the upper and intermediate RdP a marked gradient perpendicular to the estuary axis is observed, with higher values along the southern coast. Over the Barra del Indio shoal, a gradient parallel to the estuary axis occurs, with concentrations decreasing offshore. This distribution well resembles what is obtained from observations.

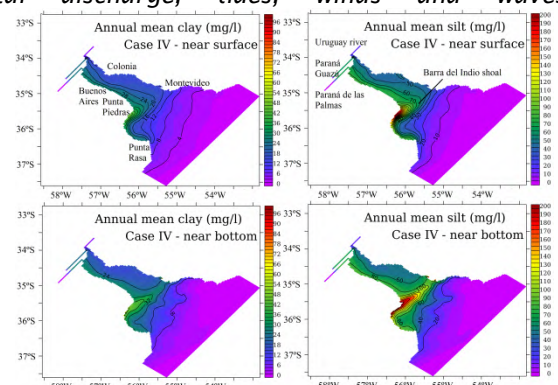


Figure 1. Suspended clay (left) and silt (right) near surface (upper) and near bottom (lower) from Case IV.

Conclusions

The distribution of suspended sediments in the RdP presents two different regions with well-marked gradients: (i) one at the upper and intermediate estuary, which is perpendicular to the estuary axis, with higher concentrations along the Argentine coast and, (ii) the second is parallel to the axis of the estuary and occurs in the exterior RdP, where the concentration of suspended sediment decreases abruptly downstream of the Barra del Indio Shoal. The largest amount of sediments is brought to the system by the Paraná River (through Guazú-Bravo and Parana de las Palmas branches), whereas the Uruguay River has a much lower sediment discharge. Tidal waves come from the southeast and propagate as Kelvin waves along the Argentine coast first and then along the Uruguayan, dissipating their energy by bottom friction along that path. Those characteristics contribute to the increase of suspended sediments concentration on the southern coast, generating the gradient observed in the interior. After the sediments are spilled into the RdP from the tributaries, the currents speeds are strongly reduced and, consequently, the different textures are gradually deposited according to their size and fall velocities. The flocculation processes that occur in the salinity front contribute, together with the decrease in the velocity of the currents as the RdP widen and the gravitational circulation associated to the estuary, in the decrease of the concentration and its respective gradient, in the exterior zone.

References

Dragani, W. C. and Romero, S. I. (2004). Impact of a possible local wind change on the wave climate in the upper Río de la Plata. *International Journal of Climatology*, 24(9), 1149-1157.

Lazure, P. and Dumas, F. (2008). An external-internal mode coupling for a 3D hydrodynamical model for applications at regional scale (MARS). *Advances in Water Resources*, Volume 31, Issue 2, February 2008, Pages 233-250.

Le Hir, P., Bassoullet, P., and Jestin, H. (2000). Application of the continuous modeling concept to simulate high-concentration suspended sediment in a macrotidal estuary. *Proceedings in Marine Science*, Elsevier, 229-247, 2000.

Menéndez, A.N. and Sarubbi, A. (2007). A Model to Predict the Paraná Delta Front Advancement, *Workshop on Morphodynamic Processes in Large Lowland Rivers*, (Santa Fe, Argentina), pp. 25.

Urien, C.M. (1972). Río de la Plata Estuary environments. *Geol. Soc. of America Mem.*, 133, 213-234.

Estuarine morphodynamic adaptation to sediment supply and human activities: a case study of turbidity maximum

Chunyan Zhu^{1,2}, Leicheng Guo¹, Bo Tian¹, Qing He¹, Zheng Bing Wang^{2,3}

¹ State Key Lab of Estuarine and Coastal Research, East China Normal University, Shanghai 200062, China, E-mail: C.Zhu@tudelft.nl

² Faculty of Civil Engineering and Geosciences, Delft University of Technology, Delft, the Netherlands

³ Deltares, Delft, the Netherlands

Abstract

Estuarine morphodynamics undergo significant changes due to declined sediment supply from river, rising sea-level, and human interferences (Syvitski and Saito, 2007; Syvitski et al., 2009). The Yangtze Estuary is such a case whose decadal morphodynamic evolution was broadly examined. It was documented that the subaqueous delta shifted from deposition to erosion since the early 2000s due to sediment supply reduction after the Three Gorges Dam (Yang et al., 2015) while some others reported that the estuary mouth bar area sustains accretion until 2010 (Luan et al., 2016; Zhu et al., 2016). The mouth bar area of the Yangtze Estuary is where the turbidity maximum exists. To clarify the morphodynamic changes therein, we examine the two large scale shoals, i.e. the Hengsha flat and the Jiuduan shoal, based on bathymetric data between 1958 and 2016 and satellite images since 1985.

Bathymetric data were digitized and converted to the same datum-the Theoretically Lowest Water Level (TLWL). Note that the landward part of the Hengsha flat was embanked since 2003 and the super-tidal flats of the Jiuduan shoal were vegetated (Fig. 1), thus bathymetric monitoring and data are lacking in these two regions. Satellite images of the mouth bar area from Landsat are also collected to identify the boundary between bare flat and saltmarsh. The Normalized Difference Vegetation Index (NDVI) can reflect the green vegetation, specifically, positive NDVIs indicate intertidal forested wetlands and intertidal marshes with vegetation. In this study, a threshold of 0.1 ($NDVI > 0.1$) is chosen to calculate the vegetated area in each image to differentiate between vegetation and non-vegetation.

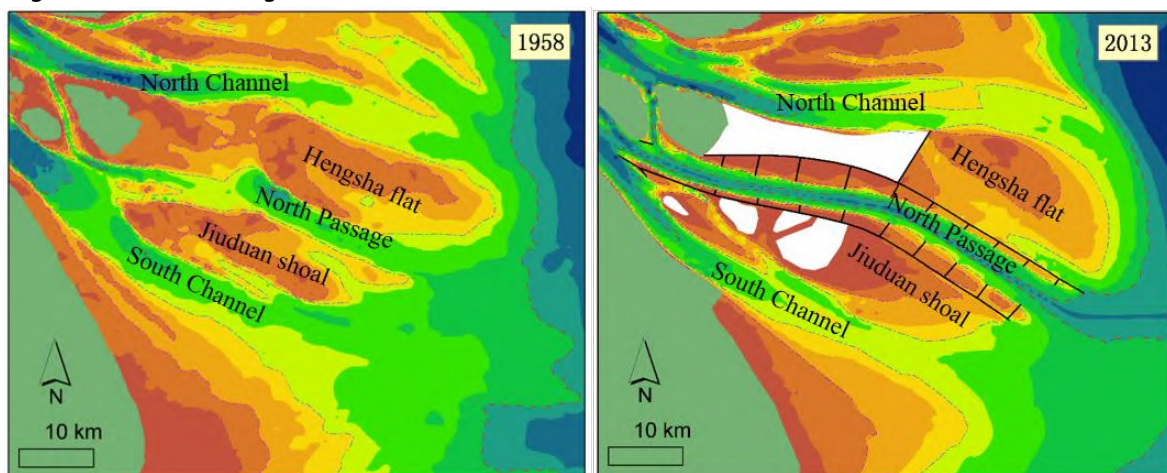


Fig. 1. Bathymetric changes with 2, 5, and 10m isobaths of the Jiuduan shoal and the Hengsha flat in 1958 and 2013. The white area was the reclaimed region in the landward part of the Hengsha flat and the vegetated super-tidal flats of the Jiuduan shoal.

We detect the morphodynamic changes of the two shoals in terms of deposition rate, hypsometry profile and saltmarsh area. Although the Hengsha flat and the Jiuduan shoal were continuously accreting prior 2010, the morphodynamic changes of these two shoals are both to a large extent influenced by human activities. In the pre-1997 period when local human activities are rare, the Jiuduan shoal accreted enormously since its isolation from the Hengsha flat while the Hengsha flat grew at a smaller rate. Since 1997, dredging and dumping activities and saltmarsh growth stimulate the growth of the Hengsha flat. However, dredging and dumping activities slow down the

development of the Jiuduan shoal and caused strong erosion in the region off the North Passage. In summary, it suggests a transition from natural morphodynamic evolution processes prior 1997 to afterwards human-driven morphodynamic adaptation.

Further, we found the accretion of the two shoals vanishes since 2010, even changes to slight erosion (Fig. 2). We argue that the upper 600-km long reaches and the region off the North Passage can supply sediment to the mouth bar area, contributing to the former accretion of the two shoals. In addition, the nearshore mud deposition belt should be taken as one of sediment sources (Liu et al., 2010). Since the erosion found off the North Passage is mainly caused by dredging activities in the North Passage, regional human activities are expected to slow down the response time of global changes. However, the reduced riverine sediment supply tends to slow down shoal accretion and initiate large scale erosion in the long term. As a result, erosion of the two shoals in recent decades is found in this study. From the evidence of erosion, we propose that the morphodynamic adaptations of the shoals lag behind the changes of the sediment load at a time scale of 10~100 years.

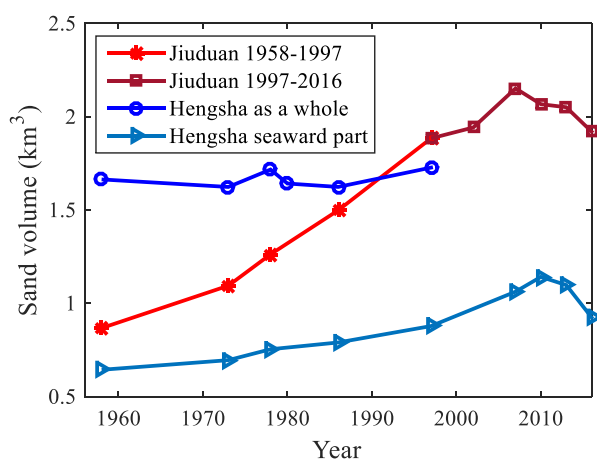


Fig. 2. Temporal sand volume (the sand volume of the flat with flat elevation <6 m) changes of the Jiuduan shoal and Hengsha flat between 1958 and 2016.

In conclusion, the two shoals in the mouth bar area of the Yangtze Estuary are influenced by complex forcing as well as strong human activities. This study deals with morphodynamic evolution of the two shoals in 60 years. The results are different from previous studies with near-instantaneous estuarine erosion. More specifically, morphology in the mouth bar area has >10 years response time for upstream sediment decline. Additionally, regional human activities play a role in buffering its response through sediment redistribution within the estuary. Such understanding of its natural behaviour and the response to human activities could also be used for research on turbidity maximum and practical projects in other highly-regulated estuaries.

Reference

- Liu H, He Q, Wang ZB, Weltje GJ, Zhang J. (2010). Dynamics and spatial variability of near-bottom sediment exchange in the Yangtze Estuary, China. *Estuarine Coastal and Shelf Science* 86: 322-330.
- Luan HL, Ding PX, Wang ZB, Ge JZ, Yang SL. (2016). Decadal morphological evolution of the Yangtze Estuary in response to river input changes and estuarine engineering projects. *Geomorphology* 265: 12-23.
- Syvitski JPM, Saito Y. (2007). Morphodynamics of deltas under the influence of humans. *Global and Planetary Change* 57: 261-282.
- Syvitski, J. P., Kettner, A. J., Overeem, I., Hutton, E. W., Hannon, M. T., Brakenridge, G. R., & Nicholls, R. J. (2009). Sinking deltas due to human activities. *Nature Geoscience*, 2(10), 681-686.
- Yang SL, Xu KH, Milliman JD, Yang HF, Wu CS. (2015). Decline of Yangtze River water and sediment discharge: Impact from natural and anthropogenic changes. *Sci Rep* 5: 12581.
- Zhu L, He Q, Shen J, Wang Y. (2016). The influence of human activities on morphodynamics and alteration of sediment source and sink in the Changjiang Estuary. *Geomorphology* 273: 52-62.

Turbulence and flocculation in an estuarine tidal channel

Figuerola Steven M., Guan-hong Lee, and Ho Kyung Ha

Department of Oceanography, Inha University, 100 Inharo, Incheon, 22212, South Korea
E-mail: stevenmiquelfiguerola@gmail.com

Introduction

The spatial and temporal variability of flocculation and turbulence in estuaries is a relatively new area of research because instruments to make accurate measurements have only recently been developed. Laboratory studies, such as Milligan and Hill (1998) and Verney *et al.* (2011), have demonstrated that floc size is affected by suspended sediment concentration and turbulence. Field deployments of floc cameras in estuarine turbidity maxima and on intertidal mudflats (Manning, 2004) have provided insights into temporal relationships of floc size, concentration, and turbulence. However, high resolution vertical measurements of these relationships in the bottom boundary layer and water column of estuaries, such as provided by Wang *et al.* (2013), are rare. The objective of this study is to better understand the spatial and temporal relationships between floc size, suspended sediment concentration, and turbulence in a tidal channel. Furthermore, the relationship between floc size and sediment flux is considered.

Materials and methods

Simultaneous bottom mooring and ship-borne casting were conducted for two tidal cycles in summer 2016 in a channel near the head of the macrotidal Geum Estuary, South Korea. The mooring consisted of a downward oriented Aquadopp-HR and an upward oriented Signature1000 that measured the current profile, including the bottom boundary layer. Their fast sampling rates allowed for Reynolds decomposition of the flow

$$u = \bar{u} + u' \quad (1)$$

where the instantaneous along-channel velocity, u , is the sum of a steady term, \bar{u} , and a fluctuating term, u' . The fluctuating terms were then used to estimate vertical profiles of turbulent stresses per fluid mass as well as turbulent kinetic energy (TKE) per fluid mass, E ,

$$E = (\overline{u'^2} + \overline{v'^2} + \overline{w'^2}) / 2 \quad (2)$$

where v' and w' are the fluctuating terms of the across-channel and upward velocities, respectively, and overbars denote burst averaging. Spectral analysis of the velocity components in the frequency domain provided estimates of TKE dissipation rate per fluid mass, which was then used to estimate the microscales of the flow. The ship-borne casting adjacent to the mooring allowed estimation of the gradient Richardson number to evaluate the effect of water column density stratification on turbulence, and profiles of floc size distributions by volume concentration were measured by laser in-situ scattering and transmissometry (LISST). In addition, water samples were filtered to calibrate casted optical backscatter sensor (OBS) turbidity measurements to compare suspended sediment mass concentration with floc size as well as to characterize the timing of flocculation with sediment flux in the channel.

Results

Surface currents achieving 0.9ms^{-1} were observed during the flood phase. TKE was concentrated in the bottom boundary layer and was greatest during the flood acceleration at 0.1Jkg^{-1} . Turbulence resuspended sediment from the channel bed and diffused them upward, increasing the concentration in the water column more than an order of magnitude, from 0.02kgm^{-3} to 0.40kgm^{-3} . The concentrated suspension at this time fully absorbed the LISST laser and prevented measurement, however measurements before and after revealed median floc sizes of $250\mu\text{m}$ breaking up in the turbulent and concentrated conditions down to a nearly homogenous suspension of $50\mu\text{m}$ median floc size, which subsequently rapidly flocculated to median size of $250\mu\text{m}$ in the surface water over a two hour period as the suspended sediment concentration and TKE abated. The greatest sediment flux occurred during the flood phase, and was followed by relatively less turbulent and more dilute conditions during ebb, which maintained median floc sizes greater than $250\mu\text{m}$ even during peak flow. A following tidal cycle exhibited a similar trend, and cumulative landward flux of sediment was observed. Both flocculation and turbulence in the tidal channel were characterized by tidal asymmetry, where a short, fast flood current was followed by a relatively long lasting high tide slack. The trend in top-to-bottom salinity difference also provided evidence that tidal asymmetry was being enhanced by the process of strain-induced periodic stratification, which occurred semi-diurnally during ebb phases. Ebb stratification reduced vertical turbulent mixing of

the water column, resulting in lesser eddy viscosity and greater vertical shear of along channel velocity. While the ebb stratification reduced TKE and promoted flocculation, the flocculated suspended sediments in the channel were trapped above a halocline, below which the stabilizing effect of the vertical density gradient exceeded the destabilizing effect of the vertical velocity gradient, represented by the gradient Richardson number.

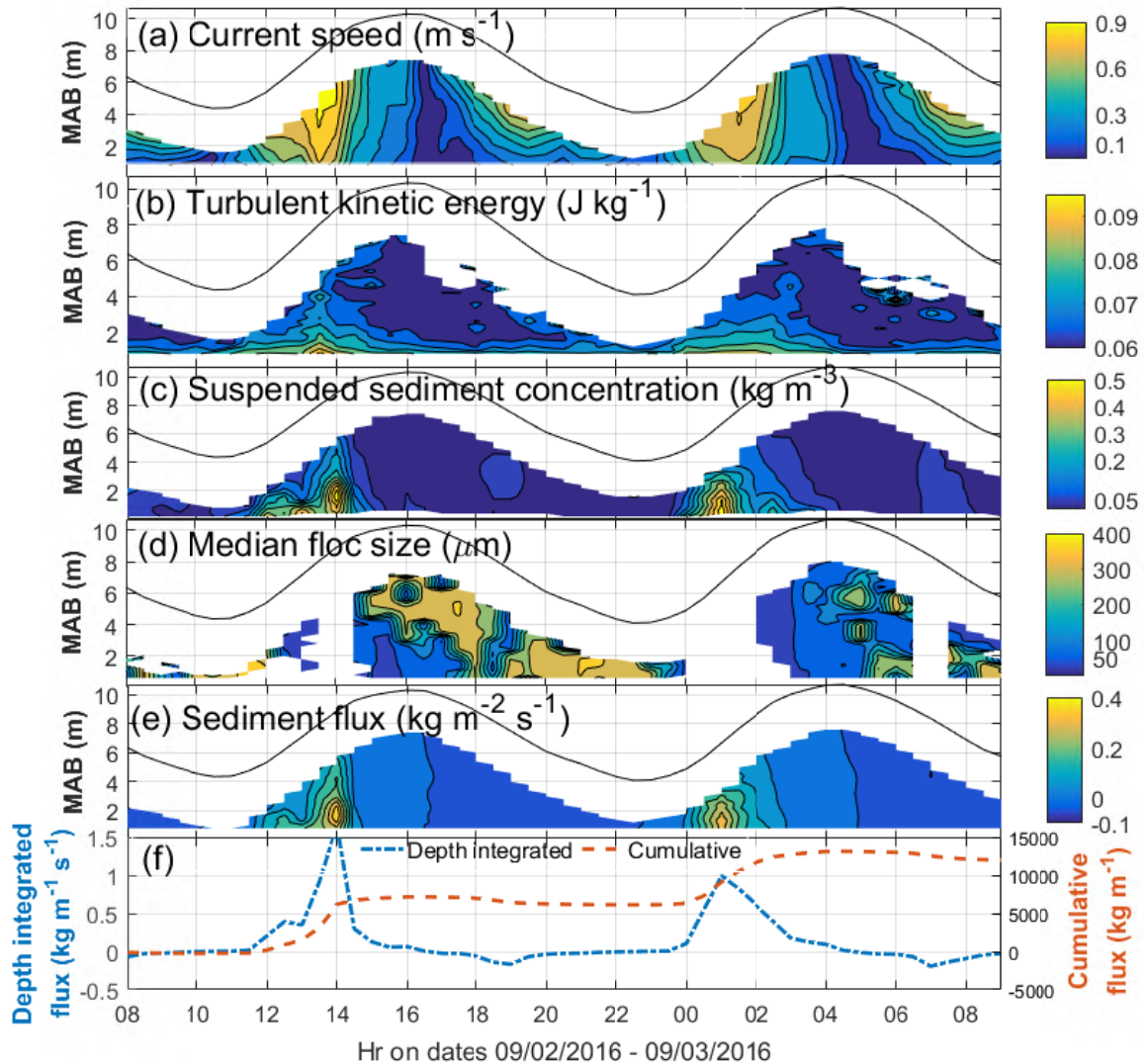


Fig. 1. Spatiotemporal variability of turbulence and flocculation in a tidal channel obtained by simultaneous mooring and ship-borne casting: (a) current speed (m s^{-1}), (b) turbulent kinetic energy per fluid mass (J kg^{-1}), (c) suspended sediment concentration (kg m^{-3}), (d) median floc size (μm), (e) sediment flux ($\text{kg m}^{-2} \text{s}^{-1}$), and (f) the depth integrated sediment flux (dash-dot line, $\text{kg m}^{-1} \text{s}^{-1}$) and cumulative sediment flux (dotted line, kg m^{-1}). Positive fluxes are directed landward. MAB is meters above the bed.

References

- Manning A.J. (2004). Observations of the properties of flocculated cohesive sediment in three western European estuaries. *Journal of Coastal Research*, SI41:70-81.
- Milligan T.G. and P.S. Hill. (1998). A laboratory assessment of the relative importance of turbulence, particle composition, and concentration in limiting maximal floc size and settling behaviour. *Journal of Sea Research*, 39(3):227-241.
- Verney R., R. Lafite, J.C. Brun-Cottan and P. Le Hir. (2011). Behaviour of a floc population during a tidal cycle: laboratory experiments and numerical modelling. *Continental Shelf Research*, 31(10):S64-S83.
- Wang Y.P., G. Voulgaris, Y. Li, Y. Yang, J. Gao, J. Chen, and S. Gao. (2013). Sediment resuspension, flocculation, and settling in a macrotidal estuary. *Journal of Geophysical Research: Oceans*, 118(10):5591-5608.

Disturbance of cohesive sediment dynamics in the world's largest tidal power plant: Lake Sihwa, South Korea

Ho Kyung Ha, Jong-wook Kim and Seung-Buhm Woo

Department of Ocean Sciences, College of Natural Sciences
Inha University, Incheon 22212, South Korea
E-mail: hahk@inha.ac.kr

Lake Sihwa, an artificial lake formed by a seawall, is located in the southern part of Gyeonggi Bay, on the west coast of South Korea. After the construction of the seawall, leading to the restriction of free exchange between freshwater discharge and seawater, sedimentation and water pollution worsened with continuous point and non-point contaminant inputs from agricultural and industrial wastes (Han and Park, 1999). To solve such problems, the Sihwa tidal power plant (TPP) was constructed and started operation in August 2011. The increase in the exchange of seawater due to the operation of TPP exhibited advantages for the improvement of the water quality in Lake Sihwa and the power generation. However, the jet-flow associated with the operation of TPP caused an imbalance in erosion and sedimentation near the Sihwa area. To date, the research has been focused on the water quality improvements of Lake Sihwa. There are few studies on the erosion and sedimentation due to the operation of TPP in outside Lake Sihwa (Bae *et al.*, 2010). The primary objective of this study is to examine the impacts of periodic artificial discharge on the variations in velocity and suspended sediment concentration (SSC).

Three mooring systems were installed for the purpose of understanding the sediment transport processes at stations M1, M2 and M3 (2.0, 2.6 and 3.3 km away from the Sihwa TPP, respectively) (Fig. 1). Each mooring system was equipped with a 600-kHz acoustic Doppler current profiler (ADCP), Conductivity-Temperature-Depth (CTD) sensors, and an optical backscatter (OBS) sensor. The downward-looking ADCP recorded velocities and acoustic backscatter at every depth bin. In order to estimate ADCP-derived SSC, the acoustic backscatter calibration was performed with the modified sonar equation of Denies (1999) and Ha *et al.* (2011).

The velocities and SSC exhibited the great variability in response to artificial discharge (Fig. 2). During ebb phase, the strong jet-flow ($>2 \text{ m s}^{-1}$) associated with artificial discharge caused the suspension of bed sediments, and high SSCs ($> 30 \text{ mg l}^{-1}$) were periodically observed in entire water column. At the end of ebb phase, the anticlockwise rotating vortex was fully developed due to the jet-flow and strong ebb currents. After turning into flood phase, the anticlockwise rotating vortex produced the secondary peaks of the SSC, transporting the suspended sediment toward the Sihwa TPP. During the presentation, it will be mainly discussed how the periodic artificial discharge can disturb the cohesive sediment dynamics in the TPP.

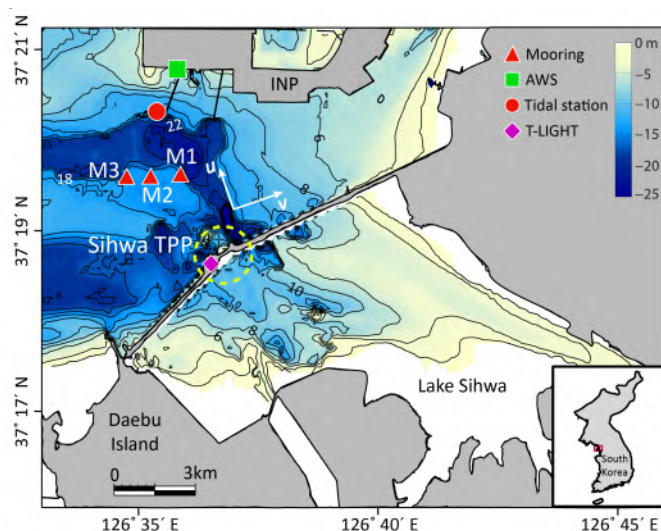


Fig. 1. Map showing Lake Sihwa and the adjacent region. Hydrographic data was collected at three mooring sites (red triangles, M1, M2 and M3).

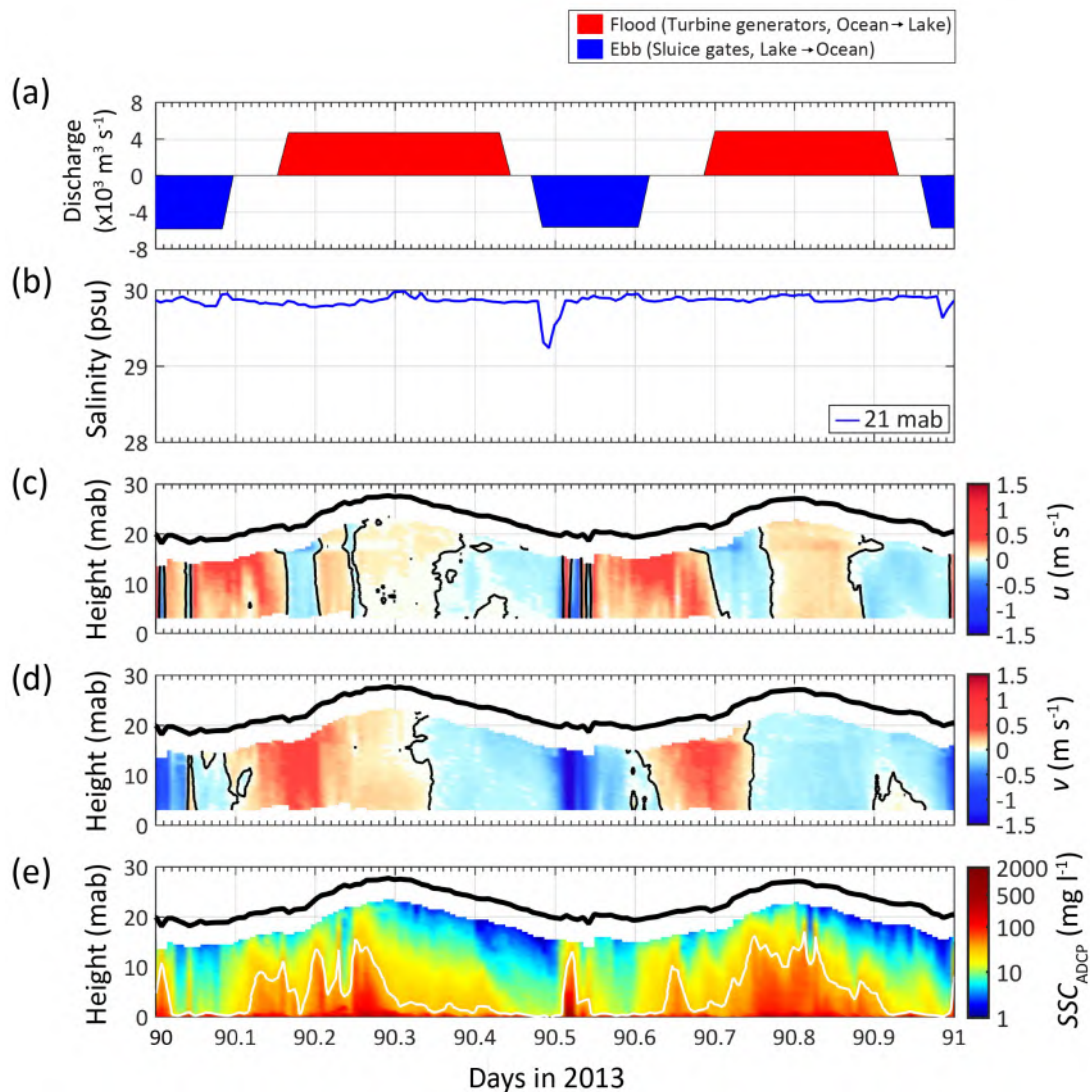


Fig. 2. Representative time series data from mooring M1: (a) discharge, (b) salinity, (c) along-channel velocity, (d) across-channel velocity, and (e) ADCP-derived SSC (SSC_{ADCP}). Thick and thin black lines indicate water height (c, d and e) and zero velocity (c and d), respectively. White line in (e) indicates 30 $mg\ l^{-1}$, as the upper limit of bottom suspension.

References

- Bae, Y. H., Kim, K. O., Choi, B. H. (2010). Lake Sihwa tidal power plant project. *Ocean Engineering* 37, 454–463.
- Deines, K. L. (1999). Backscatter estimation using broadband acoustic Doppler current profilers. *Proceedings of the 6th IEEE Working Conference on Current Measurement*. San Diego, CA, pp. 249–253.
- Ha, H. K., Maa, J. P. -Y., Park, K., Kim, Y. H. (2011). Estimation of high-resolution sediment concentration profiles in bottom boundary layer using pulse-coherent acoustic Doppler current profilers. *Marine Geology* 279, 199–209.
- Han, M. W., Park, Y. C. (1999). The development of anoxia in the artificial Lake Shihwa, Korea, as a consequence of intertidal reclamation. *Marine Pollution Bulletin* 38, 1194–1199.

Wave attenuation by brushwood dams in a mud-mangrove coast

A. Gijón Mancheño¹, S.A.J. Tas¹, P.M.J. Herman^{1,2}, A.J.H.M. Reniers¹, W.S.J. Uijttewaal¹, J.C. Winterwerp¹

¹ Department of Hydraulic Engineering, Faculty of Civil Engineering and Geosciences, Delft University of Technology, Delft, the Netherlands. E-mail: a.gijonmancheno-1@tudelft.nl

² Deltares, Boussinesqweg 1, 2629 HV Delft, PO Box 177, the Netherlands.

During recent decades, mangrove forests have experienced severe degradation due to unsustainable land use. Restoration of mangrove ecosystems requires the recovery of their habitat, considering ecology, hydrology, hydrodynamics, and sediment transport. In a first pilot in 2013, brushwood dams were built on the eroding coast of Demak, Indonesia, in order to emulate the function of mangrove roots and provide the physical conditions for natural colonization. However, at present there is little research on how soft structures affect the local hydrodynamics. The present study aims to improve the understanding of wave attenuation by permeable brushwood dams in Demak, combining field observations and hydrodynamic modelling using Delft3D. The findings of the study will be used to develop a landscape bio-morphodynamic model, which will be applied for planning future mangrove restoration efforts.

Introduction

Mangrove ecosystems are present along intertidal areas of tropical regions and provide multiple ecosystem services. They are natural habitats for numerous species, provide food and fuel wood, sequester carbon and act as a natural flood protection against hazards (Giesen et al., 2007, McIvor, 2012).

During recent decades mangrove forests have experienced severe degradation due to unsustainable land use (Winterwerp et al., 2013). In the province of Demak, Indonesia, mangrove removal for the construction of aquaculture ponds altered the sediment balance and produced high erosion rates at the coast. The measured retreat rates are over 100 m/year at some locations of the coastline, and around 6000 villages are at risk of being swallowed by the sea.

Restoration of mangrove ecosystems requires recovering their habitat, considering the ecology, hydrology, hydrodynamics and sediment transport. A first pilot was carried out in Demak in 2013, where permeable brushwood dams were built to emulate the function of mangrove roots. The dams attenuated waves in the areas that they confined, favouring sedimentation behind them and providing the physical conditions for vegetation to grow. After the stormy season of 2015 (November-February), 0.5 m of accretion was measured behind the dams and natural recruitment of *Avicennia marina* was observed to occur in the area.

In 2015 a large-scale project started with a consortium of Dutch companies (Ecoshape) in cooperation with the Indonesian Ministry of Marine Affairs and Fisheries (MMAF). The purpose of the project is to protect 20 km of coastline by a buffering mangrove belt. The BioManCO research project builds further on this initiative. It aims to expand the scientific knowledge on mud-mangrove coastlines and to develop a bio-morphodynamic landscape model that can be used to plan future restoration efforts.

Studying and quantifying wave damping by brushwood dams is a necessary step for the development of the landscape model. Substantial literature exists on the effect of permeable granular structures on incident waves (e.g. Sollit and Cross, 1976; Losada et al., 1995; Ting et al., 2004 among others). A number of authors have represented the effect of the structures in terms of reflection and transmission coefficients, empirically related to wave properties (wave height, wave steepness, wave number) and to the characteristics of the structure (geometry, porosity). However, little research has been done with soft structures such as brushwood dams.

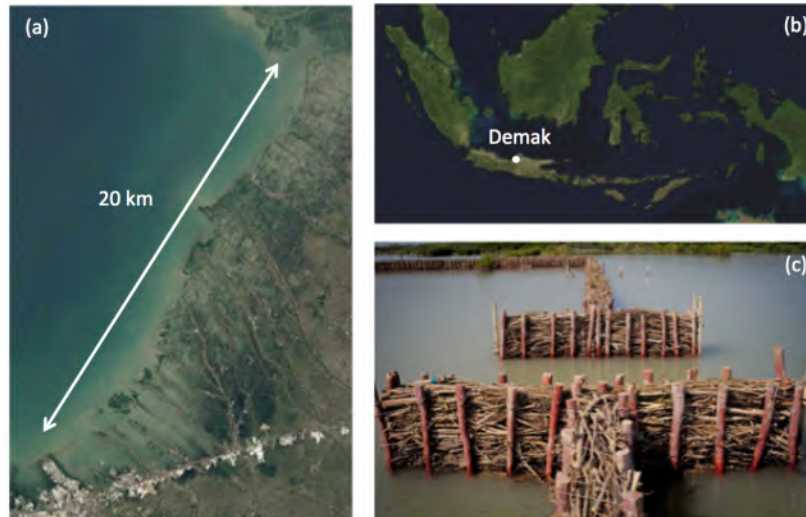


Figure 1. (a) Stretch to be protected by a mangrove belt (b) Location of Demak (c) Picture of one of the permeable dams.

Methodology

In order to improve the understanding of wave attenuation by permeable dams in the area of Demak, a combination of field observations and hydrodynamic modelling are being performed. Field measurements are conducted in order to quantify wave attenuation over the existing dams, and to characterize the soil properties at their location. The effect of the dams on flow and waves is parameterized in a submodel, included in a larger-scale Delft3D model of hydrodynamics and morphodynamics along the coast of Demak. The findings of this study will allow further development of the landscape model. This model will be applied in selecting suitable sites for the use of the permeable dams as a means to foster natural mangrove colonization and subsequent restoration of degraded mangrove ecosystems.

References

- Giesen, W., Wulffraat, S., Zieren, M., Scholten, L. (2007). Mangrove Guidebook for Southeast Asia.
- Losada, I. J., Losada, M. A. and Martin, F. L. (1995). Experimental study of wave-induced flow in porous structure, *Coastal Engineering* 26: 77-98.
- McIvor, A., Möller, I., Spencer, T., Spalding, M. (2012). Reduction of Wind and Swell Waves by Mangroves. *Natural Coastal Protection Series*, 1-27.
- Sayah, M. S. (2006). Efficiency of brushwood fences in shore protection against wind-wave induced erosion. PhD thesis, No. 3424, Ecole Polytechnique Fédérale de Lausanne.
- Sollitt, C. K. and Cross, R. H. (1976). Wave reflection and transmission at permeable breakwaters, Technical Report 76-8, US army corps of engineers - Coastal engineering research center.
- Ting, C.L., Lin, M. C. and Cheng, C. Y. (2004). Porosity effects on non-breaking surface waves over permeable submerged breakwaters, *Coastal Engineering* 50: 213-224.
- Winterwerp, J.C., Erfemeijer, P.L.A., Suryadiputra, N., van Eijk, P., Zhang, L. (2013). Defining eco-morphodynamic requirements for rehabilitating eroding mangrove-mud coasts. *Wetlands*, 33(3): 515-526.

Wave transformation on the mangrove-mud coast of Demak, Indonesia

S.A.J. Tas¹, A. Gijón Mancheño¹, P.M.J. Herman^{1,2}, A.J.H.M. Reniers¹, W.S.J. Uijttewaal¹, J.C. Winterwerp^{1,2}

¹ Department of Hydraulic Engineering, Faculty of Civil Engineering and Geosciences
Delft University of Technology, PO-box 5048, 2600 GA Delft, The Netherlands
E-mail: s.a.j.tas@tudelft.nl

² Deltares
P.O. Box 177, 2600 MH Delft, The Netherlands

Abstract

In this paper the typical hydrodynamics on mangrove-mud coasts are studied. Worldwide, these coasts experience serious erosion problems, and while the importance of mangrove ecosystems is becoming widely recognised, mangrove restoration projects frequently fail due to poor understanding of the system, especially the hydrodynamics. Therefore, a landscape model of the eroding coastline of the Demak district in Indonesia is developed to analyse the typical hydrodynamics associated to mangrove-mud coasts. Owing to the fine sediment, these coastlines are characterised by gentle slopes, in the order of 1:1000 or less. Both the theoretical and numerical wave transformation have to be re-evaluated on such slopes, which is done by combining models with field measurements. Also the current patterns and density effects are studied in detail to generate a full understanding of the hydrodynamics on mangrove-mud coasts.

Introduction

The erosion of mangrove-mud coasts is a serious problem worldwide, affecting millions of people in their daily life. For example, income drops of 60-80% and halving of commercial sea fishing over the last 5-10 years have been reported in eroding areas of Java, Indonesia, largely attributed to the loss of mangrove spawning and sheltering grounds (Manumono, 2008).

The objective of the current research project is to develop a bio-morphodynamic landscape model for mangrove-mud coasts. The algorithms for the physical and biological processes will be developed based on laboratory and field work, the latter carried out at the extremely eroding Demak coastline, Java, Indonesia.

The focus of this paper is the hydrodynamics on these muddy coasts. Due to the fine sediment, muddy coastlines are characterised by extremely gentle slopes, in the order of 1:1000 or less. On such slopes, the subtle balance between dispersion and shoaling of waves has to be re-established, and numerical models such as SWAN have experienced issues with quadruplet wave-wave interactions (Tas, 2016). Long waves are known to be less affected by these mild slopes, resulting in a lower peak frequency nearshore (Phan Khanh Linh et al., 2015). Also the effect of viscous wave damping by the soft muds on the seabed, and the effect of stratification due to river outflow is investigated.

A retreating coastline, such as the Demak coastline, is the net response to an imbalance in sediment transports. The sediment balance of muddy coasts typically consists of two huge gross fluxes, erosion and sedimentation, and results in a significantly smaller net effect. We hypothesise that the relatively weak effect of vegetation on the sediment may stabilise this inherently unstable system. One of the main drivers of sediment transport is the hydrodynamics nearshore. Therefore, the first step towards protection and/or restoration of mangrove coasts is a thorough understanding of the hydrodynamics of the system.

Methods

In order to understand the hydrodynamics at the Demak coastline, a numerical landscape model has been set up. For this, Delft3D is used, a 3D modelling suite to investigate hydrodynamics, sediment transport and morphology and water quality for fluvial, estuarine and coastal environments (Deltares, 2016). The modelled hydrodynamics are compared with currently available data (summarised below) and data taken from the field campaign which is scheduled in the Summer of 2017.

The domain is chosen sufficiently large, to prevent interaction between possible river plumes and boundary effects. This domain is illustrated in Figure 1. For the waves, an even larger domain is used in order to prevent that shadow zones induced by the boundaries affect the region of interest, i.e. the Demak coastline.

Since the Demak district has been a pilot site for coastal protection over the past years, there is already some information available, which is used to set up the boundary conditions of the model. A tidal station in Semarang, the city bordering the Demak district to the south, indicates the tide depicts a clear diurnal signal, with a small semi-diurnal component. The tidal range varies between 40cm and 60cm. There is a long-term average residual flow towards the east, resulting in a net fine sediment transport. Bed slopes are of the order of 1:1000 close to shore, further offshore steepening towards 1:500, all with a muddy substrate, although the thickness of the mud layers is unknown. Based on 14 years of wave data near Semarang, the mean wave height in the area is 0.46m and the maximum wave height lies between 2.6m and 3m. Due to the monsoon climate, all relevant waves have a direction between N and WNW. The wet season is from November to March. During this NW monsoon the river plumes are diverted to the east and pushed against the shoreline, inducing a gravitational circulation along large parts of the coast, keeping fine sediments close to the coastline. During the dry season, there are only local gravitational circulations (Winterwerp et al., 2014).

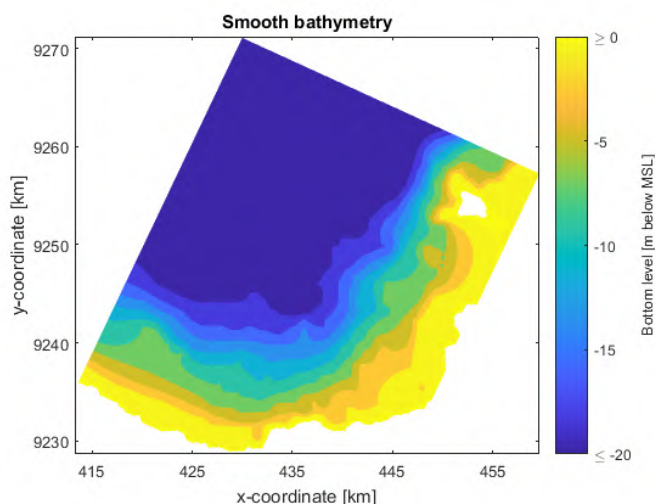


Figure 1: Domain with bathymetry of Delft3D model

Results

Wave transformation in the model is compared to wave measurements (wave height and period, orbital velocities) along transects in order to assess model performance. Non-linear wave-wave interactions (especially the quadruplets), dispersion, shoaling and wave damping by the soft muds on the seabed are analysed individually, in order to determine whether the wave transformation on these gentle slopes is modelled accurately.

Furthermore, current patterns (flow velocities and directions) are identified and analysed in order to identify the main driver(s) and to assess the presence of residual currents. Finally, density differences (salinity, temperature) are investigated over the seasons, to assess the presence of stratification.

Discussion

Understanding the hydrodynamics of the area is mandatory to gain insight in the causes of coastal erosion in Demak, moreover, it can be used to design successful coastal protection and restoration strategies. For example, by identifying the main processes driving wave transformation on gentle slopes, wave attenuating measures can be designed to tackle specific processes, and negative effects can be minimised.

Although the model is set up for the Demak area, several conclusions (such as the wave transformation on gentle slopes, the effect of stratification on sediment transport and specific protection and restoration measures) are applicable to many other mangrove coasts worldwide. However, it is important to note that, due to the sheltered character of the Java Sea, the Demak coastline is only exposed to wind waves. Therefore, the wave transformation and impact of swell waves on mangrove coasts will need to be analysed based on another case study.

References

- Deltares. (2016). Delft3D Functional Specifications. Delft: Deltares.
- Manumono, D. (2008). Perubahan Perilaku Masyarakat Kawasan pesisir Akibat Penurunan Pendapatan sebagai dampak abrasi dan rob di Kabupaten Demak/Behaviour change of coastal community as an impact of abration and rob in Demak Regency. In National Seminar of Dynamics of Agriculture and Rural Development.
- Phan Khanh Linh, Van Thiel De Vries, J. S. M., & Stive, M. J. F. (2015). Coastal Mangrove Squeeze in the Mekong Delta. *Journal of Coastal Research*, 31(2), 233-243. <http://doi.org/10.2112/JCOASTRES-D-14-00049.1>
- Tas, S. A. J. (2016). Coastal protection in the Mekong Delta. Wave load and overtopping of sea dikes as function of their location in the cross-section, for different foreshore geometries. Delft University of Technology.
- Winterwerp, J. C., van Wesenbeeck, B. K., van Dalftsen, J., Tonneijck, F., Astra, A., Verschure, S., & van Eijk, P. (2014). A sustainable solution for massive coastal erosion in Central Java.

Sediment trapping in the Zeebrugge Coastal Turbidity Maximum

D.S. (Bas) van Maren^{1,2}, Julia Vroom²

¹ Delft University of Technology, Civil Engineering and Geoscience, Stevinweg 1, 2628 CN Delft, the Netherlands

² Deltares, Boussinesqweg 1, P.O. Box 177 2600 MH Delft, the Netherlands
E-mail: Bas.vanMaren@deltares.nl, j.vroom@deltares.nl

Abstract

The mechanisms leading to the formation and maintenance of a Coastal Turbidity Maximum (CTM) along the Belgian coastline was investigated using a complex 3D numerical model. Interpretation of model results suggests that the sediment concentration in this CTM may have strongly increased as a result of human interventions in the 1980's. The large amount of sediment that became available then triggered self-organizing mechanisms that maintain or strengthen the CTM.

Introduction

A Coastal Turbidity Maximum (CTM) exists in the Belgian coastal zone, with elevated sediment concentrations up to ~100 mg/l near-surface and several g/l near the bed. These high suspended sediment concentrations lead to high maintenance dredging in the nearby Port of Zeebrugge (Fig. 1a) and its approach channels. However, despite the great costs associated with port maintenance, the mechanisms responsible for this CTM are poorly known. One of the potential mechanisms may be erosion of the seabed, which locally consists of consolidated mud (deposited there during lower sea levels earlier in the Holocene). Large quantities of mud may be eroded from the seabed due to human interventions, such as the seaward extension of the breakwaters of the Port of Zeebrugge (see Fig. 1b). A second potential mechanism is trapping by salinity-induced density currents: the CTM is located near the mouth of the Scheldt River. Additional mechanisms contributing to the CTM may be related to dredging and disposal strategies, tidal asymmetry, and residual circulation patterns.

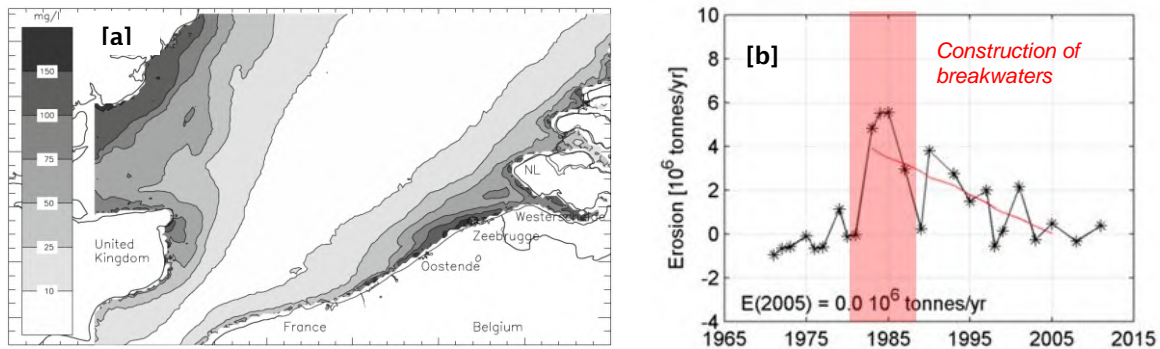


Fig. 1: The Zeebrugge coastal turbidity maximum (a, from Fettweis, 2010) and the erosion of mud following the extension of the breakwaters (in red) of the port of Zeebrugge

Approach

In order to investigate the processes responsible for the formation and maintenance of the CTM, a numerical model was setup. The overall strategy was to first setup and calibrate a complex 3D model in which all relevant processes and spatial scales are incorporated, and subsequently exclude individual processes to investigate their effect on the CTM. The model is setup with several mud fractions and with sand, and a dredging and disposal scheme based on actual dredging and disposal. Important features of this model include the effect of sediment on the density of the water-sediment mixture, a simple parameterization of near-bed hindered deposition, buffering of mud in the sandy seabed, and a local consolidated mud bed consisting of compact clays. The hindered deposition term is a simple way of accounting for several complex and poorly understood processes in the near-bed boundary layer related to hindered settling, flocculation, and consolidation which become important at high suspended sediment concentrations (SSC). The hydrodynamic model was calibrated against extensive datasets including waterlevels, velocity and salinity. The sediment module was calibrated against aggregated satellite observations, *in situ* long-term observations of SSC, and dredging volumes.

Results

The CTM can be generated with the model in two ways: through erosion of the underlying seabed or by including the hindered deposition term (Fig. 2). Over long timescales, erosion of the seabed cannot be responsible for the elevated sediment concentrations because a bed source is finite. After a certain amount of time the bed sediment would become depleted, and the sediment concentrations consequently would decrease. When hindered deposition is active, the CTM is maintained by salinity-driven and sediment-induced density effects (Fig. 3), effectively pushing the CTM towards the shore. However, hindered deposition is a process that becomes important at higher suspended sediment concentrations. This requires a condition in which sediment concentrations near the bed are already high. It is hypothesized that this initial state of elevated sediment concentrations is triggered by human interventions (such as the seaward expansion of the breakwaters illustrated by Fig. 1b). The large amount of sediment that became available triggered self-organizing mechanisms that maintain or strengthen the CTM.

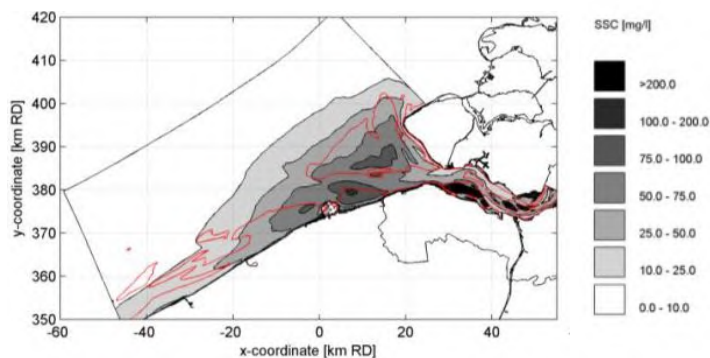


Fig. 2: Modelled average surface sediment concentration

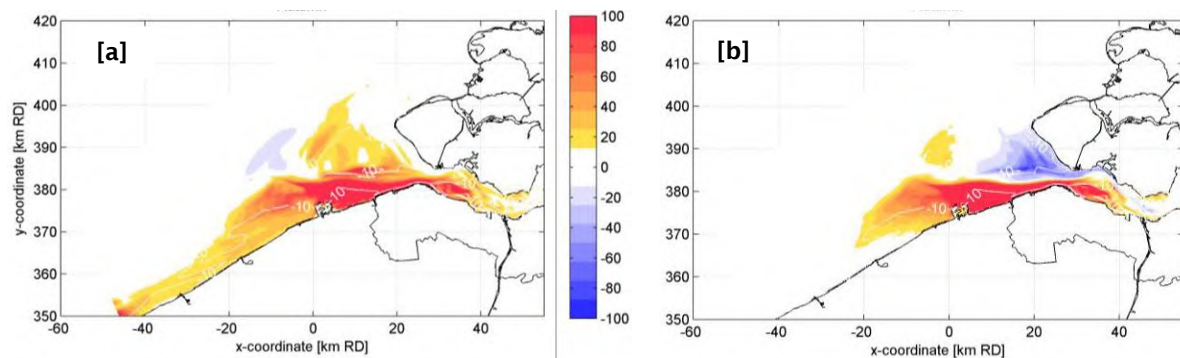


Fig. 3: Effect of sediment-induced density effects (a) and salinity (b) on the near-bed sediment concentration

References

Fettweis, M., Francken, F., Van den Eynde, D., Verwaest, T., Janssens, J., and Van Lancker, V., (2010). Storm influence on SPM concentrations in a coastal turbidity maximum area with high anthropogenic impact (southern North Sea). *Cont. Shelf Res.* 30, 1417–1427.

Flume experiment of fluid mud dynamics around navigation channel

Yasuyuki NAKAGAWA¹ and Futoshi Murayama²

¹ Coastal and Estuarine Sediment Dynamics Research Group, Port and Airport Research Institute, Nagase 3-1-1, Yokosuka, 239-0826, Japan E-mail: y_nakagawa@ipc.pari.go.jp

² Niigata Port and Airport Office, Hokuriku Regional Development Bureau, Ministry of Land, Infrastructure, Transport and Tourism, Irifune-cho 4-3778, Chuo-ku, Niigata, 951-8011, Japan

Introduction

Channel siltation is crucial topics for safety navigation of ships (e.g. PIANC, 2008). Mechanisms of the siltation depend on the sediment transport processes around navigation channels governed by several factors, such as sediment types, force conditions (waves and current) and sediment discharge through the river. A better understanding of the process is essential for selecting an effective countermeasure and minimizing siltation.

The aim of this study is to elucidate siltation process in a navigation channel which is dredged in a river mouth area. Field survey was conducted around a navigation channel under a flood condition with highly turbid water discharge and the data shows fluid mud layers in the dredged channel. Dynamics of the mud flows were studied through experiments with a circulating flume.

Study site

The study site is in the Port of Niigata, which is one of the biggest port located in the west coast of the Japanese main island (Fig.1) and the port has been developed around the mouth of the Shinano river, which is the longest one in Japan with the total length of 367 km. The channel of the port has been suffering from the siltation by the discharged sediment through the river and maintenance dredging is required around 800,000 m³ annually to keep the depth of -5.5 to -12 m in the channel and harbour basin.

Field measurements

The surveys were carried out in the summer of 2013 and the several data were taken just under a flood condition with relatively higher turbid water discharge from the upper tributary. Measured vertical profiles of salinity and SSC in the navigation channel shows apparent pycnocline beneath 3 m from the water surface (Fig.2 (a)), also with rapid increase in SSC near the bed. In this near bottom layer, high concentrated mud layer with the bulk density of around 1,200 kg/m³ appears, detected by an in-situ density measurement (Fig.2 (b)). This high concentration layer does not appear permanently according to previous field measurements during normal discharge rate condition. The near bed high concentrated layer (Fig. 2 (c)) could be formed by fluid mud transport from the upstream, which is the same mechanism as one observed on shelves off river delta (e.g. Fan et al. 2004).

Fluid mud experiments with circulating flume

Flume experiments were also carried out to examine dynamics of fluid mud flow in the vicinity of dredged channel at river mouth port (Fig.3). The flume used in the study is a circulating flume at Port and Airport Research Institute. In the experiments, the pycnocline was reproduced with upper fresh water and lower saline water at the dredged channel (Fig.4) and dynamic behaviours of turbid water discharged from upstream were measured with several turbid sensors. The experimental data will be precisely demonstrated in the paper and presentation.

Conclusions

Several field surveys were carried out to elucidate the siltation mechanism in the navigation channel located at the mouth of the Shinano River in Japan. The survey successfully captured the formation of high concentrated mud layer in the deeper dredged channel under the river flood condition with high turbid water discharge. We will also discuss, in the paper and presentation, flume experiments which were carried out to examine the fluid mud behaviours at dredged channel.

References

- PIANC (2008). Minimizing harbour siltation. The World Association for Waterborne Transport Infrastructures, Report 102. 75p.
- Fan S. et al. (2004). River flooding, storm resuspension, and event stratigraphy on the northern California shelf: observations compared with simulations, *Marine Geology*, 201, pp.17-41.

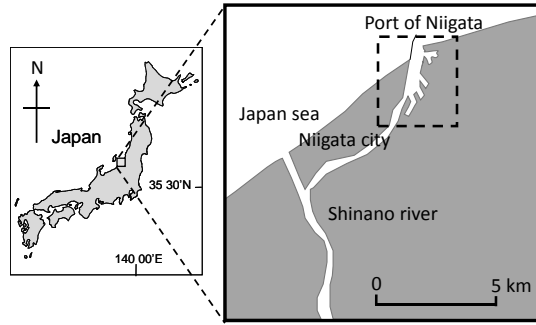


Fig. 1. The location of Port of Niigata (indicated in the dotted box)

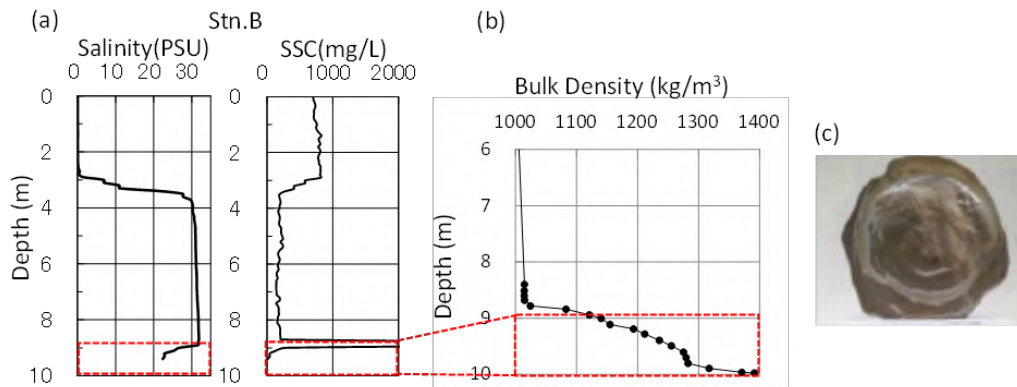


Fig. 2. Observed (a) Salinity and SSC, (b) vertical profile of bulk density and (c) sediment sample in the study site.

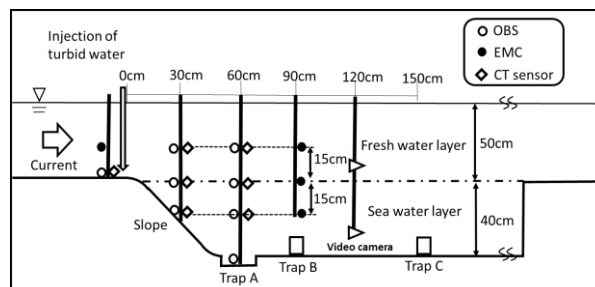


Fig. 3. Sketch of instruments layout in flume experiment.

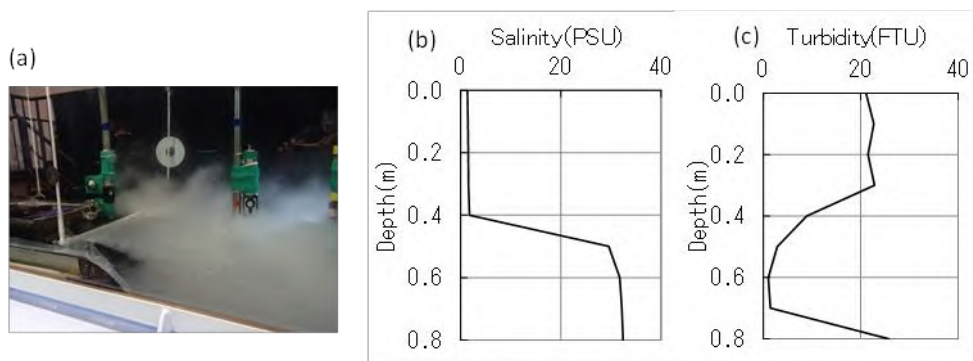


Fig. 4. (a) Flume experiment of fluid mud behaviours using Kaolinite clay in a circulating flume. (b) Salinity and (c) turbidity measured in the flume experiment.

SPM dynamics in a mud bank area crossing an estuary mouth. The case of Kaw mud bank in the Mahury Estuary (French Guiana)

Abascal Zorrilla Noelia¹, Huybrechts Nicolas², Vantrepotte Vincent¹, Gardel Antoine¹, Orseau Sylvain¹, Morvan Sylvain¹ and Lesourd Sandric³

¹ USR-LEEISA, CNRS-Guyane
Centre de Recherche de Montabo,IRD. 275, route de Montabo, Cayenne, France
E-mail: noelia.abascal-zorrilla@cnrs.fr

² Sorbonne Universités, Université de Technologie de Compiègne, CNRS, UMR 7337 Roberval, LHN (joint research unit UTC-CEREMA EMF)
Compiègne, France

³ M2C, UMR 6143
Université de Caen, PO Box 24 Caen 14000, France

Introduction

The Mahury estuary area, located in French Guiana, belongs to the coastal system under the influence of the Amazon. This 1500km-long coast of South America, between the Amazon and the Orinoco River mouths, is the world's muddiest. This is due to the huge suspended-sediment discharge of the Amazon River ($10^6 \times 754 \text{ tons yr}^{-1} \pm 9\%$), part of which is transported alongshore as mud banks (Anthony et al., 2010). When a mud bank migrates alongshore across an estuary mouth, the combined effects of waves, current, tide and wind induce mud resuspension and severe sediment settling usually affecting the navigation channel.

From in situ surveys, Orseau (2016) have analyzed the sediment dynamics focusing mainly on the processes occurring inside the Mahury estuary (Fig.1.). The aim of the present study is to further investigate how offshore sediment sources together with the seasonality in wind, oceanographic currents and waves influence the SPM dynamics inside the estuary as well as over the mud bank, located at the eastern part of the mouth of the Mahury estuary. The proposed methodology combines information provided from high spatial resolution satellite sensors (Landsat 8), in situ surveys and 3D hydrosedimentary modelling (Opentelemac).

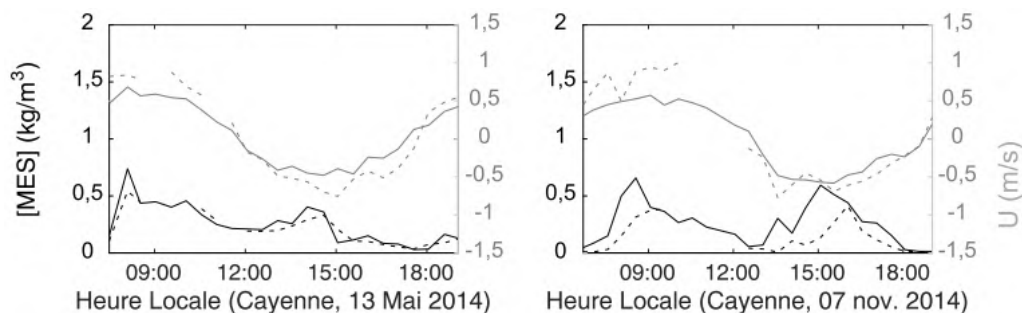


Fig. 1. SPM (kg/m^3) variation and current velocity U (m/s) over a spring tide cycle during A) the wet season and B) the dry season (Orseau, 2016). Surface values (at the mouth of the estuary) are represented by a dashed-line and bottom values with a solid line. Positive velocities correspond to downstream flow.

Results

Remote sensing

In total, 86 Landsat 8 images (04/2013; spatial resolution: 30m) have been processed from Level 1 to Level 2, using a Sun Glint correction algorithm first, and ACOLITE software (version 20160520.0) for the atmospheric correction. Surface SPM concentration was then retrieved from remote sensing

reflectance at the Landsat 8 band centered at the wavelength 665nm, using the algorithm of Han et al. (2016) (Fig. 2.). This algorithm is based on two standard semi-analytical equations calibrated for low-to-medium and highly turbid waters, respectively, using a mixing law for intermediate environments. SPM maps have been used for delineating mud bank extension and provide input data at the sea surface for the model development and validation.

3D hydrosedimentary model

The Telemac-3D model of the Mahury area has 40km long integrating, therefore, the Mahury River and its main tributaries. The river discharge was imposed upstream whereas tide was imposed offshore. Wind field was interpolated on the mesh and served to generate the Guiana current. The current velocities, tidal and salinity levels were calibrated using data gathered from several field campaigns (shipboard and mooring data, Orseau, 2016). Mud transport model consists primarily in the adjustment of different parameters in the model of consolidation, the laws of erosion and deposition and the fall velocity of the sediment. The characteristics of the bottom were taken into account using measurements coming also from different in situ campaigns (Orseau,2016).

In-situ monitoring

For monitoring SPM dynamics in the area, seismic measurements were conducted with a sub-bottom profiler (4-24KHz), well adapted for working in such shallow waters and for providing high resolution imagery over cohesive sediments. Such data allow estimating the thickness and the volume of displaced mud with time. Turbidity measurements were also conducted using OBS and STBD instruments, to characterize sediment distribution within the water column.

Conclusion

This work will emphasize the interest of combining in situ and satellite data for improving the understanding of the sediment dynamics through the development of modelling activities within the morphologically complex coastal domain of French Guiana.

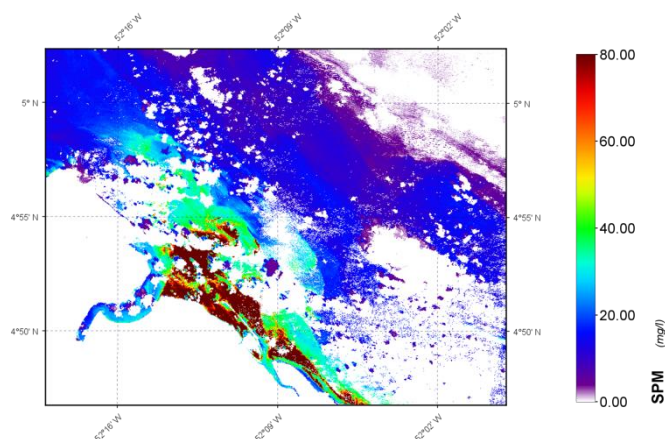


Fig. 2. LandSat 8 map of the surface SPM concentration (mg/l) in the area of study the 18th of November of 2015

References

Anthony, E. J. , Gardel, A., Gratiot, N., Proisy, C., Allison, M. A. , Dolique, F., Fromard, F. (2010). The Amazon-influences muddy coast of South America : a review of mud-bank-shoreline interactions. *Earth-Science reviews* 103, 99-121.

Han, B., Loisel, H., Vantrepotte, V., Mériaux, X., Bryère, P., Ouillon, S., Dessailly, D., Xing, Q., Zhu, J. (2016). Development of a semi-analytical algorithm for the retrieval of suspended particulate matter from remote sensing over clear to very turbid waters. *Remote Sens.* 2016, 8, 211.

Orseau, S. (2016). Dynamique sédimentaire d'un estuaire tropical sous influence Amazonienne : le cas de l'estuaire du Mahury. PhD thesis, Université du Littoral Côte d'Opale.

Plume measurements in the AMORAS underwater cell

Bart De Maerschalck¹, Styn Claeys¹, Erwin De Backer¹ and Stefaan Ides²

¹ Flanders Hydraulics Research, Berchemlei 115, 2140 Antwerp, Belgium
E-mail: bart.demaerschalck@mow.vlaanderen.be

² Antwerp Port Authority, Zaha Hadidplein 1, 2030 Antwerp, Belgium

Abstract

Since end 2011 maintenance dredging material from the port of Antwerp (right bank) is mechanically dewatered by the AMORAS dewatering installation. Before the dredged material is pumped to the AMORAS site, it is temporally stored in an underwater storage cell in one of the port shelter-docks. The fresh maintenance dredging material is disposed into the underwater cell by split and hopper dredgers. The presented paper investigates the behaviour of freshly disposed sediments in the underwater cell by means of an in situ measurement campaign, monitoring mud volume changes and tracking the disposed sediment plumes during and after a disposal of 5400m³ fresh sediment.

Introduction

In 2006 the Flemish authorities in association with the Antwerp port authority launched the AMORAS project as a sustainable solution for maintenance dredging material from the port of Antwerp. AMORAS stands for Antwerp Mechanical Dewatering (Ontwatering), Recycling and Application of Sludge. The construction of the site started in October 2008. End of 2011 the installation became operational.



Fig. 1: AMORAS production sites (left): 1. under water cell, 2. Sand separation, 3. Piping, 4. Consolidation ponds, 5. Dewatering installation, 6. Water treatment, 7. Storage. Right: Location of the underwater cell in the shelter dock for push-tow barges

After separating the sand from the dredged material, the remaining muddy sediment is mechanically dewatered and stored, see Fig. 1. The ambition is to finally recycle the dewatered sediment for other beneficial uses, e.g. in construction materials. This application is currently under investigation.

AMORAS Under Water Cell

Freshly dredged material is temporarily stored in the AMORAS underwater cell, step 1 in Fig. 1. An electrically powered cutter suction dredger picks up the sediments from the underwater cell and pumps it to the sand separation installation: step 2 in Fig. 1. The underwater cell is a local deepening, up to 16.2m depth (-12.0m TAW) in the shelter dock. The cell is separated from the navigation channel by a submerged steel sheet pile reaching up to 9.2m below the surface (-5.0m TAW).

In 2014 and 2015 the underwater cell has been monitored intensively by means of single- and multi-beam surveys and RheoTune measurements (De Maerschalck at al. 2015). It was observed that in times of intensive dredging and disposal activities, mud levels in the underwater cell rise faster than was expected, leading to up to 50% of sediment losses. Based on these observations, local authorities adjusted their port maintenance strategy.

Disposal plume measurements

In spring 2016 the single-beam/RheoTune survey was repeated during a five week monitoring campaign. In order to optimise port maintenance dredging costs, the Flemish authorities responsible for the port fairways wish to bring the MS Artvelde into action. This trailing suction hopper dredger has a hull capacity of more than 5400m³, which is significantly more than the hopper dredgers used before. Therefore it was decided to do a complementary intensive monitoring campaign to map the disposal plume during and after the disposal by the MS Artevelde.

The disposal plume was monitored simultaneously by two Acoustic Doppler Current Profilers (ADCP), a YSI multi-parameter probe, RheoTune and water samples. The disposal location has a unique setting: there are no currents nor waves and the disposal site is a confined space separated from the neighbouring fairways by a submerged dam. This made it possible to track the whole sediment plume at a high spatial and temporal resolution. The behaviour of the disposed sediments was monitored in the first minutes till hours after disposal.

It was observed that during the disposal the volume of the disposed sediment increases with a factor 5 to 7, see Fig. 2 below. The measured mean density of the fresh sediment in the underwater cell directly after the disposal was around 1.03ton/m³, while the mean hull density was around 1.2ton/m³. Based on the measured volume changes and in situ densities it was estimated that during disposal 10 to 25% of the sediments comes into suspension into the water column above the underwater cell (Fig. 3). Part of the suspended sediment is captured within the contours of the underwater cell. However, when the top of the mudlayer rises, less free space will be available within the cell and more of the suspended sediment will be distributed over the submerged dam to the neighbouring docks and channels.

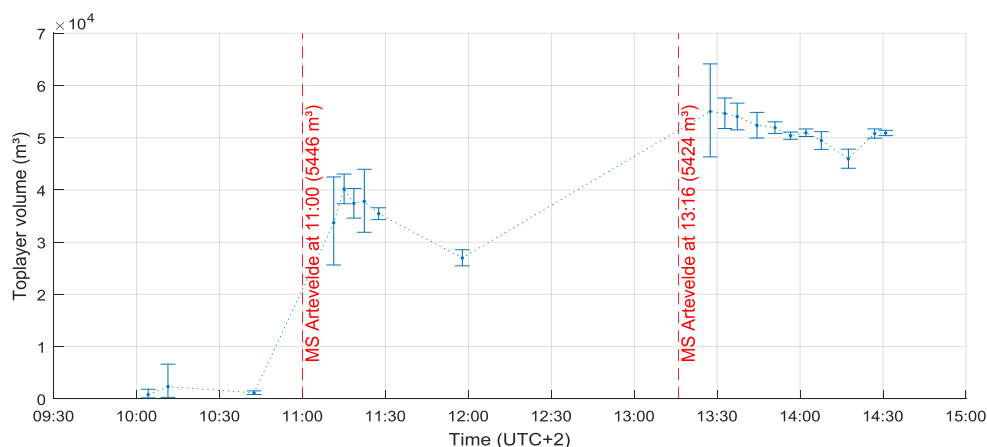


Fig. 2: Mud volumes in the underwater cell before and after disposal (disposal vol. in hull \approx 5400m³, dens. In hull \approx 1.2 ton/m³, disposal times are marked by the dashed red lines)

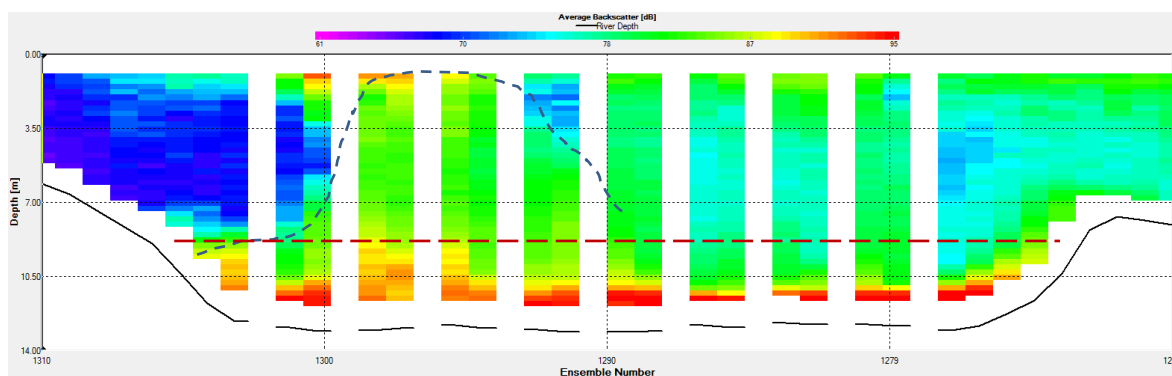


Fig. 3: ADCP backscatter intensity, sailed transect across the underwater cell 18 minutes after the first disposal. The black line is the top of the mudlayer within the UWC as detected by the ADCP bottom detector, the dashed line indicates the core of the sediment plume, the red dashed line indicates the depth of the submerged steel sheet pile (\approx 9.2 m below the surface).

References

De Maerschalck, B.; Van Esbroeck, M.; Ides, S.; Plancke, Y. (2015a). Monitoring sludge spill of the AMORAS underwater cell. INTERCOH2015: 13th International Conference on Cohesive Sediment Transport Processes. Leuven, Belgium, 7-11 September 2015. VLIZ Special Publication, 74: pp. 158-159.

Local study of erosion with a transparent model cohesive sediment

Zaynab TARHINI¹, Sébastien JARNY¹ and Alain TEXIER¹

¹ Pprime Institute, UPR 3346 CNRS–Université de Poitiers–ISAE ENSMA
BP 30179, 86962 Futuroscope Chasseneuil Cedex, France
E-mail: sebastien.jarny@univ-poitiers.fr

Abstract

A transparent model sediment with the same rheological properties than a natural one is used to study erosion in a narrow channel or a flume. Optical measurements allow access to local velocity fields within water and transparent sediment simultaneously.

Introduction

Cohesive sediment is a complex material of inorganic mineral, organic material and biological functions lead to viscoplastic and thixotropic characteristics, Toorman (1997). To characterize their erosion two parameters are to be identify: bed shear stress from hydrodynamic forces and erosion rate from suspended sediment concentration. In a macroscopic framework, previous experimental studies on erosion have already defined different thresholds sediment behaviour, Van Rijn (1993), Jacobs *et al.* (2011). This study is based on the development of transparent model cohesive sediment to allow optical measurements and lead to local kinematic information during erosion tests. First, the transparent cohesive sediment is elaborated with similar rheological properties than a natural one, Pouv *et al.* (2014). Secondly, erosion tests are carried out of the flume using particle image velocimetry (PIV) both to lead to, in the same time, the water velocity field and the deformation and the displacements of the transparent sediment.

Material development

The transparent model cohesive sediment is prepared with classical modifier agent of viscosity: synthetic clay, laponite RD (Rockwood), and polymer, carboxymethylcellulose (Prolabo). Laponite leads to thixotropic properties and carboxymethylcellulose (CMC) enhances viscoplastic effects of the mixture.

CMC solution is prepared first with powder sprinkle in deionized water in 0.5% mass concentration. The solution is stirred at 600rpm with a magnetic agitator for 1 hour. In the same time, Laponite suspension with 1% mass concentration is prepared sprinkling laponite powder in deionized water. The suspension is then mixed during 15 minutes at 11000rpm with a homogeneizer Ultraturax T25 (IKA). Finally the laponite suspension is added to the CMC solution for 1 hour mixing at 1100rpm with the magnetic agitator. The transparent sediment has a density close to $1\text{kg}\cdot\text{m}^{-3}$. For experiments this mother suspension is 70% mass diluted after 20 days at rest.

Rheological measurements

The rheological characterisation of the transparent sediment is carried out with a DHR–2 rheometer (TA Instruments) using plate–plate geometry of 4cm diameter. Both surfaces are covered with sand paper with a mean roughness of $58.5\mu\text{m}$ to prevent slippage effects. Each measurement is realised for a $300\mu\text{m}$ gap. Before flow curve measurements and to ensure a reproducible proceeding a pre–shear is applied with a shear rate of 10s^{-1} during 120s following by a 600s rest period. Then shear rate steps ranging from 10^{-3} to 10^3s^{-1} are applied in a logarithmic repartition to obtain up and down curves. Each curve is corrected using Rabinowicz formula to minimize potential existing error on the estimation of shear rate by using plate–plate geometry. The down curves of obtained rheogram follow a Herschel–Bulkley model.

Flume measurements

Experiments are realised in a transparent PMMA flume with a square section ($160\text{mm}\times 160\text{mm}$). The channel is close to defined bounded flow and to prevent from the gravity effect. Hydraulic pumps allow applying an average velocity up to $5\text{cm}\cdot\text{s}^{-1}$. Particle image velocimetry (PIV) measurements are obtained from a set Yag laser, CCD cameras devices and PIV controller. Polyamide particles (Vestosint) with a mean diameter of $20\mu\text{m}$ are dispersed in the flow.

To define a water reference flow case, at first, channel measurements are realised with no sediment. Then, the visualized channel background is lay down with the transparent sediment which has almost the same refractive index than the water. Comparisons between the complementary flow fields are conducted. Kinetic energy, laminar and turbulent shear stresses fields are then calculated to reach local quantitative data.

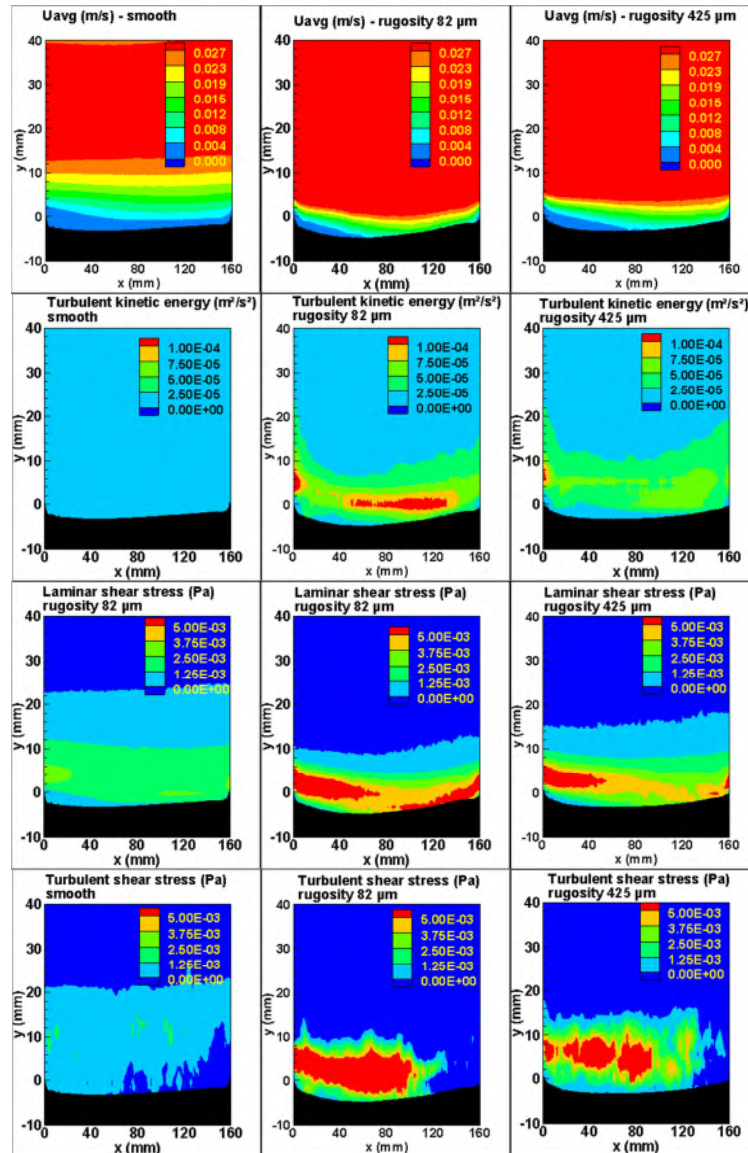


Fig. 1. For a flow rate velocity of 2.5 cm/s and three rugosity conditions: average velocity field, kinematic energy field, laminar and turbulent shear stress.

Conclusion

A transparent model sediment with the same rheological properties than a natural one is used to study erosion in a flume. Density and granular properties are not taking into account in this study. These fundamental properties of real sediments have a major impact on the flow and turbulence fields. Grain size has a major impact on the boundary layer development and turbulence intensity. The most critical point is the gravity effect and the flow down of particles during erosion. This work is the first step of a kinematic and dynamic study to understand local phenomena operating during erosion processes. A next experimental step will be to simultaneously add concentration measurements to PIV process and to use free surface flows for gravity effects. Combined with the rheological data, the final goal of this study is to rebuild the local shear stress field during erosion experiments.

References

- Jacobs W., Le Hir P, Van Kesteren W., Cann P. (2011). Erosion threshold of sand-mud mixtures. *Continental Shelf Research*, 31:14–25.
- Pouv K.S., Besq A., Guillou S., Toorman E.A. (2014). On cohesive sediment erosion: A first experimental study of the local processes using transparent model material. *Advances in Water Resources*, 72:71–83.
- Toorman E.A. (1997). Modelling the thixotropic behaviour of dense cohesive sediment suspensions. *Rheologica Acta*, 36:56–65.
- Van Rijn L. (1993). Principles of sediment transport in rivers, estuaries and coastal seas. Aqua Publications.

A tri-modal flocculation model coupled with TELEMAC for suspended cohesive sediments in the Belgian coastal zone

Xiaoteng Shen^{1*}, Erik Toorman¹ and Michael Fettweis²

¹ Hydraulics Laboratory, Department of Civil Engineering
KU Leuven, Kasteelpark Arenberg 40, B-3001 Leuven, Belgium
E-mail: xiaoteng.shen@kuleuven.be

² Operational Directorate Natural Environment, Royal Belgian Institute of Natural Sciences
Gulledelle 100, B-1200 Brussels, Belgium

Introduction

Estuarine and coastal regions are often characterized by a high variability of suspended sediment concentrations (SSC). The Belgian coastal zone is one of those areas where dredging works are conducted to maintain harbours and navigation channels (Fettweis et al., 2016). To investigate the SSC dynamics it is essential to understand the flocculation processes of estuarine mud, since it alters the sediment settling flux by aggregating individual clay particles into larger flocs. Previous curve fitting analysis of measured floc size distributions (FSDs) in the Belgium coastal zones showed that the multimodal FSDs can be decomposed into four log-normal FSDs to identify groups of primary particles, microflocs, macroflocs, and megaflocs, respectively (Lee et al., 2012). A two-class population balance model (PBM2C) was firstly developed using size-fixed class 1 particles (primary particles + microflocs) and size-varying class 2 particles (macroflocs + megaflocs) to describe the aggregation and breakage process of cohesive sediments. This simple model was validated by settling column test (Lee et al., 2011) and some field data collected in Zeebrugge (Lee et al., 2014), and later was coupled in the open source TELEMAC system and validated by using the same data set (Ernst, 2016). However, this two class assumption may be oversimplified as it does not address the large megaflocs that form after the peak of algae bloom periods. Moreover, the maximum errors for estimating the settling flux may largely decrease by tracking three size classes instead of two (Lee et al., 2012). For these reasons, a three-class population balance model (PBM3C) was developed in this study, also coupled with the open source TELEMAC modelling suite for the hydrodynamic and turbulence sections, to simulate the characteristic sizes of three size classes, i.e., microflocs (including primary particles), macroflocs, and megaflocs, respectively. A more recent data set from the WZBuoy in the Belgian coastal zone is used to validate the newly developed PBM3C. The objective of this study is to develop the PBM3C and implement it in TELEMAC to mimic flocculation processes of cohesive sediments, especially to reasonably address the population of megaflocs that previous PBM2C simply ignored.

Numerical modelling

Hydrodynamic model

The general open source software TELEMAC developed by the LNHE (Laboratoire National d'Hydraulique et Environnement) of EDF (Electricité De France) is used to solve the Navier-Stokes equations for variable water depth and velocity components, and to solve the tracer transport equation for various active and passive tracers. The transport of tracers is of major importance in the implementation of a flocculation model in TELEMAC3D.

Flocculation model

The PBM3C is developed to describe the flocculation processes, as an improvement of the previous PBM2C. As shown in Fig. 1, a system of equations are set up to track (1) the number of microflocs, macroflocs and megaflocs per unit volume, with symbol N_P , N_{F1} , and N_{F2} , respectively, (2) the total number of microflocs in all macroflocs (but not in megaflocs) per unit volume N_{T1} , and (3) the total number of microflocs in all megaflocs (but not in macroflocs) per unit volume N_{T2} . Take a one-dimensional vertical case as an example, the governing equation can be written as:

$$\frac{\partial N_i}{\partial t} + (w - \omega_{s,i}) \frac{\partial N_i}{\partial z} = \frac{\partial}{\partial z} \left(v_t \frac{\partial N_i}{\partial z} \right) + (A_i + B_i) \quad i = P, F1, F2, T1, T2 \quad (1)$$

where N_i is number concentration (in unit of m^{-3}), w is the vertical velocity of fluid, ω_s is the settling velocity, and v_t is the eddy viscosity. A_i & B_i are source and sink terms, which include (1) the aggregation of two microflocs, or two macroflocs, or two megaflocs, (2) the aggregation of a microfloc and a macrofloc, or a microfloc and a megafloc, or a macrofloc and a megafloc, and (3) the breakage of a macrofloc, or a megafloc. The average number of microflocs in one macrofloc per unit volume is $N_{C1} = N_{T1} / N_{F1}$, and the average number of microflocs in one megafloc per unit volume is $N_{C2} = N_{T2} / N_{F2}$. Thus, the sizes of macroflocs and megaflocs can be determined as $D_{Fi} =$

$D_p N_{Ci}^{1/nf}$ ($i = 1, 2$), where D_p , D_{F1} , and D_{F2} are the characteristic sizes of microflocs, macroflocs, and megaflocs, respectively, and nf is the fractal dimension. The five parameters, i.e., N_p , N_{F1} , N_{F2} , N_{T1} , and N_{T2} , are defined as tracers in TELEMAC as long as flocculation is toggled on (e.g., a predefined logical variable PBM3C is set to true). This PBM3C flocculation model can be included in the TELEMAC software with appropriate modification of the subroutines VITCHU, WCHIND, CLSEDI, SOULSBYFLOC3D, FONVAS, etc. in TELEMAC.

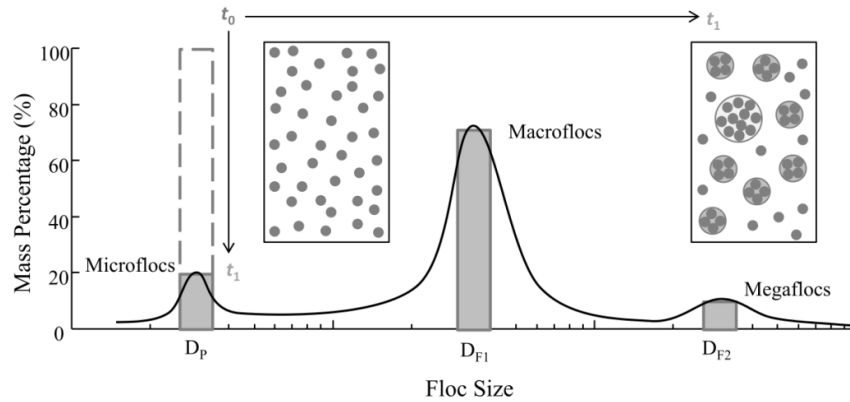


Fig. 1. Conceptual diagram for three-class population balance model (PBM3C).

Field measurements

The station WZBuoy is located about 2km outside the entrance of Zeebrugge harbour which is situated in the coastal turbidity maximum area along the southern North Sea near the Belgian coast (Fettweis et al., 2016). Although measurements were conducted with tripods for several years, only the data for several selected tidal cycles around Julian Day 322 in the year 2013 were used to validate the model. Velocity profiles and water surface elevation were recorded by an upward looking ADCP (Acoustic Doppler Current Profiler) which was mounted together with the tripod. The time series of FSDs were collected by the LISST (Laser In-Situ Scattering and Transmissometry), and temperature, salinity, and SSCs were measured or derived from the ADCP backscatter strength. Time series of water depth and the average temperature and salinity are treated as inputs to drive the model, while the velocity profiles, SSC profiles, and FSDs are used to validate the model outputs.

Results and conclusions

The PBM3C enabled TELEMAC software is validated by the flow, sediment and floc size distribution data from the WZBuoy station in the Belgian coastal zone within an intra-tidal time scale. More complicated processes such as the effect of biofilms and interaction with microplastic particles will be included in this system in a later stage.

Acknowledgements

This research was funded by the BelSPO (Belgian Science Policy Office) in the framework of the BRAIN-be (Belgian Research Action through Interdisciplinary Networks) INDI67 project, and by the JPI Oceans (Joint Programming Initiative Healthy and Productive Seas and Oceans) in the framework of the WEATHER-MIC (Microplastic Weathering) project.

References

- Fettweis M., Baeye M., Cardoso C., Dujardin A., Lauwaert B., Van den Eynde D., Van Hoestenbergh T., Vanlede J., Van Poucke L., Velez C., Martens C. (2016) The impact of disposal of fine-grained sediments from maintenance dredging works on SPM concentration and fluid mud in and outside the harbor of Zeebrugge. *Ocean Dynamics*, 66: 1497-1516.
- Lee B.J., Toorman E., Molz F.J., Wang J. (2011) A two-class population balance equation yielding bimodal flocculation of marine or estuarine sediments. *Water Research*, 45: 2131-2145.
- Lee B.J., Fettweis M., Toorman E., Molz F.J. (2012) Multimodality of a particle size distribution of cohesive suspended particulate matters in a coastal zone. *Journal of Geophysical Research*, 117:C03014.
- Lee B.J., Toorman E., Fettweis M. (2014) Multimodal particle size distributions of fine-grained sediments: mathematical modelling and field investigation. *Ocean Dynamics*, 64: 429-441.
- Ernst S. (2016). Implementation of a flocculation model in TELEMAC-3D. MSc thesis, Dept. of Civil Engineering, KU Leuven. xvi+151p.

The Importance of Wind-induced Sediment Fluxes on Tidal Flats

Irene Colosimo¹, Bram C. van Prooijen¹, D.S. (Bas) van Maren^{1,2},
Johan C. Winterwerp¹ and Ad J.H.M. Reniers¹

¹ Delft University of Technology, Civil Engineering and Geoscience, Stevinweg 1, 2628 CN Delft, The Netherlands

E-mail: I.Colosimo@tudelft.nl, B.C.vanProoijen@tudelft.nl, A.J.H.M.Reniers@tudelft.nl,
J.C.Winterwerp@tudelft.nl

² Deltares, Boussinesqweg 1, P.O. Box 177 2600 MH Delft, The Netherlands

E-mail: Bas.vanMaren@deltares.nl

Background & Research Question

Port maintenance and nature preservation are two often conflicting aspects of coastal management. Within a *Pilot Project* in the Western Wadden Sea (the Netherlands - see Figure 1a) we test a win-win solution that could reduce harbour siltation while simultaneously stimulate saltmarsh development. For this purpose, fine material, dredged in the Port of Harlingen, is used to increase the bed level of the intertidal flats at North-East of the harbour. The sediment is not disposed directly on the mudflat but at the North-East edge of the Kimstergat Channel (Figure 1b).

The strategy is based on the presumption that the flood dominant system results in an extra net sediment transport onto the Koehool Mudflat (Figure 1b). The imposed higher mud supply will gradually feed the mudflat (hence the name of the project: *The Mud Motor*) and is expected to accelerate the rate of bed level increase and, as consequence, the switch from a bare to a vegetated mudflat state.

The success of the Pilot Project *Mud Motor* relies on the sediment transport capacity from the channel to the mudflats. We therefore carried out a field campaign to unravel the role of the various hydrodynamic forcing that determine the fate of the disposed sediment.

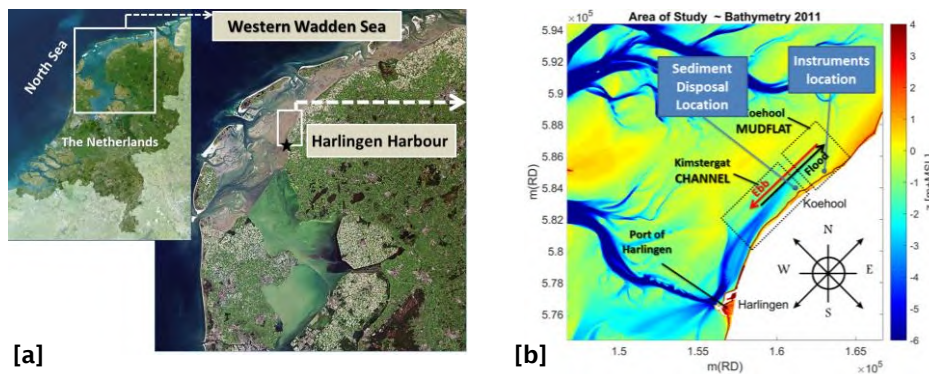


Figure 1: a) Frame of reference of the investigated area: Western Wadden Sea (the Netherlands). b) Study Area: Kimstergat CHANNEL - Koehool MUDFLAT System. The definitions for the flood direction (towards northeast) and ebb direction (towards southwest) are indicated.

Method

In Spring 2016, a 30 days' field campaign was carried out. Wave, flow and sediment concentration data were collected, at high frequency, using Wave Loggers, Acoustic Doppler Velocimeters (ADV) and Optical Back Scatter sensors (OBSs). The instruments were installed on two frames, located at 900m from each other, along a cross-section in the southern Koehool mudflat (Figure 1b).

Results and Interpretation

The dataset covers a variety of combinations of wind, waves and tidal conditions. Despite the meteorological variations, most tides show the following trends (see for example the second tide in Figure 2):

- The tides are flood-dominant, with larger flow velocities during flood (from channel to mudflat) than during ebb (from mudflat to channel).
- The Suspended Solid Concentrations (SSC) are highest during conditions with very shallow water, i.e. when the bed is more exposed to the effect of waves and when flow velocities are relatively high; SSC values are very low (often close to zero) during high water slack, when waves do not penetrate to the bed and when the flow velocity is close to zero.

The weather during the full measurement period was overall calm, but wind events showed that the above-mentioned flow and concentration patterns can drastically change. Such a different behaviour is observed in the first tidal cycle of Figure 2. The weak wind from the South during the rising tide did not result in sediment resuspension. During the falling tide, the wind changed in southwestern direction. This led to: (i) reversal of the flow, with the velocity flow remaining in flood direction during the full tidal cycle (Figure 2c); (ii) a slight water level set up (Figure 2a); (iii) relatively high wave height over depth ratios (Figure 2a, 2c). The consequence was that the falling tide phase resulted in a significant sediment flux towards the mudflat. Figure 2d shows that the accumulated flux of the “atypical” first tide, is more than 3 times larger than the accumulated sediment flux of the “typical” second tidal cycle.

The first tide of Figure 2 is representative for the case of flux enhancement in the North-East direction, but other tidal cycles, with opposite wind (from North-East), show net sediment fluxes towards the channel (Figure 3).

The analysis of the full dataset (totally 56 tidal cycles) shows that for the majority of the time, the tide-induced sediment transport result in a net flux in the flood direction. This typical pattern can be modified by the wind, (i.e. by wave forcing and wind-driven flow) and can induce a significant net sediment flux towards one direction for the full tide (respectively: from channel to mudflat with south-western wind and from mudflat to channel with north-eastern wind). The six events highlighted by the green squares in Figure 3, show that the sediment fluxes towards the mudflat, cumulated in long periods, can be “lost” in a few tides if wind reverses the tidal flow in the channel direction. Over the full investigated period, in fact, a small net flux is observed (0.5×10^4 kg/m), due to 3 reversed tide in the South-West direction (3rd, 5th and 6th wind events indicated by the green boxes in Figure 3).

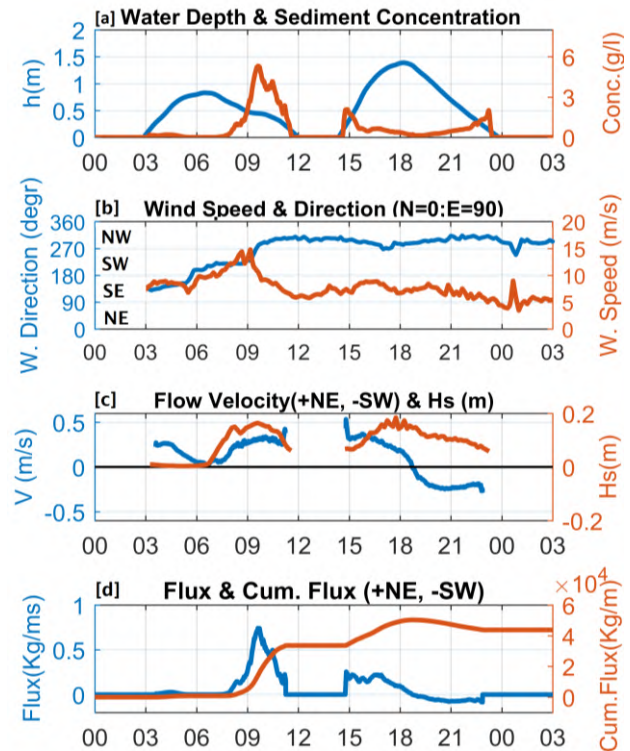


Figure 2 - Time series of : [a] Water Depth (m) and SSC (g/l); [b] Wind Speed (m/s) and Direction (degrees); [c] Flow Velocity Magnitude (m/s) and Significant Wave Height (m); [d] Fluxes (kg/ms) and Cumulative Fluxes (kg/m).

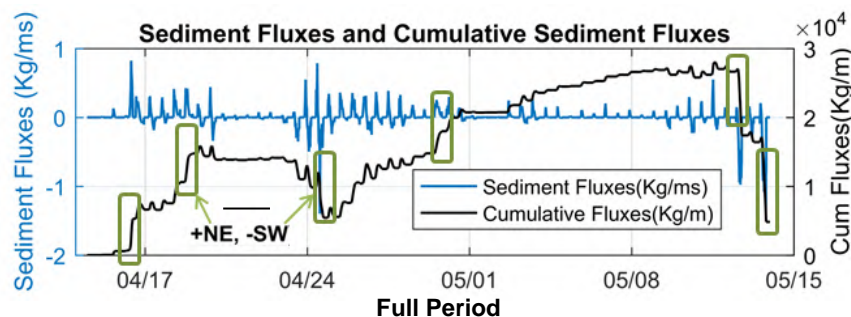


Figure 3 - Gross Fluxes (positive: N-E direction; negative: S-W direction) (kg/ms) and Cumulative Fluxes (kg/m) in the full measurement period. The boxes indicate wind events with speeds above 12 m/s.

Conclusions

This study shows that wind plays a major role on the sediment transport in shallow intertidal areas. It is therefore important to take this into account in the morphological modelling, especially in the shallower tidal flat zone. These relatively common wind-events (more than 10% of the tides in the measurement period presented a reversed velocity profile) are expected to influence the yearly averaged sediment transport and therefore, in the case of the *Mud Motor*, the effectiveness of a successful transport towards the mudflats.

Space - and time-varying bed roughness at Mixed Continental Shelves

Oliveira Kyssyanne¹, and Valéria da Silva Quaresma¹

¹ Departamento de Oceanografia, Centro de Ciências Humanas e Naturais, Universidade Federal do Espírito Santo, Vitória - Espírito Santo, Brazil
E-mail: kyssyanne.samihra@gmail.com

Introduction

Bed roughness in natural water systems has traditionally been studied extensively. It strongly affects water levels, propagation of tides, widening or retreat of beaches, the rate and composition of the suspended load and bedload transport, and consequently large-scale morphodynamics of the sea bed. Previous studies (Swinkles et al., 2012) on the effect of bed characteristics spatial variation showed that considering this variation may significantly improve the prediction of the water levels and currents in shallow areas. The flow conditions can influence the bed roughness in space as in time. Thus, an improvement in the flow representation is expected when both variation in time and space are considered. The aim of this study is to evaluate the Delft3D Modelling System performance in the tidal level hindcasting, along a stretch of the eastern Brazilian continental shelf, considering a spatially constant bed roughness, spatially varying bed roughness, and space-and time-varying bed roughness.

The study area is part of eastern Brazilian continental shelf, with the Espírito Santo Bay as its southern boundary and as the northern limit, the Doce River mouth. This study area presents a heterogeneous bed sediment distribution. At the south of study area can be observed a more uniform sediment grain size distribution, while the area near the Doce River mouth (North) presents a larger range of sediment grain sizes (Bastos et al., 2015). The influence of bed roughness in the prediction of tidal level was evaluated for two tide gauge stations: the first is located at the Tubarão Harbour, at Espírito Santo Bay; and the second station is located at the Barra do riacho, close to Doce River mouth.

Databases and Methods

Delft3D settings

To evaluate the influence of different bottom boundary conditions in the prediction of tidal level, a 2DH numerical model has been set up using the modeling system Delft3D. The hydrodynamics within the Delft3D-FLOW module are computed based on unsteady shallow water equations. To perform the numerical experimental, bathymetry, sediment grain sizes, and tidal phase and amplitude data were used.

The bathymetry database was obtained by digitizing the original bathymetric charts produced by the Brazilian Navy Hydrographic Office. Sediment grain size data (d50) was based on a compilation of published and unpublished dataset and were used to calculate the bed roughness without consider sediment in the simulations. The model was forced with tides extracted from the global tidal model FES 2012, and included 15 constituents, specifically the M2, S2, N2, K2, K1, O1, P1, Q1, Mf, Mm, MS4, MU2, N2, NU2 and M4. Three open boundaries are defined at the northern, seaward and the southern sides of the model domain. The seaward open boundary is a water-level type, with Neumann boundaries prescribed on the northern and southern sides.

Bed Roughness Conditions

In 2D calculations, the bed roughness is represented by the Chézy coefficient. This coefficient is used to determine the flow induced bed shear stress. The bed roughness can be computed using different formulations in Delft3D (Chézy, Manning, White - Colebrook and Z_0), and in this study we use the White - Colebrook's formulation (Equation 1). The White Colebrook's formulation requires the specification of a geometrical roughness of Nikuradse k_s ($k_s = 2.5 d_{50}$) [m]. Using this roughness, the Chézy coefficient is calculated as follows:

$$C = 18 \log_{10} \left\{ \frac{12h}{k_s} \right\} \quad (1)$$

Three different bed roughness conditions were tested: a spatially constant bed roughness ($k_s = 0.0011\text{m}$), spatially varying bed roughness, and space-and time-varying bed roughness (Van Rijn,

2007). The constant value of k_s was calculated considering the median sediment grain size of the study area. We adopted the roughness predictor of Van Rijn (2007) to calculate the space-and time-varying bed roughness. In this formulation, the bed roughness will be varying at all times and at all points in space, according to sediment grain size, water depth and flow velocity. A time step of six minutes was used for updating roughness.

Response of Tidal level

The influence of the three different bed roughness conditions was investigated comparing the tidal elevation modelled with the tidal level observed. The model is applied for the period between April and August of 2014. In the simulations, only the bed roughness varied. Correlation coefficient and Root Mean Square Error (RMSE) were used to indicate the degree to which model estimates reproduced observed values.

Results and Conclusions

Tidal elevation data were analyzed for two tide gauge stations, for the month of August 2014. Both correlation coefficient and RMSE (Table I) showed the tidal elevation being well reproduced by the model at the Tubarão Harbour and Barra do Riacho stations. Also, can be seen an prediction improvement when was used the spatially varying bed roughness, and an even greater improvement when the space-and time-varying bed roughness was used (Table I).

Table I: Correlation coefficient and Root Mean Square Error (RMSE [m]) considering the three different bed roughness conditions, for the two tide gauge stations (Barra do Riacho and Tubarão Harbour).

Barra do Riacho			
Statistic Parameters	Constant bed roughness	Spatially varying bed roughness	Space-and time-varying bed roughness
RMSE	0,1909	0,1889	0,1693
Correlation Coefficient	0,8926	0,8938	0,9159
Tubarão Harbour			
Statistic Parameters	Constant bed roughness	Spatially varying bed roughness	Space-and time-varying bed roughness
RMSE	0,1785	0,1764	0,1658
Correlation Coefficient	0,9345	0,9353	0,9481

Comparing the results at the two tide gauge stations, when the space-and time-varying bed roughness was used, was noted that the improvement is higher at the Barra do Riacho station. The continental shelf close to Barra do Riacho station presents a higher variation of sediment grain sizes when compared to the section of the continental shelf near the Tubarão Harbour, indicating that is recommended the use of the space-and time-varying bed roughness in areas with great sediment grain sizes variations become crucial for a proper flow representation.

References

- Bastos, A. C., Quaresma, V. S., Marangoni, M. B., D'agostini, D. P., Bourguignon, S. N., Cetto, P. H., Silva, A. E., Amado Filho, G. M., Moura, R. L., Collins, M. (2015). Shelf morphology as an indicator of sedimentary regimes: A synthesis from a mixed siliciclastic-carbonate shelf on the eastern Brazilian margin. *Journal of South American Earth Science* 63, 125-136.
- Swinkels, C.M., Bijlsma, A.C. (2012). Understanding the hydrodynamics of a North Sea tidal inlet by numerical simulation and radar current measurements. *Proceedings of 3rd International Symposium on Shallow Flows*, Iowa City, USA, June 4 - 6, 2012.
- Van Rijn, L.C. (2007). Unified view of sediment transport by currents and waves. 1: Initiation of motion, bed roughness and bed-load transport. *Journal of Hydraulic Engineering*, 133(6), 668-689.

Reoccurrence of high-energy events: how is a shallow coastal lagoon impacted? A study based on in situ and numerical investigations

Pernille L. Forsberg¹, Verner B. Ernstsen¹, Ulrik Lumborg², Nils Drønen², Thorbjørn J. Andersen¹, Aart Kroon¹

¹ Institute of Geosciences and Natural Resources, University of Copenhagen, Øster Voldgade 10, DK-1350 Copenhagen, Denmark. pefo@ign.ku.dk

² Department of Coastal and Estuarine Dynamics, DHI, Agern Allé 5, DK-2970 Hørsholm, Denmark

Introduction

Coastal lagoons are shallow water bodies separated from the sea by shore-parallel barriers, which dampen wave and current conditions (Kennish and Paerl, 2010). Due to the sheltered characteristics, coastal lagoons are typically inhabited by seagrass and marine fauna, which contribute to the individual lagoon characteristics and functioning (e.g. De Wit, 2011). The ecosystem health of coastal lagoons is vulnerable to increasing turbidity levels caused by e.g. sediment suspension. Increasing turbidity causes hindered light penetration, which affects the growth of seagrass (Middelboe et al., 2003). A proposed future increase in storminess due to climate change (IPCC, 2007) could exacerbate the local turbidity levels due to increased sediment resuspension (Madsen et al., 1993), and likewise, a sediment spill related to offshore construction work may pose a threat to the coastal lagoon health. The lagoon of the present study, Rødsand lagoon in southeast Denmark, is protected by the European Commission as a Natura 2000 area; a designation that prohibits a permanent disruption of the natural habitat. Comprehending the local sediment dynamics of a coastal ecosystem and potential future stressors is an important step towards appropriate management; a topic which has been stressed in several recent studies, e.g. Ferrarin et al. (2016), Gaertner-Mazouni and De Wit (2012) and Spalding et al. (2014). Three classical lagoon types have been proposed by Kjerfve (1986), depending on the wave energy, tidal range and water exchange with the adjacent sea i.e. “Choked”, “Restricted” and “Leaky”. Rødsand lagoon holds a morphological difference in terms of a connecting strait that generates additional flushing, which complicates assigning the lagoon to one of the classical lagoon types. The aim of the present study is to investigate the impact of a series of high-energy events (HEEs) on the suspension of sediment in Rødsand lagoon and use the results to improve the modelling of fine-grained sediment dynamics in the entire lagoonal system with the following objectives: to measure and compute wave energy, flow conditions and sediment suspension; to describe and explain the relationships between the hydrodynamic and sediment parameters; to model the flow and sediment dynamics on a lagoonal scale by integrating the in-situ observations; and finally, to evaluate the impact of increased storminess and a temporary sediment spill from nearshore construction work on the lagoonal turbidity levels.

Field work

The Rødsand lagoon in southeast Denmark is connected to the inner Danish waters through a north-eastern strait and faces the energetic strait Fehmarn Belt to the south that connects the Baltic Sea with the inner Danish waters; the lagoon is sheltered by two barrier islands and a spit (fig. 1). Rødsand lagoon is inhabited by *Zostera Marina* (eelgrass), which is present in the western and shallow part of the lagoon (FEMA, 2013). An extensive monitoring program has been in place in Rødsand lagoon from 2013 until 2015. The program included permanent stations along the coast of Lolland and within Rødsand lagoon and provided continuous measurements of the flow and sediment dynamics. In 2015 and 2017 periodic stations were deployed in the western and eastern part of Rødsand lagoon, respectively, as well as in the north-eastern strait. The periodic deployments supplied high-frequency data with information about the flow, turbidity and sediment composition in the water column. In addition, three bed sampling campaigns and subsequent laboratory erosion experiments were conducted. The in-situ observations were used as calibration parameters to improve the numerical model of Rødsand lagoon.

Preliminary results and discussion

Hydrodynamics

A total of eleven high wind speed events ($>10.8\text{m s}^{-1}$) with a duration of more than six hours were captured during the 2015 periodic deployment (instrumented platform); the events were

the first of the season. The HEEs caused increasing wave heights and energetic flow conditions. All the HEEs had westerly wind directions with exception of one event from southeast. The water level was inversely related to the wind speed; during rising water level the currents were easterly directed and vice versa. This behaviour suggested a seiche within the lagoon.

Sediment dynamics

The increasing wave energy during HEEs caused an increase in the turbidity. The energy required for particle suspension decreased with time suggesting that the erosional nature of the lagoon bed depended on the occurrence of previous HEEs. The eelgrass cover was significantly reduced during the period of investigation (diver observations). The impact of the vegetation reduction could be observed in the turbidity measurements, which showed an increase in the turbidity relative to the bed shear stress subsequent to the reduction.

Numerical model

The expected principal modelling result is an identification of the flow circulation in Rødsand lagoon and its coupling to the fine-grained sediment dynamics. The numerical model will be utilized to assess the system response and sensitivity to amplified storminess and increased sediment import in relation to a sediment spill. A conceptual model of the lagoonal flow and sediment dynamics will be proposed and compared to the classical lagoon types proposed by Kjerfve (1986).

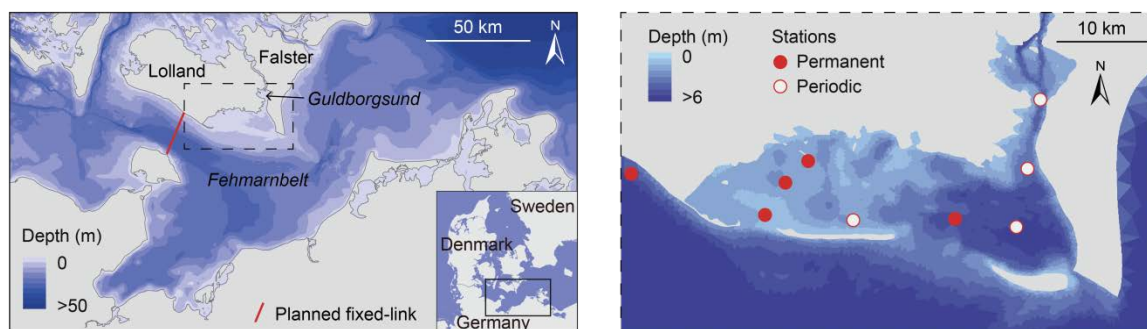


Fig. 1. Location of Rødsand lagoon (left) and zoom-in on the lagoonal bathymetry used for the numerical modelling along with the locations of in-situ measuring stations (right).

Acknowledgements

This study is part of the research project “SEDILINK” co-funded by Femern A/S, DHI and the Department of Geosciences and Natural Resource Management, University of Copenhagen.

References

- De Wit, R., 2011. Biodiversity of Coastal Lagoon Ecosystems and Their Vulnerability to Global Change, in: Grillo, O. (Ed.), *Ecosystems Biodiversity*. InTech, pp. 30–40.
- FEMA, 2013. Fehmarnbelt Fixed Link EIA. Marine Fauna and Flora – Baseline Benthic Flora of the Fehmarnbelt Area. Report No. E2TR0020.
- Ferrarin, C., Umgiesser, G., Roland, A., Bajo, M., De Pascalis, F., Ghezzi, M., Scroccaro, I., 2016. Sediment dynamics and budget in a microtidal lagoon — A numerical investigation. *Mar. Geol.* 381, 163–174. doi:10.1016/j.margeo.2016.09.006
- Gaertner-Mazouni, N., De Wit, R., 2012. Exploring new issues for coastal lagoons monitoring and management. *Estuar. Coast. Shelf Sci.* 114, 1–6. doi:10.1016/j.ecss.2012.07.008
- IPCC, 2007. *Climate Change 2007: Synthesis Report. An Assessment of the Intergovernmental Panel on Climate Change, Synthesis Report*. IPCC. doi:10.1256/004316502320517344
- Kennish, M.J., Paerl, H.W., 2010. Coastal Lagoons: Critical Habitats of Environmental Change, in: Kennish, M.J., Paerl, H.W. (Eds.), *Coastal Lagoons*. CRC Press, pp. 1–16.
- Kjerfve, B., 1986. Comparative Oceanography of Coastal Lagoons, in: Wolfe, D.A. (Ed.), *Estuarine Variability*. Academic Press, pp. 63–81.
- Madsen, O.S., Wright, L.D., Boon, J.D., Chisholm, T.A., 1993. Wind stress, bed roughness and sediment suspension on the inner shelf during an extreme storm event. *Cont. Shelf Res.* 13, 1303–1324. doi:10.1016/0278-4343(93)90054-2
- Middelboe, A.L., Sand-Jensen, K., Krause-Jensen, D., 2003. Spatial and interannual variations with depth in eelgrass populations. *J. Exp. Mar. Bio. Ecol.* 291, 1–15. doi:10.1016/S0022-0981(03)00098-4
- Spalding, M.D., Ruffo, S., Lacambra, C., Meliane, I., Hale, L.Z., Shepard, C.C., Beck, M.W., 2014. The role of ecosystems in coastal protection: Adapting to climate change and coastal hazards. *Ocean Coast. Manag.* 90, 50–57. doi:10.1016/j.ocecoaman.2013.09.007

Diachronic numerical modelling of the turbidity maximum dynamics in the macrotidal Seine estuary (France) from 1960 to 2010

Florent Grasso¹, Pierre Le Hir¹ and Nicolas Chini²

¹ IFREMER – DYNECO/DHYSED, Centre de Bretagne, CS 10070, F-29280 Plouzané, France
E-mail: florent.grasso@ifremer.fr

² ACRI-HE, "Le Grand Large", quai de la douane, 29200 Brest, France

Abstract

The estuarine turbidity maximum (ETM) is one of the main drivers of longshore and cross-shore sediment transfers in macrotidal estuaries. Besides the quantification of the ETM sediment mass and its spatial expansion, the challenge is to understand its dynamics associated with the long term (~50 years) estuary morphodynamics. This study is based on a realistic 3D hydro-sediment dynamics modelling of the Seine estuary (France) in order to quantify the influence of hydro-meteorological forcing on ETM characteristics. The diachronic analysis of years 1960, 1975 and 2010 provides understanding on the influence of the different bathymetries on the ETM dynamics. The ETM seaward migration from 1960 to 1975 and its upstream migration from 1975 to 2010 is related to extensive engineering works through the 20th century that lead to significant tidal asymmetry changes.

Introduction

The estuarine turbidity maximum (ETM) is a key pattern in estuarine sediment dynamics. This highly-concentrated zone of suspended particle matters buffers sediment exchanges between continental and coastal waters, controls channel siltation and drives bio-geo-chemical processes. The mass and the location of the ETM is known to be strongly modulated by the river discharge and the tidal range. Nevertheless, waves may also significantly affect the ETM dynamics, resuspending flushed out ETM sediments and hence accelerating ETM reformation. Besides the quantification of the ETM sediment mass and its spatial expansion, the challenge is to characterize its dynamics associated with the long term (around 50 years) estuary morphodynamics. Based on a realistic process-based numerical model, this study investigates the ETM dynamics of the macrotidal Seine estuary (France). Since the deepening of the navigation channel of Rouen, the Seine ETM has been translated downstream close to the mouth, which is exposed to strong westerly wind-waves. Here, the main objectives are to explore the ETM sensitivity to different hydrodynamic and hydrological forcing (tide, waves, river discharge) and to quantify its evolution during the last fifty years (1960-2010) due to morphological changes.

Methods

The realistic 3D numerical modelling is based on the MARS3D hydrodynamics model forced by main tidal components at the sea boundary, a realistic river discharge and wind stresses provided by a meteorological model. Waves are simulated using the WAVE WATCH III[®] model on a series of embedded computational grids, from a large-scale model of the Atlantic Ocean down to a local model at the same resolution as the circulation model. The hydrodynamics model is coupled with a multilayer sediment model for sand and mud mixtures (Le Hir *et al.*, 2011) considering the advection/diffusion of five particle classes (median diameter $d_{50} = 20, 100, 210, 800, 5000 \mu\text{m}$) and taking into account consolidation processes (Grasso *et al.*, 2015). The hydro- and sediment dynamics models were validated on the reference year 2010. This hydro-meteorological forcing was then applied on the 1960 and 1975 bathymetries. Consequently, the diachronic analysis between the three periods (1960, 1975 and 2010) consists in comparing the influence of the different bathymetries on the ETM dynamics.

Results and discussion

The simulation of year 2010 confirms that the Seine ETM location (x_{ETM}) is strongly driven by the Seine river discharge, shifting seaward during high river flow (Fig. 1a). The river-discharge detrended analysis provides insights on the tide-induced ETM location ($x_{TR, ETM}$) and bottom salinity gradient location ($x_{TR, Salinity}$) after removing the river-induced trend ($x_{TR, Salinity, ETM} = x_{(Salinity, ETM)} - x_{Q, (Salinity, ETM)}$). It reveals that the ETM would be dominated by the tidal pumping mechanism for spring tide and dominated by the salinity gradients for neap tide (Figs. 1b and c). Moreover, the tidal range change (dTR), characterizing the neap-to-spring (and spring-to-neap) period, influences significantly the ETM location through a hysteresis response due to the delay for tidal pumping and stratification to occur.

The ETM mass is highly related to the tidal range, reaching 500,000Tons for spring tide, and modulated by the tidal range changes (Fig. 2b). This relationship proves to be non-linear, with a clear resuspension increase for tidal range larger than 6 m. Surprisingly, it appeared that the river discharge did not significantly affect the ETM mass (Fig. 2a), whereas it strongly controlled the tide-averaged location (Fig. 1a). Waves were observed to substantially influence the ETM dynamics in increasing the ETM mass by 10 to 50% during energetic conditions (i.e. for waves larger than the median value), especially during high river flow when the ETM is located close to the wave-exposed estuary mouth.

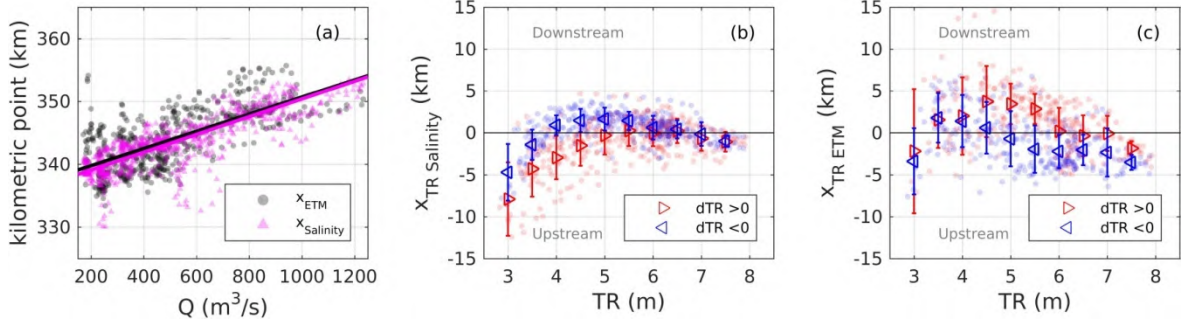


Fig. 1. 2010 period. (a) Simulated ETM x_{ETM} and salinity front $x_{Salinity}$ locations versus the Seine river discharge Q . River-discharge detrended locations of (b) near bottom salinity front $x_{TR Salinity}$ and (c) ETM $x_{TR ETM}$ versus tidal range TR for neap-to-spring ($dTR > 0$, red circles) and spring-to-neap ($dTR < 0$, blue circles) phasing. In panel (a), black and purple lines represent linear regression laws for x_{ETM} and $x_{Salinity}$, respectively. In panels (b) and (c), triangles and vertical brackets represent data average and standard deviation, respectively, associated with TR ranges for neap-to-spring (red rightward triangles) and spring-to-neap (blue leftward triangles) phasing.

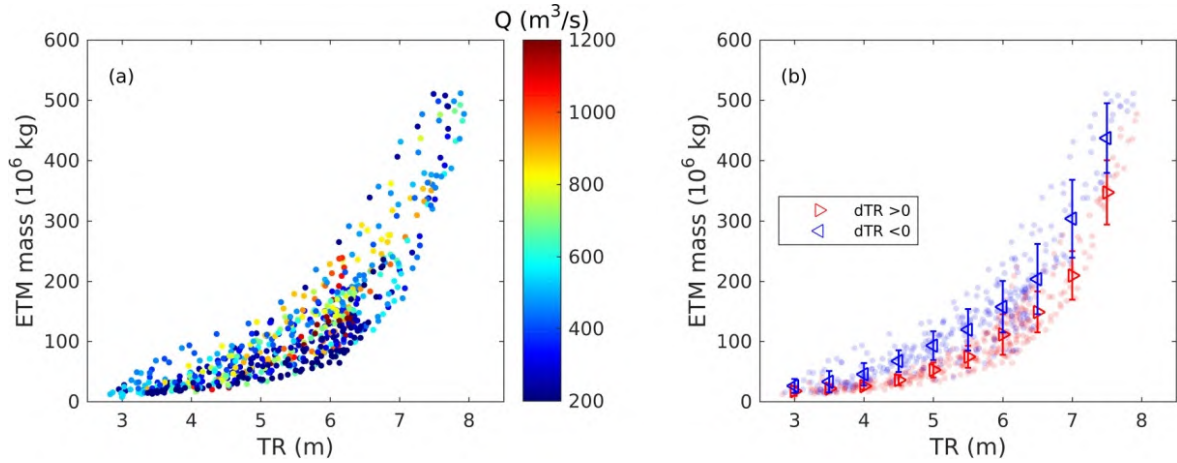


Fig. 2. 2010 period. Simulated tide-maximum ETM mass versus tidal range TR related to (a) the Seine river discharge Q and (b) neap-to-spring ($dTR > 0$, red circles) and spring-to-neap ($dTR < 0$, blue circles) phasing. In panel (b), triangles and vertical brackets represent data average and standard deviation, respectively, associated with TR ranges for neap-to-spring (red rightward triangles) and spring-to-neap (blue leftward triangles) phasing.

Measurements and simulations provide evidences that the ETM location in 2010 is situated up to 10 km upstream of the location observed by Avoine *et al.* (1981) in 1978, contrasting with the downstream migration observed from 1955 to 1978. The diachronic simulations are in agreement with these changes as the tidal asymmetry in 1975 was lower than in 1960 and 2010. It would induce a reduction of tidal pumping and thus the ETM downward location in 1975. The reduction of tidal asymmetry from 1960 to 1975 is associated with the dyking of the lower estuary in order to enhance ebb-flow currents, whereas the tidal asymmetry increasing from 1975 to 2010 is related to the estuary mouth narrowing after engineering works to extend Le Havre harbour.

Acknowledgements

This study is conducted in the framework of the ANPHYECO and HYMOSED projects funded by the Seine-Aval 5 scientific research program.

References

- Avoine, J., Allen, G., Nichols, M., Salomon, J., and Larssonneur, C. (1981), Suspended-sediment transport in the Seine estuary, France: effect of man-made modifications on estuary—shelf sedimentology, *Marine Geology*, 40(1-2):119-137.
- Grasso, F., Le Hir, P., and Bassoullet, P. (2015). Numerical modelling of mixed-sediment consolidation. *Ocean Dynamics*, 65(4):607-616.
- Le Hir P., Cayocca F., and Waeles B. (2011). Dynamics of sand and mud mixtures: A multiprocess-based modelling strategy, *Continental Shelf Research*, 31(10):S135-S149.

Quantitative clay mineralogy as provenance indicator for the recent muds in the southern North

Adriaens Rieko¹, Edwin Zeelmakers¹, Michael Fettweis², Elin Vanlierde³, Joris Vanlede³, Peter Stassen¹, Jan Elsen¹, Jan Srodon⁴, Noël Vandenberghe¹

¹ Department of Earth and Environmental Sciences, KU Leuven, Celestijnenlaan 200E, 3001 Heverlee, Belgium

² Royal Belgian Institute of Natural Sciences, OD Nature, Gulledele 100, 1200 Brussels, Belgium
E-mail: mfettweis@naturalsciences.be

³ Flanders Hydraulics Research, Berchemlei 115, 2140 Antwerp, Belgium

⁴ Institute of Geological Sciences, Polish Academy of Sciences, Research Centre in Kraków, ul. Senacka 1, PL-31002 Kraków, Poland

Introduction

In order to assess the present state of a marine sedimentary environment and to predict changes induced by natural variability, human activities or climate change, qualitative understanding and quantitative estimates of sediment fluxes and budgets are needed. Although sediment fluxes and budgets are a key element to assess the fine-grained sediment dynamics on a regional scale, data are often not available to qualitatively understand the fluxes on a time-scale longer than the duration of in-situ measurement campaigns. One of the difficulties lays in the fact that regional fine-grained sediment dynamics is the sum of all the local sources and sinks, such as rivers, coastal erosion and accretion, deposition in inter- or subtidal areas and erosion of the geological substratum that are often not well known and that reflects the recent geological history of the area. This is also the case for the fine-grained sediment transport, the coastal turbidity maximum and the cohesive sediment deposits in the French-Belgian-Dutch nearshore area and in the Scheldt estuary, where the provenance is still under debate. The existing hypotheses for the mud provenance are based on the residual flow patterns and general sedimentological considerations (e.g. Prandle et al. 1996; Fettweis et al. 2007). The aim of the current study is to make a new contribution towards qualitative and quantitative fine-grained sediment budgets and dynamics in the southern North Sea by identifying how the provenance of the fine-grained bottom and suspended sediments is related to regional and local fine-grained sediment sources.

Method

As provenance indicator clay minerals have been used. The advantage of clay minerals is the obvious abundance of these minerals in the mud deposits and in the SPM and their stability or very minor changes if any during transport between provenance and deposition areas. Clay minerals can be considered as representative tracers as the transport of fine-grained sediment occurs either in flocs or as suspended particulate matter (e.g. Irion and Zöllmer 1999). The clay minerals have been determined using the robust quantitative analyses of Środoń & McCarthy (2009) and Hubert et al. (2009, 2012).

An extensive sampling campaign was set up in different phases to characterize the clay mineral composition of the mud deposits off the Belgian nearshore (further referred to as BCS), the SPM in the English Channel and the southern North Sea, and its possible source areas. These comprise both present-day sources, which were sampled by collecting bottom mud and/or suspension water samples, outcrop material and older, geological sources, which were sampled from borehole core material. For each source area, the clay mineral composition <2µm, referred to as the clay fraction, was quantified and compared with the mud composition from the BCS.

Results

The clay mineral compositional field for each analyzed source area is shown in Figure 1 with reference to the BCS muds and SPM compositional field. This figure demonstrates that English Channel waters, outcropping Paleogene sea floor bottom and Rhine-Meuse river water and deposits have to be excluded as an important clay mineral source of the BCS muds. The BCS muds and SPM clay mineral composition is also found in the SPM occurring in the Dutch coastal waters. This demonstrates that the clay minerals in the Dutch coastal waters do not originate from the Rhine-Meuse River but have as major source the turbidity maximum overlying the BCS muds. The turbidity maximum in the Belgian nearshore area is thus formed by erosion of the BCS mud.

The close relationship between the mud from the Scheldt estuary and the BCS mud raised the question whether the estuary effectively discharges the mud to the BCS where it is deposited or whether the inverse happens and BCS mud is imported into the estuary by tidal currents. As demonstrated in Figure 1, this combined fluvial discharge clay mineral composition plots very close

to the Scheldt estuary and BCS mud composition. It can be concluded that the BCS mud composition can only be produced by Scheldt river system.

The current tidal regime of the Scheldt estuary is, however, marine-dominated with only small amounts of fluvial mud being discharged into the North Sea (Verlaan, 2000). Presently, marine SPM dominates the estuary. This apparent contradiction with the results of the clay mineral provenance analysis can only be satisfactorily solved if the short period of hydrodynamic and sediment flux measurements in the estuary since the start of the measurements represents an unusual situation compared to the much longer period before when larger amounts of fluvial mud was exported from the river basin to the sea. The geological history suggest that the mud deposition with the BCS clay mineral composition has started since a few 100.000 years in contrast to the present hydrodynamics in the estuary and the coastal zone that exhibits a fine-grained sediment flux from out of the estuary towards inside. A consequence of this analysis is that the modern mud is derived from the erosion and resuspension of previously deposited mud. Resuspended muds contribute to a large part to the coastal turbidity maximum and represent a significant source of material in the estuary itself.

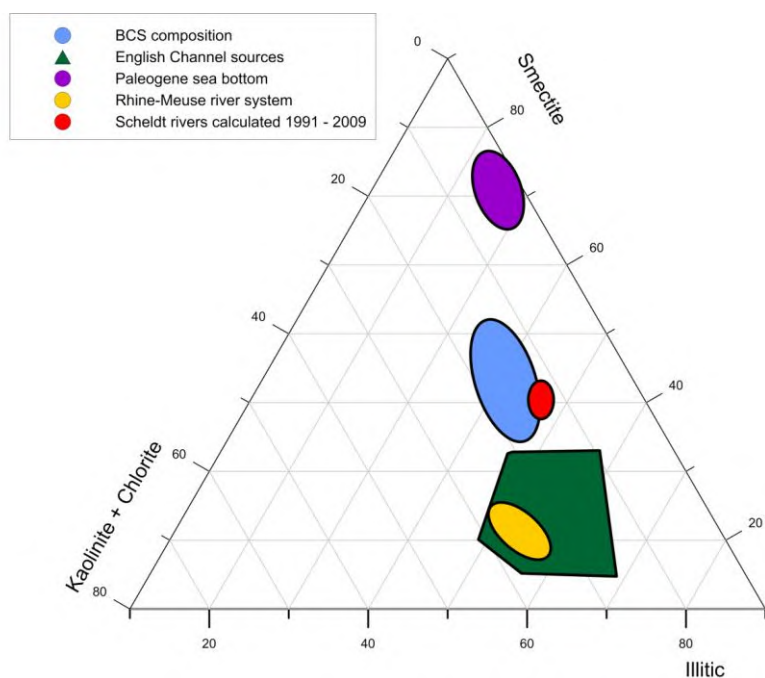


Fig. 1: Triangular diagram of the quantitative clay composition $<2\mu\text{m}</math> of the different analyzed regional sources and comparison with the compositional domain of the Belgian nearshore area (BCS).$

References

- Fettweis M, Nechad B, Van den Eynde D. (2007). An estimate of the suspended particulate matter (SPM) transport in the southern North Sea using SeaWiFS images, in-situ measurements and numerical model results. *Continental Shelf Research*, 27, 1568–1583.
- Hubert F, Caner L, Meunier A, Lanson B. (2009). Advances in characterization of the soil clay mineralogy using X-ray diffraction: from decomposition to profile fitting. *European Journal of Soil Science*, 60, 1093-1105.
- Hubert F, Caner L, Meunier A, Ferrage E. (2012). Unraveling complex $<2\mu\text{m}</math> clay mineralogy from soils using X-ray diffraction profile modeling on particle-size sub-fractions: Implications for soil pedogenesis and reactivity. *American Mineralogist*, 97, 384-398.$
- Irion G, Zöllmer V. (1999). Clay mineral associations in fine-grained surface sediments of the North Sea. *Journal of Sea Research*, 41, 119-12.
- Prandle D, Ballard G, Flatt D, Harrison AJ, Jones SE, Knight PJ, Loch SG, McManus JP, Player R, Tappin A. (1996). Combining modelling and monitoring to determine fluxes of water, dissolved and particulate metals through the Dover Strait. *Continental Shelf Research*, 16, 237-257.
- Srodon J, McCarty DK. (2009). Surface area and layer charge of smectite from CEC and EGME/H₂O-retention measurements. *Clays and Clay Minerals*, 56, 155–174.
- Verlaan PAJ. (2000). Marine vs Fluvial Bottom Mud in the Scheldt Estuary. *Estuarine, Coastal and Shelf Science* 50, 627-638.

Seasonal variation of sediment flocculation and the modeling thereof as function of biochemical factors

Zhirui Deng¹, Qing He¹, Claire Chassagne², Johan C. Winterwerp²

¹ State Key Laboratory of Estuarine and Coastal Research, East China Normal University, Zhongshan N. Road 3663, Shanghai 200062, China
E-mail: Z.Deng-1@tudelft.nl

² Delft University of Technology, Department of Geosciences and Engineering, 2628 CN Delft, NL, P.O. box 5048, the Netherland

Abstract

The flocculation process and modelling of suspended sediment transport in estuarine regions is a hot topic in estuarine science [Winterwerp, 1999]. The flocculation is greatly influenced by biochemical parameters [De Lucas Pardo, 2014]. In this paper, we analyse the impact of algae on the processes of flocculation in the Yangtze Estuary, and we identify the mechanisms which are responsible for their changes. The amount of algae (phytoplankton biomass) is linked to the chlorophyll α concentration which we measured [Uncles *et al.*, 1998]. The measurements were performed in the maximum turbidity zone. The seasonal variations of phytoplankton lead to changes in the flocculation dynamics and the composition of suspended particle matter. We recorded the floc size changes in the Yangtze Estuary and we found that: (1) the flocs are significantly influenced by tidal dynamics, as the floc size during slack water is larger than ebb tide and flood tide, (2) there is a correlation between the Chlorophyll concentration and sediment concentration, (3) the floc size is correlated to the algae-sediment mass ratio, (4) in winter, with high salinity and small river discharge, the region has a significant stratification and the floc size was smaller than the one in summer (fig.1).

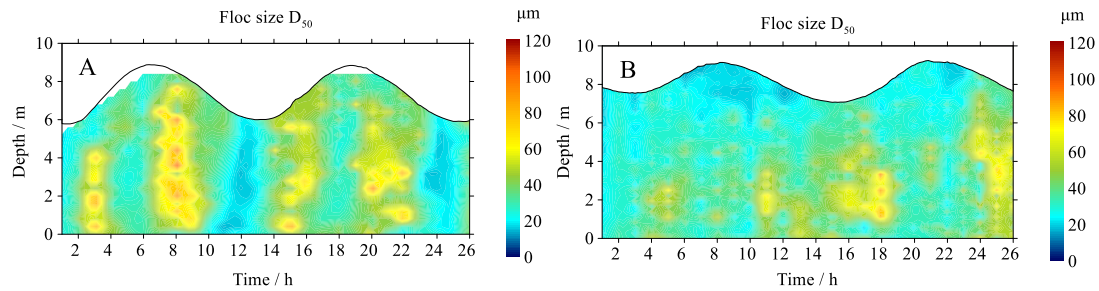


Fig. 1. The floc size distribution for different seasons ((A) summer (B) winter).

In order to better identify the parameters that influence most the flocculation and try to model it, a series of laboratory experiments were performed. Parameters such as salinity, shear rate, phytoplankton (and EPS (extracellular polymeric substances) produced by this phytoplankton) and sediment concentration were systematically varied [Mietta, 2010]. The floc size as function of time was modelled according to:

$$N_i(t) = \frac{a_1}{1+a_2 \exp\left(-\frac{t}{t_a}\right)} \left[a_3 + \exp\left(-\frac{t}{t_b}\right) \right] \quad (1)$$

where $N_i(t)$ represents the number of flocs of size i as function of time and the parameters of a_1 , a_2 , a_3 , t_a , t_b are fitted to the data. The dependence of these parameters on the environmental conditions will be discussed. the full particle size distribution (PSD) obtained from fitting each class is given in fig.2.

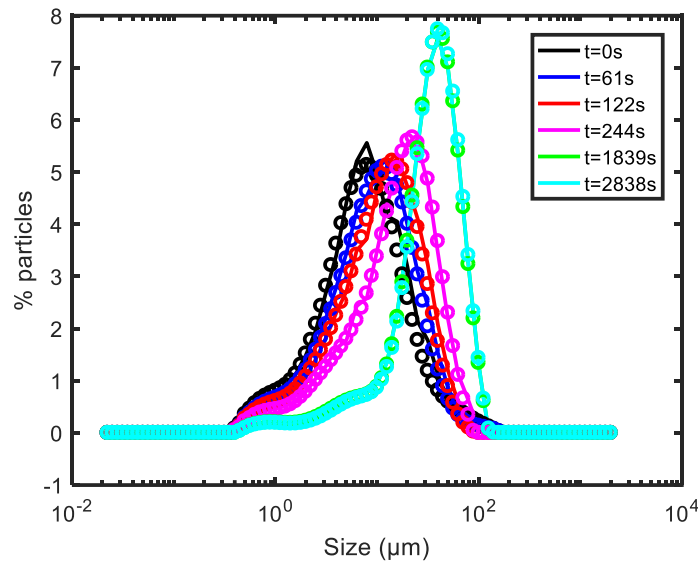


Fig. 2. The time dependent PSD of a suspension composed of 0.7g/l Yangtze sediment and 2mg/g EPS and 0.3mol/l NaCl.

We will show by comparing the lab experiments and in-situ data, that more insight can be given in the flocculation process by phytoplankton. The ultimate goal is to apply the model to in-situ flocculation data and hereby improve large scale sediment transport models.

References

- De Lucas Pardo, M. (2014), Effect of biota on fine sediment transport processes: A study of Lake Markermeer, TU Delft, Delft University of Technology.
- Mietta, F. (2010), Evolution of the floc size distribution of cohesive sediments, TU Delft, Delft University of Technology.
- Uncles, R., A. Easton, M. Griffiths, C. Harris, R. Howland, I. Joint, R. King, A. Morris, and D. Plummer (1998), Concentrations of suspended chlorophyll in the tidal Yorkshire Ouse and Humber Estuary, *Science of The Total Environment*, 210-211, 367-375, doi:10.1016/s0048-9697(98)00024-2.
- Winterwerp, J. C. (1999), On the dynamics of high-concentrated mud suspensions, TU Delft, Delft University of Technology.

Revealing suspended sediments variability in highly-turbid estuaries through spectral methods: a comparison of observations and model predictions

Isabel Jalón-Rojas¹, Sabine Schmidt², Aldo Sottolichio¹ and Katixa Lajaunie-Salla¹

¹ Univ. Bordeaux, EPOC, UMR5805, F33600 Pessac, France
E-mail: ijalonrojas@gmail.com

² CNRS, EPOC, UMR5805, F33600 Pessac, France

Motivation and Methods

Suspended particulate matter (SPM) is a key variable of estuarine systems that influences physical and biogeochemical processes. SPM concentration varies strongly over time scales ranging from second to years under the influence of multiple environmental forcings, including deterministic (tidal cycles, tidal range) and stochastic (river flow, wind, turbulence) components (Schoellhamer, 2002). Understanding the variability of SPM concentration related to each forcing is particularly important inasmuch as environmental forcings are not steady but evolve in time under multiple effects, such as climate change and human activities (Winterwerp and Wang, 2013).

The aim of this work is to quantify the variability of SPM concentrations at time scales characteristic of environmental forcings in the highly-turbid Gironde and Loire estuaries (west France). It involves identifying turbidity variability at forcing frequencies and estimating the relative contribution of these frequencies to the total variability. For this purpose, different spectral methods were combined and applied to the high-frequency multiannual turbidity time series recorded in both systems by automated monitoring networks. In particular, the Singular Spectrum Analysis (SSA) was combined with the Lomb-Scargle periodogram (LSP) for a multiannual analysis, and with the Continuous Wavelet Transform (CWT) for a seasonal analysis (Jalón-Rojas *et al.*, 2016a). This approach gives an indicator of the relative influence of different forcings on turbidity variability that allows evaluating the consequences of changes in forcings on such variability. In addition, the combined spectral methods were applied to numerical (SIAM-3D, Lajaunie-Salla *et al.*, in revision) and semi-analytical (iFlow, Jalón-Rojas *et al.*, 2016b) simulations of SPM concentrations as a validation test of the prediction of variability frequencies and their relative contribution to the total variability.

Results

Frequencies of the main environmental factors affecting turbidity variability were identified in both estuaries and subsequently grouped in three categories: river flow (hydrological regime and discharge variability), tidal range (semimonthly and monthly tidal cycles), and tidal cycles. Their relative contributions to the total turbidity variability depend on the estuarine region (lower and upper estuary) and the time scale (multiannual or seasonal) and follow similar patterns in both estuaries. On multiannual time scale (Fig. 1), the contribution of tidal forcings decreases by a factor of 2.5 up-estuary, from about 50% to 20% in the case of tidal cycles (from 15% to 6% for tidal range). In contrast, the influence of river discharge increases drastically toward upstream, from about 3% to 42-49%. On the seasonal time scale, the relative influence of forcings frequencies remains almost constant in the lower estuary, dominated by tidal frequencies (60% and 30% for tidal cycles and tidal range, respectively); in the upper reaches, it is more variable depending on hydrological regime, even if tidal frequencies are responsible for more than half of the turbidity variance.

The interest of these quantifications was further discussed: (1) as indicator of long-term changes in turbidity due to the potential evolution of environmental factors and (2) to compare nearby and overseas systems. This includes a comparison of trends between the Gironde, the Loire, the San Francisco Bay (Schoellhamer, 2002) and the Blyth (French *et al.* 2008) estuaries that shows a similar influence of tidal frequencies on turbidity in their lower reaches.

Finally, the application of spectral methods to concentration prescribed by a numerical model (SIAM-3D) in the Gironde estuary suggested that the current parametrization of the model underestimates intratidal variability, in particular the quarter-diurnal. The parameterization of setting velocity was optimized in order to reproduce SPM variability and turbidity maximum dynamics. Semi-analytical predictions from iFlow showed a good approximation to observations of the proportion of the semi-diurnal and quarter-diurnal variabilities. Interestingly this approach allowed quantifying the percentage of the variance that this idealized model is overestimating for these two time scales at the expense of higher variabilities frequencies.

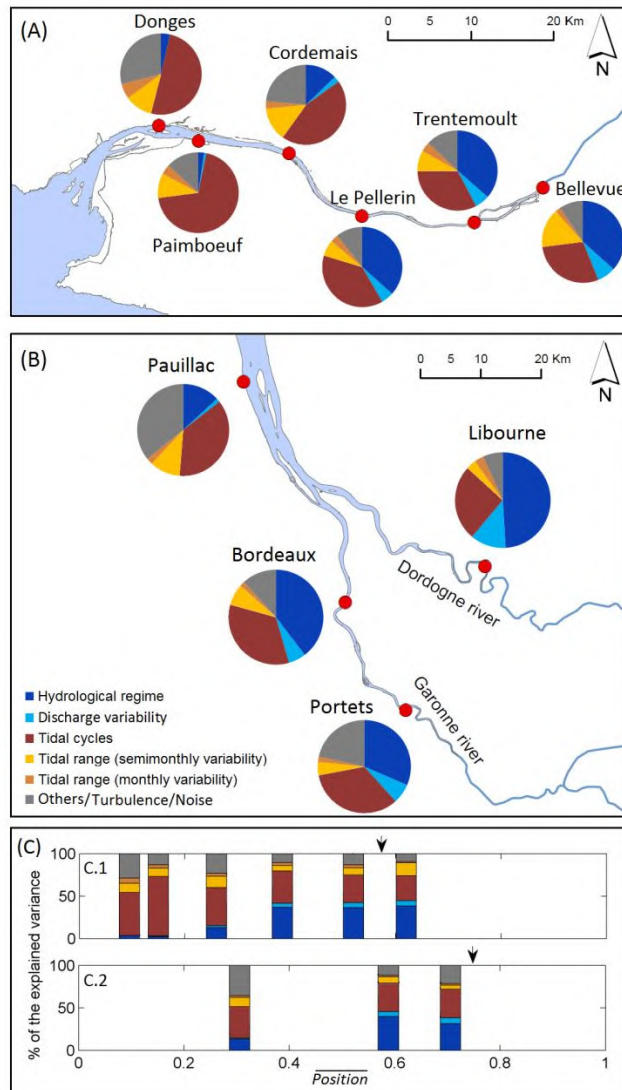


Fig. 1. Contribution (%) of each forcing to turbidity variability, estimated from the application of SSA to time series of the Loire (A, C.1) and Gironde (B, C.2) estuaries. In (C) the distance from the mouth of each station is normalized by the total length of the corresponding estuary (Position) and only the best documented axis of the Gironde (Gironde-Garonne tidal river) is plotted.

References

- French, J.R., Burningham, H., Benson, T. (2008). Tidal and Meteorological Forcing of Suspended Sediment Flux in a Muddy Mesotidal Estuary. *Estuaries and Coasts*, 31:843–859.
- Jalón-Rojas, I., Schmidt, S., Sottolichio, A. (2016a). Evaluation of spectral methods for high-frequency multiannual time series in coastal transitional waters: advantages of combined analyses. *Limnol. Oceanogr. Methods*, 14(6):381–396.
- Jalón-Rojas, I., Sottolichio, A., Dijkstra, Y., Schuttelaars, H., Hanquiez, V., Brouwer, R., Schmidt, S. (2016b). Multidecadal evolution of tidal patterns in a highly turbid macrotidal river and implications for sediment dynamics. *Book of Abstract, 18th PECS*, 9-14 October, The Netherlands.
- Lajaunie-Salla, K., Wild-Allen, K., Sottolichio, A., Thouvenin, B., Litrico, X., et Abril, G. (in revision). Impact of urban effluents on summer hypoxia in the highly turbid Gironde 1 estuary, applying a 3D model coupling hydrodynamics, sediment transport and biogeochemical processes, *Journal of Marine Systems*.
- Schoellhamer, D.H. (2002). Variability of suspended-sediment concentration at tidal to annual time scales in San Francisco Bay, USA. *Cont. Shelf Res.*, 22:1857–1866.
- Winterwerp, J.C., Wang, Z.B. (2013). Man-induced regime shifts in small estuaries—I: theory. *Ocean Dyn.*, 63:1279–1292.

Mud dynamics in the harbor of Zeebrugge

Joris Vanlede^{1,2}, Arvid Dujardin^{3,1} and Michael Fettweis⁴

¹ Department of Mobility and Public Works, Flanders Hydraulics Research, Berchemlei 115, B-2140 Antwerp, Belgium
E-mail: joris.vanlede@mow.vlaanderen.be

² Faculty of Civil Engineering and Geosciences, Delft University of Technology, Delft, The Netherlands

³ Antea Group, Buchtenstraat 9, B-9051 Gent, Belgium

⁴ Royal Belgian Institute of Natural Sciences, Operational Directorate Natural Environment, Gulledele 100, B-1200 Brussels, Belgium

Abstract

One year of SPM concentration (SPMC) and Velocity data are analyzed to gain insight in the mud dynamics in the harbor of Zeebrugge. Seasonal dynamics are inferred from satellite images, depth soundings and SPMC data.

Study Site

The harbor of Zeebrugge is situated in the coastal turbidity maximum area along the Belgian coast (southern North Sea). About 5,3 million tons (dry matter) of mainly fine-grained sediments is dredged annually in the port (15.000 TDS/day). The fluid mud inside the port has a mean layer thickness of up to 3m in front of the entrance of the Albert 2 dock (see Figure 4).

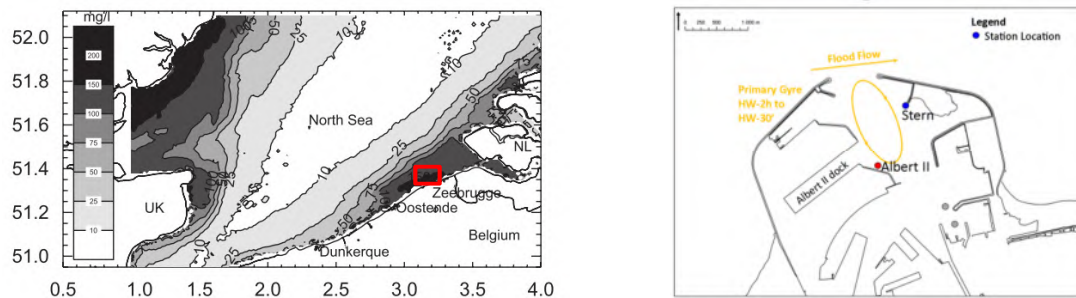


Figure 1 - Depth averaged SPM in Southern North Sea (left, Fettweis, 2007) and harbor of Zeebrugge (right)

Measurements at fixed locations inside the harbor

SPM concentration and current velocity were measured at four locations inside the harbor (see Figure 1) at two depths in the water column. Each measuring point was equipped with a point velocimeter (Aquadopp), an OBS3+ and a CT-probe (Valeport 620). The data were collected every 10 minutes for a measurement campaign lasting 400 days (March 2013 to April 2014).

The time series of SPM concentration are split-up into individual tidal cycles, and grouped according to neap, average and spring tide conditions in an ensemble analysis to study tidal dynamics.

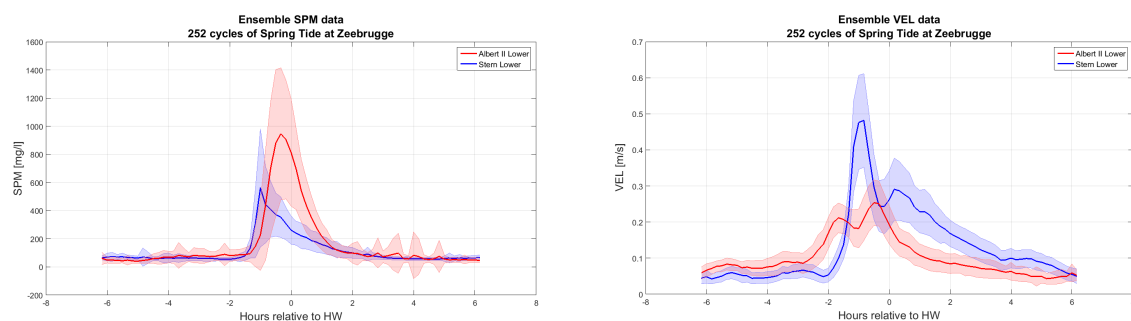


Figure 2 - Ensemble analysis of SPMC (left) and velocity data (right) for the lower set of sensors at locations Stern (in blue) and Albert II (in red) during spring tide conditions

Natural Evolution of the Top of the Mud Layer

The top of the mud layer is measured by the 210 kHz echo sounder reflector. A simple volume balance is set up to decompose the measured depth change Δh^m in the effect of dredging Δh^d and the natural evolution Δh^n .

$$\Delta h^m = \Delta h^n + \Delta h^d$$

$$\Delta h^d = -\frac{m^d(\rho_g - \rho_w)}{A \rho_g(\rho_b - \rho_w)}$$

The natural evolution Δh^n of the top of the mud layer corresponds to the cumulative effect of resuspension and consolidation (negative sign) and deposition (positive sign) and is calculated from daily depth soundings in Albert II dock (Figure 3).

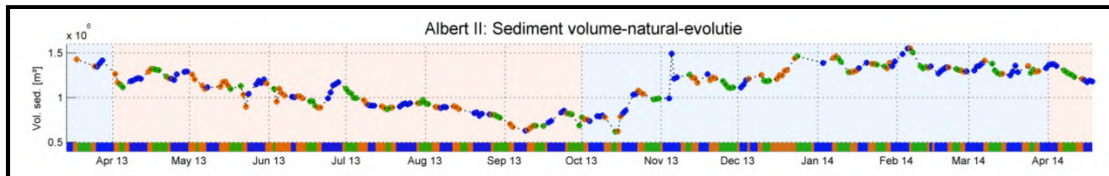


Figure 3 - Natural evolution of the mud volume in Albert II-dock during summer (red background) and winter (green background). Colored dots and (baseline) show tidal conditions: neap tide (green), average tide (orange) and spring tide (blue).

Results and Discussion

Intra-tidal variation

Both SPMC and velocity peaks at location Albert II are 50 minutes delayed to location Stern (Figure 2). The peak concentration at Albert II is higher than at Stern, even though the velocity is lower. This is explained by sediment being advected in the harbor and transported in a primary gyre, and settling out between locations Stern and Albert II. This is consistent with the analysis of Vanlede et al. (2014), who showed that horizontal transport is the most important component of the gross sediment exchange at the harbor mouth of Zeebrugge, and that most horizontal sediment exchange happens from 2h before high water to high water.

Spring-neap variation

Sediment import into the harbor during spring tide is 3 (2 to 4) times higher than during neap tide. This is consistent with the spring-neap variation of SPMC observed at a nearby station in the North Sea and with the spring-neap variation of peak SPMC observed inside the harbor.

Seasonal Variation

The mud volume in the Albert II dock is largest in winter, and reaches a minimum at the beginning of autumn (Figure 3). Density profiles also show that the sediment layers are less consolidated in winter than in summer. Figure 4 shows a striking seasonal pattern in the shape of the mud layer in the Albert II dock. Where the top of the mud layer is flat in winter, it shows a height difference of 1m (max. slope 1/400) in summer. The seasonal variations are believed to be linked to seasonal variations in the floc properties of the SPM (Fettweis & Baeye, 2015) that might influence consolidation and strength properties of the bed.

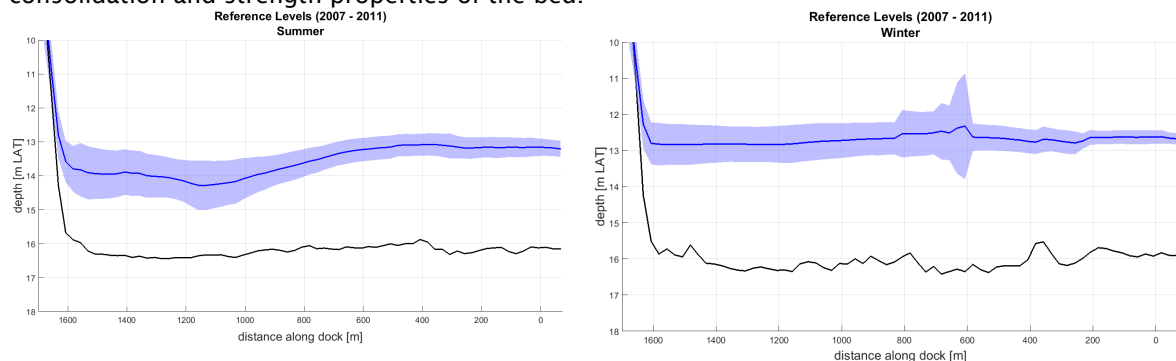


Figure 4 - Seasonal variation of levels in Albert II dock. 210 kHz level (and 1σ) in blue for summer (left) and winter (right). 33 kHz in black.

References

Fettweis, M., Baeye, M., 2015. Seasonal variation in concentration, size and settling velocity of muddy marine flocs in the benthic boundary layer. *J. Geophys. Res.* 120, 5648-5667. doi: 10.1002/2014JC010644

Vanlede, J., & Dujardin, A. (2014). A geometric method to study water and sediment exchange in tidal harbors. *Ocean Dynamics*, (11), 1631-1641. doi:10.1007/s10236-014-0767-9

On best practice for in situ high-frequency long-term observations of suspended particulate matter concentration using optical and acoustic systems

Fettweis Michael¹, Rolf Riethmüller², Romaric Verney³, Marius Becker⁴, Joan Backers¹, Matthias Baeye¹, Marion Chapalain³, Stijn Claey⁵, Jan Claus⁶, Tom Cox⁷, Julien Deloffre⁸, Davy Depreiter⁶, Flavie Druine⁸, Götz Flöser², Steffen Grünler⁹, Frederic Jourdin¹⁰, Robert Lafite⁸, Janine Nauw¹¹, Bouchra Nechad¹, Rüdiger Röttgers², Aldo Sottolichio¹², Wim Vanhaverbeke¹, Thomas Van Hoestenbergh¹³, Hans Vereecken⁵

¹ Royal Belgian Institute of Natural Sciences, OD Nature, Gulledele 100, 1200 Brussels, Belgium
E-mail: mfettweis@naturalsciences.be

² Helmholtz-Zentrum Geesthacht, Institute for Coastal Research, Max-Planck-Str. 1, 21502 Geesthacht, Germany

³ IFREMER, Hydrodynamics and Sediment Dynamics Laboratory (DYNECO/PHYSED), BP 70, 29280 Plouzané, France

⁴ MARUM, Centre for Marine Environmental Sciences, University of Bremen, Leobener Str. 8, 28359 Bremen, Germany

⁵ Flanders Hydraulics Research, Berchemlei 115, 2140 Antwerp, Belgium

⁶ IMDC, Van Immerseelstraat 66, 2018 Antwerp, Belgium

⁷ University of Antwerp, Ecosystem Management Research group, Universiteitsplein 1C -C.0.32, 2610 Wilrijk, Belgium

⁸ Normandie University Rouen, UMR CNRS 6143 M2C, 76821 Mont Saint Aignan, France

⁹ Bundesanstalt für Wasserbau, Wedeler Landstr. 157, 22559 Hamburg, Germany

¹⁰ Service Hydrographique et Océanographique de la Marine (SHOM), 13 rue du Chatellier, 29228 Brest, France

¹¹ Royal Netherlands Institute for Sea Research, PO Box 59, 1790 AB Den Burg, The Netherlands

¹² University of Bordeaux, EPOC, UMR5805, 33600, Pessac, France

¹³ Fluves, Waterkluiskaai 5, 9040 Gent, Belgium

Abstract

Water clarity or turbidity is an important parameter to understand the marine ecosystem and is mainly controlled by suspended particulate matter concentration (SPMC). Measurements of SPMC spanning long time and large spatial scales have therefore become a matter of growing importance in the last decades. On many places worldwide observation platforms were installed to capture the temporal and spatial SPMC variability on scales ranging from turbulent fluctuations to entire basins. The infrastructure on which the sensors are attached is as diverse as the time scale of the processes studied, and includes fixed and moving platforms or a combination of both. The same holds for SPMC itself that may cover the range from very low to hyper-turbid conditions and concerning its composition from organic to mineral and from non-cohesive to cohesive properties.

Long-term in-situ measurements of SPMC involve in general one or several optical and acoustical sensors of similar or different technical specifications and, as the ground truth reference, gravimetric measurements of filtered water samples. The combination of indirect and reference measurements require two main calibration steps (sensor and model parameter calibration) at different moments during the workflow in order to extract reliable and homogeneous SPMC. These calibration steps are essential to be able to relate possible changes in calibration constants (sensor and model parameter) to sensor degradation or to natural variability in SPM inherent properties. The SPMC in long-term measurements is thus a surrogate of the real SPMC. A variety of parameters, particle (floc) size and composition have an impact on the optical and acoustical inherent properties of the SPM and thus on the sensor output. In case of long-term measurements, where multiple methods are often used in parallel, different sensor SPM concentration are obtained that represents surrogates or proxies that are not necessarily the same

The estimation of SPMC by optical and acoustical surrogates generally results from the combination of a number of technically independent calibration measurements and regression or inverse models. This includes all aspects of the measuring strategy, from the planning of the measurements to the

measurements itself and the post processing of the data (Figure 1). As long as measurements are carried out during a cruise with staff and laboratories ready to control the proper functioning of sensors and to react on changes in the actual field conditions, uncertainties in the separate steps can be minimized and errors quantified to some degree or even avoided. The situation is different for autonomous, long-term implementations or large-scale observation networks. The parallel or consecutive operation of numerous sensors requires additional (inter-)calibration effort to assure data homogeneity. Variabilities in the state of the studied system change the inherent particle properties which may require repeated field surveys for water sampling; electronic drift, mechanical threats or growing coverage of sensor transmitter/receiver windows by living (biofouling) or non-living matter (fouling) requires regular maintenance and sensor cleansing with sensor monitoring against well-defined references.

Direct or indirect measurements of SPMC are thus inherently associated with a number of uncertainties along the whole operational chain from planning over laboratory work, to system problems during mostly unsupervised deployment and to converting the observed continuous proxy values of optical and acoustical signals to SPMC. The aim of the study is to present and discuss potentials and limitations related with the use of optical and acoustical backscatter sensors, to describe challenges and yet unsolved problems with long-term observations of SPMC and to formulate recommendations as a basis to acquire quality-assured SPMC data sets. On the basis of examples the main sources of errors as well as means to quantify and reduce the uncertainties associated with SPMC measurements are illustrated.

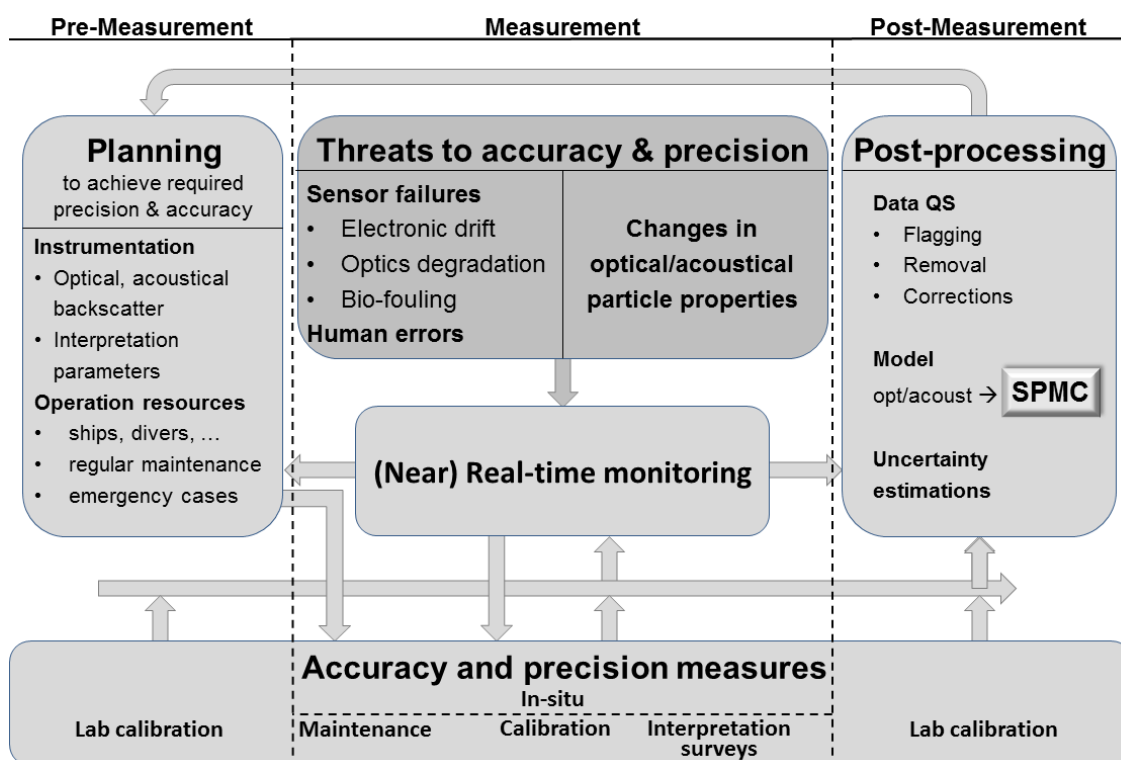


Fig. 1. Workflow of activities and tasks to be performed in long-term SPMC measurements. The arrows indicate the flow of information between the tasks and activities over the measurement phases. The measurement phases are plotted in serial order, but may overlap in the course of long-term installations.

Response of SPM concentrations to storms in the North Sea: investigating the water-bed exchange of fine sediments

Hendriks Erik^{1,2}, Bram C. van Prooijen¹, Johan C. Winterwerp¹ Stefan G.J. Aarninkhof¹, Carola M. van der Hout³ and Rob Witbaard³

¹ Department of Hydraulic Engineering, Civil Engineering and Geosciences, Delft University of Technology, Delft, the Netherlands. E-mail: H.C.M.Hendriks@tudelft.nl

² Deltares, Delft, the Netherlands

³ Royal Netherlands Institute for Sea Research (NIOZ), Den Burg (Texel), the Netherlands

Introduction

Shallow coastal seas are subject to an increasing pressure by offshore operations. Further to a direct influence these operations impose on benthic and pelagic organisms, an indirect influence is caused by changes in sediment dynamics and morphodynamics. Temporal variations in SPM have a large effect on the timing and rate of primary production, thereby also affecting higher trophic levels. Field measurements along the Dutch coast indicate significant seasonal variations in concentrations of SPM (Suijlen and Duin, 2001; Witbaard et al., 2015). These seasonal variations originate from a marked seasonality in wind climate and the occurrence of storms. During storms, increases in SPM occur simultaneously in large parts of the Dutch coastal zone of the North Sea (Suijlen & Duin 2001), demonstrating that on short timescales, the vertical exchange between the sea bed and the water column is dominant. Model concepts with two discrete seabed layers (a fluffy top layer and a sandy lower layer) turned out to capture these fine sediment dynamics, see van Kessel *et al.* (2011). However, the underlying physical processes resulting in the water-bed exchange of fines are still to be unravelled.

Therefore, this study aims to investigate the resuspension of fines from the bed during and after storms, accounting for the tidal variation due to the spring-neap tide cycle. This will lead to a more specific conceptualization and related parameterization of the water-bed exchange, thereby enabling to study both the direct and indirect impact of offshore operations.

Methods

To investigate the water-bed exchange of fines, data from a bottom lander is analysed. The lander was placed 1.2 km off the Dutch coast, at Egmond aan Zee (see Figure 1). It collected data on hydrodynamics and sediment concentrations continuously during a period of 21 months, from March 2011 until November 2012 (van der Hout *et al.*, submitted). The following data collected with the lander are analysed: (i) current velocity over the entire water column, measured by an upward looking RDI ADCP; (ii) near bed velocities, measured with a Nortek Vector current meter, positioned at 30cm above the seabed; (iii) SPM concentrations at four heights above the bottom, i.e. 30, 80, 140 and 200cm, measured with ALEC Compact-CLW's.

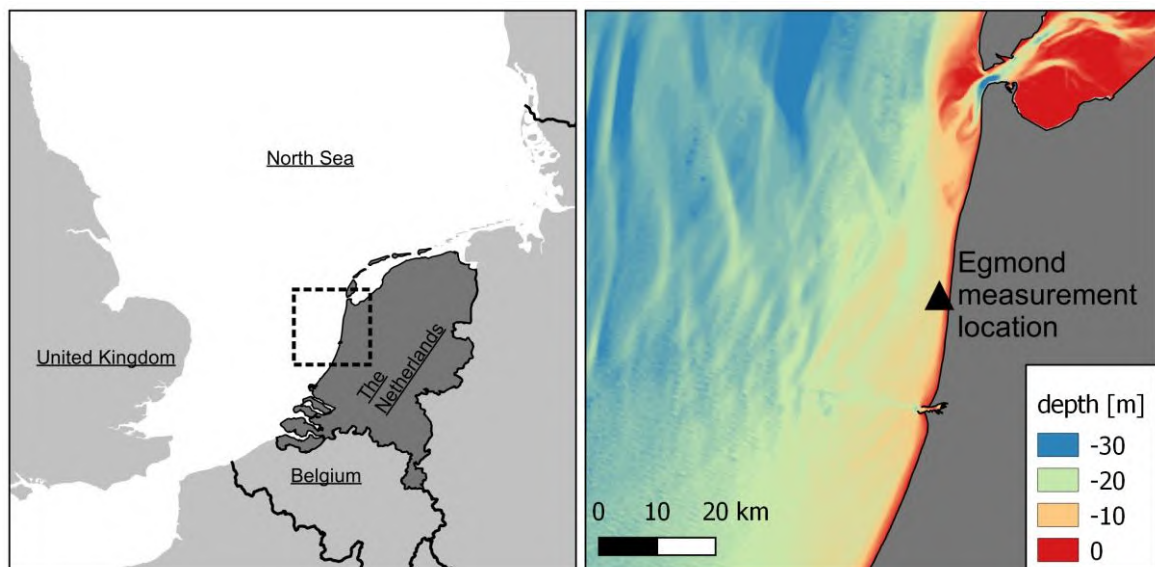


Figure 1: Location of the bottom lander, also showing the bathymetry of the study area

Results

The 21-month deployment allows comparing high-energetic conditions with low energetic conditions. Here, we highlight a period of 25 days: 10 August 2011 until 4 September 2011. Figure 2a shows the water depth variation with a dominant semi-diurnal tide and spring-neap cycle. Panel 2b shows the computed variation in bed shear stress by waves and currents, whereas panel 2c shows measured SPM concentrations at 0.3 and 2.0 meters above the bed (mab). Two storm events can be distinguished, and are indicated by grey bands. During these storms, the bed shear stress increases due to wave action. An increase in SPM concentration is also observed during this storm period. A quarterly diurnal cycle can be identified, which can be related to increased mixing during higher tidal flow velocities. After the storm events, the bed shear stress decreases, but the SPM concentrations remained high for approximately a week. During the period from 12 August - 26 August (i.e. between the storm events) similar bed shear stresses lead to large differences in SPM concentrations. The first week after the storm event is characterized by generally high SPM concentrations, whereas SPM concentrations are low throughout the second week after the storm event. This indicates that more fine sediment is available for resuspension in the study area after the storm event. After approximately a week, the response of SPM concentrations to the computed bed shear stress is similar to pre-storm response. Before the onset of the second storm, around the 28th of August, SPM concentrations at 0.3 mab are lower than 100 mg/l. After the storm event, similar bed shear stresses lead to SPM concentrations of almost 500 mg/l at 0.3 mab.

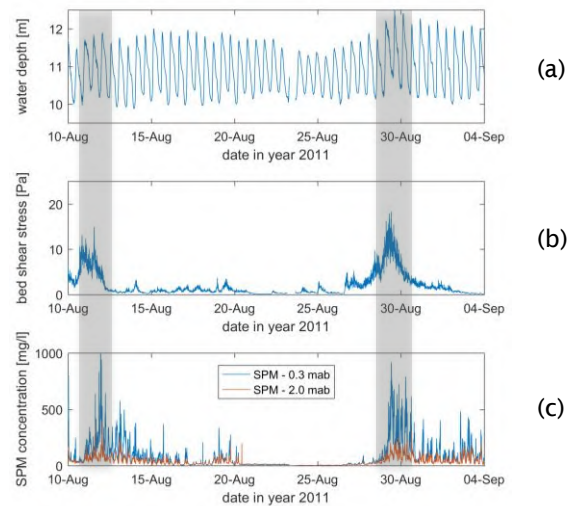


Figure 2: Measured water levels (a), computed bed shear stress (b) and measured SPM concentrations at 0.3 and 2.0 meters above the bed (c), from 10 August 2011 until 04 September 2011.

Interpretation and Conclusions

The variations in SPM concentration indicate that waves play a crucial role in remobilizing fine sediment from the mostly sandy seabed. After remobilization, tidal flow is essential for mixing the sediment higher up in the water column. The resulting SPM-time series show a semidiurnal cycle (mixing by the flow) modulated by the wave-induced bed shear stress. Before and shortly after storms, the response of SPM concentrations to similar bed shear stresses is clearly different. This difference can be attributed to the burial of fines into the seabed. However, this burial is not instantaneous but takes approximately one week of calm conditions. Hence, the predominant processes that lead to the burial of fine sediments in the seabed should work on these timescales as well.

In conclusion, the North Seabed depicts a profound memory to previous meteorological (and seasonal) conditions, which needs to be captured in any model describing the water-bed exchange processes in this sandy system.

Acknowledgements

This work is part of the SANDBOX project, funded by NWO-ALW. The additional funding by Boskalis is also appreciated. Data collection has been made possible by financial support of the LaMer foundation and a grant of Ecoshape within the framework of Building with Nature.

References

- [Suijlen, J.M., R.N.M. Duin, 2001.](#) Variability of near-surface total suspended matter concentrations in the Dutch coastal zone of the North Sea. Climatological study on the suspended matter concentration in the North Sea. Report RIKZ/OS/2001.150X.
- [Van der Hout, C.M., R. Witbaard, M.J.N. Bergman, G.C.A. Duineveld, M.J.C. Rozemeijer, T. Gerkema, Submitted.](#) The dynamics of suspended particulate matter (SPM) and chlorophyll-a from intratidal to annual time scales in a coastal turbidity maximum. Journal of Sea Research.
- [Van Kessel, T., J.C. Winterwerp, B.C. van Prooijen, M. van Ledden, W. Borst, 2011.](#) Modelling the seasonal dynamics of SPM with a simple algorithm for the buffering of fines in a sandy seabed, Continental Shelf Research, Vol 31, No 10-suppl, S124 -S134, doi:10.1016/j.csr.2010.04.008.
- [Witbaard, R., Duineveld, G.C.A., Bergman, M.J.N., Witte, H.I., Groot, L., Rozemeijer, M.J.C., 2015.](#) The growth and dynamics of *Ensis directus* in the near-shore Dutch coastal zone of the North Sea. J. Sea Res. 95, 95-105.

Regime shifts in a D3D schematized Scheldt model: recent progress

M A de Lucas Pardo¹, Y Dijkstra^{1,2}, B van Maren^{1,2}, J Vroom¹, T van Kessel¹, J C Winterwerp^{1,2}

¹ Deltares

² Delft University of Technology

Abstract

The Ems and Loire evolved into hyper-turbid estuaries in the course of the 20th century. Winterwerp et al. (2013 a, b) argued that narrowing and deepening of these rivers induced a regime shift towards these hyper-turbid conditions. This regime shift was presumed to be driven by a positive feed-back between tidal amplification, tidal asymmetry and sediment-induced drag reduction. As also the Sea Scheldt was/is subject to narrowing and deepening, Winterwerp et al. reasoned that also this river may be at risk to become hyper-turbid.

Currently, these arguments have not yet been sustained with quantitative data and/or model results. Therefore a number of in-depth studies have been initiated analysing such a regime shift. The study in the current report is aimed at contributing to these studies and the discussion on the causes of these regime shifts. The objective of this work is to assess whether a regime shift towards hyper-turbid conditions can be simulated with a simple state-of-the-art process-based numerical model. For this purpose, we have developed a schematized Delft3D model of the Sea Scheldt.

Several model configurations were tested aiming to observe sediment accumulation in the estuary and, eventually, a transition to a hyper turbid regime. These model configurations are defined by the inclusion of certain sediment transport processes. These are: the initial presence of sediments at the bed of the river; erosion and deposition of sediments from the water column to the bed and vice versa; the type of bed model (we have tested the standard D3D bed model and the buffer layer model of D3D) and the associated sediment transport processes (the inclusion of a fluff layer and of a deposition efficiency term is the main difference); in none of the simulations, the bed level is updated, i.e. all sediments depositing on the bed are taken into the bed, but without bed level changes.

The table below gives an overview of the model configurations tested in this study, where the sediment transport processes considered for each configuration are indicated. Salinity is considered in all model configurations. Note that one configuration with no sediments in the system is tested as well, to establish the equilibrium salinity penetration without the influence of sediments.

model configuration	type of bed model	sediment in the model	sediment at bed initially	erosion and deposition
1	standard D3D	no	no	no
2	standard D3D	yes	no	no
3	standard D3D	yes	no	yes
4	standard D3D buffer layer	yes	yes	yes
5	model D3D	yes	no	yes

Hyper-turbid conditions have not developed under the studied set of parameters yet. However, a number of important conclusions can be drawn from the current work. General conclusions from the study of model configurations:

- Erosion and deposition, in combination with tidal asymmetry, are responsible for the transport of sediments into the estuary. This is important, since without suspended sediments distributed throughout the whole system, hyper turbid conditions cannot develop under any circumstance.
- The presence of internal asymmetry (vertical stratification in sediment concentration) contributed to further increase the import of sediments into the system via two mechanisms: a. the combination of sediment mixing during high energetic conditions (and stratification during low energetic conditions) and tidal asymmetry. b. The decrease in eddy viscosity that a fluid mud layer produces and the associated tidal amplification.
- With erosion and deposition allowed in the model, and with the effect of internal asymmetry, sediment keeps accumulating in the system after 66 months.
- The initial amount of sediment in the system does not affect the equilibrium suspended sediment concentration in the water column, which is determined by the balance between erosion and deposition (given a constant sediment supply).

Within each of the studied model configurations, the sensitive of a selection of sediment and hydrodynamic parameters in the import of sediments into the river

has been studied as well. The most relevant results are from this sensitivity analysis are:

- In a starved bed, an increase in the settling velocity leads to an increase in the bed thickness and thus of the eroded sediment and the suspended sediment concentration.
- A starved bed can become alluvial by increasing the sediment input into the system.
- A more erosive bed increases the sediment concentration in the water column, but decreases the overall import of sediments into our schematized estuary.
- Spring-neap variations (or episodic erosion events) are key to mobilize the stock of sediments at the bed, increasing the sediment concentration in the water column. Once a certain concentration is reached in the water column, the rate at which the overall sediment concentration increases seems to become linear.

References

Winterwerp, J. C., & Wang, Z. B. (2013). Man-induced regime shifts in small estuaries—I: theory. *Ocean Dynamics*, 63(11-12), 1279-1292.

Winterwerp, J. C., Wang, Z. B., van Braeckel, A., van Holland, G., & Kösters, F. (2013). Man-induced regime shifts in small estuaries—II: a comparison of rivers. *Ocean Dynamics*, 63(11-12), 1293-1306.

How important is mud transport on large scale estuarine and deltaic morphodynamics?

Leicheng Guo¹, Chunyan Zhu^{1,2}, Qing He¹

¹ State Key Lab of Estuarine and Coastal Research, East China Normal University, Shanghai 200062, China, E-mail: candleguol@gmail.com

² Faculty of Civil Engineering and Geosciences, Delft University of Technology, PO-Box 5048, Delft, the Netherlands

Abstract

Sediment transport provides a critical bridge between hydrodynamics and morphodynamics. Sediment transport behaviour has obvious impacts on morphodynamic development. Long-term morphodynamic modelling enables examination of large scale morphological patterns, such as channel-shoal patterns in estuaries and deltaic channel structures. Non-cohesive sand is mostly used as the material in shaping morphology. However, most of estuaries and deltas in nature are partly or fully dominated by cohesive sediment or mud. There are researches on sand-mud interactions and their implications on total sediment transport (van Ledden, 2003). It is increasingly aware that adding mud to the system can make a big differences on the large scale morphodynamic development behaviour (Edmond and Slinger, 2009; Gelynese et al., 2010; Caldwell and Edmond, 2014). However mud transport is notoriously difficult to be defined properly in the model given the combined sensitivity to a few fundamental parameters (Partheniades, 1965; Mehta, 2014). It is thus not clearly known how mud have controls on development of large scale morphodynamics and the sensitivity to the mud property.

In this work we construct a long-term morphodynamic model based on the DELFT3D in an idealized 300 km long and 100 km wide river-estuary-sea system. Long-term simulation is assisted by the morphological factor approach. Both sand and mud are put on the river bed for erosion while the river supplies mud into the system as well. Dry bed erosion is considered to stimulate sand bar and channel migrations. Sand and mud interactions are considered by defining transport layers. By varying the content of mud and the mud properties, we run a number of sensitivity scenarios under combined river and tidal forcing.

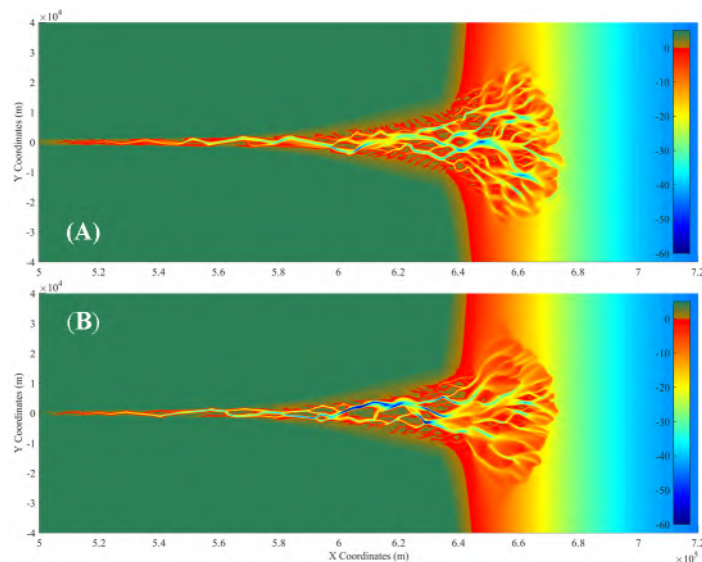


Figure 1. Modeled morphology after 100 years in scenarios with (A) sand only and (B) sand plus 30% of mud

The model results suggest that inclusion of mud on the sandy environments induces less bifurcated and less braided channel-shoal pattern (Figure 1). Instead, more merged sand bars and less meandered channels forms in sand-mud mixture environment. Increasing mud content leads to straighter channel pattern. The tidal flats and sand bars are more accreted in elevation and more sediments are retained inside the estuary due to the presence of mud. We argue that the impacts of mud on large scale estuarine and deltaic morphodynamic development can be explained by its

cohesiveness which increases erosion resistance and fine sediment transport rate once in motion. More sensitivity simulations and in-depth analysis results will be presented in the conference.

References

- Caldwel R.L., Edmond D.A., 2014. The effects of sediment properties on deltaic processes and morphologies: a numerical modelling study, *Journal of Geophysical Research: Earth Surface* 119, doi:10.1002/2013JF002965.
- Edmond D.A., Slingerland R.L., 2009. Control of delta morphology by sediment cohesion. *Nature Geosciences*, doi: 10.1038/ngeo730.
- Gelynese N., Storms J.E.A., Stive M.J.F., Jagers H.R.A., Walstra D.J.R., 2010. Modeling of a mixed-load fluvio-deltaic system. *Geophysical Research Letters* 37, L05402, doi:10.1029/2009GL042000.
- Mehta A.J. (2014). *An introduction to hydraulics of fine sediment transport*. World Scientific Publishing, Singapore. 1039p.
- Partheniades E., 1965. Erosion and deposition of cohesive soils. *Journal of the Hydraulics Division, ASCE*, 91(1), 105-139.
- van Ledden M., 2003. *Sand-mud segregation in estuaries and tidal basins*, PhD dissertation of Delft University of Technology, Delft, the Netherlands.

On the homogeneity of suspended matter concentration data in an integrated coastal ocean observing system

Götz Flöser, Rolf Riethmüller, Wolfgang Schönfeld

Helmholtz-Zentrum für Geesthacht, Centre for Materials and Coastal Research, Max-Planck-Straße 1,
21502 Geesthacht, Germany
E-mail: floeser@hzg.de

Introduction

The Helmholtz Zentrum Geesthacht aims to generate comprehensive data sets of coastal ocean key state variables on an operational basis. In general, the observational data originate from various types of in-situ measurements and satellite remote sensing.

Maps of near-surface suspended matter concentration (SPMC) are provided by satellites measuring ocean colour and subsequently converting spectral radiances into SPMC by means of inverse models. The outcome depends critically on the comparison to water samples in order to calibrate the model parameters. In coastal waters, the inherent optical properties of the suspended particles are highly variable in time and space. This variability is not reflected in the limited number of available satellite overfly match-up SPMC data from water samples. Hence, incommensurable results are expected compared to other in-situ observations which are needed to extend the satellite observation into the vertical and to fill observational gaps due to cloud obstruction. The distribution of SPMCs shows strong gradients and patchiness in concentration and inherent particle properties (Figure 1). Hence, the combination of remote sensing and in-situ SPMC data is expected to be a challenging task.

Methods

The Helmholtz-Zentrum Geesthacht operates since 2007 the observing system COSYNA (Coastal Observing System of Northern and Arctic Seas). Main observation area is the German Bight, a shallow coastal shelf sea characterised by significant inflow of fresh water from the major rivers Elbe and Weser and the intertidal Wadden Sea as its coastal fringe (Baschek et al., 2016). These data are used for ground-truthing of satellite scenes.

A direct comparison of satellite remote sensing data from ENVISAT/MERIS scenes, taken between 2002 and 2012, to match-up water samples yields only some 50 out of 5000 water samples. In order to extend the amount of match-up cases both in time and space, we took advantage of the numerous in-situ measurements of optical backscatter (turbidity) data collected by the different COSYNA observing platforms: time series from pole stations in the East and North Frisian Wadden Sea, profiler data during occasional ship surveys and horizontal transects across the German Bight taken by means of an undulating fish towed behind a cruising vessel. Turbidity was converted into SPMC by repeated calibration with SPMC from simultaneously taken water samples. These turbidity values were in turn compared to isochronous spectral radiances from MERIS generated by the ESA standard processor developed for CASE II waters.

Results

The relationship between sample SPMC and turbidity could be well described by linear regression in most cases (Figure 2, left). There are, however, significant regional differences in the slope up to a factor of two between East Frisian Wadden Sea, North Frisian Wadden Sea, off-shore German Bight and Elbe river plume areas indicating different inherent optical properties of the suspended particles. The number of turbidity match-up cases is about one order of magnitude larger than the direct comparison to water samples. This allowed regional differentiation of correlation parameters between in-situ SPMC and turbidity. The differing correlation parameters (turbidity – SPMC) are most probably due to differences in particle size and specific densities.

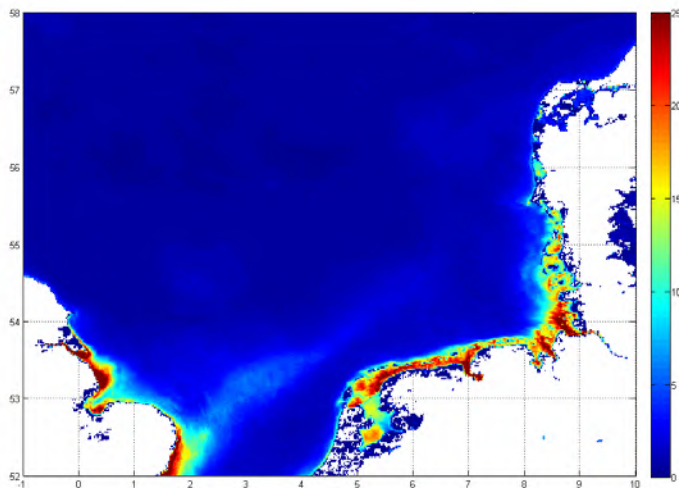


Figure 1: composite map of ENVISAT/MERIS TSM results, averaged over the year 2010.

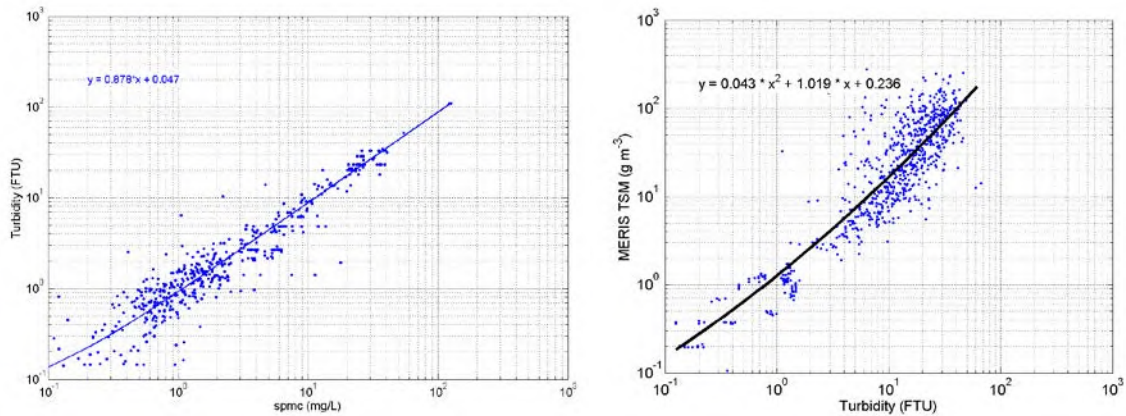


Figure 2: Correlation optical backscatter - SPMC for all ship cruises in the offshore German Bight where turbidity was measured, 2009-2012 (left). Correlation of ENVISAT/MERIS TSM to turbidity data from several stations and ship cruises in the Wadden Sea and German Bight (right).

The scatter of the correlation diagram of MERIS TSM with in-situ turbidity data (Figure 2, right) is still large, but the preliminary results indicate that there is some universal nonlinear correlation irrespective of the area considered.

The results indicate the need for detailed in-situ calibration of turbidity in coastal waters to adapt the conversion algorithms to consider spatial, and in case of extreme events, temporal variation.

References

Baschek, B., Schroeder, F., Brix, H., Riethmüller, R., Badewien, T. H., Breitbach, G., Brüggel, B., Colijn, F., Doerffer, R., Eschenbach, C., Friedrich, J., Fischer, P., Garthe, S., Horstmann, J., Krasemann, H., Metfies, K., Ohle, N., Petersen, W., Pröfrock, D., Röttgers, R., Schlüter, M., Schulz, J., Schulz-Stellenfleth, J., Stanev, E., Winter, C., Wirtz, K., Wollschläger, J., Zielinski, O., and Ziemer, F.: The Coastal Observing System for Northern and Arctic Seas (COSYNA), *Ocean Sci. Discuss.*, doi:10.5194/os-2016-31, in review, 2016.

Evaporation reduces the erodibility of mudflats in Plum Island Sound, Massachusetts, USA

Fagherazzi S.¹ A.M. Vieillard¹, R.W Fulweiler^{1,2}, G. Mariotti^{1,3}, T. Viggato¹,

¹Department of Earth and Environment, Boston University, Boston Massachusetts USA

²Department of Biology, Boston University, Boston Massachusetts USA

³Department of Oceanography and Coastal Sciences, Louisiana State University, Baton Rouge Louisiana USA

Abstract

Large areas of mesotidal estuaries become subaerial during low tide. Here we study the effect of several meteorological and hydrodynamic parameters on the erodibility of mudflat substrates when they are subaerial. Field measurements carried out over a two week period in September 2011 in Plum Island Sound, Massachusetts USA, indicate that high evaporation rates and long subaerial periods are associated to low sediment erodibility. Sediment concentrations in the water column during submergence depend on bottom shear stresses triggered by tidal currents. Surprisingly, they are also related to the total evaporation that occurred in the previous emergence period. We conclude that low erodibility of mudflat sediments is linked to subaerial desiccation at low tide. This strengthening effect is not lost during the following submerged period, thus limiting the erosive effect of tidal currents. We thus show that not only subaqueous but also subaerial processes might control the erodibility of mudflats. Global warming and other climatic variations regulating long-term evaporation rates can therefore directly affect the stability of mudflats in mesotidal environments.

Methods

A two-week study into the daily variability in the erosion threshold of tidal flat sediments was conducted in September 2011 in a tidal flat bordering the Rowley River in Plum Island Sound, Massachusetts, USA. Field observations were used to investigate how changes in environmental conditions impact the erosion threshold of tidal flat sediments during emersion. Additionally, hydrological and meteorological sensors located in proximity of the study site were used to model the hydrodynamic processes occurring during submergence. This approach was used to determine whether sediment resuspension during submergence was related to meteorological conditions during the previous emersion period.

A rectangular transect six meter by one was established on a mudflat near the Rowley river. The transect, divided in six 1x1m squared plots, stretched from the salt marsh scarp to the channel (Figure 1). The total change in elevation along the transect was less than 0.4 meters. High-resolution measurements of critical shear stress, chlorophyll a concentration, dry density, and organic content were taken daily. An acoustic Doppler velocimeter (ADV) was deployed 3 m upstream to monitor hydrological conditions (Figure 1). A meteorological station located approximately 2.9 miles from the study site was used to monitor weather conditions during the experiment.

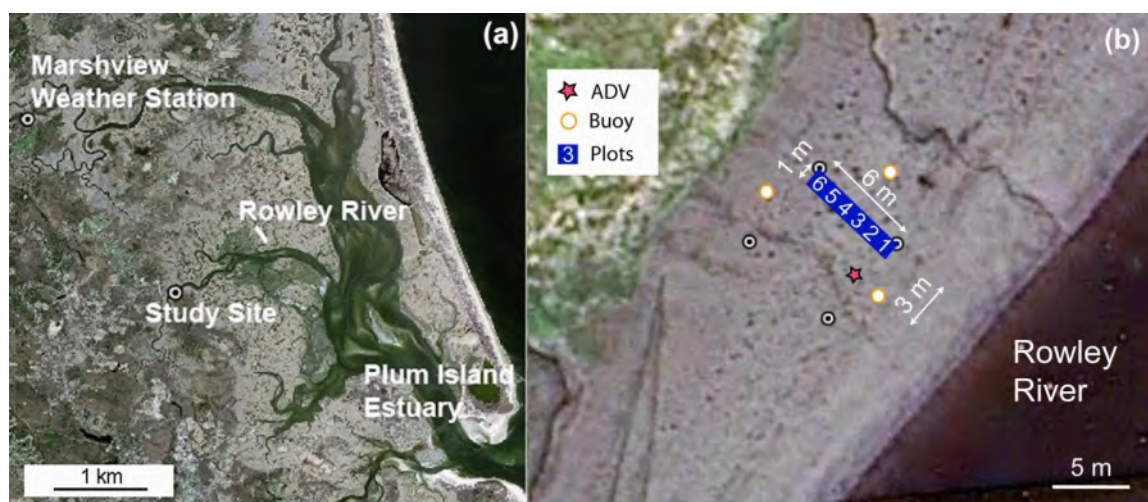


Figure 1:(a) Map of Plum Island Estuary including study site and Marshview weather station. (b) Map of study site transect and ADV location during the measurements. Image courtesy of Google Earth, Imagery Date (a) 04/17/2008, (b) 06/18/2012

Results

Factors controlling substrate critical shear stresses

A significant difference was found in the daily erosion threshold measurements taken within the same plots on different days ($p < 0.05$), implying that variations in daily environmental conditions were affecting sediment erodibility within the plots.

Correlation analysis showed that the length of exposure to air prior to the CSM measurement cannot explain the differences in erosion threshold. In fact, the variability in erosion threshold increased as sediments were subaerial for a longer period of time. When the daily evaporation rate was considered together with the length of exposure (total evaporation), a monotonic trend was detected, with erosion threshold growing as a function of total evaporation (Kendall's $\tau = 0.30$ with $p < 0.05$, Spearman's $\rho = 0.42$ with $p < 0.05$). Moreover a significant linear correlation between the erosion threshold and total evaporation was found ($R^2 = 0.44$, $p < 0.05$, statistical power $\pi = 0.95$).

A negative linear relationship was present between chlorophyll *a* and the erosion threshold of tidal flat sediments ($R^2 = -0.23$, $p < 0.05$, statistical power $\pi = 0.58$) (Table 1, Figure 6B), indicating that microphytobenthos were fewer when the sediment was stronger (Kendall's $\tau = -0.37$ with $p < 0.05$, Spearman's $\rho = -0.56$ with $p < 0.05$). A weak relationship was found between chlorophyll *a* concentration and the total evaporation calculated prior to the CSM measurements ($p = 0.08$, statistical power $\pi = 0.41$). It should be noted that the time at which chlorophyll *a* samples were taken was not recorded and we used the time of the CSM measurements as a proxy. As a consequence the relationship between total evaporation and chlorophyll *a* may be stronger than depicted in this analysis. The erosion threshold of tidal flat sediments was also found to be significantly correlated to the average distance between ADV and sediment bed ($p = 0.03$).

A multiple regression analysis was used to determine which significant variables from the correlation analysis were collectively contributing to changes in the observed erosion threshold of the tidal flat sediments. Average change in bottom elevation was not significant when combined to total evaporation in a multiple regression analysis. Similarly, total evaporation and chlorophyll *a* were not significantly correlated with erosion threshold when considered together in a multiple regression analysis.

Factors affecting turbidity on the Rowley River tidal flats

Acoustic backscatter recorded by the ADV during the flood period was used as a proxy for sediment resuspension occurring on the tidal flat as well as for sediments remobilized in several tidal flats within Plum Island Sound and then funneled in the Rowley River.

The sediment concentration recorded by the ADV appears to grow with maximum shear stress exerted locally on the tidal flat (Kendall $\tau = 0.34$ with $p < 0.05$, Spearman $\rho = 0.46$ with $p < 0.05$) and to decrease as a function of total evaporation recorded during the previous tidal cycle (Kendall $\tau = -0.37$ with $p < 0.05$, Spearman $\rho = -0.51$ with $p < 0.05$). The logarithm of the sediment concentration also linearly correlates with the logarithm of the maximum shear stress ($R^2 = 0.34$, $p < 0.05$, statistical power $\pi = 0.98$) and the total evaporation during the previous cycle ($R^2 = -0.28$, $p < 0.05$, statistical power $\pi = 0.87$). A multiple linear regression analysis showed that the total evaporation occurring during the previous tidal cycle and the maximum shear stresses exerted on the tidal flat during flood are independent factors, both controlling the maximum sediment concentration and therefore sediment resuspension. Both factors remain statistically significant when considered together and explained approximately 53% of the variability in the logarithm of sediment concentration ($p < 0.05$).

Conclusions

The results of this study show that evaporation is likely associated to daily variations in sediment erodability of tidal flat sediments. The erosion threshold of the substrate seems to increase as evaporation occurs over the emersion period. The extent of evaporation that tidal flat sediments undergo depends on meteorological conditions (temperature, relative humidity, wind conditions, and solar radiation) as well as the duration of exposure to air. As these conditions change between emersion periods, so does the rate of evaporation and therefore the erosion threshold of the tidal flat sediments.

The influence of turbulence on suspended sediment concentrations within a rapidly prograding mangrove forest

Julia C. Mullarney¹, Erik M. Horstman¹ and Karin R. Bryan¹

¹Coastal Marine Group, Faculty of Science and Engineering, University of Waikato, Private Bag 3105, Hamilton, 3240, New Zealand
E-mail: julia.mullarney@waikato.ac.nz

Introduction

Mangrove forests constitute much of the intertidal vegetation at tropical and sub-tropical latitudes. These ecosystems provide a variety of vital services and hence support many coastal communities (Kathiresan and Bingham, 2001). Additionally, mangrove forests have been shown to enhance coastal resilience from storms by dissipating wave energy and reducing erosion (Horstman *et al.*, 2014). In many parts of the world, these valuable areas are threatened by changes in land-use and total global coverage has declined by around half since the pre-industrial epoch (Giri *et al.*, 2011). However, there are a few notable exceptions to this global trend. One such area is the Firth of Thames mangrove forest in the North Island of New Zealand (Fig. 1). Over the past 60 years, the mangrove forest has prograded rapidly (>800m), owing to increased sediment loads from catchment deforestation and engineering works on the rivers that discharging into the Firth of Thames (Swales *et al.*, 2015).

In this work, we explore relationships between the hydrodynamics, in particular turbulence characteristics, and sediment transport within these rapidly expanding mangroves. This work aims to elucidate the physical mechanisms underlying this unusual trend.

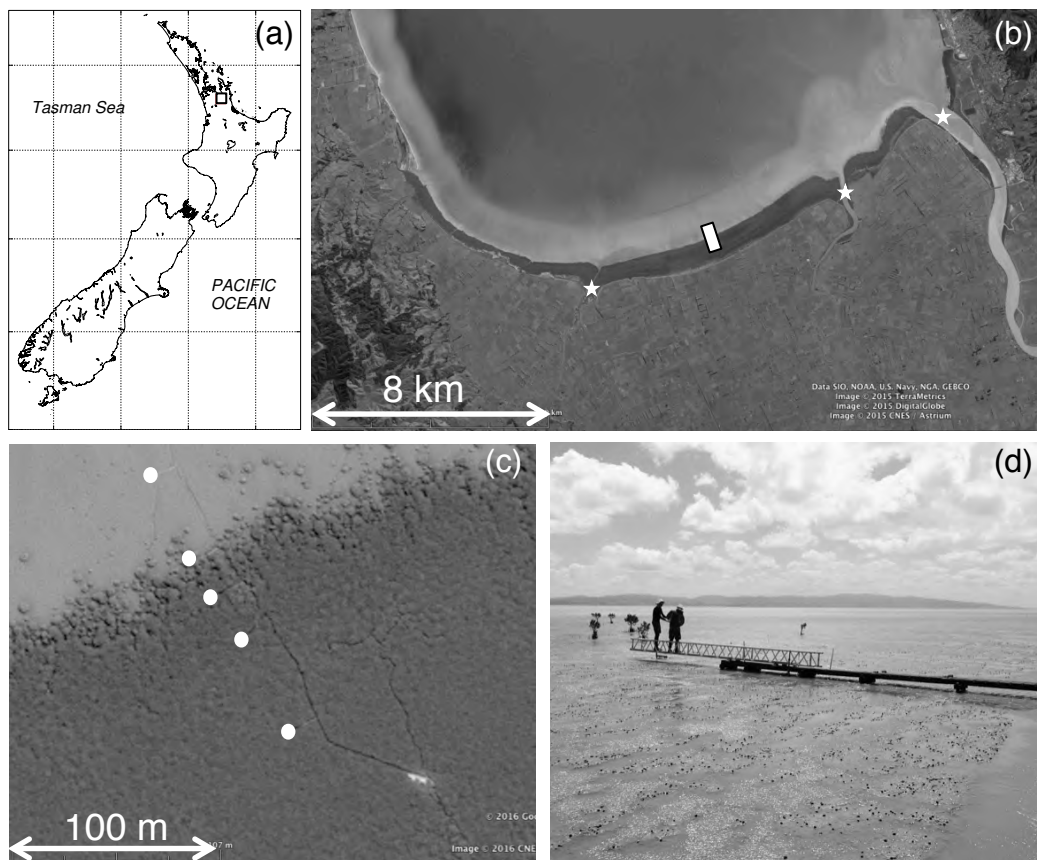


Fig. 1. (a) Location of Firth of Thames in New Zealand (black box), Google Earth images of (b) location of main transect (white box) within mangrove forest with rivers supplying sediment indicated by stars, (c) instrument deployment sites (circles), (d) Photograph of system used to deploy instruments with minimal disturbance of seabed.

Field Site and Measurements

Data was collected along a transect close to the centre of the Firth of Thames mangrove forest (Fig. 1b). The forest is composed of small *Avicennia* mangrove trees with average heights of ~3m. The transect encompassed several zones from the bare mudflat, through to the sparsely-populated fringe region to the densely populated forest interior (Fig. 1c). Measurements of hydrodynamic conditions and sediment concentrations were taken over 10 consecutive days in November 2016, using a variety of acoustic current meters and optical backscatter sensors. In particular an array of three vertically-stacked Nortek Vectrino Profilers was used to obtain high-resolution velocity profiles (each profile was 3 cm in length with 1 mm vertical resolution with a sampling rate of 50Hz) through the water depth. An access boardwalk with 5 side-arms and cantilevered bridge systems allowed the deployment of instruments with minimal disturbance of the sediment bed (Fig. 1d). The average grain size (D50) at the field site was 5-10 μ m.

Results

Preliminary results from a single tidal cycle are shown in Fig. 2. On this day, the Vectrino Profilers were deployed within the forest (central white circle, Fig. 1c) and small (0.5 m) waves were observed to propagate into the forest. During flood tide, turbulence (characterised by the dissipation rate of turbulent kinetic energy, ϵ) was lowest at the bed and increased with height above the bed, likely owing to the larger wave velocities within the upper part of the water column. Relatively high SSCs are observed (~2.5g/L). At mid-height in the water column, SSCs decreased during the tide, while conversely, turbulence increased. This inverse relationship may suggest that sediment supply from outside the forest is the dominant control on SSCs during the flood stage of the tide, instead of the local turbulence conditions. Future work will explore this possibility in order to elucidate the relation between sediment concentrations and turbulence properties throughout the tidal cycle and under different hydrodynamic conditions

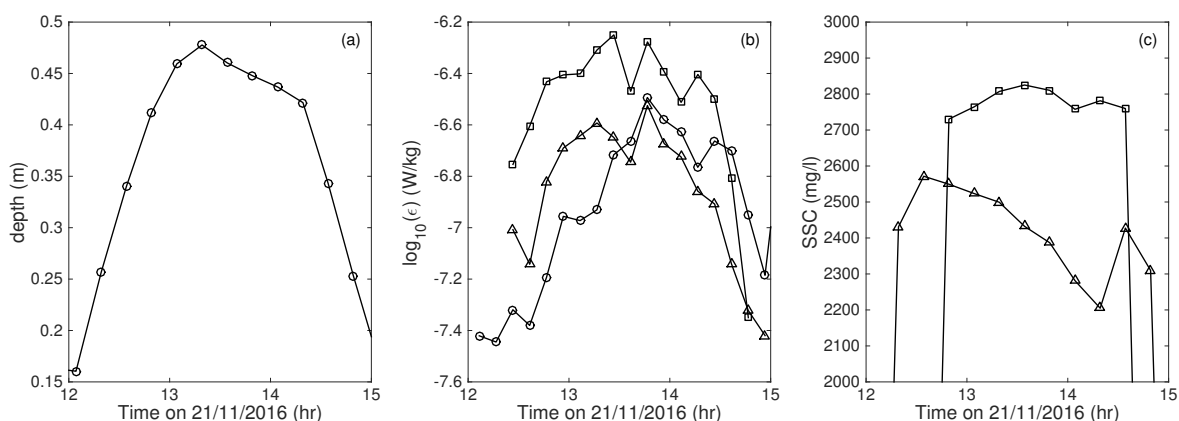


Fig. 2. Data from just inside mangrove forest (centre dot, Fig. 1c). (a) Water depth (b) 10-min averaged dissipation rate of turbulent kinetic energy (ϵ) at 1cm (circles), 18.5cm (triangles) and 22.5cm (squares) above the bed, (c) burst-averaged suspended sediment concentrations at 14cm (triangles) and 29.5cm (squares) above the bed.

Acknowledgments

We thank the Marsden Fund of New Zealand for funding (grant number 14-UOW-011), Dean Sandwell, Chris Morcom, Dave Culliford, Rex Fairweather, Hieu Nguyen, Caitlyn Gillard and Carol Robinson for assistance with field-work. We also thank the construction crew of the boardwalk especially Iain MacDonald, Nicola Lovett, Chris Eager and Matt Davis.

References

- Giri, C., Ochieng, E., Tieszen, L. L., Zhu, Z., Singh, A., Loveland, T., Masek, J., & Duke, N. (2011). Status and distribution of mangrove forests of the world using earth observation satellite data. *Global Ecology and Biogeography*, 20, 154–159. doi:10.1111/j.1466-8238.2010.00584.x.
- Horstman, E. M., Dohmen-Janssen, C. M., Narra, P. M. F., van den Berg, N. J. F., Siemerink, M., & Hulscher, S. J. M. H. (2014). Wave attenuation in mangroves: A quantitative approach to field observations. *Coastal Engineering*, 94, 47–62. doi:10.1016/j.coastaleng.2014.08.005.
- Kathiresan, K., & Bingham, B. L. (2001). Biology of mangroves and mangrove ecosystems. *Advances in marine biology*, 40, 81–251.
- Swales, A., S. J. Bentley, and C. E. Lovelock, 2015: Mangrove-forest evolution in a sediment-rich estuarine system: opportunists or agents of geomorphic change? *Earth Surface Processes and Landforms*, 40 (12), 1672–1687, doi:10.1002/esp.3759.

Biophysical controls on sediment deposition in mangroves

Erik M. Horstman¹, Julia C. Mullarney¹ and Karin R. Bryan¹

¹ Coastal Marine Group, Faculty of Science and Engineering, University of Waikato, Private Bag 3105, Hamilton 3240, New Zealand
E-mail: erik.horstman@waikato.ac.nz

Introduction

Mangrove ecosystems are found in sheltered intertidal areas of tropical and sub-tropical coastlines. The characteristic aerial root systems of mangrove trees and their canopies provide a significant source of drag to the tides and waves propagating into the forest, resulting in delayed asymmetric tidal currents (van Maanen *et al.*, 2015) and substantial wave attenuation (Horstman *et al.*, 2014). Consequently, mangroves are known as efficient sinks for suspended sediments, often flocculated muds, which are imported on flood tides and settle in the quiescent conditions of the forest. (Furukawa *et al.*, 1997). Although the physical mechanisms facilitating the sediment retention in mangroves are roughly known, the relative contribution of the intertidal elevation, root types and densities and sediment properties are yet to be disentangled (Krauss *et al.*, 2014). The present study addresses the deposition across contrasting mangrove fringes and identifies linkages between sediment deposition rates the sediment properties, vegetation parameters and tidal flow characteristics.

Field sites & methods

Data have been collected in four estuarine mangrove regions: in the Firth of Thames and Whangapoua Harbour in New Zealand and in the Palian and Kantang estuaries in Thailand (Fig. 1). Mangroves in New Zealand are mono-specific, consisting of relatively small *Avicennia* trees of height 1.5-4 m. The study sites in Thailand accommodated multiple species of e.g. *Avicennia* and *Rhizophora* with trees of up to 20 m height. All field sites had a characteristic fringing region between the bare mudflat fronting the mangroves and the denser forest further inland. Trees are sparse in this fringing region, yet there is a dense cover of pneumatophores (pencil roots) protruding from the bed.

At each field site sediment deposition was monitored over periods ranging from a single tidal cycle to a full spring-neap cycle. Concurrent observations of the tidal flows were collected with Aquadopp current profilers and Vector current meters (Nortek), covering each of the three characteristic zones along the transects: the bare flat fronting the mangroves, the pneumatophore dominated fringe of the forest and the dense(r) mangrove forest in the back. Other biophysical parameters that were quantified for each zone were: numbers (N) and diameters (d) of vegetation elements to compute the cross-sectional vegetation density ($\phi = N\pi d^2/4$), the sediment grain sizes and the contents of organic matter (OM) and Chlorophyll-a (Chl-a) of the top 2 cm of the bed.

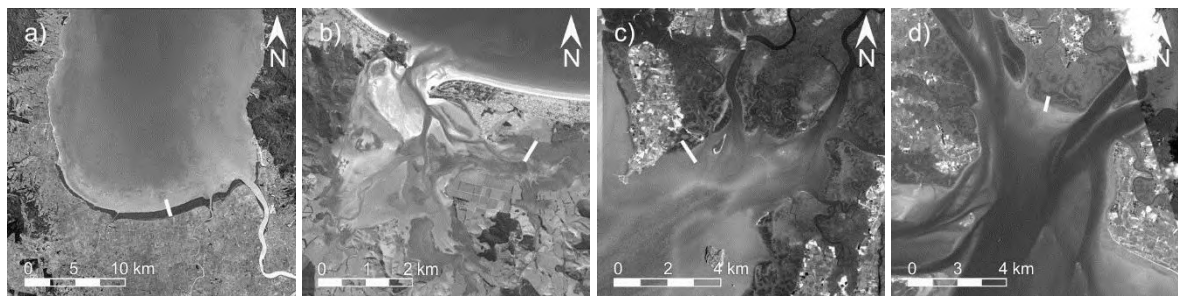


Fig. 1. Mangrove transects in (a) the Firth of Thames and (b) Whangapoua Harbour, both in northern New Zealand, and (c) the Palian estuary and (d) Kantang estuary, both in southern Thailand.

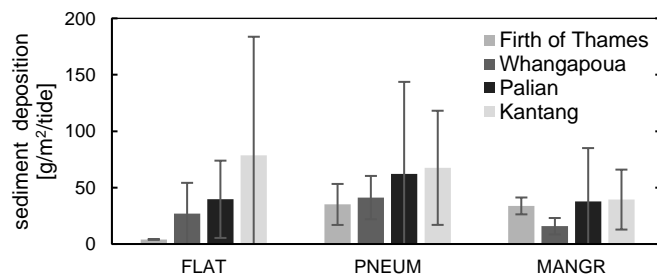


Fig. 2. Deposition rates for the three distinct zones at each study site.

Table I. Biophysical conditions for each of the characteristic vegetation zones at the study sites.

		H_{max} [m]	$V_{flood,max}$ [m/s]	$V_{ebb,max}$ [m/s]	ϕ [-]	D_{50} [μ m]	OM [%]	Chl-a [μ g/g]
Firth of Thames	flat	1.7	0.22	0.10	0	7.45	10.0	4.9
	pneum	1.3	0.09	0.07	0.0083	10.2	9.5	5.9
	mangr	1.3	0.11	0.10	0.0135	10.1	9.3	12.7
Whangapoua	flat	1.5	0.24	0.14	0	198	1.9	14
	pneum	1.5	0.13	0.07	0.0053	232	1.9	15
	mangr	1.4	0.07	0.04	0.0081	245	3.0	23
Palian	flat	1.9	0.08	0.10	0	85.3	8.3	-
	pneum	1.3	0.02	0.05	0.0194	70.9	6.6	-
	mangr	0.9	0.02	0.02	0.0407	74.0	12.3	-
Kantang	flat	1.9	0.10	0.03	0	159	10.3	-
	pneum	1.3	0.04	0.03	0.0200	115	10.2	-
	mangr	0.8	0.05	0.04	0.0150	96.9	9.3	-

Results

The observed sediment deposition was converted into a deposition rate per unit area per tide (Fig. 2). Deposition rates showed greatest inter- and intra-site variability on the bare flats fronting the mangroves, coinciding with the greatest difference in velocities between flood and ebb tide (Table I). Even though tidal forcing was quite similar across the sites, as indicated by the inundation depth of these intertidal areas, maximum tidal velocities in the New Zealand sites were more than 2 times greater, partially explaining the limited deposition at these sites.

At the pneumatophore fringes and within the forests, tidal velocities were more similar, generally less than 10 cm/s, with the lower velocities observed in the denser vegetation at the Thai sites (Table I). Likewise, deposition rates for these zones showed a reduced variability between the sites and highest deposition rates were observed at the Thai sites (Fig. 2).

Apart from the tidal forcing, there is a spectrum of biophysical controls which determines sediment transport and deposition in mangroves. Even though mean grain sizes (D_{50}) of the bed material varied from clay to fine sand, the generally high organic matter content increased sediment cohesivity. At the Whangapoua site, the lack of organic matter might be compensated by a greater density of microphytobenthos reflected by the higher Chlorophyll-a content (Table I).

Outlook

Although the tidal current velocities provide a first indication of the differences in the observed sediment deposition rates across the studied mangroves, these do not provide a full explanation for the inter- and intra-site differences that were observed. Further data analysis will address the correlations between the hydrodynamics, vegetation densities, sediment properties and biological activity. These analyses could be complemented with the critical erosion thresholds that have been quantified for the New Zealand sites, as a quantifier for the erosion and deposition threshold for fresh deposits.

The comprehensive analysis of these data should provide quantitative information on the factors facilitating and limiting sediment deposition in mangroves, providing new insights in the thresholds to sedimentation in these highly dynamic ecosystems.

Acknowledgements

This research is funded by the Royal Society of New Zealand's Marsden Fund (14-UOW-011). Data collection in Thailand was funded by the Singapore-Delft Water Alliance (R-264-001-024-414) and was consented by the National Research Council of Thailand (Project-ID2565). We are grateful for assistance in the field by Dean Sandwell, Chris Morcom, Dave Culliford, Rex Fairweather, Hieu Nguyen, Caitlyn Gillard, Carol Robinson, Iain MacDonald, Nicola Lovett, Chris Eager, Matt Davis, Martijn Siemerink, Niels-Jasper van den Berg, Thorsten Balke, Demis Galli, Dan Friess and Edward Webb.

References

- Furukawa K., Wolanski E. and Mueller H. (1997). Currents and sediment transport in mangrove forests. *Estuarine, Coastal and Shelf Science*, 44(3): 301-310.
- Horstman E.M., Dohmen-Janssen C.M., Narra P.M.F., Van den Berg N.J.F., Siemerink M. and Hulscher, S.J.M.H. (2014). Wave attenuation in mangroves: A quantitative approach to field observations. *Coastal Engineering*, 94: 47-62.
- Krauss, K.W., McKee K.L., Lovelock C.E., Cahoon D.R., Saintilan N., Reef R. and Chen L. (2014). How mangrove forests adjust to rising sea level. *New Phytologist*, 202(1): 19-34.
- Van Maanen B., Coco G. and Bryan K.R. (2015). On the ecogeomorphological feedbacks that control tidal channel network evolution in a sandy mangrove setting. *Proceedings of the Royal Society of London A: Mathematical, Physical and Engineering Sciences*, 471(2180): 1-24.

Mixing tank experiments on floc size distributions of suspended cohesive sediment in Yangtze River Estuary

Yuyang Shao^{1,2}, Xiaoteng Shen³

¹ College of Harbor, Coastal and Offshore Engineering
Hohai University, Nanjing 210098, Jiangsu Province, P.R.China
E-mail: syy@hhu.edu.cn

² Virginia Institute of Marine Science, Gloucester Point, Virginia 23062, U.S.A

³ Hydraulics Laboratory, Department of Civil Engineering
KU Leuven, Kasteelpark Arenberg 40, B-3001 Leuven, Belgium

Introduction

Cohesive sediments do not exist as single particles, but exist as flocs that consist of many particles gathered together in estuary waters. The size and density of flocs changed with many factors, such as the suspended sediment concentrations (SSC), clay minerals, local shear rate, floc strength, ions in the water, and organic matter contents (Shen and Maa, 2015). Therefore, experiments that can isolate various affecting factors in order to understand the significance of each affected parameter in flocculation are important.

In this study, a tank mixer system was designed to explore the flocculation processes of cohesive sediments. Turbulence shear rate, salinity, and the SSC are selected as control factors that inflecting the flocs size distributions in natural environments. The sediment from North Passage of Yangtze River estuary (with its D50 about 8 micron) and commercial kaolinite were used in the experiments. The effect of turbulence shear, which practically limits the maximum floc size around the size of the Kolmogorov micro-scale, was discussed for different SSCs and salinities. The results of this study can be used to further enhance any flocculation model in the future.

Methods

Experiments

The cylindrical tank with a 33 cm blade was constructed in Hohai University (see Fig.1). The height of the tank is 158cm and the inside diameter is 76cm. The red point is the measuring point (about 80cm above the bottom). An Optical Backscatter Sensor (OBS-300) calibrated with pumped water samples is used to measure the SSC. The Laser In Situ Scattering and Transmissionmetry (LISST-100, Type C) is used to measure the floc size distributions and its volume concentration.

Hydrodynamic model

A hydrodynamic model was built using the Ansys Fluent software. The Acoustic Doppler Velocimeter (ADV-16Mhz) was used to measure the velocity and turbulence kinetic energy. The output data of ADV are used to calibrate the hydrodynamic model. Based on the output of model, the details of flow field and turbulent shear rates in the device and the influence by instrument in the device are discussed.

Results and conclusions

The experiments describe the influences of shear rate, salinity, and SSCs on sediment flocculation. The relationship between floc size distribution and settling velocity was also addressed. Flocculation model can benefit from these experiments and improved in a later stage. It will also provide theoretical support for flocculation processes in other sediment transport models.

Acknowledgements

This research was funded by the State Key Program of National Natural Science of China (Grant No. 51339005 & 41230640) and the National Natural Science Foundation of China (Grant No. 51409081), and by the financial support from China Scholarship Council.

References

Shen X., Maa, J. P-Y. (2015). Numerical simulations of particle size distributions: Comparison with analytical solutions and kaolinite flocculation experiments. *Marine Geology*, 379:84-99.

Figures

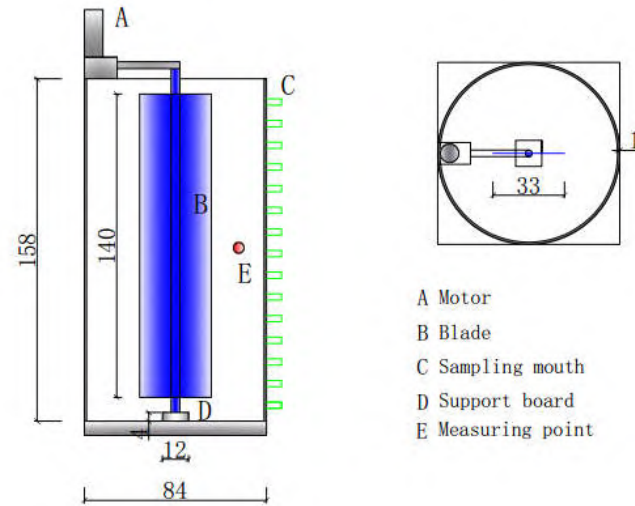


Fig. 1. The sketch of settling tanks

A three dimensional coupled wave-current model for mud transport simulations in the Persian Gulf

Afshan Khaleghi¹, and S. Abbas Haghshenas¹

¹ Institute of Geophysics, University of Tehran, Tehran, Iran,
North Kargar Ave, PO Box 14155-6466, Tehran 1439951113, Iran
E-mails: afshan.khaleghi@yahoo.com, and sahaghshenas@ut.ac.ir

Introduction

The Arvand River which is located in the south west of Iran, on the border with Iraq, is one of the largest inland waterways in the area, formed by the confluence of the Euphrates, the Tigris and the Karoon River. The Karoon River, a tributary which joins the waterway from the Iranian side, deposits large amounts of fine sediments into the river. Mud deposits originated from the Arvand River branches at the north-western part of the Persian Gulf have mainly affected the coastlines in over a vicinity of more than 100 km in diameter, extending to Deylam Bay in the east and Kuwait Bay in the west. The fine deposits in this area are of two dominant origin; clastic mud coming from Zagros Range and carbonate mud deposited in the water column (Purser, 1973).

The hydrodynamic of this area is governed by tidal, wind-induced and wave induced currents. Moreover, the wave climate is highly affected by the existence of muddy deposits and relevant dissipation originated by wave-mud interaction (Soltanpour et al., 2008).

In this case accurate prediction of current velocity and bottom shear stress, which both can be significantly influenced by wind generated waves, is essential for sediment transport predictions in the coastal environment (Ma and Madsen, 2012).

This paper presents a small-scale 3D coupled wave-current numerical model to predict the rate of cohesive sediment transport. The model performance is verified against field measurements, geomorphological evidences and shoreline data extracted from satellite imagery.

Numerical modeling and the case study

Delft 3D is assumed among the strongest models for areas with complex hydrodynamic systems and is able to capture small scale variations in wave-current-morphology simulation for coastal areas. An important target for this model is to estimate appropriate conditions for carbonate mud precipitation in the study area.

A general 2D hydrodynamic model is set up for the entire Persian Gulf to simulate general currents due to tides and winds for one year which provides water level elevations in five points for the local model. The 3D online coupled wave-current model results for one year over the area covered by fine sediments are adopted to simulate the sediment transport rate, ultimately. Wave height attenuation due to wave-mud interaction is simulated using a multi-layer fluid system introduced by Maa (1986) and assuming viscoelastic rheological behavior for the fluid mud layer.

As the case study, Deylam Bay is considered in which the model results are verified against an available set of 37-day wave and current measurements at two, nearshore and offshore, stations. This bay is located on the margin of the area affected by fine sediments and studies show that while the western margin of Deylam Bay is influenced by mud deposits up to 20 m in some areas, very fine sand with oolitic origin is dominant at the eastern part. Near the most northern point of the bay there is a small village with a newly constructed port, called Shah-Abdollah, where repeating sequences of soft mud and fine sand could be observed on the beach, indicating that this location is the marginal point of the sandy and muddy sediments. Hence, it is believed that the long-term pattern of suspended mud transport in the North-Western Persian Gulf is the main cause for determination of mud affected margins in this area (Khaleghi et al., 2014).

Results and Discussion

The results of various model runs are presented here. First of all the general hydrodynamic model over the Persian Gulf has simulated the general currents over the entire Persian Gulf (Figure 1(a)) and successfully predicted current velocities at the offshore measurement station for a 37-day period in late winter 2007 as shown in Figure 2.

The coupled wave and current model has reasonably predicted current velocities at shallow water station, as depicted in Figure 1(b), as well as suspended sediment concentrations. As a result the long-term pattern of suspended mud transport, the consequent spatial pattern of the formed bed constituents at Shah-Abdollah coastal village is in fair agreement with model results presented in Figure 1 (b) in which the net mud transport rate in front of this village is estimated to be zero.

In short, the established model is capable of simulating currents and sediment transport rates over the north-western Persian Gulf.

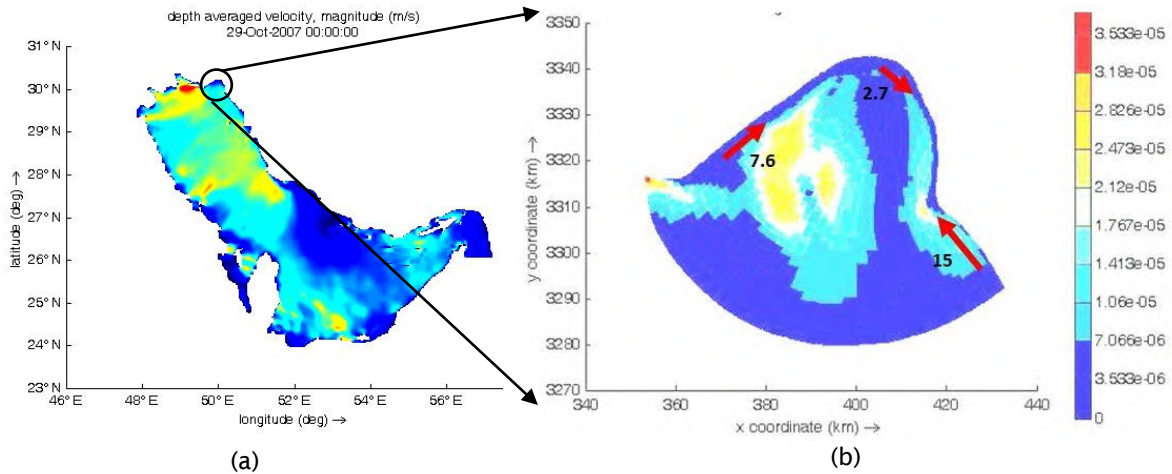


Figure 1. (a) Depth averaged velocity in the Persian Gulf model, (b) Longshore sediment transport in Deylam Bay ($1000 \text{ m}^3/\text{year}$)

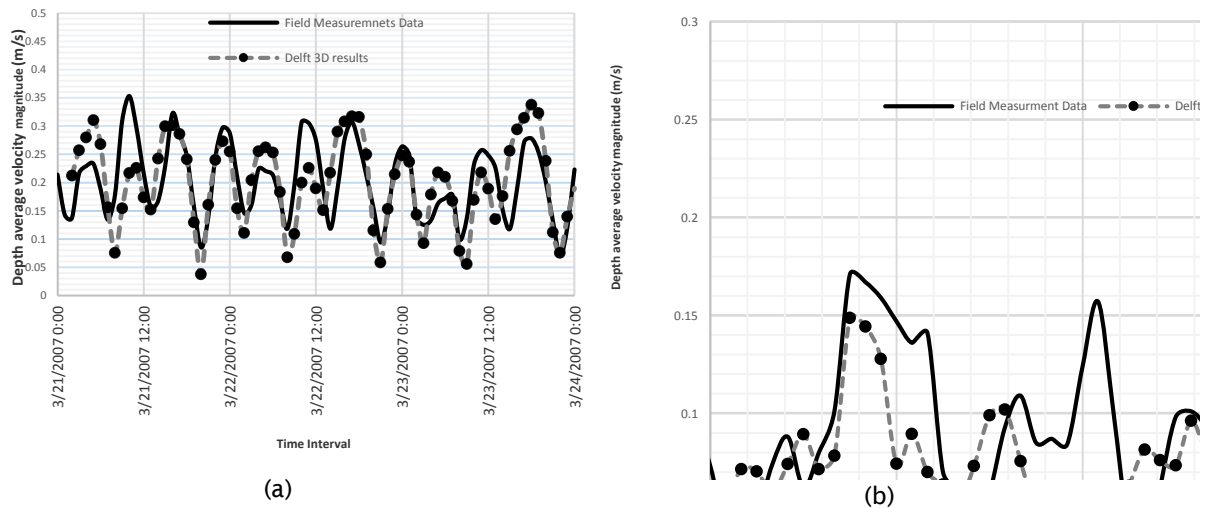


Figure 2. (a) Comparison of calculated and measured depth-averaged velocity at offshore station, (b) Comparison of calculated and measured depth-averaged velocity at nearshore station

References

- Khaleghi A., Soltanpour M., Haghshenas S. A. (2014). A study on the sand-mud mixture at north-west of the Persian Gulf. *Coastal Engineering Proceedings*, 1(34), sediment.79.
- Ma P F, Madsen O S. (2012). A 3D sediment transport model for combined wave-current flows. *Coastal Engineering Proceedings*, 1(33), sediment.21.
- Maa, P.-Y., 1986. Erosion of soft mud by waves. Ph.D. dissertation, University of Florida, Gainesville, FL, 276p.
- Purser B.H. (1973). **The Persian Gulf: Holocene Carbonate Sedimentation and Diagenesis in a Shallow Epicontinental Sea.** Springer-Verlag Berlin Heidelberg, Germany. vi 471 p.
- Soltanpour, M., Haghshenas, S. A., & Shibayama, T. (2008). An integrated wave-mud-current interaction model. 31th International Conference on Coastal Engineering (ICCE 2008), ASCE, Hamburg, Germany (pp. 2852-2861)

Mud rheology in the North-Western Persian Gulf by contrast with sediment constituents

Farzin Samsami², Samane Ahmadi¹, S. Abbas Haghshenas¹, Abbasali Aliakbari Bidokhti¹, and Michael John Risk³

¹ Institute of Geophysics, University of Tehran
North Kargar Ave., Tehran PC 1439951113, Iran
E-mails: ahmadi.samane@ut.ac.ir, sahaghshenas@ut.ac.ir, and bidokhti@ut.ac.ir

² Department of Civil Engineering, West Tehran Branch, Islamic Azad University
Tehran, Iran
E-mail: samsami@wtiau.ac.ir

³ PO Box 1195 Durham ON N0G 1R0, Canada
E-mail: riskmj@mcmaster.ca

Introduction

The North-Western part of the Persian Gulf is covered with mud deposits which were believed to be mainly originated from the Arvand River catchment area. However, recent findings show that precipitated carbonate mud forms considerable portion of fine sediments in the mentioned area. This study aims to correlate sediment constituents to the general rheological behaviour of mud deposits in the study area.

Sediment constituents in the study area

Mud deposits up to 20 meters thickness is observed at the very shallow coasts extending from Shah-Abdollah and Hendijan Fishery Ports in the east towards the Arvand River mouth and surrounding area of Kuwait Bay in the west. Aragonite can be found in sediments of certain locations in the Persian Gulf (Purser, 1973). True aragonite needle muds are chemically-precipitated type of sediment which are found in warm, shallow, saline, agitated water, usually where strong currents exist. They are chemically-precipitated from water that becomes oversaturated with CaCO_3 . The percentage of carbonate constituent in studied samples typically exceeds 30%. The solubility of carbonate in warm water is already low, and wave agitation blows off more CO_2 , which leads to an increase in pH and helps the precipitation process to happen more easily. Small particles are picked up off the bottom, and carried up into surface waters of high pH, where carbonate precipitates around the particles as coatings of aragonite. The true aragonite needle muds are too fine grained to be studied with a light microscope. Figure 1 shows a photograph of a selected mud sample from the shoreline of Hendijan Port taken by a scanning electron microscope (SEM). The sediment texture consists of ordinary clay flakes together with aragonite needle mud with a length/breadth ratio of 6/1 to 12/1. The dimension of the figured needles vary from $0.1 \times 0.5 \mu$ to $0.2 \times 1.7 \mu$. The carbonate fraction in the sediment constituents are estimated to exceed 30 percent in the nearshore and offshore samples with an average value of 28% based on XRF tests; while the water content ratio of sediment mixture is measured between 60 and 80 percent.



Figure 1. SEM photograph of a selected mud sample from the shoreline of Hendijan Port

Rheometry investigations and sediment constituent analysis

The selected samples from the Hendijan Coast and the Musa Estuary of the Persian Gulf were analyzed using an Anton Paar Physica MCR301 rheometer capable of performing rotary and

oscillatory tests. Vane geometry was used as the measuring system at a constant temperature of 20°C. The oscillatory tests are operated in terms of controlled shear stress (CSS) in the form of amplitude sweep (keeping the frequency at a constant value; usually the angular frequency sets as 10 rad/s) (Mehta et al., 2014). The yield and flow stresses were determined from the amplitude sweeps tests with controlled-strain deformation ramp mode in a range of 0.01 to 100 (%). The rotary tests were operated in terms of controlled shear rate (CSR) and the shear rate was considered in the range of 0.1 to 100 1/s. The constituents of the sediment samples were examined by conducting XRF and XRD tests. Moreover, a number of samples were fabricated by mixing kaolinite and various percentage of carbonate material and it is tried to regenerate similar rheological properties with the artificial samples. Figure 2 shows sample results of rheometric behaviour of Hendijan mud sample in comparison with one of the artificial sediment sample with zero carbonate content. Yield and flow stresses of Hendijan mud can be obtained from oscillatory test whose curve is presented in Figure 3. As it is observed the yield stress from rotary test is about 100 pa, while the yield stress from oscillatory test is about 10 pa and the flow stress is about 129 pa.

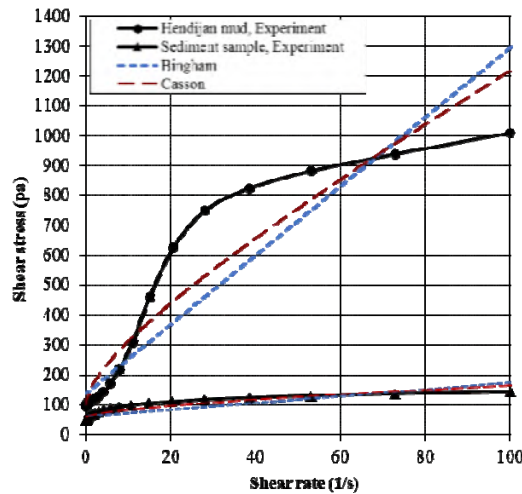


Figure 2. Flow curves for Hendijan mud and sediment sample

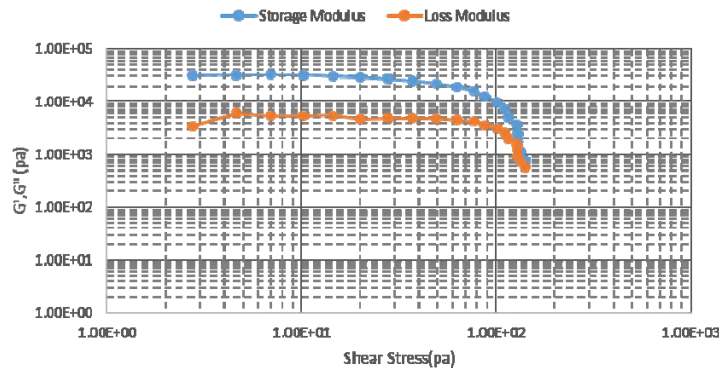


Figure 3. Oscillatory test results on Hendijan mud sample

Summary

Considerable amount of carbonate constituent is observed in muddy sediments over the shallow coasts of North-Western Persian Gulf. This carbonate fraction seems to play an important role in mud rheological behaviour, something which is tried to be investigated in this study. Moreover, it is tried to regenerate similar behaviour as PG mud samples by fabricating artificial muds consisting of kaolinite and various amounts of carbonate material.

References

- Mehta A., Samsami F., Khare Y., and Sahin C. (2014). Fluid Mud Properties in Nautical Depth Estimation. *J. Waterway, Port, Coastal, Ocean Eng.*, 140(2): 210–222.
- Purser B.H. (1973). *The Persian Gulf: Holocene Carbonate Sedimentation and Diagenesis in a Shallow Epi-continental Sea*. Springer-Verlag Berlin Heidelberg, Germany. vi 471 p.

An application of Artificial Neural Network for analyzing sediment erodibility data

Ebrahim Hamidian J.¹, S. Abbas Haghsheenas¹, Lawrence P. Sanford², Farhang Ahmadi Givi¹

¹ Institute of Geophysics, University of Tehran, Tehran, Iran,
North Kargar Ave, PO Box 14155-6466, Tehran 1439951113, Iran
E-mails: eb_hamidian@ut.ac.ir, sahaghshenas@ut.ac.ir, ahmadig@ut.ac.ir

² Horn Point Laboratory, University of Maryland Center for Environmental Science (UMCES), 2020
Horns Point Rd, Cambridge, MD 21613, USA
Email: lsanford@umces.edu

Introduction

Erosion is one of the most significant coastal and estuarine processes which may lead to drastic geomorphological changes, dispersing contaminants and fine-grained materials in to the water, resultant probable habitat loss and environmental problems. The prediction of sediment erosion is an important issue while dealing with coastal and estuarine dynamics. The erosion resistance of sediments is characterized by introducing critical shear stress and erodibility. These two parameters, as the major sediment erosion properties, are dependent on many parameters which should be identified through an exploratory analysis of factors affecting sediment erodibility. Although understanding of erosion especially in cohesive sediments is not thoroughly obtained, for gaining a better understanding of erosion and analysis of erodibility data, paying attention to some parameters affecting on erosion is inevitable; parameters such as: sand, silt and clay content, sediment grain size, organic content, water content, Atterberg limits, plasticity index, specific gravity, consolidation condition, bulk density and etc. Many researchers have tried to correlate sediment erodibility with these sediment properties, including: Parchure and Mehta (1985), Winterwerp and van Kesteren (2004), van Prooijen and Winterwerp (2010), Jacobs *et al.* (2011), Winterwerp *et al.* (2012) and Kimiaghali *et al.* (2015); however, the relations they have suggested for correlating sediment erodibility and other sediment properties are highly dependent on location and sediment origin. Hence, erosion like many other natural processes depends on many factors which makes it a complicated problem. This issue makes ordinary statistical methods less effective to interpret and analyze such data. Moreover, it is so probable that there would be a gap in our measured dataset which will influence on the statistical analysis results.

This study aims to propose a conceptual framework for analyzing erosion data of cohesive/non-cohesive/mixed sediment beds using some specific soft computing techniques in order to 1) determine effective parameters and evaluating the level of effectiveness, and 2) establish a general framework to correlate physical parameters of the sediment to the erodibility parameter.

Artificial Neural Network

ANN -Artificial Neural Network-is one of the most well-known machine learning methods which is used for many different purposes, such as: function approximation and curve fitting, pattern recognition and classification, clustering, feature extraction and data dimension reduction, input-output time-series prediction, forecasting, single time-series prediction, dynamic modelling and so on. It is inspired by human nervous system. It consists of many neurons which enable data to be processed. As the capability of every single neuron is so limited in processing data, setting neurons adjacent to each other and making networks so that the output of one neuron will be the input for the next neuron seems inevitable. For dealing with complicated problems it is needed to imitate (or it has been proved that imitating) brain function and make parallel networks or in order to decrease the calculation time remarkably. Furthermore, optimization, data training and finding the relationship between different parameters are some of the other most important applications of artificial neural network which are going to be used in this study to meet the challenge of reaching to a better correlation.

To reach this goal, neural fitting toolbox in Matlab for a multiple-conditioned set of data was applied. A two-layer feed-forward network with 10 sigmoid hidden neurons and linear output neurons was applied. 70% of input samples were dedicated to training and 15% to each validation and testing parts. The network was trained with Levenberg-Marquardt backpropagation algorithm. As the first trained network is not necessarily the best one, a couple of network retraining has been performed to gain a better correlation value.

An exploratory application of ANN

As regular statistical regressions are not usually fitted on the majority of data points and usually do not consider more than two variables in every try, such artificial intelligence methods are getting more and more popular in recent decades.

As a case study, the erosion data set provided from Kimiaghalam *et al* (2014) and Jacobs *et al* (2011), encapsulated in Table 1, is adopted to find an appropriate correlation between critical shear stress and other sediment properties. According to Kimiaghalam *et al* (2014) several undisturbed natural soil samples were taken from different river banks in Manitoba, Canada. The samples mainly contained clay and silt with 24–94% clay content. For each sample 13 different physical, mechanical, and electrochemical properties were measured. Previously using Kimiaghalam data set and managing to get to almost high correlation values encourages us to expand our data set to a set of data with a vast range of diversity-even in its conditions- in order to investigate our results and the efficiency of ANN. Hence, a set of data has been extracted from Jacobs *et al* (2011) which was belong to artificially generated samples with different conditions. According to Jacobs *et al* (2011) their erosion tests were taken on artificially generated sand-mud mixture. The composition of soil samples are vastly varied in silt, sand and clay percentages and clay mineralogy. Hereby, it has been used of organic matter to link these multiple-conditioned sets of data and play the role of a joint in this new table. Adopting and training the described network, Figure 1 shows ANN estimated values for critical shear stress versus observational data.

Summary

In this study a framework is proposed based on ANN to analyze erosion data of different conditions to obtain a tool for estimating sediment properties. Applying a selected network to a diverse combination of two sets of data (from intact and artificially generated sediment samples), a reasonably fair agreement is achieved between observations and ANN estimated values.

Table1. The applied data set, consists of Jacobs' [1] and Kimiaghalam [2] data sets

#	xcl (%)	xsl (%)	xsa (%)	Pin (%)	ω(ave.)	OM	p(ave.)	τ(ave.)	Ref.	#	xcl (%)	xsl (%)	xsa (%)	Pin (%)	ω(ave.)	OM	p(ave.)	τ(ave.)	Ref.
1	2	49	49	0	21.0	0	2034.0	0.278	[2]	21	12	41	47	7.8	31.5	0	1879.5	0.927	[2]
2	0	4	96	0	27.0	0	1948.0	0.222	[2]	22	16	42	42	11	37.0	0	1817.5	1.419	[2]
3	2	8	90	1.3	21.5	0	2028.0	0.177	[2]	23	5	19	76	5	25.0	0	1976.0	0.520	[2]
4	5	19	76	3.2	20.5	0	2050.5	0.258	[2]	24	6	24	70	6.6	23.5	0	1993.0	0.333	[2]
5	6	24	70	4	21.0	0	2033.5	0.316	[2]	25	11	44	45	13.5	37.0	0	1817.0	0.717	[2]
6	11	45	44	7.5	28.5	0	1924.0	0.980	[2]	26	16	63	21	19.7	49.0	0	1704.0	0.990	[2]
7	16	64	20	10.7	39.0	0	1794.0	0.929	[2]	27	33	28	39	29	39.0	2.2	1823.7	9.380	[1]
8	2	5	93	1.3	22.0	0	2014.0	1.146	[2]	28	27	25	48	12	29.0	1	1825.4	0.980	[1]
9	4	10	86	2.7	21.0	0	2028.0	1.146	[2]	29	41	41	18	34	44.0	9	1741.0	9.550	[1]
10	7	19	74	5	22.5	0	2009.0	0.513	[2]	30	40	43	17	40	54.0	6.6	1744.8	1.720	[1]
11	12	30	58	8	30.0	0	1897.5	1.197	[2]	31	42	44	14	21	28.0	1.1	2005.8	7.810	[1]
12	17	42	42	11.1	38.0	0	1802.0	1.596	[2]	32	50	45	5	24	34.0	1	2066.3	10.250	[1]
13	3	19	78	2	17.0	0	2120.0	0.273	[2]	33	94	4	2	27	35.0	1.4	1915.7	4.850	[1]
14	5	19	76	3.2	20.0	0	2058.5	0.439	[2]	34	60	34	6	17	27.0	1.4	1920.2	8.570	[1]
15	6	19	75	4	22.0	0	2017.5	0.414	[2]	35	65	33	2	14	23.0	1.9	1777.4	1.620	[1]
16	7	18	74	5	23.5	0	1995.5	0.924	[2]	36	56	27	17	24	40.0	2.8	1929.2	2.680	[1]
17	8	18	74	5.4	24.0	0	1984.5	0.899	[2]	37	54	45	1	18	38.0	2.1	2214.9	2.740	[1]
18	2	49	49	1.6	20.5	0	2049.0	0.250	[2]	38	24	37	39	13	17.0	1.2	2156.3	1.600	[1]
19	5	47	47	3.7	23.0	0	2004.5	0.323	[2]	39	25	50	25	5	22.0	1	2131.3	0.310	[1]
20	8	46	46	5.7	28.5	0	1924.5	0.545	[2]										

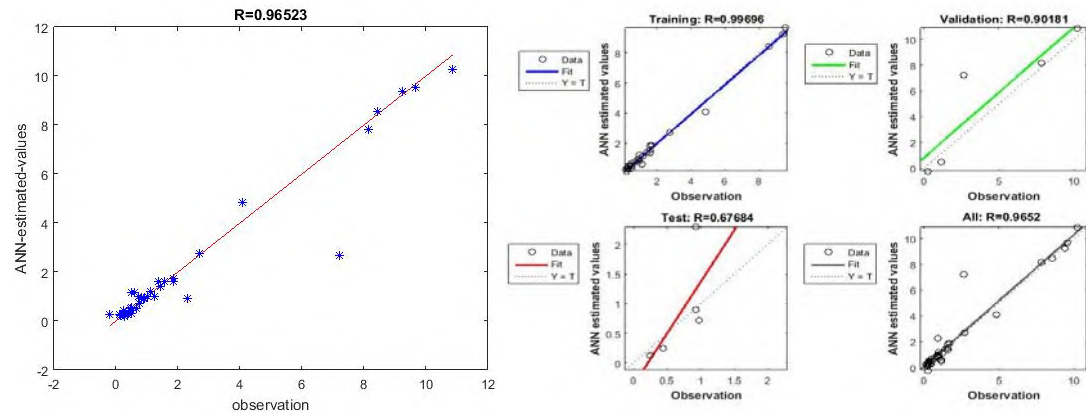


Figure 1. The overall training + Correlation values in different stages of network training

References

- [1] Jacobs, W., Le Hir, P., Van Kesteren, W., & Cann, P. (2011). Erosion threshold of sand–mud mixtures. *Continental Shelf Research*, 31(10), S14-S25.
- [2] Kimiaghalam, N., Clark, S. P., & Ahmari, H. (2016). An experimental study on the effects of physical, mechanical, and electrochemical properties of natural cohesive soils on critical shear stress and erosion rate. *International Journal of Sediment Research*, 31(1), 1-15.
- [3] Parchure, T. M., & Mehta, A. J. (1985). Erosion of soft cohesive sediment deposits. *Journal of Hydraulic Engineering*, 111(10), 1308-1326.
- [4] van Prooijen, B. C., & Winterwerp, J. C. (2010). A stochastic formulation for erosion of cohesive sediments. *Journal of Geophysical Research: Oceans*, 115(C1).
- [5] Winterwerp, J. C., Kesteren, W. G. M., Prooijen, B., & Jacobs, W. (2012). A conceptual framework for shear flow–induced erosion of soft cohesive sediment beds. *Journal of Geophysical Research: Oceans*, 117(C10).

Field investigations of effects of macro flora on fine-grained sediment transport

Lumborg, Ulrik

¹ DHI
Agern Alle 5, DK2970 Hørsholm, Denmark
E-mail: ulu@dhigroup.com

Introduction

Sediment dynamics in near coastal areas has during the recent decades been extensively studied by means of numerical models. These models are often calibrated by comparing measured and modelled sediment concentrations. Although very good calibrations have been presented some patterns remain to be modelled correctly. This is often explained as being due to benthic biology. In this study, it is attempted to improve a numerical modelling tool to include combined seagrass/sediment effects.

Currently there is a good understanding of how suspended sediment affects seagrasses (e.g. De Los Santos et al., 2010). But essential for our ability to quantify effects are also how biology works back on sediment transport. For instance, that vegetation can act as sediment traps.

Seagrass induce hydrodynamic drag on the flow. This reduces water velocity and attenuates wave energy (e.g. Carr et al., 2010). The plants can also be so extensive that the sea bed is mechanically protected from hydrodynamic forces. Combined, these effects reduce the resuspension of sediments and increase sedimentation in the seagrass area (Gacia and Duarte, 2001). On the contrary some authors suggest that the vegetation may increase near bed turbulence and in this way increase the bed shear stress and enhance erosion (e.g. Lefebvre et al., 2010).

Seagrasses require light for growth; thus reduced resuspension, and the corresponding increase in light availability for growth and photosynthesis creates a positive feedback for their growth. On the other hand suspended sediments can limit the growth and thus the protective cover. This may create a negative feedback on the plants. The effect of plants on hydrodynamics has been studied well in the laboratory and during shorter field periods. But seasonal changes are less well studied (Hansen and Reidenbach, 2013). Therefore there is currently a knowledge gap preventing more precise model predictions of eelgrass growth and sediment transport taking into account the interaction between plants and sediment.

In this study it will be attempted to quantify the effect of *Zostera Marina* (eel grass) in a non-tidal lagoon. The effect is studied by means of time series of hydrographic and sedimentological parameters along with mapping of the eel grass. The study will be conducted during a period where the biomass of eel grass is increasing.

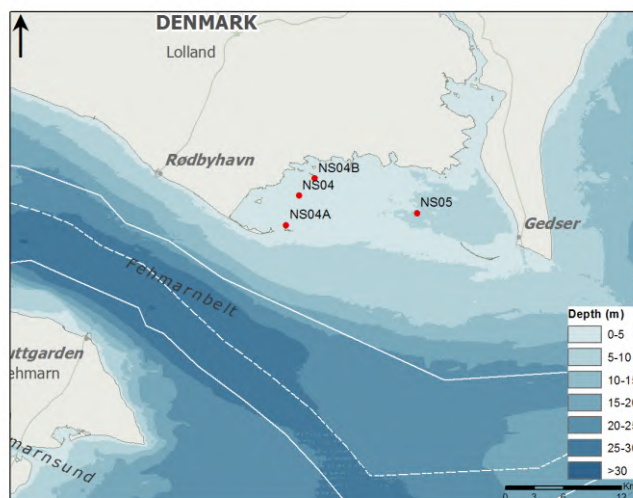


Fig. 1. Rødsand Lagoon. The study area was selected as it is an important habitat located close to Fehmarn Belt. The area is generally shallow and has widespread patches of eel grass.

Non-tidal lagoon used as a study area

The study is conducted in Rødsand lagoon which is a non-tidal lagoon in the inner Danish Waters. The area is located next to Fehmarnbelt and is protected by a coastal spit as well as two semi-submerged sand barriers. The lagoon is located north of the strait Fehmarnbelt and covers an area of approximately 150 km². Water exchange with Fehmarnbelt takes place through three openings towards the South. The water level variation is forced mainly by water level changes in Fehmarnbelt. Fehmarnbelt itself a part of the inner Danish waters. These waters is the transition zone between the salty North Sea and the brackish Baltic Proper. Fehmarnbelt is responsible for 70-75% of the water exchange (Sayin and Krauss, 1996). Rødsand lagoon also has an opening towards the North, Guldborgsund which occasionally contribute to the water exchange.

Online stations to monitor hydrographic and sediment parameters

From April 2014 to October 2015, hydro- and sediment dynamics were studied by means of four online monitoring stations. The stations logged currents and waves as well as turbidity and other water quality parameters. The stations were equipped with automatic remote controlled water samplers so water samples could be extracted also in rough weather. The data set provided very good data to establish a conceptual model of the area and in many periods high correlations between bed shear stress and suspended sediment concentration was observed.

Based on the data from the stations a 3D numerical model was set up (Forsberg et al., n.d. (in review)). Through calibration it was possible to reproduce the main features of the measured turbidity time series. It was however also clear that the eel grass in the lagoon affected the sediment dynamics. Therefore a subsequent study has now been initiated to study the effect of the eel grass on sediment transport.

Quantifying the effect of eel grass on sediment dynamics

A monitoring platform will be placed on a feasible site where eelgrass is present. The station will monitor hydrodynamics with a higher detail also close to the sediment bed. At the same time the eel grass will be documented with respect to area cover, canopy height, shoot density and biomass. An additional station will be placed at a similar site without vegetation.

The overall aim is to improve our ability to predict growth of eelgrass and (fine-grained) sediment dynamics, by being able to model the interaction of sediment dynamics as a function of eelgrass shoot density/biomass, as well as the eelgrass growth dynamics as a function of sediment dynamics. Essentially, this initial study will focus on establishing changes in critical bed shear stress for erosion and deposition. Time series of sediment, hydrodynamic and biological parameters will provide a data basis for understanding the temporal dynamics and quantify critical shear stress and sedimentation/erosion.

References

- Carr, J., D'Odorico, P., McGlathery, K., Wiberg, P., 2010. Stability and bistability of seagrass ecosystems in shallow coastal lagoons: Role of feedbacks with sediment resuspension and light attenuation. *J. Geophys. Res. Biogeosciences* 115, 1-14. doi:10.1029/2009JG001103
- De Los Santos, C.B., Brun, F.G., Bouma, T.J., Vergara, J.J., Pérez-Lloréns, J.L., 2010. Acclimation of seagrass *Zostera noltii* to co-occurring hydrodynamic and light stresses. *Mar. Ecol. Prog. Ser.* 398, 127-135. doi:10.3354/meps08343
- Forsberg, P.L., Lumborg, U., Bundgaard, K., Ernstsen, V.B., n.d. Impact of mussel bioengineering on the fine-grained sediment dynamics in a non-tidal coastal lagoon: a numerical modelling investigation. *J. Mar. Syst.*
- Gacia, E., Duarte, C., 2001. Sediment Retention by a Mediterranean *Posidonia oceanica* Meadow: The Balance between Deposition and Resuspension. *Estuar. Coast. Shelf Sci.* 52, 505-514. doi:10.1006/ecss.2000.0753
- Hansen, J.C.R., Reidenbach, M.A., 2013. Seasonal Growth and Senescence of a *Zostera marina* Seagrass Meadow Alters Wave-Dominated Flow and Sediment Suspension Within a Coastal Bay. *Estuaries and Coasts* 36, 1099-1114. doi:10.1007/s12237-013-9620-5
- Lefebvre, A., Thompson, C.E.L., Amos, C.L., 2010. Influence of *Zostera marina* canopies on unidirectional flow, hydraulic roughness and sediment movement. *Cont. Shelf Res.* 30, 1783-1794. doi:10.1016/j.csr.2010.08.006
- Sayin, E., Krauss, W., 1996. A numerical study of the water exchange through the Danish Straits. *Tellus A* 48A, 324-341.

Modelling net-deposition of cohesive sediments within the ETM

Roland F. Hesse¹

¹ Institute of River and Coastal Engineering, Hamburg Technical University
Denickestraße 22, D-21073 Hamburg, Germany
Email: roland.hesse@tuhh.de

Study area and sediment dynamics

In the navigation channel of the Weser estuary (Northern Germany), net-deposition of predominantly cohesive sediments leads to a high maintenance effort by dredging to guarantee safe shipping traffic to adjacent ports. The estuary is the tidal influenced reach of the Weser river between the weir in the south (km 0) and the North Sea. The average river discharge amounts $326\text{m}^3/\text{s}$ and can vary between 60 and $3500\text{m}^3/\text{s}$. The average tidal range is 2.8m in the outer estuary, but reaches 4.1m at the weir. Thus, the estuary can be classified as hypersynchronous and meso- to macrotidal. The average location of the brackish zone (2 to 20ppt) is located between Weser km 45 to 70 for slack high water and between km 60 to 90 for slack low water. An estuarine turbidity maximum (ETM) occurs in this reach and has been described by Grabemann, *et al.* (1997) based on turbidity measurements. Its position is generally between Weser km 30 and 90 according to Kösters, *et al.* (2014). The core area for maintenance dredging of the navigation channel coincides with the typical, frequent location of the ETM, reported by the German Federal Institute of Hydrology, Eberle and Fiedler (2014). Fig. 1 shows the location of the Weser estuary and the relevant reach where the ETM is located for moderate river discharges.

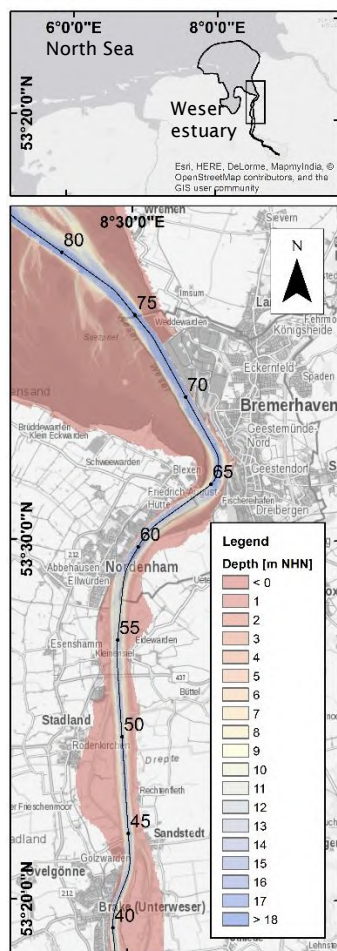


Fig. 1: Location and extent of Weser estuary (model domain) and reach of the navigation channel between km 40 to 80 with depth below chart datum [m NHH]

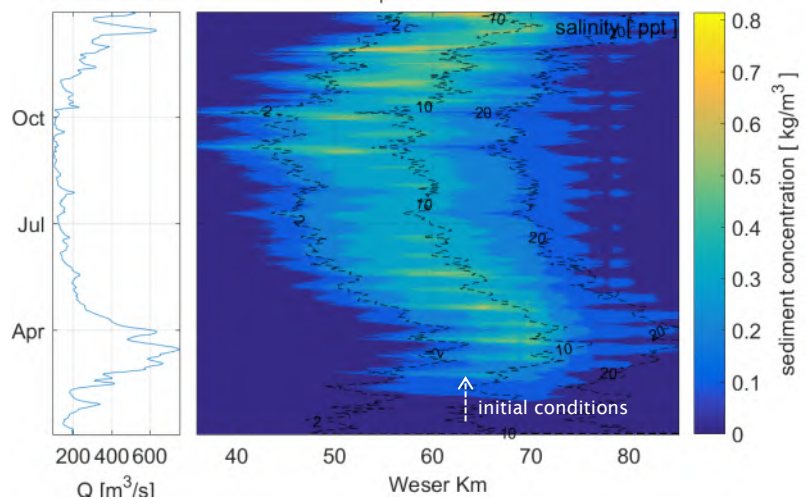


Fig. 2: Modelled, tide- and depth averaged sediment concentration, isohalines (---) and river discharge (Q) for the year 2009

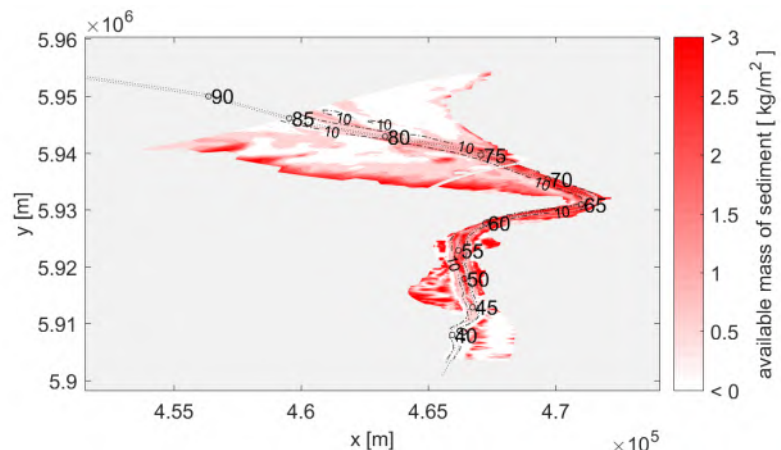


Fig. 3: Modelled areas of net-deposition indicated by available mass of sediment in the lower bed layer after one year at the end of the simulation with navigation channel (· · ·) and isobaths (---) of 10m average water depth (distorted view; coordinate system UTM)

In general, the ETM formation can be explained by the interaction of the effective settling velocity and residual hydrodynamic transport processes induced by salinity gradients in estuaries. More recently, it was shown by Burchard and Hetland (2010) that tidal straining might in some cases have a higher contribution to the ETM formation than gravitational circulation. This is assumed to be valid for the Weser as well. Field studies by Schrottke, *et al.* (2006) show that at times, a concentrated benthic suspension (CBS) is present at the ETM. Schrottke reasons that a small part of CBS is not resuspended during one tide, but deposits with increasing erosion stability. This might be due to different processes (e.g. consolidation) and could explain net-deposition in the presence of high bed shear stresses in the navigation channel. Though, this process is not understood in detail yet.

Modelling approach

To reproduce and investigate the described findings, a hydro-numerical 3D-model has been set up. Two basic characteristic effects shall be simulated with the model:

- Formation of the ETM by sediment transport from the model boundaries and residual accumulation processes in the water column induced by the estuarine residual circulation/tidal asymmetries rather than instantaneous local erosion.
- Net-deposition in the reach of the ETM due to
 - a high settling flux of the accumulated sediments (sediment availability) and
 - an increasing erosion resistance of the deposited sediments (erosion reduction).

The focus of the model approach is to reproduce the sediment transport fluxes, budgets and average variation in a seasonal scale on a big spatial domain, namely the ETM formation and shifting during one year as well as the resulting net-deposition areas according to measured turbidity and dredged volumes. This can be achieved by a simplified parametrization which still enables the reproduction of the described effects but also leads to a passable computational effort.

Model setup and results

The model of the whole estuary is set up using Delft3D. The spatial domain has an extent from north to south of about 100km (Fig. 1, top) and is discretized by about 15,000 elements with 10 vertical layers. The simulation period is the year 2009 with appropriate boundary conditions. Water level and salinity along the navigation channel can be reproduced adequately with root mean square errors smaller than 30cm and 3ppt, respectively. To ensure that the ETM does not evolve merely due to local erosion, no initial sediment distribution is provided and sediment concentrations are only specified at the open model boundaries for the current model stage. Besides, a constant settling velocity $w_s = 1\text{mm/s}$ is used. To be able to reproduce the described objectives the 2-layer-concept by van Kessel, *et al.* (2011) is applied. This concept extends the bed exchange parametrization of Partheniades-Krone with an additional fast responding upper fluff layer. Here, this concept is adopted to reproduce the short scale tidal dynamics of sediments in the water column and the resulting residual transport from the boundaries as well as an increasing erosion resistance of the deposited sediments in areas with a temporally high CBS. Hence, the ETM formation as well as long term net-deposition in the navigation channel at the ETM can be simulated.

Fig. 2 displays the formation and shifting of the modelled ETM along the navigation channel. Fig. 3 shows the corresponding net-deposition after one year. Net-deposition takes place in the navigation channel, but is still underestimated. Though, averaged seasonal measured concentrations (not shown) can be reproduced quite well, taking into account that sediments are specified only at the open boundaries with more than an order of magnitude lower concentrations ($\sim 0.05\text{kg/m}^3$).

References

- Burchard, H. and Hetland, R. D. (2010). Quantifying the Contributions of Tidal Straining and Gravitational Circulation to Residual Circulation in Periodically Stratified Tidal Estuaries. *Journal of Physical Oceanography*, 40 (6): 1243–1262.
- Eberle, M.E. and Fiedler, M. (2014). Sedimentmanagementkonzept Tideweser. Untersuchung im Auftrag der WSA Bremen und Bremerhaven. Bericht 1794. Koblenz.
- Grabemann, I., Uncles, R., Krause, G., and Stephens, J. (1997). Behaviour of Turbidity Maxima in the Tamar (U.K.) and Weser (F.R.G.) Estuaries. *Estuarine, Coastal and Shelf Science*, 45: 235–246.
- Kösters, F., Grabemann, I., and Schubert, R. (2014). On SPM dynamics in the turbidity maximum zone of the Weser estuary. *Die Küste : Archiv für Forschung u. Technik an d. Nord- u. Ostsee ; archive for research and technology on the North Sea and Baltic Coast*, 81 (2014): 393–408.
- Schrottke, K., Becker, M., Bartholomä, A., Flemming, B. W., and Hebbeln, D. (2006). Fluid mud dynamics in the Weser estuary turbidity zone tracked by high-resolution side-scan sonar and parametric sub-bottom profiler. *Geo-Marine Letters*, 26 (3): 185–198.
- van Kessel, T., Winterwerp, H., van Prooijen, B., van Ledden, M., and Borst, W. (2011). Modelling the seasonal dynamics of SPM with a simple algorithm for the buffering of fines in a sandy seabed. *Continental Shelf Research*, 31 (10): 124-134.

Numerical modelling of flow and sediment transport under the impact of vegetation

Sina Saremi¹, Nils Drønen¹

¹ DHI

Agern Alle 5, DK2970 Hørsholm, Denmark

E-mail: Sina Saremi sis@dhigroup.com

Abstract

The presence of aquatic vegetation can alter properties such as flow resistance and turbulence in shallow water systems which consequently impacts the transport of sediment, organic flocs, nutrients and contaminants. The fate of these particles is closely linked to vegetation and may exert major influences on habitats and biodiversity. For this, it is important to take into account the presence of vegetation in hydrodynamic modelling where its results will be used for sediment transport, morphodynamic and ecological modelling, and their feedback to the hydrodynamics.

There are already models which describe the effects of vegetation on water flow and sediment transport mainly by reduction and dampening of turbulent stresses due to vegetation drag, calculated either as an excess bottom resistance (Luhar *et al.*, 2008) or as a local drag force in the vegetated volume inducing loss of momentum (Maza *et al.*, 2013; Jacobsen, 2016). The parameters used in the models are mostly obtained from laboratory experiments for specific conditions and types of vegetation (artificial or real). Besides, comparative analysis and validations on extensive datasets are still lacking therefore making the application of the results to real cases difficult.

In this study the aim is to couple the impact of vegetation on hydrodynamics and fine sediment transport (and ultimately on morphology, nutrients transport and light) and the feedback on the growth and biomass (ex. shoot density) of the vegetation.

The impact of vegetation on the hydrodynamics of waves and currents will be modelled by defining the vegetation as a 3D porous medium in the MIKE3-HD model. As an example, in figure 1, the impact of a vegetated area on wave field is shown, where it causes velocity dampening and phase lag. The porosity and the drag coefficients will be a function of the vegetation type and properties. The hydrodynamic model is coupled with the sediment transport (MIKE-MT) and the ecological model (MIKE-EcoLab), where the altered flow properties impact the transport, erosion and deposition of sediments and other nutrients and particles in the flow, influencing the light and water quality around the vegetated area. The ecological model then reacts on changes in light and water quality and controls the growth rate of vegetation in the bottom.

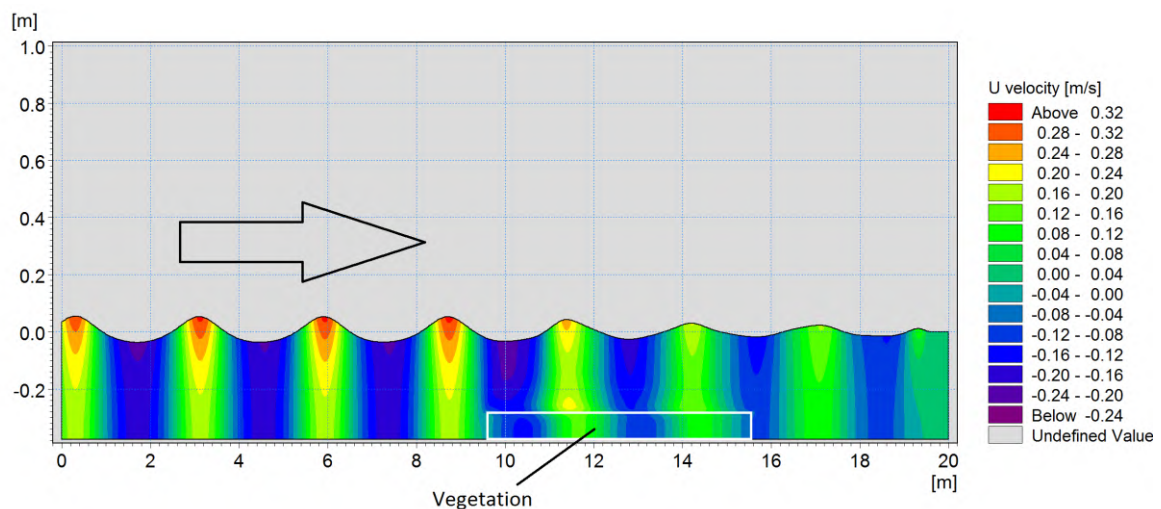


Fig. 1. Impact of vegetation on propagating waves in form of dampening and change in velocities and phase

This study will be accompanied by a field investigation in Rødsand lagoon which is a non-tidal lagoon in the inner Danish Waters. A monitoring platform will be placed on a feasible site where eelgrass is present. The station will monitor hydrodynamics with a higher detail also close to the sediment bed. At the same time the eel grass will be documented with respect to area cover, canopy height, shoot density and biomass. An additional station will be placed at a similar site without vegetation. In this way, the influence of vegetation on the flow properties and concentration levels can be determined. These results will then be used for calibration of the model parameters for implementing the vegetation effects such as drag coefficients and porosity values.

Coupling the hydrodynamics, sediment transport and the ecological modelling of the growth and decay of vegetation enables a better understanding and predicting of the dynamics of the fine sediments transport in vegetated areas and their feedback on the vegetation's growth and local habitats.

References

- Jacobsen N. G. (2016). Wave-averaged properties in a submerged canopy: Energy density, energy flux, radiation stresses and Stokes drift. *Journal of Coastal Engineering*, 117 (2016) 57-69
- Vargas-Luna A., Crosato A., Uijttewaal W.S.J. (2015). Effects of vegetation on flow and sediment transport: comparative analysis and validation of predicting models. *Journal of Earth Surface Processes and Landforms*, 40 (2015) 157-176
- Maza M. , Lara J.L., Losada I.J. (2013). A coupled model of submerged vegetation under oscillatory flow using Navier-Stokes equations. *Journal of Coastal Engineering*, 80 (2013) 16-34

Influence of Salinity on the Coastal Turbidity Maximum in the Southern Bight of the North Sea

Diem Nguyen^{1,2}, Joris Vanlede^{2,3}, and Bart De Maerschalck²

¹ Antea Group, Buchtenstraat 9, 9051 Gent, Belgium
E-mail: ThiThuyDiem.Nguyen@anteagroup.com

² Flanders Hydraulics Research, Berchemlei 115, 2140 Antwerp, Belgium

³ Delft University of Technology, Faculty of Civil Eng. and Geosciences, Stevinweg 1, 2628 Delft, the Netherlands

Introduction

In the Southern Bight of the North Sea, a Coastal Turbidity Maximum (CTM) can be observed in the Belgian coastal area around the port of Zeebrugge. Understanding the dynamics of this turbidity maximum is of great importance in coastal zone management. Our research studies the CTM with a numerical process model (model domain shown in Fig. 1).

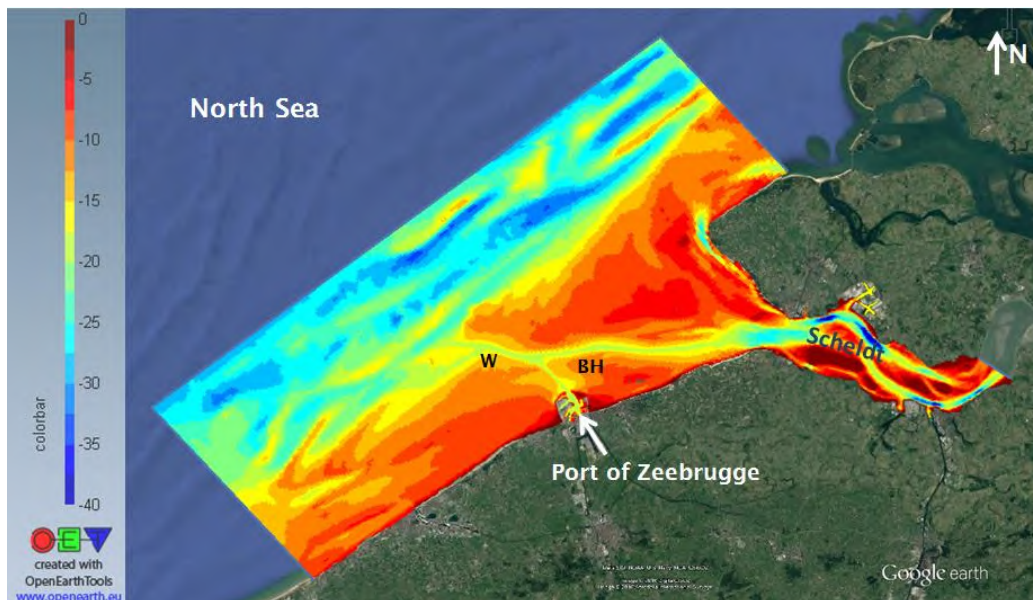


Fig. 1: Model domain and bathymetry. Letters W and BH indicate the location of the observation stations Wandelaar and Bol van Heist

Methods

The hydrodynamics is simulated using a 3D hydrodynamic model, developed within the Delft3D model suite (Deltares, 2011) and is then passed on to a sediment transport model implemented in Delwaq (Deltares, 2014). In this way the sediment dynamics in the area is modelled in an 'offline' mode. Two methods of taking into account the effect of waves are examined: importing the calculated wave field and applying a simple fetch length approach. The sediment transport is modelled using a two-layer bottom model as described in van Kessel et al. (2011).

The model starts running without prescribed initial sediment, neither in the bed nor in the water column. The sediment supply comes from the model boundaries and the model gradually builds up to a dynamic equilibrium. This modelling approach is suitable for studying CTM (and ETM) dynamics, as the resulting turbidity maximum is not forced through the provided initial condition, but is an internal solution of the system.

Results

The turbidity maximum in front of the port of Zeebrugge is found to be robust to a wide range of parameter settings (e.g. Fig. 2). The mechanisms controlling the suspended sediment concentration are studied in detail.

This paper focuses on the effects of salinity on the formation of the CTM. The results of suspended sediment concentration obtained from the simulations in baroclinic mode (with salinity) and barotropic mode (without salinity) are compared (Fig. 2a,b). The density-induced residual circulation due to salinity (Fig. 3a,b) causes more sediment being trapped within the turbidity maximum.

Due to the feedback mechanism of the system, the change of the model settings leads to the change in the sediment pattern of the whole system. As the result of the change in the turbidity maximum pattern in the vicinity of the port of Zeebrugge, the exchange of sediment through the port, the dredging (and thus dumping) amount are affected. These, in turn, modify the turbidity maximum in the area. This feedback intervention will be thoroughly discussed.

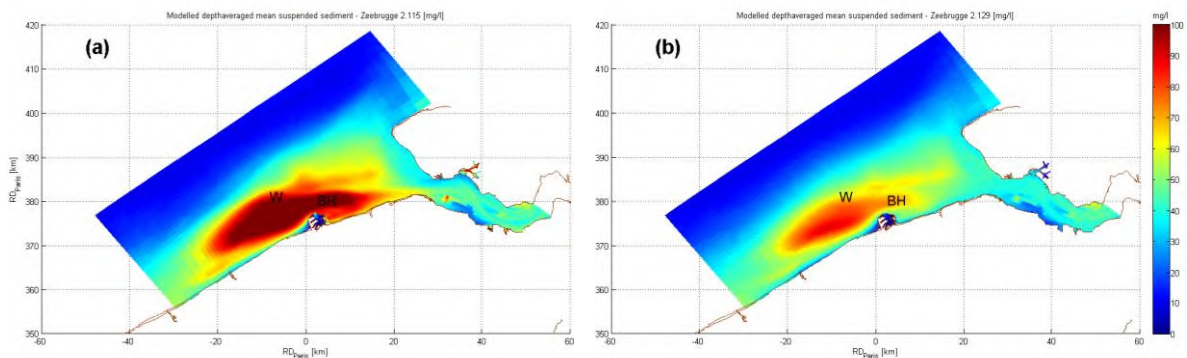


Fig. 2: Depth-averaged suspended sediment concentration (averaged over a spring-neap cycle) computed (a) with salinity and (b) without salinity

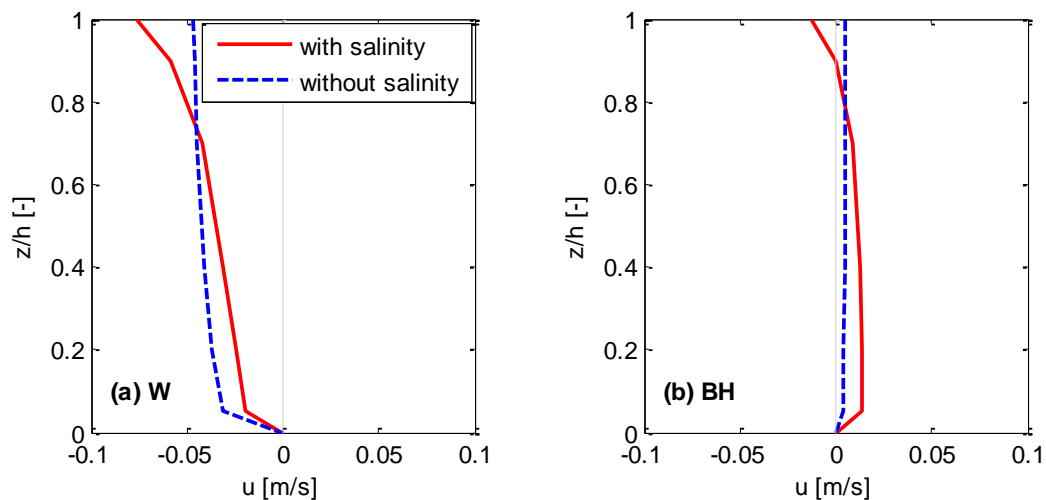


Fig. 3: Spring-neap averaged current velocity profiles computed at (a) Wandelaar (W) and (b) Bol van Heist (BH) (see Fig. 1 & 2 for the locations). Positive values indicate currents directed landward

References

- Deltares (2011). Delft3D-flow: Simulation of multi-dimensional hydrodynamic flows and transport phenomena, including sediments. User manual.
- Deltares (2014). D-Water Quality: Water Quality and Aquatic Ecology Modelling Suite. User Manual.
- Van Kessel, T., Winterwerp, H., Van Prooijen, B., Van Ledden, M., & Borst, W. (2011). Modelling the seasonal dynamics of SPM with a simple algorithm for the buffering of fines in a sandy seabed. *Continental Shelf Research*, 31(10): S124-S134.

Dynamics of the suspended particle matter transport in an estuary with morphology strongly modified by human activities

Beatriz M. Marino¹, Luis P. Thomas¹, Ricardo N. Szupiany², Manuel A. Gutierrez¹

¹ Grupo Flujos geofísicos y Ambientales, Centro de Investigaciones en Física e Ingeniería
CONICET – Universidad Nacional del Centro Prov. Buenos Aires, Pinto 399, 7000 Tandil, Argentina
E-mail: lthomas@exa.unicen.edu.ar

² Facultad de Ciencias Hídricas
Universidad Nacional del Litoral, CC 217, 3000 Santa Fe, Argentina

Introduction

In brackish waters, suspended particles rarely exist in their primary state; instead, they are typically found as aggregated and heterogeneous assemblages of mineral grains, biogenic debris, bacteria and organic material. The texture, size and density of the particles are largely controlled by flocculation, which acts as one of the key factors determining the transport and deposition of suspended particulate matter (SPM) in estuaries. In these environments particle transport processes are governed by tidal currents, river flow, waves, salinity gradients and SPM characteristics; they are driven by a well-known cycle: suspension, flocculation, settling, deposition, erosion, and resuspension. In addition, the SPM concentration depends mainly on the kind of estuary (i.e. highly stratified, partially mixed, well mixed), the magnitude and variability of riverine discharges, the characteristics of the hydrodynamics processes (i.e. friction effects, residual circulation), the sediment characteristics (i.e. granulometry, flocculation, settling velocity), the maximum turbidity and the sediment residence time, among others.

The high spatial and temporal variability of suspended sediment and its associated components (including contaminants and living organisms), in conjunction with the typically low flow velocities, has generated an increasing interest in the characterisation and quantitation of the estuarine transport of SPM in order to study the distribution patterns and the associated deposition-erosion processes. Therefore, measurements with optical and acoustic instruments require careful calibration and interpretation due to they depend greatly upon a variety of parameters (particle size, composition, shape, environmental characteristics). The aim of the present study is to characterise the transport of SPM in the Quequén Grande River estuary where flocculation processes occur analysing the records obtained with two acoustic Doppler current profilers (ADCP) and one diffractometer.

Methodology

The estuary, located in southeastern Buenos Aires Province in Argentina, is a microtidal coastal plain primary system between 150 and 200 m wide, and its head is marked by minor falls at 13.7 km from the mouth. Measurements were performed during the survey conducted on 23–24 August 2016, during complete tidal cycles. Six measurement stations were set at 1.36, 1.99, 2.89, 7.44, 8.41 and 11.35 km upstream of the jetties position. The prevailing quiet meteorological conditions in the days prior to the survey meant that the estuarine system was stratified. The river discharge had values close to minimum mean values and the wind did not significantly affect the estuarine flows. A *Horiba* U-50 multiparameter water quality meter was employed to obtain salinity profiles.

Two *Workhorse Río Grande* ADCPs of 600 and 1200 kHz (*Teledyne RD Instruments*) and a global positioning system were placed on the same side of a small boat for simultaneous measurement of the water column. Sailing transversally and longitudinally to the main current (back and forth, twice) in selected places, the distributions of the water velocity and SPM backscatter intensity were determined employing *Winriver 2.08* software and plotted with *VMT* software (Parsons et al., 2013). For each run, the backscatter intensity of any ADCP was transformed, cell by cell, into concentration using calibration curves, while using both equipment simultaneously the flocs size distribution was determined. In addition, the total flow crossing a given cross-section was obtained by multiplying the concentration by the velocity and area in each cell and integrating the whole cross-section.

The backscatter signals measured with each ADCP were averaged during the time in which LISST-25X (*Sequoia Sci. Inc.*) measurements were also performed. These average values were corrected by taking into consideration the attenuation of the sound waves due to beam spreading, the absorption due to the water viscosity and the presence of fine sediments (Latosinski et al., 2014). The results were then correlated with the SPM concentration obtained from the measurements performed with the LISST-25X to find the calibration curves.

Results

A great variability of the flocs size is found, which is consistent with a variable composition of organic and inorganic matter. Flocs consist of fine inorganic matter, basically silt and clay carried by the river, and organic matter provided presumably by the waste waters from the cities located next to the estuary and port activities. These suspended elements remain in the system long enough to allow aggregations to be formed, which results from the combination of the low river discharge and the small tidal amplitude. The poor flushing of the estuary also has an important impact on the nutrient enrichment of estuarine waters and consequently on the abundance of organic matter.

The SPM is transported to the harbour (where the aggregation processes are more intense) in the faster surface layer that develops on the SW side and covers all the estuary cross-section near the estuary mouth. The flow stops at slack tide and the suspended particles start to separate from the surface layer to settle on the bottom. During the flood tide, most of flocs have just settled and the flow velocity in the harbour area is too slow to transport sediments upstream (see for instance Figure 1). Thus, the combination of the deposition times, dynamics of the exchange flows, stratification and particular bathymetry generates that the flocs are retained in the harbour bed, tending to fill the space artificially created by dredging. This occurs independently of the river contributions, at least when river and tidal flows are low. A detailed description of the flocs deposition in the 12m deep harbour zone by analysing the concentration and size profiles in the measurements stations located there is reported by Thomas et al (2017).

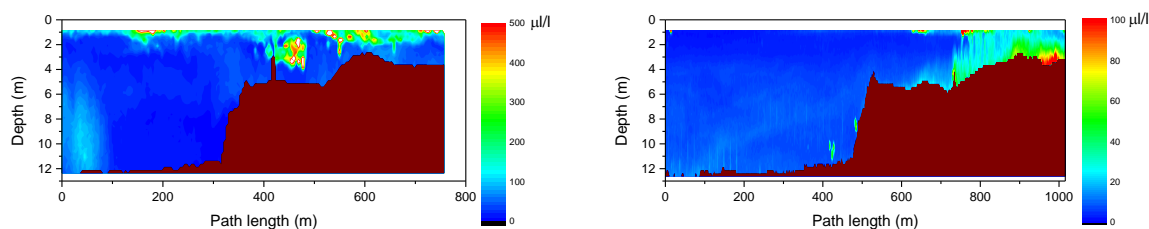


Fig.1. SPM concentration distributions along a longitudinal path that passes through the abrupt depth step at the end of the ebb-tide (left), and during the maximum flood (right).

Conclusions

Stratified, unsteady, non-uniform flows and flocculation processes in estuaries present important challenges for the characterisation of the dynamics of the suspended matter transport and require the use of combined techniques. Velocity and backscatter intensity measurements, carried out along and across the flow, as well as previous bathymetric studies were combined to analyse the circulation and sediment dynamics of the Quequén Grande River estuary. The information obtained enables us to move forward with the comprehension of the SPM transport and relate it with morphology and circulation. As a consequence of the significant modifications caused by human intervention in this estuary, the deepening and widening of the natural watercourse by dredging generated a decrease of the water velocity and turbulence in the harbour area. Thus, different circulations in the deep harbour zone and in the shallow part of the estuary are induced, affecting the settling of SPM. Particularly, the two-ADCP method employed by Guerrero et al. (2013) in rivers (where the sediment mainly consists of sand) showed to be highly effective for determining the SPM size distributions in a non-intrusive way in brackish and salt water, and then the SPM flow. The presence of flocs as acoustic targets, which are greater than single organic and inorganic particles, is an additional advantage, since flocs cause more intense backscatter intensity. Moreover, the speed at which measurements can be made can allow the detection of spatial and temporal variations due to changes in the local current velocity.

References

- Guerrero M., Szupiany R.N., Latosinski F. (2013). Multi-frequency acoustics for suspended sediment studies: an application in the Parana River. *J. Hydraulic Research*, 51 (6): 696-707.
- Latosinski F., Szupiany R.N., García C.M., Guerrero M., Amsler M.L. (2014). Estimation of Concentration and Load of Suspended Bed Sediment in a Large River by Means of Acoustic Doppler Technology. *J. Hydraulic Eng.*, 10.1061/(ASCE)HY.1943-7900.0000859, 04014023.
- Parsons D., Jackson P., Czuba J., Engel F., Rhoads B., Oberg K., Best J., Mueller D., Johnson K., Riley J. (2013). Velocity Mapping Toolbox (VMT): a processing and visualization suite for moving-vessel ADCP measurements. *Earth Surface Processes and Landforms*, 38(11): 1244-1260.
- Thomas L.P., Marino B.M, Szupiany R.N, Gutierrez M. (2017) Influence of the flocculation on the deposition of the suspended particle matter in specific places of a modified estuary. INTERCOH 2017, Montevideo, Uruguay.

Dynamics of the settling of the flocculated suspended particle matter in specific places of a modified estuary

Luis P. Thomas¹, Beatriz M. Marino¹, Ricardo N. Szupiany², Manuel A. Gutierrez¹

¹ Grupo Flujos geofísicos y Ambientales, Centro de Investigaciones en Física e Ingeniería
CONICET – Universidad Nacional del Centro Prov. Buenos Aires, Pinto 399, 7000 Tandil, Argentina
E-mail: lthomas@exa.unicen.edu.ar

² Facultad de Ciencias Hídricas
Universidad Nacional del Litoral, CC 217, 3000 Santa Fe, Argentina

Introduction

The ability to predict the sediment and nutrients circulation within estuarine waters is of significant economic and environmental importance. In these systems, flocculation is a dynamically active process that is directly affected by the prevalent environmental conditions. Consequently, the floc properties continuously change, which greatly complicates the characterisation of the settling of suspended particle matter (SPM). In this study, two techniques are combined in a stratified estuary under quiet weather conditions and with a low river discharge to provide a solution to this problem. The challenge is to obtain the concentration and size profiles of suspended elements at selected sites using ADCP records and diffractometer measurements for calibration. The usefulness of this methodology lies in its practicality for obtaining information in situ with high temporal and spatial resolutions.

Measurements were performed in the Quequén Grande river estuary (QGRE), located in southeastern Buenos Aires Province in Argentina. The QGRE is a microtidal coastal plain primary system between 150 and 200m wide and 13.7km long. The saline wedge enters about 10km from the sea. The Quequén Harbour, mainly associated with grain exports, is located in the last 2 km of the estuary and its 12–14 m depth is maintained by regular dredging. Further upstream, the thalweg is 3–4 m deep, with an irregular topography exhibiting small canals, 5–7 m deep, formed by local currents. This generates an artificial abrupt depth step that separates the estuary into two parts. Typically, the river discharge crosses this zone slightly mixed with salt water, in a 1–3 m surface layer with a halocline below, with salinities reaching over 30 practical salinity units (PSU), homogeneous down to the bottom. Two jetties prevent the entry of sand from the sea, except during severe storms

The goal of the present study is to describe the settling of the SPM in the harbour zone, which is favoured by the flocculation of the sediments transported by the river. The dynamics of the SPM transport throughout the estuary is described in the separated paper by Marino et al. (2017).

Materials and Methods

Data for the description were obtained in two measurement stations set at 1.36 and 1.99km upstream of the jetties position during complete tidal cycles. The prevailing quiet meteorological conditions in the days prior to the survey meant that the estuarine system was stratified.

Two *Workhorse Río Grande* ADCPs of 600 and 1200 kHz (*Teledyne RD Instruments*) were placed on the same side of a small boat (that remained at rest) for simultaneous measurement of the water column. The backscatter intensity of any ADCP was transformed, cell by cell, into concentration using calibration curves, while using both equipment simultaneously the flocs size profile was determined. The backscatter signals measured with each ADCP were averaged during the time (about 5min) in which LISST-25X (*Sequoia Sci. Inc.*) measurements were also performed. These average values were corrected by taking into consideration the attenuation of the sound waves due to beam spreading, the absorption due to the water viscosity and the presence of sediments. The results were then correlated with the SPM concentration obtained from the measurements performed with the LISST-25X to find the calibration curve. The diffractometer provides the Total Sauter Mean Diameter of the complete sample between 2.50 and 500 μm , and the Sauter Mean Diameter of the coarse fraction between 63 and 500 μm , thereby yielding information about the mean sizes of the total and coarse fractions of suspended particles, respectively. It also determines the total suspended sediment volume concentration and the coarse suspended sediment volume concentration from 0.10 to 1000 mg/L. A *Horiba* U-50 multiparameter water quality meter was employed to obtain salinity profiles.

Results

Fig. 1 shows the concentration (a) and size (b) profiles obtained with the 1200kHz ADCP and the two-ADCPs method (lines), respectively, and with LISST-25X (black points) at different times, at the

end of the ebb-tide. The greatest concentrations and sizes are observed in the 1.5m-thick brackish surface layer. Below this layer, profiles relatively constant in depth are obtained although with significant size fluctuations (50–350 μm). At the beginning of the flood-tide (Fig. 2), the profiles shape changes drastically. The SPM concentration substantially increases and the maximum value is at an ever increasing depth, which is consistent with a quick sedimentation of the SPM. This implies that, during the transition from the ebb- to the flood-tide, flocs are separated from the lighter surface layer, pass through the freshwater-saltwater interface, and fall rapidly toward the bed. The suspended particles have the same mean size in the surface layer; the size decreases at a depth of 1.5m, and from a depth of 2.5m to the bed the flocs size increases. Thus, a separation of the suspended elements as function of the water depth is obtained. LISST-25X records shows a great variability partly because the quick evolution of the profiles shape during the measurement time (= 5min), and also to the fluctuations of the SPM concentration that increases with depth.

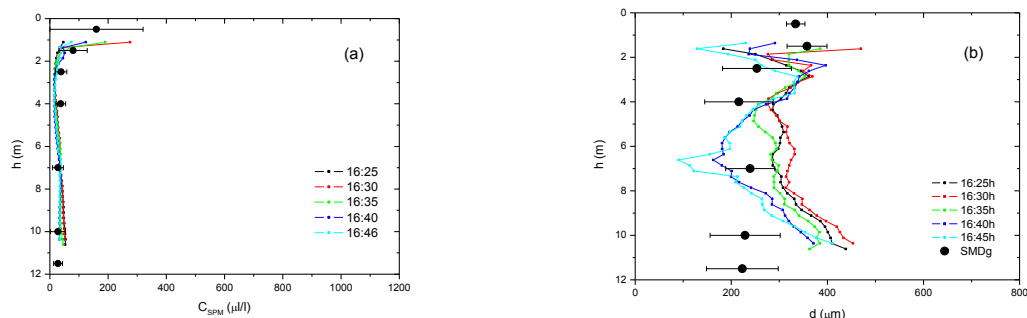


Fig. 1. Profiles of (a) concentration and (b) size of the SPM at the end of the ebb-tide. They were obtained using ADCPs (lines) and LISST-25X (black points). The bars represent de standard deviations of the mean values obtained with the diffractometer.

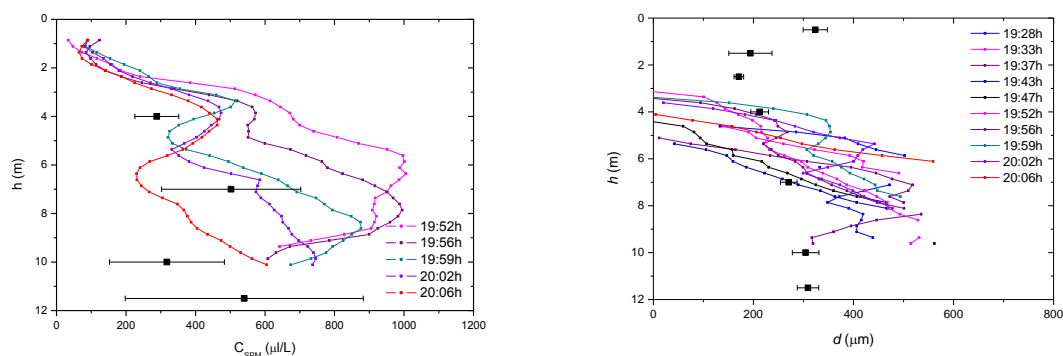


Fig. 2. Profiles of (a) concentration and (b) size of the SPM at the flood-tide.

Conclusions

Measurements performed in the harbour zone offer a global overview of the deposition process in the Quequén Grande River estuary. After the ebb-tide finishes, the river freshwater containing sediments (mainly silt and clay) and organic matter occupy the surface layer throughout the harbour zone. All this SPM forms aggregations with average sizes of up to 400 μm . The slackwater creates the proper physical conditions for a quick sedimentation of flocs, and the water depth of 12m is enough for a separation by size in depth (since the greatest flocs fall quicker than the smallest ones).

Although the concentration profiles determined using the intensity of the backscatter acoustic signal largely reproduce the measurements performed with LISST-25X, the ADCPs information is continuous in the whole water column unlike the point measurements provided by the diffractometer. In addition, the estimate of the flocs size employing the two-ADCPs technique is reasonable when a uniform size distribution in depth exists as occurs during the ebb-tide (Fig. 1b). However, incorrect results are obtained when important variations of concentration and size take place as occurs at the beginning of the flood-tide. In a future work, the necessary theoretical modifications to calculate the sizes under this situation will be studied.

References

Marino B.M., Thomas L.P., Szupiany R.N., Gutierrez M.A. Dynamics of the suspended particle matter transport in an estuary with morphology strongly modified by human activities. INTERCOH 2017, Montevideo, Uruguay.

Study of dimensionless wave attenuation rate on fluid mud beds

Sima ghobadi¹, Mohsen soltanpour¹

¹ Department of Civil Engineering, K. N. Toosi University of Technology, No. 1346, Vali-Asr St., PO Box 19967-15433 Tehran, Iran
E-mail: soltanpour@kntu.ac.ir

Abstract

Considerable energy dissipation is observed when waves pass over fluid mud layers. Water depth, wave characteristics and mud properties are all effective on damping of wave energy. As the details of the physical processes in the complex wave-mud interaction are not well understood, the applications of the techniques of data mining look beneficial. Employing available laboratory data, the present study offers an empirical dimensionless expression for the wave attenuation rate based on the most effective parameters. M5' model tree as a machine learning approach is employed and the performance of the derived formula is examined.

Introduction

Regression trees are simple and efficient models to deal with domains of large number of variables. They are obtained by dividing the given training data into smaller subsets. Within Machine Learning, most research efforts concentrate on classification (or decision) trees, in comparisons to regression trees and M5 (Quinlan, 1992; Wang and Witten, 1997).

Dimensionless parameters of the model

A number of laboratory and numerical studies have been conducted in order to study the effective parameters on wave height attenuation over fluid mud layer. The results show that wave energy dissipation depends on water depth and wave characteristics, such as wave height and wave period, and thickness of fluid mud and its properties, such as density and rheological behaviour. By dimensional analysis of above governing parameters, different dimensionless quantities can be derived. Table I presents the list of the adopted dimensionless quantities where μ , f , H , ρ_m , ρ_w , d , k_i , h and g stand for dynamics viscosity, wave frequency, wave height, mud density, water density, mud depth, wave attenuation rate, water depth and gravitational acceleration, respectively.

Table I. Dimensionless parameters used in M5 algorithm

Dimensionless parameters	Physical meaning
$\frac{k_i}{k_s}$	dimensionless Wave height attenuation
$\frac{\omega^2 d}{g}$	relative mud depth
$\frac{\omega^2 h}{g}$	relative water depth
$\frac{\omega^2 H}{g}$	wave steepness
$\frac{\nu}{h^2 \omega}$	dimensionless viscosity
$\frac{\rho_m}{\rho_w}$	Relative density
$\frac{\nu}{\sqrt{g h^3}}$	dimensionless viscosity
$k_s H$	dimensionless wave height

Model tree modelling and results

The data set includes laboratory experiments of Sakakiyama and Bijker (1989), Jiang (1983), Soltanpour and Samsami (2011) and Hsu et al. (2013). Each set of laboratory data was examined to study the relationship between dimensionless wave height attenuation and dimensionless parameters of Table 1. M5 algorithm was then used to predict the best relation for the dimensionless wave attenuation rate. All data of 182 runs were randomly divided to two training (75%) and testing (25%) groups. As only linear relationships can be modelled by M5' model tree, logarithmic values of the parameters were employed to prevail this limitation. The nonlinear formula for dimensionless wave attenuation can be derived as

$$k_i/k_s = \left(\frac{\omega^2 H}{g}\right)^{0.197} \times \left(\frac{\rho_m}{\rho_w}\right)^{3.6619} \times \left(\frac{\omega^2 h}{g}\right)^{-0.786} \times \left(\frac{v}{\omega h^2}\right)^{0.2346} \times e^{-4.065} \quad (1)$$

Following the statistical parameters of Willmott et al. (2012), Table II shows the accuracy of the proposed formula. Scatter diagram of the measured versus predicted dimensionless parameters is presented in figure 1. It is observed that the derived relationship is capable to predict the damping of passing waves on fluid mud beds.

Table II. Validation indices between predicted and measured dimensionless wave attenuation rate

Correlation coefficient (R^2)	Relative error (E)	Index of model performance (d_r)
0.873	0.087	0.96

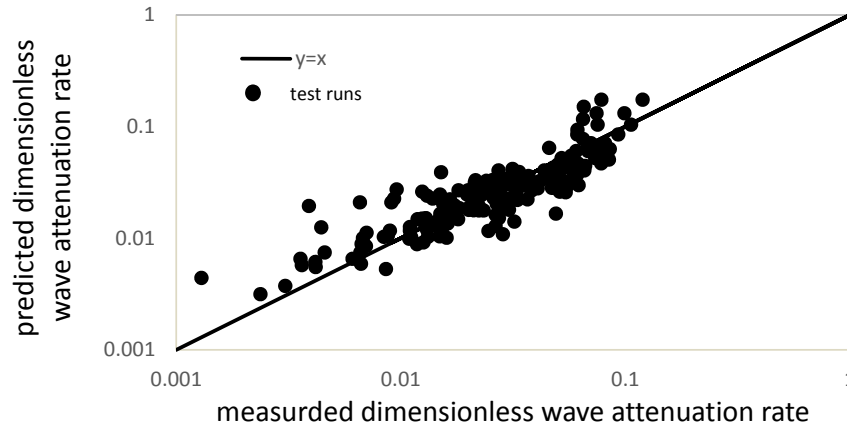


Fig. 1 Measured and predicted dimensionless wave attenuation rates

References

- Hsu W. Y., Hwung H. H., Hsu. T. J., Freyermuth A. T. and Yang R. Y. (2013). An experimental and numerical investigation on wave-mud interactions. *Journal of Geophysical Research, Oceans*, 118(3), 1126-1141.
- Jiang F. (1993). Bottom and transport due to water waves. Ph.D. Dissertation, University of Florida, Gainesville, 222p.
- Quinlan J.R. (1992). Learning with continuous classes. *Proc. of the 5th Australian Joint Conference on AI'92 (Adams & Sterling)*, 343-348.
- Sakakiyama T. and Bijker E. W. (1989). Mass transport velocity in mud layer due to progressive waves. *Waterway Port Coastal Ocean Eng*, 115, 614-633.
- Soltanpour M. and Samsami F. (2011). A comparative study on the rheology and wave dissipation of kaolinite and natural Hendijan Coast mud, the Persian Gulf, *Ocean Dynamics*, 61(2-3), 295-309.
- Wang Y. and Witten I. H. (1997). Inducing model trees for continuous classes. In *Proceedings of the Ninth European Conference on Machine Learning*, 128-137.
- Willmott C. J., Robeson S. M. and Matsuura K. (2012). A refined index of model performance. *International Journal of Climatology*, 32(13), 2088-2094.

How settling velocity impacts modeled intratidal ssc patterns and residual sediment fluxes

Anna Zorndt¹, Steffen Grünler¹, Frank Kösters¹, Marius Becker²

¹ Bundesanstalt für Wasserbau, Federal Waterways Engineering and Research Institute, Wedeler Landstraße 157, 22559 Hamburg, Germany.
Corresponding author e-mail: anna.zorndt@baw.de

² MARUM Center for Marine Environmental Sciences, Bremen University, Leobener Straße, 28359 Bremen, Germany.

Introduction

Carefully assessing impacts of human interventions on sediment transport in estuaries has become increasingly important due to the high ecological importance of these systems. Quantifying these changes is commonly done by numerical modeling. Especially for suspended sediment concentration (ssc), model results rely on the applied model formulations and model parameters, settling velocity being a key parameter. The validation of ssc is therefore important, but is often difficult due to limited measuring data. However, small variations of settling velocities can lead to relevant variations of the overall residual sediment fluxes in the whole estuary.

Objective

In this study, an estuary model of a macro-tidal and well- to partially mixed estuary is used to study intratidal ssc patterns for different settling velocities, compare them to measurements and in a second step, assess the impact of settling velocity on the residual sediment fluxes over a hydrological year.

Study area and methods

The study area is the Weser estuary, which discharges into the south-eastern North Sea (Germany). Strain induced periodic stratification is assumed to be the main contributor to the estuarine circulation. In measurements and simulations, sips can be observed especially during high river runoff and neap tides. Over the tidal cycle, high variations in suspended sediment concentration (ssc) from <10mg/l to over 1g/l occur. This is due to the processes of local resuspension and advection with flood and ebb currents, followed by settling and finally deposition during slack tides.

The employed hydrodynamic modeling tool, based on the shallow water equations, is Un-TRIM (Casulli and Zanolli, 2002) coupled with the SediMorph module which calculates the transport of suspended sediment and bed load. The model of the estuary stretches from beyond the limit of freshwater influence to the limit of tidal influence at the tidal weir (Fig. 1a). Realistic boundary conditions are considered, including modeled and / or measured water levels, river runoff, waves, salinities, temperature and ssc. A comparison of model water levels, salinity and temperature to measurements has shown very good agreement. Sediment transport is calculated with a multi-fractional approach with up to five suspended sediment fractions. Each is assigned a settling velocity based on the Dietrich formulation. The initial distribution on the bed is based on surface samples.

The model is run for an initial spin-up phase and consecutively for a time span covering the below mentioned ADCP measurements in 2009, as well as the hydrological year 2012.

To determine the intratidal ssc patterns, cross-sectional hydro-acoustic profiling data over a full tidal cycle were collected, using two vessel-mounted simultaneously direct reading ADCPs (300Hz, 600Hz). The measurements were carried out at three locations within the etm in three consecutive years (2009 - 2011). In order to cover the change of acoustic properties of the particles, vertical profiles of CTD, OBS and LISST as well as water samples were taken every 30 minutes.

To study the residual sediment fluxes in the whole estuary, exact transport rates at the edges of the elements of the numerical grid are integrated during the simulation and later aggregated over control volumes representing relevant morphological units.

Results and discussion

A comparison of the modeled current velocities to the ADCP measurements shows very good agreement. At many instances in the tidal cycle, the spatial patterns observed and modeled ssc are in good agreement, as shown in Fig. 1b for the sum of all fractions.

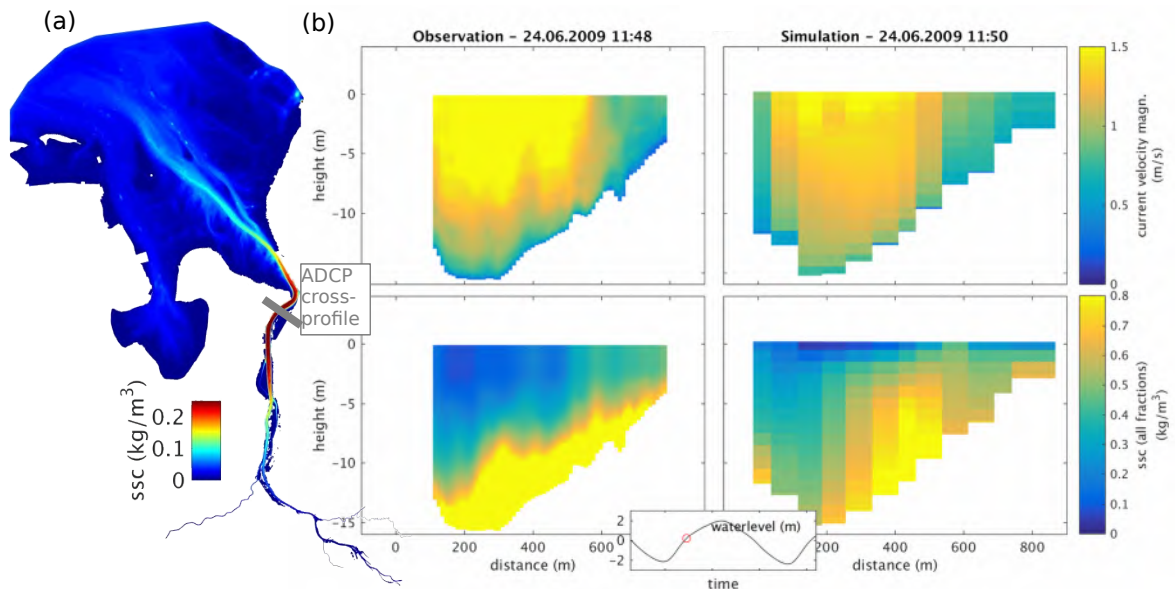


Fig. 1. (a) Tidally averaged ssc in the Weser estuary model with position of ADCP measurement cross-section; (b) Measured (left) and simulated (right) current velocity magnitude (upper) and suspended sediment concentration (lower panel), at full flood current 2h20min after low tide.

However, a comparison of different sediment fractions with different settling velocities reveals that the settling velocity has a strong impact on the agreement of modeled and observed patterns. This is most evident during slack water time. Then, sediment with lower settling velocity does not settle fast enough and the suspended matter remains in the water column for a longer period in the simulations than in the observations. Sediment with slightly higher settling velocity settles faster and the intratidal ssc patterns are in better agreement to the observations.

The remaining of the suspended matter with lower settling velocities in the water column has implications for the residual sediment fluxes in the estuary. This is shown by means of sediment budgets for one hydrological year calculated at cross sections in the outer estuary. Overall, the budgets are expected to show a net sediment import into the estuary over the year. Due to the baroclinic circulation, fractions with their main load being transported in the lower part of the water column, are transported upstream. Sediments with lower settling velocities, which are distributed more evenly over the water column, are not captured equally well by this import mechanism with the same magnitude. This leads to downstream directed residual fluxes and may lead to an overall loss of sediment from the etm in the long run.

Summary

When modeling suspended sediment in estuaries, looking at intratidal ssc patterns enables to study detailed short-term effects of different settling velocities. Comparisons of such patterns to ADCP cross-profile observations show if the spatial and temporal ssc variations are realistic. However, only by looking at residual sediment fluxes over longer periods, it can be evaluated if a certain choice of settling velocity approach yields to plausible results for the whole estuary domain.

Literature

Casulli, V.; Zanolli, P. (2002): Semi-implicit numerical modeling of nonhydrostatic free-surface flows for environmental problems. In: *Mathematical and Computer Modelling* 36 (9-10), S. 1131-1149. DOI: 10.1016/S0895-7177(02)00264-9.

Impacts of maintenance dredging on suspended sediment dynamics in the Seine estuary

Jean Philippe Lemoine¹, Pierre Le Hir² and Florent Grasso²

¹ GIP Seine-Aval, Pôle Régional des Savoirs, 115 boulevard de l'Europe, 76000 Rouen, FRANCE
E-mail : jplemoine@seine-aval.fr

² IFREMER, laboratory DYNECO/DHYSED, Centre de Bretagne, CS 10070, 29820 Plouzané, France

Abstract

This paper addresses the impact of maintenance dredging in the mouth of the Seine estuary through the use of numerical sediment marking.

Context

The macrotidal Seine estuary shelters two of the major French harbours. Rouen harbour is located 80 km upstream from the mouth, its navigation channel is crossing a very morphodynamic area which needs to be maintained by continuous dredging operations. Le Havre harbour is opened to the Baie de Seine nearby the estuary mouth, and is subject to fine sediment settling especially after storms in the area and/or when the estuarine turbidity maximum is located downstream, during high river discharge.

The respective amounts of sediment annually dredged are 1.8 M.t for Le Havre Harbour (88% mud) and 4.5 M.t. for the navigation channel to Rouen (66 % mud). These quantities have the same order of magnitude as the sum of river input (550 kt/year of fine), and the loosely known global sedimentation of the Seine estuary mouth (around 7M.t per year considering a bulk density of 1.8).

Therefore, dredging plays an important role on the sediment budget of the estuary. In this context, several questions arise on the role of maintenance dredging on sediment dynamics in the Seine estuary:

- renewal of turbidity maximum, and possible increase of its mass
- contribution to the sedimentation patterns in the area, and to the fate of tidal flats,
- consequences on the estuarine morphological evolution

These features get an increased interest since the actual dumping site for material from the navigation channel is becoming saturated, and should be replaced by another location, more offshore.

Methods

The 3D hydrodynamic model used is based on the code Mars 3D. A curvilinear grid is used and realistic forcing is considered: tidal components offshore, real 2DH wind forcing, waves from WaveWatch III and diurnal Seine river flow. Suspended sediment transport is simulated by solving advection/diffusion equation for 5 sediment types (1 gravel, 3 sands and 1 mud) (Le Hir et al., 2011). Consolidation is taken into account. This hydro-sedimentary model was validated in hydrodynamics and suspended particle matters dynamics (Grasso et al., 2017).

In the model dredging and dumping are explicitly accounted for when sediment elevation is not compliant with the draught specified by port authorities, sediments are removed from the sea bed and instantaneously released in the bottom layer of the water column above the dumping sites. The model distinguishes 9 dredging sites where the dredged masses and sediment composition are known. In order to follow the fate of dredged materials, the latter are numerically marked by affecting them to specific state variables of the model that respect the particle type (sands or mud). The corresponding concentrations of these new variables can be computed either in the water column (suspensions) or in the layered surficial sediment. Their contributions to the total suspended sediment mass of the estuary or to the siltation rate can then be evaluated.

Dredging and dumping model is calibrated against in-situ data gathered on dredging vessels. The robustness of the model was first evaluated regarding the temporal and spatial variability of dredging efforts in the Seine Estuary. Finally, the volume of settled sediment in the dumping area constitutes a second validation dataset. The agreement between numerical and in-situ dredged sediment grain size was also tested. Except the tolerance of the dredging strategy, and the dredged depth when it applies, there is no specific calibration of the numerical procedure, so that results are dependent on the overall validation of the sediment transport model.

Results

The figures illustrate the distribution of "already dredged sediment" at the Seine estuary mouth, after 6 month, either in suspension (Fig.1), or deposited (Fig.2). Fig. 1 shows that a part of dredged sediment is advected to the north while a significant fraction comes back in the estuary and joins the turbidity maximum zone.



Fig. 1: Percentile 50 over a semi-diurnal tidal cycle of the marked suspended mud concentration (*i.e. previously dredged in the navigation channel*) at the Seine estuary mouth. Dredged sediment marking started 6 months before. Area A represents the dumping site of Rouen harbour. The estuary turbidity maximum zone is located in area B at this period of the year, and extends seawards for high river discharge.

The distribution of previously dredged material in the surficial sediment (fig. 2) indicates maxima in the vicinity of the dumping site, with a dominant dispersion northward, but also some dispersion towards the estuary, either around the sandy Ratier shoal or in the northern flood channel and on the intertidal mudflat “vasière nord” located East of Le Havre harbour. It appears that some dumped sediment can be found in the dredged area of Rouen and Le Havre harbour too, suggesting that Le Havre harbour is dredging sediment previously dredged by Rouen harbour. As the measured stability of the dumping site is estimated to be 70%, this result indicates that dredging and dumping clearly interfere with the siltation in the estuary.

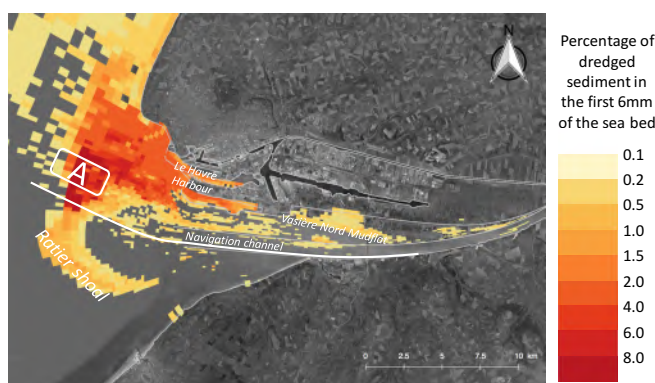


Fig. 2: Percentage in mass of sediment dredged in the navigation channel, naturally dispersed in the upper 6mm of the seabed, after 6 months of numerical marking. Area A represents the dumping site of Rouen harbour.

Conclusions and perspectives

Our study improves our knowledge on natural and anthropogenic factors interactions within the Seine estuary. The main challenge is to approach a steady state of marked quantities in order to quantify the weight of dredging activities in the sediment dynamics of the Seine estuary. Another perspective is to model middle term (10 years) morphodynamic evolutions in response to different dredging strategies.

Acknowledgments

This work is part of the MEANDRES Project funded by the Seine-Aval research program. Data were provided by harbour authorities of Rouen (GPMR) and Le Havre (GPMH).

References

- Grasso F. (2017). Diachronic numerical modelling of the turbidity maximum dynamics in the macrotidal Seine estuary (France) from 1960 to 2010, submitted to INTERCOH 2017.
 Le Hir P., Cayocca F., and Waeles B. (2011). Dynamics of sand and mud mixtures: A multiprocess-based modelling strategy, *Continental Shelf Research*, 31(10):S135-S149.

Mud-induced periodic stratification in the hyperturbid Ems estuary

Marius Becker¹ and Christian Winter¹

¹ Center for Marine Environmental Sciences, Bremen University
 Leobener Straße, 28359 Bremen, Germany
 E-mail: mbecker@marum.de

Introduction

Feedback of sediment-induced stratification on the flow plays a significant role in estuarine transport (e.g., Winterwerp, 2001). Talke et al. (2009) and Donker and de Swart (2013) modelled subtidal dynamics in the hyper-concentrated Ems estuary and showed how sediment-induced longitudinal density gradients influence the location of the turbidity maximum. By contrast to the increasing number of such modelling studies, few experimental results were published on the actual vertical structure of the water column, or on the intratidal dynamics of stratification and mobile mud layers, which were sporadically observed to move independent from the tidal flow (e.g., in the Severn estuary, Kirby, 1989). Based on data collected in the Ems estuary, we found sediment-induced restratification during flood to effectively decouple the upper and the lower half of the water column, inducing the formation of a density current in the mobile mud layer.

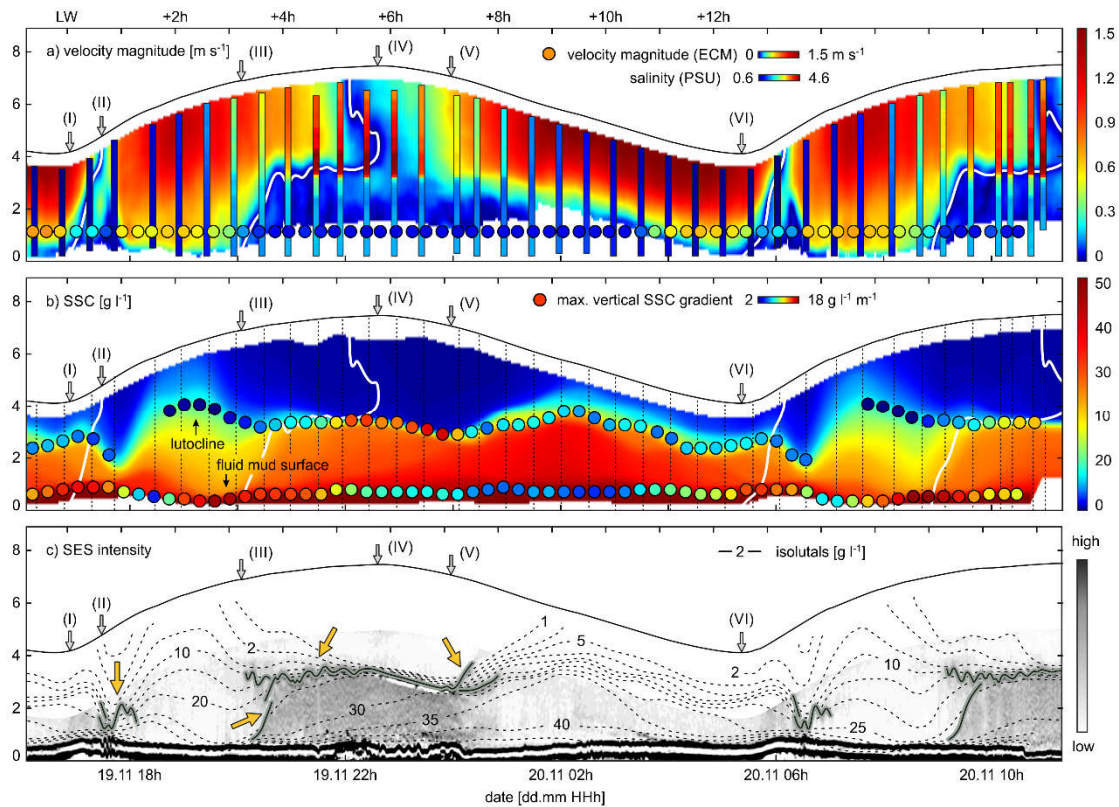


Fig. 1. Vertical distribution of ADCP current velocity (a), SSC interpolated from OBS casts (b, vertical dashed lines), and echo sounder intensity (c, SES-2000, Innomar) during 17 h at Lemgum. White lines (a, b) separate flood and ebb directed flow. Salinity (a) is shown by vertical bars. Coloured circles (a) indicate magnitude and location of ECM measured current velocity in the mobile mud layer. Coloured circles (b) indicate strength and location of the maximum vertical SSC gradients.

Observations

Figure 1 shows the variability of sediment-induced stratification in the center of the turbidity zone of the Ems estuary, measured November 2014 during moderate discharge, at one side of the navigation channel. Layers were separated by strong gradients in suspended sediment concentration (SSC), i.e., a lutocline on top of a mobile mud layer, and an interface separating the mobile mud from a higher concentrated fluid mud layer below (SSC > 50 g/l). According to electro-magnetic current meter data (ECM, not shown), the fluid mud layer was stationary.

During the first half of the flood tide (Figure 1b, II-III), the mobile mud layer was entrained. We observed the formation of the mobile mud layer (restratification) during an unexpectedly early stage of the flood phase (III). Subsequently, the flow was decoupled between the upper and the lower layer, separated by the lutocline, approximately in the middle of the water column. The flow was flood directed towards the surface, while velocities in the mobile mud layer were ebb directed (Figure 1a). The mobile mud layer remained unaffected by entrainment for a period of 4.5 h around high water and moved with an average velocity of 0.08 m/s in ebb direction, with a peak velocity of 0.12 m/s above the fluid mud surface, directly following flow reversal (III).

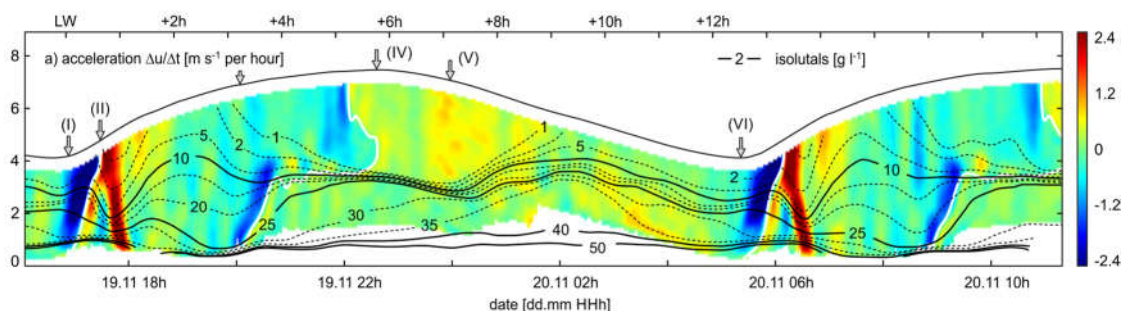


Fig. 2. Horizontal flow acceleration. During flood acceleration (II) the mobile mud layer is moved upstream. Deceleration during restratification (III) affects the lower part of the water column.

Interpretation

In general, these data describe a significant intratidal asymmetry in vertical mixing, which is strongly controlled by the properties of flocculated cohesive sediments (Winterwerp, 2002). Settling and restratification during flood is interpreted to result from a super-saturated situation after the acceleration phase. High SSC in the upper part of the water column is not sustained during stagnating flow. The settling flux is rapidly increased, inducing the collapse of the SSC profile through feedback by increased turbulence damping (Winterwerp, 2001). Consequently, the region of highest velocity shear moved vertically from the fluid mud surface to a location above the lutocline.

In addition, significant flow deceleration was observed in the lower part of the water column, over the vertical extent of the mobile mud layer before flow reversal, indicating a situation of forced convection (Figure 2, III). The required ebb directed momentum is provided either by the downstream bottom slope or, most probably, by the downstream SSC gradient. We believe that the collapse of the SSC profile causes a corresponding change in the vertical distribution of the sediment-induced downstream density gradient, acting against the flood momentum to decelerate the lower part of the water column and reverse the flow direction.

The collapse of the SSC profile has a substantial impact on the flow structure and transport. The restratification is implicitly responsible for the differential advection of saline water over the mobile mud layer, observed at the end of the flood phase. Moreover, the restratification may reduce upstream transport of sediments. Flood entrainment after low water provides the main pulse of near-bed upstream transport and controls tidal pumping of sediments. During flood, this pulsed transport is obviously limited by restratification and the associated rapid increase of the downstream density gradient in the lower part of the water column.

Neglecting consolidation, upstream transport would increase the downstream density gradient on a longer time scale. However, the probability of rapid restratification would increase at the same time. It follows that mud-induced period stratification could be interpreted as a self-organizational process in hyperturbid estuaries, balancing and limiting further upstream transport. In any case, our observations demonstrate the importance of intratidal processes, here the mud-induced mixing asymmetry, on subtidal estuarine fluxes.

References

- Donker, J.J.A., de Swart, H.E. (2013) Effects of bottom slope, flocculation and hindered settling on the coupled dynamics of currents and suspended sediment in highly turbid estuaries, a simple model. *Ocean Dynamics*, 63, 311-327.
- Talke, S.A., de Swart, H.E., Schuttelaars, H.M. (2009) Feedback between residual circulations and sediment distribution in highly turbid estuaries: An analytical model. *Continental Shelf Research*, 29, 119-1357.
- Winterwerp, J.C. (2001) Stratification effects by cohesive and non-cohesive sediment. *Journal of Geophysical Research*, 106, 22559-225747.
- Winterwerp J.C. (2002) On the flocculation and settling velocity of estuarine mud. *Continental Shelf Research* 22 1339-1360.

Experimental study on continuous turbulence effects on sediment adsorption of heavy metals.

Jingjing Zhou^{1,2}, Xian Zu¹ and Naiyu Zhang²

¹ College of Harbor, Coastal and Offshore Engineering
Hohai University, 210098, Nanjing, Jiangsu Province, China
E-mail: zjj@hhu.edu.cn

² Ocean and Earth Science, National Oceanography Centre
University of Southampton Waterfront Campus, European Way, SO14 3ZH, United Kingdom

Abstract

Estuarine and coastal areas are densely populated and economically developed. Along with the Jiangsu coastal development planning as a national strategy to promote, by 2020, the per capita GDP in this area must be greater than the average level of the eastern region. This will make it become a region of important economic growth. However, large scale land reclamation, as well as practices such as sewage discharge has led to serious deterioration of water quality, and accumulation of toxic and harmful substances within the sediments. Under the condition of hydrodynamic effect, cohesive sediment will be enrolled in diffusion, transportation, deposition and re-suspension of complex movement processes. In addition, cohesive sediment is also the carrier of heavy metals, organic pollutants, and its transportation directly affects the migration and transformation of pollutants, also changes the original characteristics of sediment movement.

In this paper, in the central Jiangsu coast intertidal zone along the south side of Chuandong Port, based on the established site of beach elevation observation, four typical vertical lines are chosen for water level, velocity and sediment concentration observation, and three of which are located on the intertidal mudflat, including 5#(33°02.482' N, 120°53.667' E), 6#(33°02.744' N, 120°53.990' E), 7#(33°03.035' N, 120°54.393' E), and one in Xiyang Deep Trough(33°06.650' N, 120°57.655' E)(Figure 1). Water and sediment samples were collected once a month between July and October 2016. Heavy metal concentrations of more than 40 sediment and water samples were examined, including Chromium (Cr), Iron (Fe), Copper (Cu), Zinc (Zn), Arsenic (As), Cadmium (Cd), Mercury (Hg), and Lead (Pb). According to sea water quality standard (GB 3097-1997) and marine sediment quality standard (GB 18668-2002), the area is severely affected with high pollution of Zn, Hg and Pb. Sampling surface sediments when ebb tide occurs and beaches expose, using heavy metal Zn as an example, to clarify the effect of turbulence on continuous water sediment adsorption of heavy metals.

Experiments were subsequently carried out on collected sediment using six mini annular flumes(Figure 2); one of them was selected as raw sediment without screening and cleaning, and the other five were treated with the same clean sediment for the adsorption of heavy metal Zn. Take the first class water quality standard of upper bound 0.02g/L; sediment standard applies the first kind; the concentration of Zn is 150mg/kg. Water in the flume is 20cm high, and sediment concentration in each flume is about 1.5kg. Respectively sampling sediments from the flume in interval 3, 4, 5 and 6 days(Figure 3), the weight are always 50-100g, and then to measure concentration of heavy metal adsorption of sediment based on continuous turbulence water. The sediment in each mini annular flume is taken only once to ensure that all the samples have the same adsorption state.

The stable maximum zinc adsorption of fine sediment was found to occur at 8-10 days. Limited by short sampling intervals, the zinc was not fully absorbed onto the sediment, thus heavy metal concentrations gradually increased as the adsorption capacity reduced. After reaching a maximum value, concentrations gradually decreased but the release rate was significantly lower than the adsorption rate. Based on saturated adsorption, continuously kept under the same hydrodynamic conditions for 20 days, and then returned to still water after 32 days, it was found that heavy metal adsorption capacity of the undisturbed sediment was smallest. Microorganisms and organic matter could inhibit the adsorption of fine sediment. In the absence of an applied flow, sediment gradually settled to the bottom of the annular flumes, leaving only surface interactions between the sediment and water. When saturated adsorption was reached, the sediment gradually released heavy metal zinc into the water, resulting in a decrease in zinc adsorption in each annular flume.

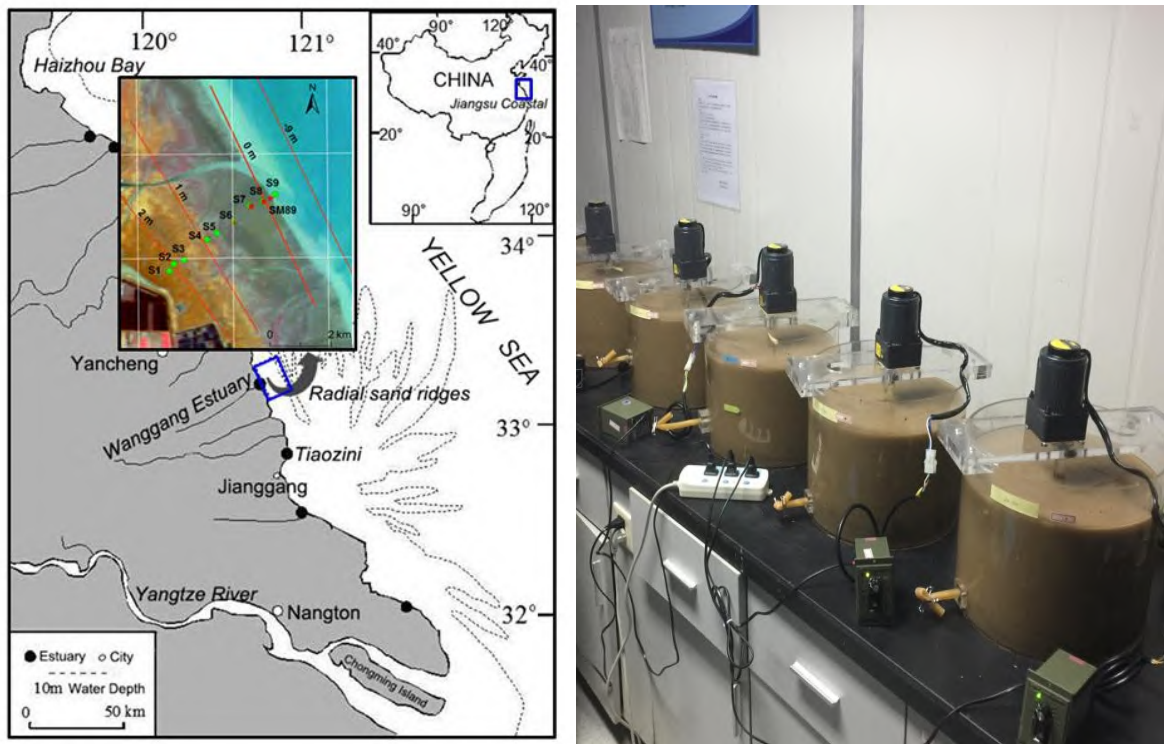


Figure 1. Jiangsu coastal area and the location of the study sites.
 Figure 2. Mini annular flumes during the experiments

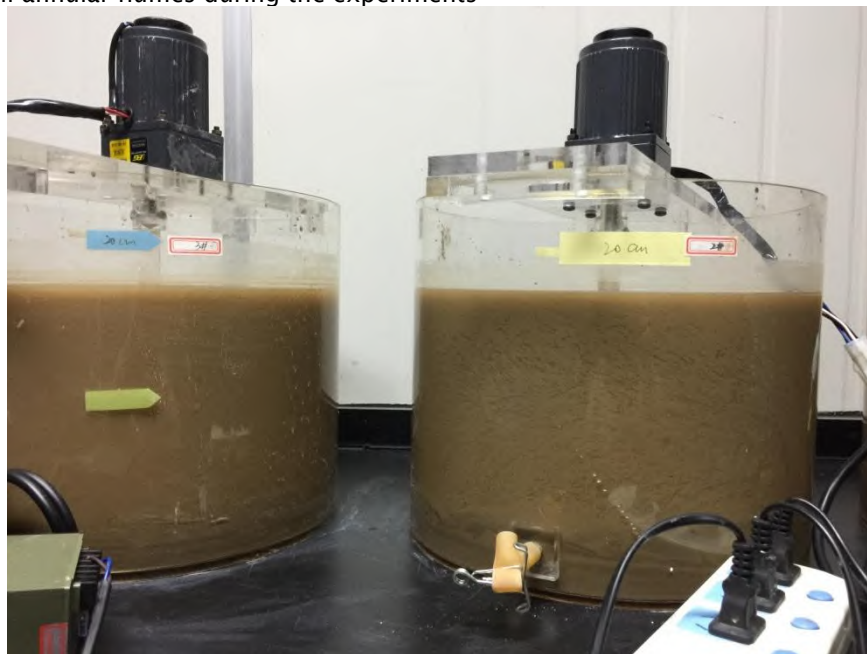


Fig. 3. After 4 and 5 days sediment sampling

Assessment of the spatio-temporal variability of sediment fluxes on the French continental shelf under the influence of natural and anthropogenic forcings

Baptiste Mengual¹, Pierre Le Hir¹, Florence Cayocca² and Thierry Garlan³

¹ Laboratoire DYNECO/DHYSED, IFREMER, centre de Bretagne, CS 10070, 29280 Plouzané, France
E-mail: bapt.mengual@hotmail.fr

² AAMP (Agence des Aires Marines Protégées), 16 Quai de la Douane, 29200 Brest, France

³ SHOM/DOPS/HOM/Sédimentologie, 13 rue du Châtelier, CS 92803, 29228 Brest, France

Context

Assessing sediment fluxes over continental shelves is crucial for many socio-economical and environmental issues such as regional sediment budgets, sediment extraction and dredging, or monitoring benthic habitats. This study focuses on the continental shelf of the Bay of Biscay, located in the north-east Atlantic. Surficial sediment is constituted of barely-consolidated mixtures of fine sand and mud. Despite the abundant literature on hydrodynamic circulation, mainly poleward and driven by wind and density gradients (e.g. Lazure *et al.*, 2008; Le Boyer *et al.*, 2013) although in a macrotidal context, sediment fluxes had never been assessed at this regional scale. Regarding sediment dynamics, previous works were mainly conducted on sediment exchanges in submarine canyons along the continental slope, turbidity dynamics and sediment fluxes at river mouths, sedimentation rates, and seabed nature. In addition to the influence of natural forcings, a few studies have already drawn attention to the fact that trawling activities are likely to significantly influence sediment dynamics over large areas of the Bay of Biscay shelf (e.g. Mengual *et al.*, 2016), as it is the case over many continental shelves worldwide. This study aims at quantifying sediment fluxes at the shelf scale under the influence of natural forcings and trawling activities.

Methods

Given the extent of study area, a numerical modelling approach was chosen. A 3D hydro-sedimentary model, based on the coupling between the hydrodynamic code *MARS3D* (Lazure and Dumas, 2008) and the mixed-sediment transport model *MUSTANG* (Le Hir *et al.*, 2011), was validated in terms of hydrodynamics, hydrology, and dynamics of suspended sediment. Two 5-year realistic simulations were run (2007-2011 period), accounting either for natural forcings only (i.e. wave, wind, tide, river discharge) or for both natural and anthropogenic forcings (i.e. trawling) in order to quantify and compare their respective contributions to sediment dynamics. Based on site-specific measurements and fishing effort data, the trawling-induced erosion is parameterized according to Mengual *et al.* (2016). More details about forcing features, initial and boundary conditions, and model settings can be found in Mengual (2016).

The first step of this work consisted in assessing typical regimes of natural-induced sediment fluxes on the continental shelf over the simulated period. One of the most popular and simple clustering algorithms (*K-means*) was applied. The residual (tide filtered) sediment dynamics have been computed and presented in terms of integrated sediment fluxes over different water depth ranges, along borders across the shelf (longshore and cross-shore), at different time scales (seasonal and annual). Lastly, the trawling contribution to sediment dynamics was investigated in terms of resuspension and horizontal fluxes at seasonal and annual scales, as well as changes in the seabed composition.

Results and conclusions

The cluster analysis (*K-means*) enabled the identification of 5 typical sediment flux regimes over the 5-year period at the shelf scale, and revealed a marked seasonality. During the autumn/winter period, results highlight a poleward/equatorward alternation of intense sediment flux regimes, well correlated with water fluxes, and largely influenced by the wind. Nevertheless, both sand and mud residual fluxes (depth-integrated) during this energetic period exhibit a clear poleward orientation. Due to less energetic conditions in terms of waves and currents, sediment flux regimes occurring during the spring/summer period are significantly weaker than the rest of the year and are confined near of the coast. Moreover, mud fluxes exhibit a poleward orientation on the inner shelf, not correlated with water fluxes, and different from sandy ones oriented more cross-shore. Our results provided evidence for the role of the tidal current asymmetry: due to contrasted settling velocities and thus different phase lags between dominant resuspension (on ebb tidal phase) and subsequent deposition, the mud flux is oriented north-westward while the fine sand flux follows the maximum current direction (west-south-westward). At the annual scale, sediment fluxes are clearly controlled by the residual poleward dynamics occurring in winter (Fig. 1), in fair agreement with the annual

residual circulation reported in the literature. A sediment budget at the scale of the French shelf, performed from sediments initially prescribed within the seabed, revealed a total loss of 2.02Mt.yr^{-1} in the same order of magnitude as the riverine input of 2.5Mt.yr^{-1} (Jouanneau *et al.*, 1999).

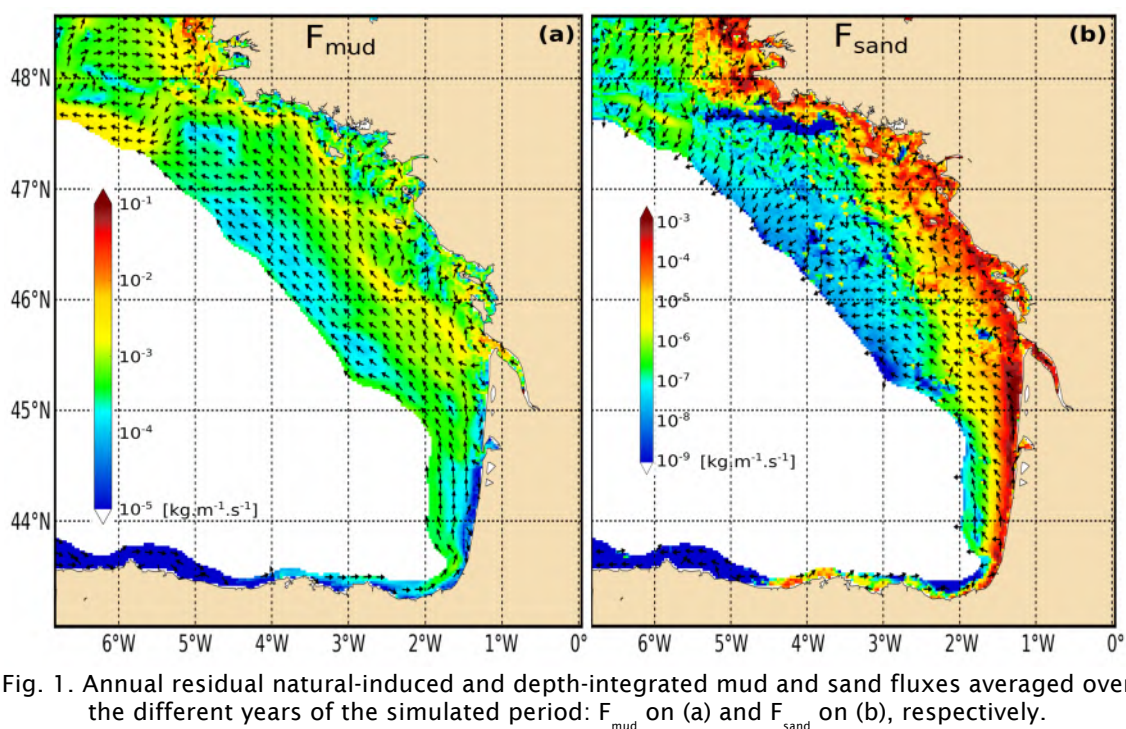


Fig. 1. Annual residual natural-induced and depth-integrated mud and sand fluxes averaged over the different years of the simulated period: F_{mud} on (a) and F_{sand} on (b), respectively.

Regarding anthropogenic forcing, trawling is responsible for a significant annual contribution to resuspension over intensively trawled muddy areas of the mid-shelf (up to 20%), more precisely over the "Grande-Vasière" mud belt where it becomes the main source of resuspension during the high fishing season. Trawling also contributes to horizontal sediment fluxes. At the annual scale, trawling enhances poleward natural mud and sand fluxes at a rate ranging from a few per cent to 40%, and significantly contributes to the natural off-shelf export of sediment: +35% and +15% of mud export along the 130m and 180m isobaths, respectively. On the contrary, trawling induces an onshore residual transport of sediment in some locations of the inner shelf. Lastly, our results highlighted a trawling-induced mud fraction decrease in the seabed over intensively trawled areas of the shelf, qualitatively in agreement with recent observations (cf. Mengual *et al.*, 2016).

Acknowledgments

This study was supported by the SHOM (Service Hydrographique et Océanographique de la Marine) and IFREMER (Institut Français de Recherche pour l'Exploitation de la Mer).

References

- Jouanneau J.M., Weber O., Cremer M., Castaing P. (1999). Fine-grained sediment budget on the continental margin of the Bay of Biscay. *Deep Sea Research Part II: Topical Studies in Oceanography*, 46:2205-2220.
- Lazure P., Dumas F. (2008). An external-internal mode coupling for a 3D hydrodynamical model for applications at regional scale (MARS). *Advances in Water Resources*, 31:233-250.
- Lazure P., Dumas F., Vrignaud C. (2008). Circulation on the Armorican shelf (Bay of Biscay) in autumn. *Journal of Marine systems*, 72:218-237. doi:10.1016/j.jmarsys.2007.09.011.
- Le Boyer A., Charria G., Le Cann B., et al. (2013). Circulation on the shelf and the upper slope of the Bay of Biscay. *Continental Shelf Research*, 55:97-107.
- Le Hir P., Cayocca F., Waeles B. (2011). Dynamics of sand and mud mixtures: a multiprocess-based modelling strategy. *Continental Shelf Research*, 31:S135-S149. doi:10.1016/j.csr.2010.12.009.
- Mengual B., Cayocca F., Le Hir P., et al. (2016). Influence of bottom trawling on sediment resuspension in the "Grande-Vasière" area (Bay of Biscay, France). *Ocean Dynamics*, 66:1181-1207. doi:10.1007/s10236-016-0974-7.
- Mengual B. (2016). Variabilité spatio-temporelle des flux sédimentaires dans le Golfe de Gascogne : contributions relatives des forçages climatiques et des activités de chalutage. Ph. D. Thesis. University of Western Brittany, France, 194p.

Fractal flocs: “primary particles” variability and consequences on floc characteristics

Romaric Verney¹, Aurélien Gangloff¹, Marion Chapalain¹, Flavie Druine², David Le Berre¹ and Matthias Jacquet¹

¹IFREMER, DYNECO/DHYSED, ZI pointe du Diable, CS10070, Plouzané, France. E-mail: romaric.verney@ifremer.fr

²UMR6143 M2C – University of Rouen, Place Emile Blondel, 76821 Mont Saint Aignan, France.

Context

In estuaries and coastal seas, suspended particulate matters (SPM) are mainly aggregated in flocs, of variable shape, size, density and hence settling velocity. The latter is crucial as it controls the SPM fluxes in coastal ecosystems, from turbidity maximum formation to turbid plume or mudflat dynamics. In 1994 Kranenburg, following Krone’s works, proposed an innovative concept of fractal flocs, assuming that flocs are self-similar objects, i.e. “a unique relationship exists between aggregate size and the number of primary particles that form the aggregate”. In practice, this concept leads to the following widely used relationship between floc size D and floc excess density $\Delta\rho$:

$$\Delta\rho = (\rho_p - \rho_w) \left(\frac{D_p}{D}\right)^{3-nf}$$

Where D_p is the primary particle size, ρ_p the primary particle density and nf the fractal dimension. These concept and relationship are used both for estimating floc settling velocity from floc size in situ measurements and for simulating floc dynamics in numerical sediment transport models. The main difficulty of the concept is to know what are basic floc particles constituting the flocs, and what are their densities. As flocculation is associated to particle cohesiveness, clay minerals are often considered as floc basic/primary particles. However, once observing flocs individually, it becomes evident that not only clay but other larger minerals as well as organic particles, often aggregated in very dense, strong basic particles, contribute to form microflocs and macroflocs. The aim of this study is to investigate the variability of the primary/basic particles forming flocs, and to examine the consequences of this variability in term of floc density and floc settling velocity.

Methods

More than 360 samples were collected in the Seine estuary, Bay of Seine and Rhone ROFI area in 2015 and 2016, at different seasons and for various hydrodynamic conditions. These SPM samples were analyzed to estimate SPM concentration (gravimetric measurements), organic matter content (loss of ignition method) and SPM deflocculated particle size distribution after agitation and ultrasonic insonification. Combining SPM concentration and volume concentration provide information on population-average excess densities. Simultaneously to SPM samples, in situ turbidity and floc size distribution were measured with an OBS3+ and a LISST100X.

Results

De-flocculated spectra: Basic/Primary particles variability

De-flocculated spectra are generally characterized by a combination of two sub-populations: a clay-like population, with a diameter around $2\mu\text{m}$ and a larger flocculi-like population featured by median diameters ranging from $10\mu\text{m}$ to $20\mu\text{m}$ (Fig. 1). During planktonic blooms, a third population is observed, featured by larger sizes (from 50 to $200\mu\text{m}$). This population is named “phytoplankton” but may also be strong bio-aggregates. These populations were quantified, both in term of PDF and representative diameters. Flocculi generally dominate the PSD, contributing from 50% to 90% of the distribution.

The presence of distinct populations is questionable: were flocs entirely de-flocculated and then do the populations correspond to the true signature of the primary individual particles or did some small but resistant flocculi persist to exist despite the ultrasonic deflocculation? This question is examined by comparing the volume concentration and the mass concentration of samples, and testing hypotheses of primary particles or small but dense aggregates.

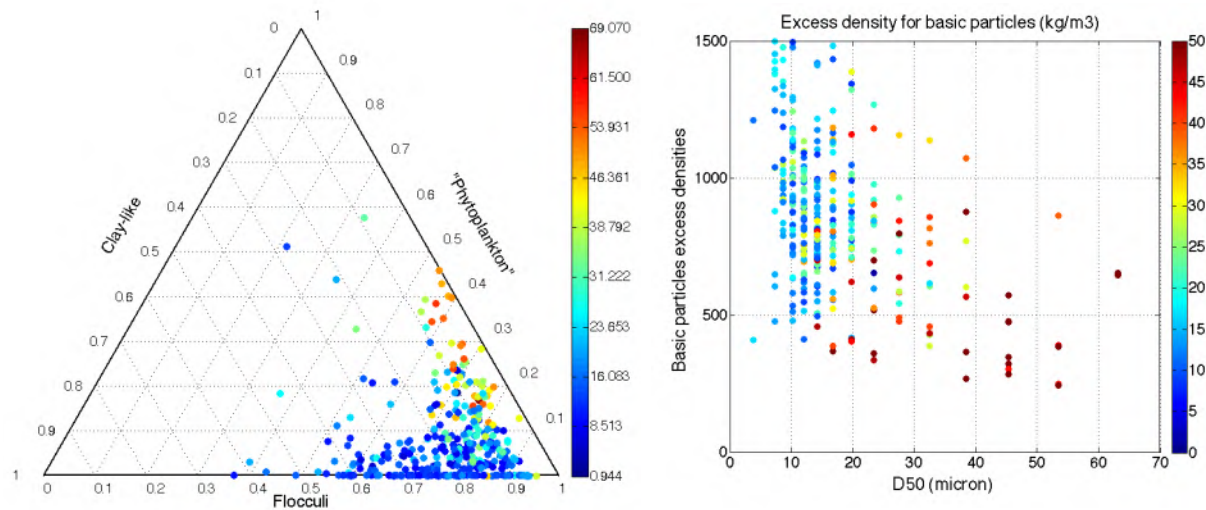


Fig. 1. Left: Synthesis of deflocculation experiments: decomposition between “primary particles” clay-like, “flocculi” and “phytoplankton” populations, in percentages of full spectrum. Color represents the organic matter content (%). Right: Basic particles excess density Vs median particle size. Color represents the organic matter content (%).

“Basic particles” features: size Vs densities

Examining population average excess densities shows that populations observed after ultrasonic insonification are mainly dense small floccs, named here “basic particles”, with excess density values ranging from $1500\text{kg}\cdot\text{m}^{-3}$ to $500\text{kg}\cdot\text{m}^{-3}$, and decreasing with increasing median floc sizes (Figure 1 - right). High organic matter content is associated with low densities, from $1000\text{kg}\cdot\text{m}^{-3}$ to $200\text{kg}\cdot\text{m}^{-3}$. If these basic particles are assumed to be self-similar (and neglecting the presence of phytoplankton, i.e. a second population of primary particle with lower density), these particles show fractal dimension ranging from 2.5 to 3.

Fractal continuity between primary particles, “basic particles” and in situ micro/macroflocs

The question addressed in this last section is the continuity of the fractal approach over floc sizes. The fractal dimension of the basic particles will be confronted to the fractal dimension of the in situ microflocs/macroflocs. For the latter populations, two assumptions are made: either primary particles are $2\mu\text{m}$ clay-like particles, or $10\mu\text{m}$ to $20\mu\text{m}$ basic particles, with their respective densities. Fractal dimensions calculated are then compared with deflocculated features, and the presence of organic matter. The implication on settling velocity estimation will then be discussed.

References

Kranenburg, C. (1994). "The fractal structure of cohesive sediment aggregates." *Estuarine, Coastal and Shelf Science* 39: 451-460.

Using real time monitoring networks for investigating sediment dynamics in estuaries: a step beyond turbidity time series analysis

Romarc Verney¹, Florent Grasso¹, Flavie Druine², Julien Deloffre², and Jean Philippe Lemoine³

¹IFREMER, DYNECO/DHYSED, ZI pointe du Diable, CS10070, Plouzané, France. E-mail:

romarc.verney@ifremer.fr

²Normandie Univ, UNIROUEN, UNICAEN, CNRS, M2C, 76000 Rouen, France.

³GIP Seine Aval, Pole Régional des Savoirs, 115 Boulevard de l'Europe, 76100 Rouen, France.

Context

Macrotidal estuaries are featured by the presence of Estuary Turbidity Maximum (ETM), where sediments are accumulated through the joint influence of tidal pumping (tidal asymmetry) and salt edge structure. ETMs are defined as areas of high suspended sediment concentration, and are characterized by a given location, extension, mass and average concentration. The ETM dynamics has been widely investigated over the last decades, mainly from short term in situ measurements of suspended solid concentration (SSC) and floc size distribution, and numerical modelling. Since 2015, the SYNAPSES automatic monitoring network was deployed within the Seine Estuary, measuring turbidity at high frequency in 6 stations along the system (3 within the ETM zone). The aim of this study is to investigate the potential of automated turbidity monitoring networks to characterize the ETM dynamics, applied to the case study of the Seine Estuary, France.

Methods

The SYNAPSES monitoring network consists in six stations deployed along the estuary, all equipped with YSI 6600V2 probes measuring conductivity, temperature, turbidity, fluorescence and O₂ concentrations every 5min. If both surface/bottom measurements are available in the ETM, this study focuses on near bed (1mab) measurements. The network has been fully operational since January 2015, supervised by the GIP Seine Aval and maintenance being operated by the Grand Port Maritime de Rouen.

The MARS3D hydrodynamics and sediment transport numerical model was implemented in the study area, and is featured by a non-orthogonal curvilinear computation grid and refined meshes within the estuary mouth. The model is forced by tidal components at the sea boundary, the ARPEGE meteorological model and waves simulated by WW3 on the studied area. Sediment dynamics is computed through the advection-dispersion equation and the process-based model developed by Le Hir et al. (2011) and Grasso et al. (2015). Five sediment classes are transported within the model: 1 gravel, 3 sands and 1 mud, representative of the sediments present in the system (Grasso et al., 2017).

Results

Turbidity time series

Turbidity measurements show that the largest turbidity is observed at Fatouville, in the central part of the expected ETM, for medium or high river discharge periods (Fig. 1). Turbidity reached values above 4000NTU close to the bed during spring tides and the lowest values during neap tides. For low river discharges, turbidity values are slightly higher at the upstream station (Tancarville), reaching values above 2000NTU during spring tides. This strong correlation with the river discharge suggests that the ETM is mainly centered close to the upstream station during low river discharge periods and close to Fatouville (central station) the rest of the year.

ETM location

Based on the simultaneous turbidity measurements at SYNAPSES stations, an estimation of the ETM location can be given by calculating the centre of gravity of the turbidity along the section covered by the three stations (Fig. 1). Results show that ETM would be effectively centered on Fatouville for medium to high river flow but between Tancarville and Fatouville during low river discharge periods. This method reaches its limit when the largest turbidity is observed at one of the upstream/downstream station: in this case, the ETM could be located upper (or lower respectively) in the estuary, but not correctly observed.

In order to analyze the reliability of this simple calculation, results are compared with ETM location calculated from model outputs (validated and then considered as the reference), evaluating the SPM mass longitudinal distribution (using information over the full model grid) every 15' and estimating the center of mass of the ETM (Fig. 1). If the trends of both methods are similar at the annual scale, the SYNAPSES-based calculation locates the ETM 5km downstream than model results.

Two approaches were then tested to improve the ETM location calculation from the SYNAPSES stations:

- A limitation identified in the SYNAPSES-based method is the “low” number of stations compared with the distance covered by the ETM at the annual scale. Based on model results, the monitoring network was then virtually optimized, moving or adding new stations.
- We also tested the hypothesis that i) the ETM, associated with large turbidity measurements, is nearly always passing at the Fatouville station and ii) if the ETM is located upstream, ETM will arrive late during ebb at Fatouville. Then we calculated the time lag (DT) between high water and the percentile 90 (P90) of turbidity during ebb. This proxy was calculated and compared both for the SYNAPSES data and model data, and results showed very good correlation. DT calculated from SYNAPSES data was then compared with the reference ETM location. Results show that a linear relationship can be found and used to reliably evaluate the ETM location from a single monitoring station (SYNAPSES DT - Fig. 1). However, this last method can be unreliable for very high river flow, if the ETM is located downstream Fatouville.

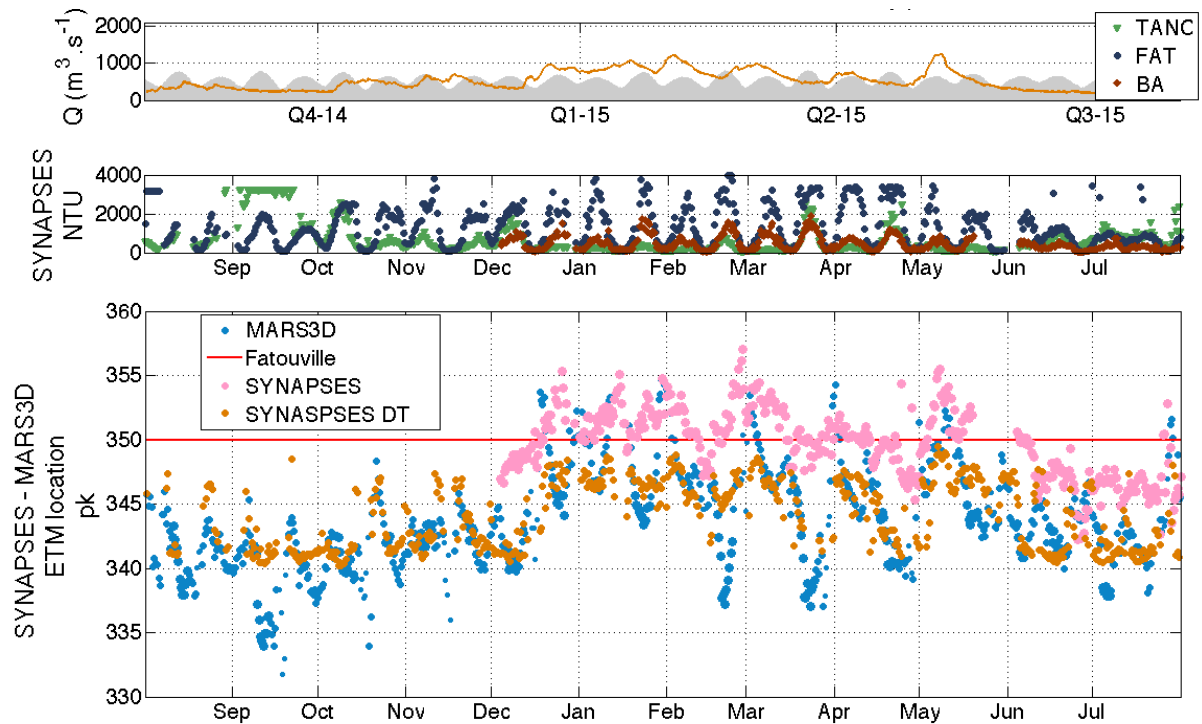


Fig. 1: Seine river discharge and tidal range (top panel), P90 turbidity measurements at the three SYNAPSES stations (middle panel) and ETM location (bottom panel). Pk 337: Tancarville (upstream), pk 350: Fatouville, pk 365: Balise A (downstream). Blue dots: MARS3D ETM location, pink dots: ETM from SYNAPSES center of gravity, orange dots: ETM estimated from time lag between high water and ebb turbidity P90

References

- Grasso F., Le Hir P., and Bassoullet P. (2015). Numerical modelling of mixed-sediment consolidation. *Ocean Dynamics*, 65(4), 607-616. <http://doi.org/10.1007/s10236-015-0818-x>
- Grasso F., Le Hir., Chini N. (2017). Diachronic numerical modelling of the turbidity maximum dynamics in the macrotidal Seine estuary (France) from 1960 to 2010. Submitted to INTERCOH 2017.
- Le Hir, P., Cayocca, F., and Waeles, B. (2011). Dynamics of sand and mud mixtures: A multiprocess-based modelling strategy. *Continental Shelf Research*, 31, S135-S149.

Equilibria and Evolution of Estuarine Fringing Intertidal Mudflats

Bram C. van Prooijen¹, Florent Grasso², Pierre Le Hir², P.M.L. (Lodewijk) de Vet^{1,4}, Zheng B. Wang^{1,4}, Brenda Walles³, Tom Ysebaert³

¹ Delft University of Technology, department of Hydraulic Engineering, Delft, The Netherlands.
E-mail: B.C.vanProoijen@TUDelft.nl, P.L.M.deVet@TUDelft.nl; Z.B.Wang@Tudelft.nl

² Ifremer, laboratory DYNECO/DHYSED, Centre de Bretagne, Plouzané, France
E-mail: Florent.Grasso@ifremer.fr, Pierre.le.Hir@ifremer.fr

³ NIOZ, Estuarine and Delta Systems, Yerseke, The Netherlands
E-mail: tom.ysebaert@nioz.nl, brenda.walles@nioz.nl

⁴ Deltares, Department Applied Morphodynamics, Delft, The Netherlands

Abstract

Fringing intertidal flats are common features of elongated estuaries. We generalized the geometry of profiles of individual intertidal flats towards a common relationship, based on extensive measurement data of various estuaries. We found a strong linear relation between the width, slope and height of linear intertidal flat profiles, which also yields well for the mild-sloped upper part of convex-up profiles. Deviations of this linear relation at the lower steeper part of the flats are the result of dominating alongshore currents.

Introduction

Elongated estuaries are fringed by tidal flats that consist of bare mudflats and at higher elevations vegetated marshes. These areas form a buffer between the channel and the dike, thereby serving as coastal protection. Furthermore, they provide valuable habitats for various species and are consequently often protected by legislations (e.g. Natura2000). Human interferences have affected and are still affecting these flats. Channel deepening, storm surge barriers and local weirs and groynes are examples of such interferences.

Profile shape (convexity or concavity) has been identified as a predictor for tidal flat development. Convex-up profiles are related to expanding systems dominated by tidal flow and concave-up profiles are linked to retreating wave-dominated systems. The theoretical basis for these relations however lies in analyses of systems dominated by cross-shore tidal flows. Limited evidence is available that supports such relations for systems with predominantly along-shore tidal flows. In this paper, we aim to identify the relations between tidal flat parameters for systems with predominantly along-shore tidal flows in order to determine predictors for future developments of fringing tidal flats.

Data

We consider fringing tidal flats in the meso-tidal systems Westerschelde and Oosterschelde (the Netherlands) and the macro-tidal Seine Estuary (France). All these flats are confined between the shore and a channel. Many of the considered tidal flats in the Oosterschelde and Westerschelde are also confined in streamwise direction by the dyke configuration. For the Oosterschelde and Westerschelde, a data set of 56 transects on 20 fringing tidal flats is available covering a period of 21 years (1993-2014) with annual RTK measurements. Furthermore, LiDAR data in combination with single-beam data is available for various years. For the Seine a local LiDAR database over 12 years is available. Numerical simulations provide the local tidal ranges and characteristic velocities in the channels. The bathymetry, tidal range and average flow magnitudes are indicated in Figure 1.

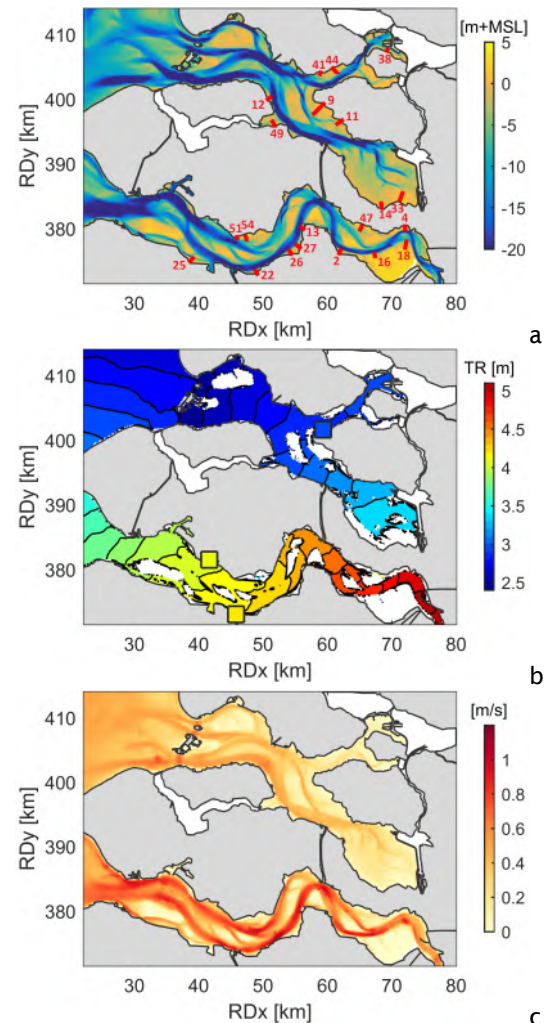


Figure 1: Westerschelde and Oosterschelde: (a) bathymetry and numbering of the tidal flats; (b) averaged tidal range; (c) average magnitude of the velocities.

Results

Oosterschelde. The tidal flats in the Oosterschelde have an S-shaped profile, where the linear part in the middle covers more than 80% of the intertidal area. The flats are therefore characterized as linear. A consistent linear relation is found for the bed level:

$$z = z_0 - s \cdot x \quad \text{with} \quad s = \frac{TR}{L \left(\frac{z_0}{\frac{1}{2}TR} + 1 \right)} \quad (1)$$

with distance from the shore or marsh x , bed level z (and z_0 at $x = 0$), tidal range TR , bed slope s and calibrated length scale $L=1000$ m. High and mild-sloped flats are therefore found when there is sufficient space between the channel and the shore.

Westerschelde. Two types of tidal flat profiles are found in the Westerschelde: (i) linear (partly concave-up) profiles; (ii) convex-up profiles with a mild-sloped upper part and a steep-sloped lower part. Linear and convex-up shapes are found for different widths and heights of the flats. The linear profiles show a similar relation between the height, slope and width as for the Oosterschelde, also with $L=1000$ m. The convex-up profiles have two distinct slopes. The slope in the upper part follows the relation as found for the linear profiles. The slope in the lower part is significantly larger. Time evolutions of the profiles show that both profiles can be stable, eroding or accreting.

Seine Estuary. The profiles in the Seine Estuary show a distinct double-sloped profile. The upper profiles approximately follow the linear relation with $L=1000$ m, using a tidal range of $TR=6.7$ m. The transition to the steeper lower part is more distinct than in the Westerschelde.

For all profiles a value of approximately $L=1000$ m was found, despite the significant variation in tidal range. No definite explanation was found yet for this linear profile. It is hypothesized that waves are important drivers. When waves are negligible, it seems that the upper part can become flat and dewatering processes generate creeks.

Conclusions and Outlook

The measured transects at the tidal flats in the three estuaries indicate that various (almost) equilibrium profiles exist. The shape itself seems not to be a direct predictor for future development. Linear profiles and convex profiles can prograde, erode or can be in equilibrium. The upper flat follows a linear profile with milder slopes and higher mean bed levels for wider flats. The exact cause for the relation for the upper flat is to be examined. Further steps will focus on determining the influence of the alongshore current and sediment abundance on the width and slope of the steeper lower part of the convex-up profile.

Acknowledgements

Rijkswaterstaat provided the Oosterschelde and Westerschelde data. Jean-Philippe Lemoine, GIP Seine-Aval, provided the Seine data. This study is funded by NWO project EMERGO (850.13.021) and Ifremer is acknowledged for hosting and funding Bram van Prooijen for a two-week stay.

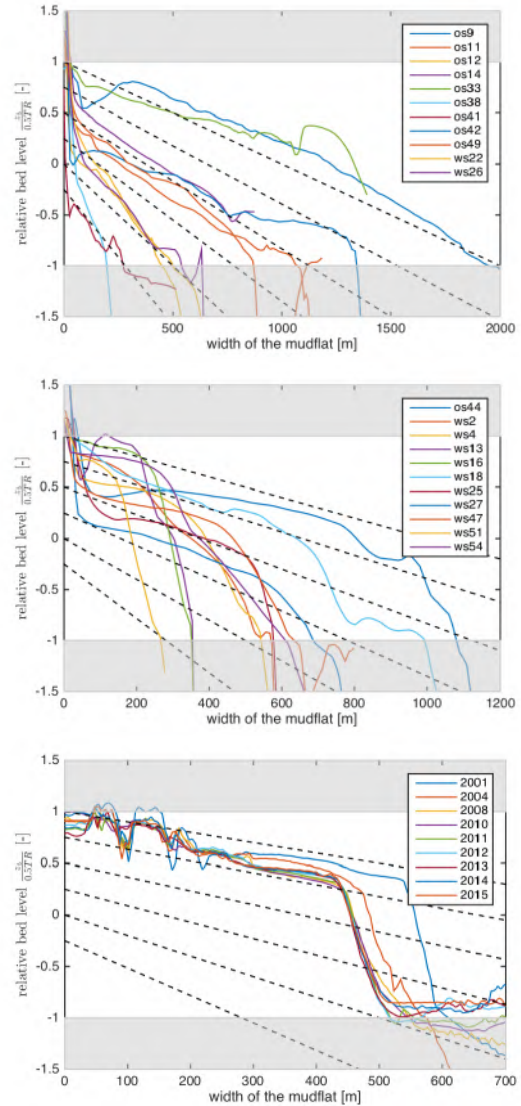


Figure: (a) Linear profiles in the Oosterschelde and Westerschelde. (b) Convex-up profiles in the Westerschelde and Oosterschelde. (c) Profiles in the Seine Estuary for different years. See Figure 1 for the location of the profiles in the Oosterschelde and Westerschelde. The vertical scale is made dimensionless by dividing by $0.5TR$. The dashed lines represent Equation (1) for various values of z_0 .

Size and settling velocities of suspended mud in the Mississippi River mouth estuary

Smith, Jarrell¹, Kelsey A. Fall^{1,2} and Michael T. Ramirez¹

¹ U.S. Army Engineer Research and Development Center, 3909 Halls Ferry Rd, Vicksburg, MS, USA
39180-6133
E-mail: jarrell.smith@usace.army.mil

² Virginia Institute of Marine Science, College of William and Mary, Route 1208 Grete Road,
Gloucester Point, VA, USA 23062-1346

Background

The Mississippi River is North America's largest river in terms of water and sediment delivery to the ocean (Milliman and Meade, 1983). The annual maximum sediment and water discharges typically occur in the spring to early summer and the annual minimum discharges occur in the late summer through autumn. During high river discharge, estuarine mixing of the river discharge occurs in the Gulf of Mexico. However, during low river flow, seawater enters the river and a salt wedge forms within the lower extent of the river, migrating as much as 100km upstream. This highly stratified river-mouth estuary produces favorable conditions for flocculation, sediment trapping, and sedimentation of suspended fine sediment.

Actively and passively controlled flow and sediment diversions exist in the lower 200km of the river. Additional river diversions are under consideration to mitigate ongoing land loss in the Mississippi River Delta. The present research is being conducted to better anticipate the potential consequences of increased river diversion on the frequency and extent of salt-water intrusion into the river channel and the associated sediment interactions that impact sedimentation.

Methods

Field measurements of water discharge, sediment discharge, and suspended sediment characteristics were conducted November 2015 and December 2016 in the lower Mississippi River during periods of sea-water intrusion. The measurements were conducted at profiling stations established between minor river distributaries located 28 to 88 km upstream of the Mississippi River outlet to the Gulf of Mexico. The river depth at these stations ranged between 15 to 45m deep. Flow velocity, vertical shear, river discharge, suspended sediment concentration, and sediment discharge were estimated with a vessel-mounted Acoustic Doppler Current Profiler (ADCP) calibrated to physical samples of Suspended Sediment Concentration (SSC). An instrumentation package was cast through the water column at the thalweg of each station to collect suspended sediment samples and measure water and suspended sediment properties. In addition to water temperature and salinity, in-situ suspended sediment size was measured by Laser In-Situ Scattering and Transmissometry (LISST-100x) (Agrawal and Pottsmith, 2000) in-situ size and settling velocity were measured with the Particle Imaging Camera System (PICS) (Smith and Friedrichs, 2011; Smith and Friedrichs, 2015).

Results

The water column was observed to be sharply stratified, with vertical salinity gradients ranging between 5-10ppt/m. The mixing zone between the overlying, seaward flowing freshwater and underlying, upstream flowing seawater was 2-4m thick. In this mixing zone, median particle size was observed to increase compared to the freshwater layer by approximately an order of magnitude from nominally 20 μ m to 200 μ m. Settling velocities also increased by a factor of 3-5 from nominally 0.1mm/s to 0.3 to 0.5mm/s. Large macroflocs with diameters between 300-500 μ m were also observed in the lower seawater lens with settling velocities between 1-3mm/s.

Additional analysis of the 2015 and 2016 data is in progress, investigating the longitudinal variations in the suspended sediment populations, floc growth in the shear layer, and floc breakup near the bed. These findings will be finalized prior to the conference.

References

- Agrawal Y.C. and Pottsmith H.C. (2000). Instruments for particle sizing and settling velocity observations in sediment transport. *Marine Geology* 168:89-114.
- Milliman J.D. and Meade R.H. (1983). World-wide delivery of river sediment to the oceans. *The Journal of Geology*, 91(1):1-21.
- Smith S.J. and Friedrichs C.T. (2011). Size and settling velocities of cohesive flocs and suspended sediment aggregates in a trailing suction hopper dredge plume. *Continental Shelf Research* 31:S50-S63.
- Smith S.J. and Friedrichs C.T. (2015) Image processing methods for in situ estimation of cohesive sediment floc size, settling velocity, and density. *Oceanography and Limnology: Methods* 13:250-264.

Dynamics of suspended particulate matter in coastal waters (Seine Bay)

Marion Chapalain¹, Romaric Verney¹, Michael Fettweis², Pascal Claquin³, Matthias Jacquet¹, David Le Berre¹, and Pierre Le Hir¹

¹ Laboratoire DYNECO/DHYSSED, IFREMER, ZI pointe du Diable, CS10070, Plouzané, France

E-mail: marion.chapalain@ifremer.fr

² Royal Belgian Institute of Natural Sciences, OD Nature, Gulledele 100, 1200 Brussels, Belgium

³ Université de Caen Basse-Normandie, BOREA, Esplanade de la Paix, CS 14032 Caen, France

Context

Suspended particulate matters (SPM) are key elements within coastal ecosystems regarding their role in sedimentary transfer, transport of contaminants, dynamics of benthic habitats and in the modulation of primary production. In coastal areas, at the interface between estuary and bay, strong turbidity gradients are observed and SPM are mainly formed by flocs, aggregates of mineral and organic matters, even if sand can episodically be resuspended associated to high-energy hydrodynamics events. SPM dynamics is driven by physical and hydrological forcings such as tidal currents, storms, river discharge, but also by the seasonal variability of organic matter (OM) content (i.e. phytoplankton blooms). All these parameters contribute to modulate flocculation/deflocculation processes and hence the characteristics (size, density) of flocs. The role of organic matter in SPM dynamics is still rising important questions, especially the understanding of the contribution of phytoplankton and Exopolymeric Substances (EPS)/Transparent Exopolymeric Particles (TEP). This work aims to examine the spatial and temporal variability of SPM characteristics at the interface between the Seine estuary and bay.

Methods

Six field campaigns were conducted in 2016 within the Seine river plume and the near Seine Bay in order to investigate flocculation dynamics and the potential relationship with the OM content. These campaigns consisted of ship-based monitoring and sampling through 12-h tidal cycle cruises carried out along the annual cycle (~ every 2 months, mainly spring tides) at two fixed stations: La Carosse (LC), at the mouth of the Seine estuary in the turbid plume, and BS1, located more offshore. During these surveys, we used a floating platform equipped with two downward looking RDI 1200kHz and 600kHz ADCPs continuously recording along the 12-h tidal cycle. Every hour, samples at the sub-surface and 1m above the bed were collected from a horizontal Niskin bottle sampler for quantifying suspended sediment concentration (SSC), TEP, total OM and chlorophyll a concentration. Finally, a frame equipped with a CTD profiler, an OBS3+, a turbidity meter (Wetlabs FLNTU) and a LISST100X was deployed to profile the water column, at 15-min intervals during the tidal cycles. Dedicated post-processing methods were developed for LISST analysis, especially in the salinity gradient (flagging the Schlieren effect), but also in low SSC conditions. Analysis of water samples taken near the bed also revealed, sometimes, the presence of both sand and flocs.

Results

First results at the station LC show that SPM dynamics at the tidal scale could be divided into 3 key patterns using hydrological parameters such as SSC and salinity: the Seine river surface plume during low tide, offshore (Seine Bay) waters during high tide in the whole water column, and resuspended bed sediments near the bottom during ebb and flood (Fig. 1). The three patterns are always observed all along the annual cycle, but with variable SPM features (SSC, Particle size distribution (PSD) and OM content).

The SSC surface plume is around 30mg/l during winter and 10mg/l in summer. This variability could be explained by the position of the turbidity maximum in the estuary, close to the mouth in winter (high river discharge), and shifted landward during summer low river discharge periods. Suspended sediments in the plume are mainly macroflocs, with sizes larger than 200 μ m. Preliminary results do not show a seasonal variability of surface plume floc sizes but this pattern is characterized by sharp salinity gradients, then LISST data require deeper and careful processing.

Regarding fine sediment resuspension patterns, a seasonal trend is also observed with SSC values reaching 100mg/l in January and March and lower values for the rest of the year. Sand particles are regularly observed close to the bed and their presence is generally correlated to spring tides, except once in December. A methodology - based on the separation of the LISST particle size distribution (PSD) into five Gaussian populations - has been developed in order to estimate the presence of sand in suspension and to calibrate the optical instruments with only fine (i.e. the flocculating) particles (Fig. 2). It consists in estimating SSC from LISST-100X PSD, testing the presence of flocs (H1) or sand in the two largest populations, macro- and mega-flocs (H2) or in mega-flocs only (H3). For H1, the excess density of each population is calculated assuming a fractal behaviour, while for H2 and H3 a fixed density of 2650kg.m⁻³ is

associated to the largest “sand” populations. The best hypothesis is validated when the calculated concentration is the nearest from the reference sample concentration (Fig. 2). This methodology will be extrapolated to all vertical profiles along tidal and annual cycles, in order to automatically detect the presence of sand in suspension.

Superposed to the hydrological cycle, a strong seasonal variability of the OM content is observed, reaching values up to 50 % during spring and summer and lower than 20 % during the rest of the year. Observations of deflocculated PSD revealed clearly the presence of a phytoplankton bloom in July. This seasonal variability of OM content is suspected to modulate SPM characteristics, and will be also investigated from the collected dataset.

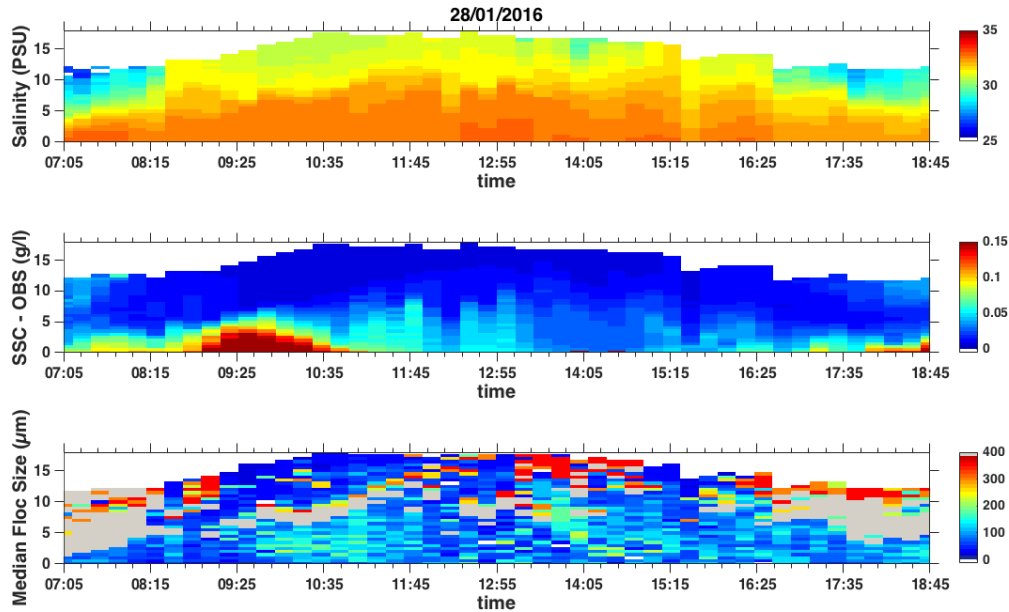


Fig. 1. Tidal profiles of salinity (PSU), SSC (g/l) given by the OBS3+ and the median floc size (μm) at the fixed station LC on 28/01/2016.

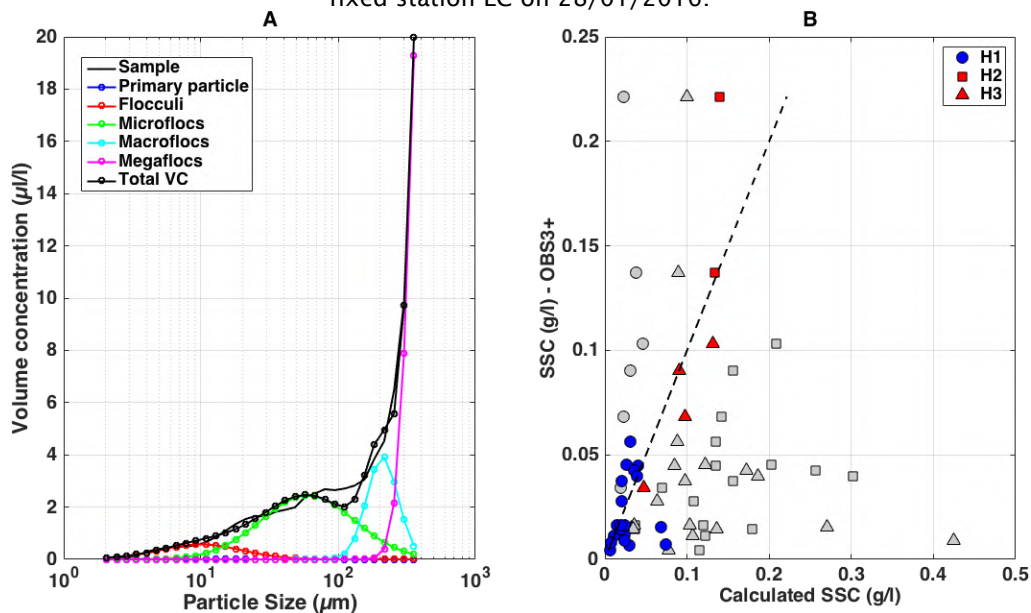


Fig. 2. (A) PSD split up into 5 Gaussian Populations for a near bed water sample at LC on 22/03/2016. (B) Comparison of SSC estimated against SSC given by OBS3+ at LC on 22/03/2016 with the 3 hypotheses: H1, only flocs are present, H2, presence of flocs and sand in the two largest populations (macro- and mega-flocs) or in mega-flocs only (H3). Grey points represent samples for which the hypotheses are not validated. Red points are samples with H2 or H3 validated (sand and flocs), blue points are for samples with H1 validated (only flocs).

In situ response of optical turbidity sensors to suspended sediment characteristics in turbid estuarine system.

Flavie Druine¹, Romaric Verney², Julien Deloffre¹, Jean-Philippe Lemoine³, and Robert Lafite¹

¹ Normandie Univ, UNIROUEN, UNICAEN, CNRS, M2C, 76000 Rouen, France
E-mail: flavie.druine@sfr.fr

² IFREMER, DYNECO/DHYSED, ZI pointe du Diable, CS10070, Plouzané, France

³ GIP Seine Aval, Pole Régional des Savoirs, 115 Boulevard de l'Europe, 76100 Rouen, France

Abstract

The development of an automated monitoring network is a key issue for both water quality (e.g. indicators) and knowledge on the fate of suspended particulate matter (SPM) in estuarine systems. Among the monitored parameters turbidity is governed by resuspension, deposition and advection of sediment. Turbidity measurement is obtained by optical methods to accurately assess the temporal variations of SPM concentrations. The main advantage of indirectly estimating SPM concentration are the continuous acquisition of data and low operating cost. On the other hand, some limitations have been identified to using turbidity sensors, as the effect of sediments characteristics on the turbidity response (Hatcher and *al.*, 2000; Merten and *al.*, 2014). This article, based on field sample and turbidity measurements, describes the effects of particle concentration, size, density and the organic matter on the turbidity signal of two optical sensors with different design. Results are applied to the Seine estuary automated water monitoring system (measuring since 2010).

The optical sensors tested were deployed to realize vertical profiling measurements of turbidity directly in the field. The data were carried out in the fluvial and Turbidity Maximal Zone (TMZ), along the Seine Estuary (Normandy, France) during 36 tidal cycles between February 2015 and June 2016. A measuring frame was deployed vertically with Sea-Bird 19plus V2 CTD associated to an OBS3+, a multi-parameter YSI 6600 V2 probe and a LISST 100X-type C. For each tidal cycle, profiles were conducted every 15' in the water column to measure sedimentary parameter such as turbidity and floc sizes. A horizontal Niskin bottle was used every hour in order to obtain SPM concentration from the sub-surface (1 m) and close to the bed (1 m), thus resulting in about 26 samples per tidal cycle. Each sample was immediately filtered on pre-weighed glass filters (Whatman GF/F) with a pore size of 0.45 μm to obtain the SPM concentration. Eight water samples were also chosen per tidal cycle and were filtered to measure the organic matter proportion by loss on ignition (480°C for 4 hours).

For each tidal cycle, a correlation coefficient between turbidity is obtained by comparing OBS3+ or YSI 6600V2 and SPM concentration. We used several methods to accurately obtain this relationship (Fig. 1A). Comparing all the data (36 tidal cycles in the fluvial or TM zone), the correlation coefficient ranges between 0.92 and 3.92 (Fig. 1B). Results show an YSI slope range between 1.12 and 1.79 mg.l⁻¹.NTU⁻¹, for TMZ, and between 0.85 and 1.97 mg.l⁻¹.NTU⁻¹, for fluvial area. Conversely, OBS calibration coefficient varies with time, showing statistically different slopes. The highest values reach close to 3.95 and 3.96 mg.l⁻¹.NTU⁻¹ and the lowest values are observed around 2.19 and 1.75 mg.l⁻¹.NTU⁻¹, respectively for TMZ and fluvial area. Various studies (Bunt and *al.*, 1999; Downing, 2006) indicate that OBS sensor signal can be altered by the variability of the particle optical properties in the environment. On the Seine estuary optical sensors are affected by particles size (D_{50}) and flocs organic matter content (Fig. 1C). Measuring sediment fluxes using automated monitoring network need to accurately estimate SPM/Turbidity relationships (Fig. 1D).

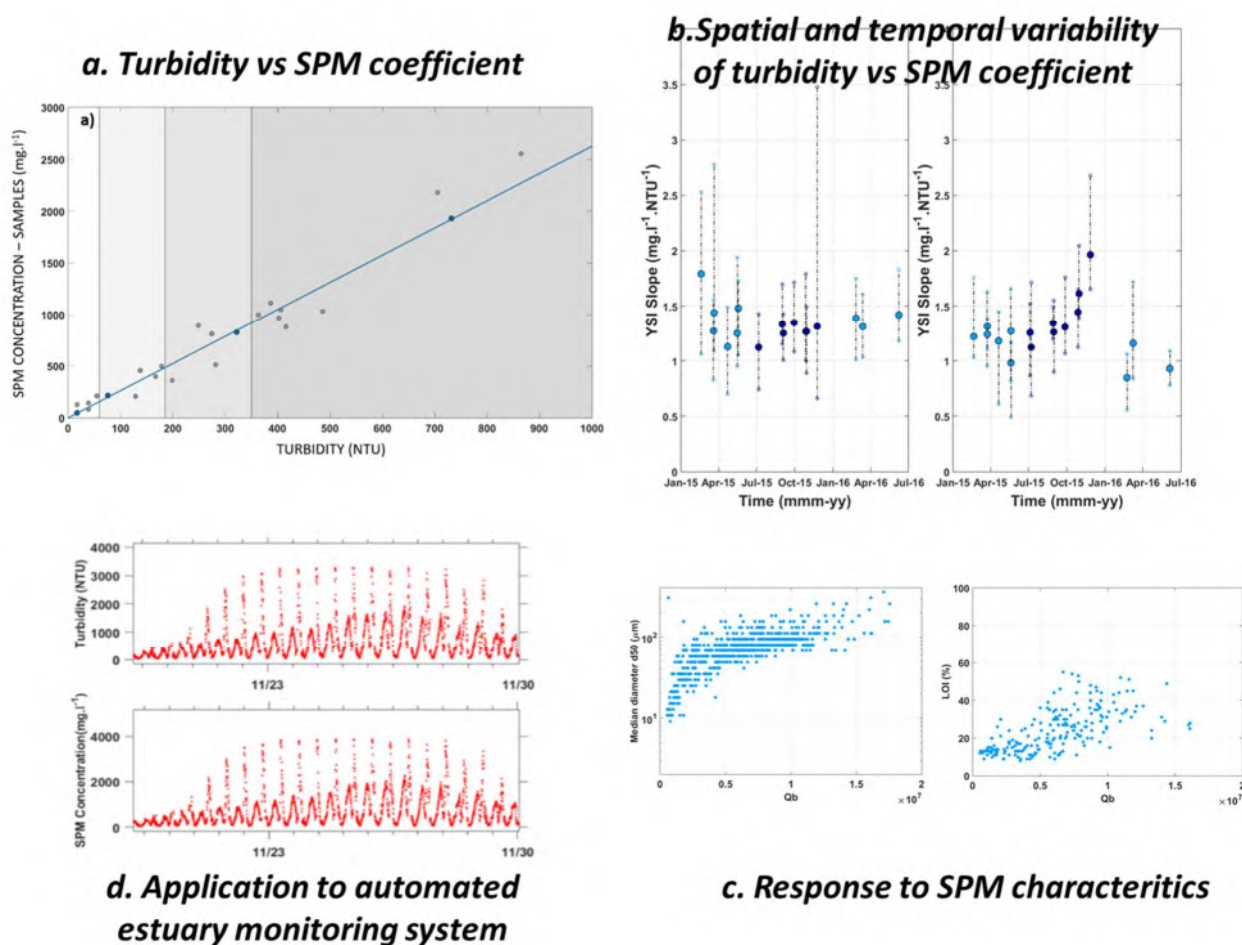


Figure 1: General scheme of the study. a: Relationship between turbidity and SPM concentration using different methods; b. Temporal variations of the Turbidity/SPM relation in the fluvial and TMZ zone; c. Response of the optical sensors to SPM characteristics (D50 and loss on ignition) and d. application of the obtained relation to the Seine estuary monitoring network.

References

- Bunt, J.A.C., Lacombe, P., Jago, C.F., 1999. Quantifying the response of optical backscatter devices and transmissometers to variations in suspended particulate matter. *Continental Shelf Research* 19, 1199–1220.
- Downing, J., 2006. Twenty-five years with OBS sensors: The good, the bad and the ugly. *Continental Shelf Research* 26, 229–2318.
- Hatcher, A., Hill, P. and Grant, J., 2001. Optical backscatter of marine flocs. *Journal of Sea Research* 46, 1–12.
- Merten, G.H., Capel, P.D. and Minella, J.P.G., 2014. Effects of suspended sediment concentration and grain size on three optical turbidity sensors. *Journal Soils Sediment* 14, 1235–1241.

Modelling morphodynamics in the sand/mud context of the Seine estuary mouth: methodology, validation and questions

Pierre Le Hir¹, Jean-Philippe Lemoine², Florent Grasso¹ and Bénédicte Thouvenin¹

¹ IFREMER, laboratory DYNECO/DHYSED, Centre de Bretagne, CS 10070, 29280 Plouzané, France
pierre.le.hir@ifremer.fr, florent.grasso@ifremer.fr, benedicte.thouvenin@ifremer.fr

² GIP Seine-Aval, 115 Bd de l'Europe, 76100 Rouen, France- jplemoine@seine-aval.fr

Abstract

Discussion on the strategy for calibrating a 3D process-based model to simulate short-term sediment dynamics (sand and mud) and long term morphodynamics.

Introduction: the Seine mouth, a dynamic system

Since the the XIXth century, many engineering works have been undertaken in the macrotidal Seine estuary, north-west of France: bank protections by dikes and the associated channelling of the estuary along 120 km, expansion of Le Havre and Rouen harbours, respectively nearby the mouth and 120 km upstream. These works have induced the development of an ebb delta split into two shoals separated by a navigation channel, both prograding seawards. In 2005, a new extension of Le Havre harbour ("Port 2000") restricted the total width of the estuary mouth, while the navigation channel along the estuary, up to Rouen, was slightly deepened. Last, the maintenance of navigation channels requires annual dredging up to 6 MT (see Lemoine *et al*, 2017).

All these features make the Seine estuary a very dynamic system. In particular, submersible dykes at the mouth, aimed at enhancing ebb sediment fluxes, have induced some shift of the turbidity maximum towards the mouth, inducing the expansion of muddy subtidal areas , while the intertidal mudflats have been considerably reduced.

In such context, it is important to predict the probable evolution of the system, accounting for possible effect of sea level rise. For this purpose, a morphodynamic process-based model has been set up.

Model description

The model solves the hydrostatic 3D Navier-Stokes equations. Suspended sediment transport is simulated by solving an advection/diffusion equation for different sediment types ranging from mud to fine and medium sand (Le Hir *et al*, 2011). A lateral erosion term allows meandering and channels divagation, intertidal flats extension, but also erosion of underwater slopes exposed to strong currents in channels. Consolidation of sand and mud mixtures is solved according to a modified Gibson equation (Grasso *et al*, 2015).

In the application to the Seine estuary, a curvilinear grid is used and the mesh size is about 70 x 200m in the area of interest. Realistic forcing is considered: tidal components offshore, real 2DH wind forcing, diurnal Seine river flow. The wave model WW3 solves the propagation of swells as well as the generation and dissipation of wind-induced waves at the same resolution as the circulation model.

In order to speed up mean and long term simulations, a morphological factor (MF) is applied in the sediment compartment to erosion and deposition exchanges, while processes in the water column are simulated at the right scale.

Methodology for calibration and validation: successive steps

The presentation will emphasize the calibration procedure. The latter requires simultaneous validation for hydrodynamics, hydrology, sediment transport, erosion and deposition patterns, surficial sediment changes and morphodynamics coupling; then it addresses short term (tidal cycle, season) and mean term (up to decades) processes.

Except the consolidation parameters that were set up thanks to laboratory experiments (Grasso *et al.*, 2015), all parameters were fitted by trial and error approaches, using field data for calibration and validation (with several sets). For hydrodynamics and tide propagation, tidal gauges were classically used, together with some current measurements. Turbulence closure and mixing parameters were fitted to simulate hydrological features (salinity gradients and stratification), by comparison with measurements at fixed stations (SYNAPSES network). Suspended Sediment Concentrations (SSC) and turbidity maximum patterns were deduced after fitting erosion and settling parameters, using SSC observations of the same SYNAPSES network. At this stage, some ambiguity remains concerning sand erosion parameters, and the wave-induced skin stress to be used. A combination of short term observations of sediment elevation (with ALTUS echosounders) and successive bathymetric charts (~ 1/year since 2001) enabled to fit them. The latter were synthesized by averaging deposition and erosion on specific areas, in order to get a representative comparison between field data and model results. Once all these settings achieved, the capacity to simulate mean and long term trends can only be partly adjusted by specifying the lateral erosion parameters and above all the initial surficial sediment distribution (size-composition, thickness and shear strength), which gradients are so large and variable that no sediment cover is accurate enough to prevent uncertainties (recommendations are provided). One of the most relevant data to fit the mean term modelling appeared to be the characterization (sand, mud...) and quantification of dredged masses in different maintained zones.

Sediment fluxes

On the other hand, after such thorough calibration, the model can be considered as reliable to provide the time evolution of sediment fluxes through different cross-sections, and especially the sediment influx from the sea, one of the most relevant feature for long term trends, and probably the most difficult to assess.

Morphological coupling

The long-term approach by using a morphological factor in mixed sediment context is also evaluated. In addition to a possible artefact in consolidation processes due to enhanced fresh deposits, the vertical structure of the layered sediment is likely to be affected, and consequently the subsequent erosion. However, the technique is proving effective.

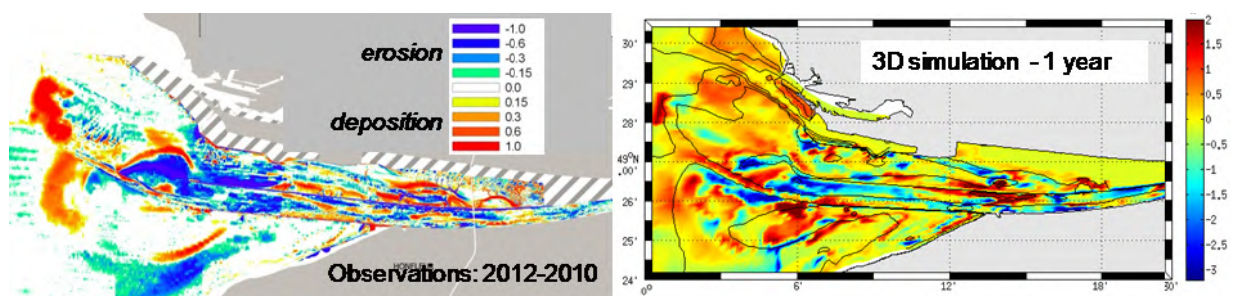


Fig. 1. Morphological evolution of the Seine estuary (in *m*)

Acknowledgements

This work is supported by the Seine-Aval 5 Scientific programme (HYMOSED & MEANDRES project). Bathymetric data are supplied by harbour authorities of Rouen (GPMR) and Le Havre (GPMH).

References

- Grasso F., Le Hir P., Bassoullet P., 2015. Numerical modelling of mixed-sediment consolidation. *Ocean Dynamics*, 65(4), 607-616.
- Le Hir P., Cayocca F., Waeles B., 2011. Dynamics of sand and mud mixtures: a multiprocess-based modelling strategy. *Continental Shelf Research*. 31, S135-S149
- Lemoine J.P., Le Hir P., Grasso F., 2017. Impact of maintenance dredging on suspended sediment dynamics in the Seine estuary, submitted to INTERCOH 2017.

Modelling the dispersal of microplastic particles: anthropogenic cohesive particles and their fate in coastal waters

Erik Toorman¹, Qilong Bi¹, Xiaoteng Shen¹, Annika Jahnke² and Jaak Monbaliu¹

¹ Hydraulics Division, Department of Civil Engineering
KU Leuven, Kasteelpark Arenberg 40, box 2448, B-3001 Leuven, Belgium
E-mail: erik.toorman@kuleuven.be

² Department of Cell Toxicology, Helmholtz Centre for Environmental Research -- UFZ
Permoserstrasse 15, DE- 04318 Leipzig, Germany

Introduction

Microplastic (MP) particles are small plastic particles with a size smaller than 5 mm, which are found in all kinds of products (paints, shower gels, etc) or result from the degradation by weathering of macroplastics by exposure to UV radiation, biotic degradation, friction, etc. These particles enter the aquatic environment via sewer inflows, sewer treatment plant overflows, or direct input from waste through rainfall runoff or from the air. These particles are believed to be a threat to the environment since during the weathering process they break up into food-sized particles and may leach toxic additives that may enter the food chain. Recent monitoring has revealed an astonishing amount of MP particles deposited in sediments along shores down to the deep ocean bottom. Thus far, little is known about the time scales and pathways for the transport of MP particles and the governing processes (Jahnke *et al.*, 2017b). The JPI Oceans funded project WEATHER-MIC (Jahnke *et al.*, 2017a) aims at investigating this aspect. Since MP particles show many similarities with cohesive sediment particles (e.g. surface charges and biofilm formation), the KU Leuven applies their expertise on cohesive sediment transport modelling to these “new” particles, including the possible interaction with cohesive particles in the aquatic environment.

Modelling of microplastics dispersal

The KU Leuven contributes to this project by setting up 3D particle transport models for two sites, i.e. the Oslo Fjord (Norway) and the Himmerfjärden Bay, south of Stockholm (Sweden), using the TELEMAC software (www.openTELEMAC.org). Open sea boundary conditions are generated by a two-dimensional depth-averaged (2DH) hydrodynamic model for the wider area covering the Skaggeak, Kattegat and Baltic Sea, in which tidal currents and wind effects are considered. Field data are collected by the Norwegian Geotechnical Institute (NGI) and Stockholm University, partners in the project.

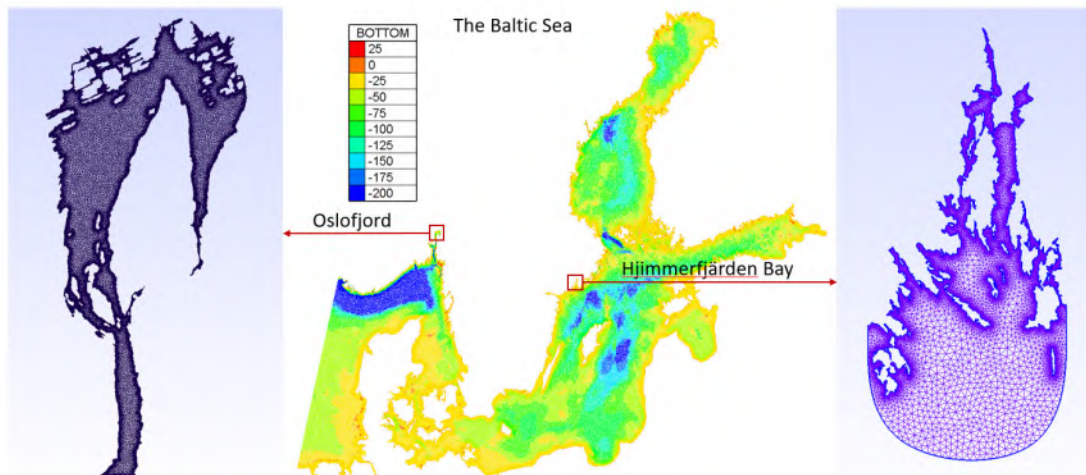


Figure 1. The unstructured meshes for the 2DH Baltic Sea model, and the 3D Oslo Fjord and Himmerfjärden Bay models

The main challenge is the development of a closure model to predict the highly variable size, density and settling velocity of the particles and their aggregates. For this purpose, the two-class population balance equation (2CPBE) flocculation model, developed by Lee *et al.* (2011), and

implemented into TELEMAC (Ernst, 2016), will be extended to 3 classes (Shen *et al.*, 2017) and adapted to be applicable to MP particles (class 1), cohesive sediment particles (class 2) and their combined flocs (class 3). Since so little is known on the changing properties of MP particles by weathering, biofilm formation and aggregation, dedicated experiments are carried out in settling columns at NGI.

Characterization of weathering microplastic particles

Complementary research is carried out by the Helmholtz Center for Environmental Research (UFZ Leipzig), Fraunhofer Institute (IKTS Dresden), the Department of Environmental Science and Analytical Chemistry (Stockholm University) and NGI (Oslo) by experimental studies to gain understanding of weathering mechanisms and their environmental impact. The effect of the following factors on MP weathering is investigated: UV light exposure, salinity, physical stress (turbulence and friction with other particles, including sediments), biodegradation, biofilm formation and temperature. The outcome of these investigations needs to be transformed into breakup and aggregation terms for the particle kinetics equations in order to calculate the evolution of the average settling velocities of MP particles and its aggregates.

For many of the partners this is the first application of their expertise to MP, which results in the innovative use of methodologies and measuring techniques never before applied to these particles.

Further information can be found on the project website <http://www.jpi-oceans.eu/weather-mic/about>

Acknowledgments

This research is supported through the Joint Programming Initiative Healthy and Productive Seas and Oceans (JPI Oceans) project WEATHER-MIC, where the contributions of KU Leuven and UFZ are funded by the Belgian Federal Science Policy Office (BELSPO, Project Grant BR/154/A1/WEATHER-MIC) and the German Federal Ministry of Education and Research (BMBF, Project Grant 03Ff0733A).

References

- Ernst, S. (2016). Implementation of a flocculation model in TELEMAC-3D. MSc thesis KU Leuven, Dept. of Civil Engineering, 151 pp.
- Jahnke, A., MacLeod, M., Potthoff, A., Toorman, E., Arp, H.P. (2017a). WEATHER-MIC—How microplastic weathering changes its transport, fate, and toxicity in the marine environment. *Fate and Impact of Microplastics in Marine Ecosystems. From the Coastline to the Open Sea*. MICRO2016. Lanzarote, 25-27 May 2016, 127-128.
- Jahnke, A., Arp, H., Escher, B., Gewert, B., Gorokhova, E., Kühnel, D., Ogonowski, M., Potthof, A., Rummel, C., Schmidt-Jansen, M., Toorman, E., McLeod, M. (2017b). Reducing uncertainty and confronting ignorance about the possible impacts of weathering plastic in the marine environment. *Environmental Sci. & Techn. Lett.*, 4 (DOI: [10.1021/acs.estlett.7b00008](https://doi.org/10.1021/acs.estlett.7b00008)).
- Lee, B.J., Toorman, E.A., Moltz, F., Wang, J. (2011). A two-class population balance equation yielding bimodal flocculation of marine or estuarine sediments. *Water Research*, 45:2131-2145.
- Shen, X., Toorman, E., Fettweis, M. (2017). A tri-modal flocculation model coupled with TELEMAC for suspended cohesive sediments in the Belgian coastal zone. INTERCOH 2017 Book of Abstracts (this volume).

Validation of satellite remote sensing for coastal turbidity monitoring by sediment transport modelling

Qilong Bi¹, Jonas Royakkers¹, Nitin Bhatia², Sindy Sterckx², Els Knaeps², Erik Toorman¹ and Jaak Monbaliu¹

¹ KU Leuven, Department of Civil Engineering, Hydraulics Section, Kasteelpark Arenberg 40, PB 2448, BE-3001 Leuven, Belgium. jaak.monbaliu@kuleuven.be

² Flemish Institute for Technological Research, Boeretang 200, BE-2400 Mol, Belgium.

Introduction

Satellite images of coastal areas can show the spatial distribution of fine suspended sediments at the surface of large water bodies. After atmospheric correction of the raw image, the intensity of the reflectance in selected frequency bands can be converted into suspended particulate matter (SPM) concentrations. Calibration and validation of the conversion algorithm requires field data (ground truthing) which is time demanding, labour intensive and restricted to a few locations. In addition, comparison can be made with images from other satellites and SPM maps generated by computer simulations.

Proba-V is a Belgian satellite designed for vegetation monitoring with daily coverage at 300 m and a 5-daily coverage at 100m resolution. The sensor onboard the satellite records data up to at least 100 km away from the coastlines. The good image quality provides opportunities for turbidity retrieval in coastal waters. Combining turbidity products from Proba-V and other typical ocean colour sensors allows for better monitoring of turbidity in dynamic near shore areas and it increases the chance to detect short term events in particular for areas with rapid changing cloud cover. An evaluation of the added value of Proba-V for monitoring turbidity, taking into accounts its limitations, is presented by Knaeps *et al.* (2017). They present the turbidity retrieval algorithm and the direct validation with in-situ data (normalized water leaving radiance sensors, SPM concentrations from OBS sensors on buoys and sampling; Fig.1) in more detail.

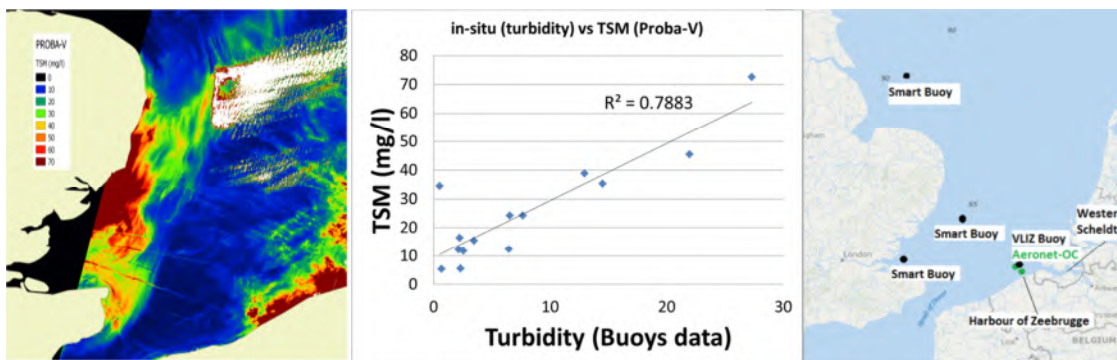


Figure 1. Left: PROBA-V TSM product (acquisition date/time 21 April 2015/11:06); Middle: Direct validation of PROBA-V TSM data through comparison with in-situ turbidity data from CEFAS smart buoys and VLIZ buoy. Right: Buoy locations.

The present study focusses on the indirect validation method, consisting of an intercalibration with a sediment transport model (using TELEMAC, solving for hydrodynamics, waves and SPM concentrations) which is used to take into account the turbidity variations between subsequent image acquisitions.

Assessing the errors and similarities of simulated SPM maps

A methodology has been developed for assessing the errors and similarities of simulated SPM maps compared with the remote sensing images. The quality of an image signal that is being evaluated can be thought of as a sum of an undistorted reference signal and an error signal. Thus, to assess the quality of simulated results, it is necessary to quantify the error signal. The methodology in this study mainly consists of three approaches.

The first one is called the distance based approach, which is used to quantify the errors between simulated results and remote sensing images. The Euclidean distance is adopted as the error index and it can be calculated at different length scale. This can give an indication of the quality of simulated results in a defined sub-domain and show the model performance at a relatively large scale.

The second approach is an assessment based on structure similarity. This approach is brought up to compensate some drawbacks in the distance based approach. The reason is that the same distance metrics may come from very different types of errors, some of which are more visible than others. Image signals are highly structured, while the distance metrics are based on pointwise signal differences and independent of the underlying signal structure. Hence, instead of estimating perceived errors, perceived changes in structural information variation can be measured in the framework of a Structural Similarity Index (SSIM) as developed by Wang et. al (2004). This index is calculated from the simulated results and is used to quantify the Structural Similarity between a modelled SPM map and a remote sensing image.

The third approach is based on pattern recognition and comparison. A method for calculating 2D cross-correlation is adopted. In general, cross-correlation is a measure of similarity of two series as a function of the displacement of one relative to the other. It is commonly used for searching a shorter, known feature or local pattern in a longer signal. It is also a method of estimating the degree to which two series are correlated. With 2D cross-correlation, it is possible to find the local pattern shift in the simulated results and quantify the displacement of simulated patterns and the ones captured in the remote sensing image.

The methodology is also applicable to assess the similarity in temporal variations. Instead of directly using simulated results at certain time frame, a temporal variation can be calculated from different time steps. Then, it is possible to apply the above three approaches to the temporal variations from the remote sensing data and the simulated results, respectively. The purpose is to check if a similar trend can be found in both remote sensing images and simulated SPM maps.

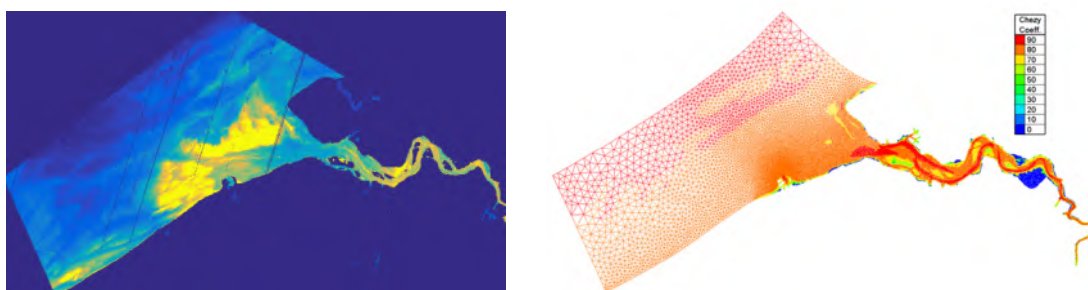


Figure 2. Left: PROBA-V image cropped to the modelling domain, of which the mesh and roughness map (cf. Bi & Toorman, 2015) is shown on the right.

Different model set-ups will be applied in order to assess the importance of potential 3D effects (e.g. vertical stratification) and the importance of flocculation (Bi *et al.*, 2016) and how they may affect the interpretation of remote sensing images.

Acknowledgements

This research is funded by the Belgian Science Policy Office (Proba4Coast project) and the European Space Agency (ESA, PV-LAC project).

References

- Bi, Q., Toorman E.A. (2015). Mixed-sediment transport modelling in the Scheldt estuary with a physics based bottom friction law. *Ocean Dynamics*, 65:555-587.
- Bi Q, Ernst S, Lee B, Toorman E. (2016). Implementation of two-class population balance equation bimodal flocculation model in TELEMAC-3D. TELEMAC-MASCARET User Conference. (Oct.2016, Paris, FR), pp. 11-13.
- Knaeps, E., Sterckx S., Bhatia N, Monbaliu J, Toorman, E. (2017). Coastal turbidity monitoring using the PROBA-V satellite, Abstract, Coastal Dynamics 2017 (12-16 June 2017, Helsingør, DK).

Wave effects on hydrodynamics and sediment transport in a deep channel of the Changjiang Estuary

Jie Jiang¹, Qing He¹, Chao Guo¹

¹ State Key Laboratory of Estuarine and Coastal Research, East China Normal University, P.R. China

E-mail: jiejiang_sklec@qq.com

Introduction

Waves and tidal currents which usually perform as interaction are vitally important to the physical processes of estuaries. The hydrodynamics induced by waves and currents have been widely discussed in various estuaries, including the flow structure under combined wave-current motion (G. Klopman, 1994), wave-induced bed shear stress, the initiation of sediment motion by waves and sediment transport under wave-current interaction (Green et al., 2014). However, few researchers have tried to measure and assess the importance of the wave-current interaction as well as wave transport of suspended sediment in deep channels compared to the much more works in shallow (<2m) water on intertidal flats (de Jonge and van Beusekom, 1995; Carniello et al., 2005). To acquire more details of the hydrodynamics and sediment dynamics under combined wave-current conditions in deep channels, a field survey was carried out in the North Passage ($\sim 12.5\text{m}$), which is located in the turbidity maximum (TM) of Changjiang Estuary (China). We aim to investigate the wave effects on flow structure within and outside bottom boundary and estimate the combined wave-current induced bed shear stress in the deep channel. This work is fundamentally valuable to evaluate the potential sediment transport under combined action of waves and currents.

Methods

The field survey was conducted in the North Passage of the Changjiang Estuary (Fig. 1a) for a month, from August 12, 2015 to September 11, 2015. The observation site (TNN) is located in the middle-lower section of the deep channel where ebb tide dynamic dominates. Flood tide and ebb tide averaged currents velocities are 0.88 m/s and 1.25 m/s during spring tide, respectively, with 0.69 m/s and 1.06 m/s during neap tide relatively. Particularly, an episodic storm happened during our survey period, which induced higher waves in 2 days from August 24 to August 26 when the significant wave height measured could exceed 1m up to 1.6m.

A tripod system (Fig. 1b) was placed at the bottom of the site with various instruments, including upward looking 600k Acoustic Doppler Current Profilers (ADCP), downward looking HR-profiler, Acoustic Doppler Velocimeter (ADV, Nortek 6.0MHz Vector), ASM (Argus Surface Meter IV), three OBS 3A at 30, 55, 75 cm above the bed, respectively. All the instruments were fixed in the tripod to get continuous synchronous datasets of hydrodynamics and sediment dynamics. Wave-induced bed shear stress (τ_w , N/m²) is obtained from the peak bottom orbital velocity U_δ (m/s) and wave friction coefficient f_w and current-induced bed shear stress (τ_c , N/m²) is calculated according to van Rijn (1993) based on the LP (log-profile) method; the combined wave-current shear stress (τ_{cw} , N/m²) refers to the Wave-Current Interaction (WCI) model proposed by Soulsby (2005).

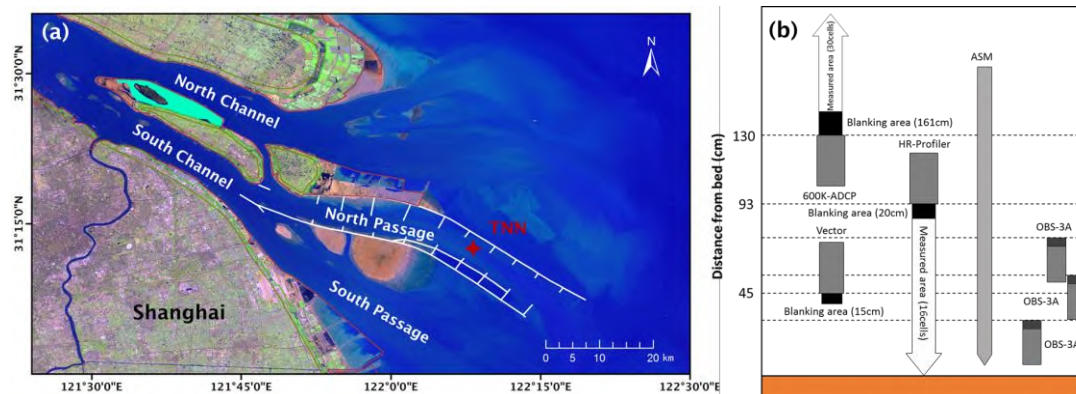


Fig. 1. (a) Sketch of the Changjiang Estuary and the measurement site (the red solid star) in the North Passage; (b) Plane figure of the instruments on the tripod system.

Results

Fig.2 shows a subset of the measurements elementarily. Current velocity matches well with the water level in the tidal scale. Obviously, there is a great difference between current velocities in windy and calm conditions although which shows the similar time series of water lever (Fig.2a). It can be partly attributed to large disparities between significant wave heights under two conditions (Fig.2c). Particular velocity profiles of main streams at the bottom (1 m above bed) of water column during a tidal cycle are shown in Fig.3. It is worth noting that flood peak current velocities are larger than ebb peak current velocities in the bottom boundary layer during both windy and calm weather when it comes to the dominance of ebb tide dynamic in situ. Moreover, only the bottom velocity data is plotted by logarithmic function when considering upper flow field is seriously disturbed by windy waves, which is used to estimate current-induced bed shear stress. Results perform very well in according to the value of R^2 .

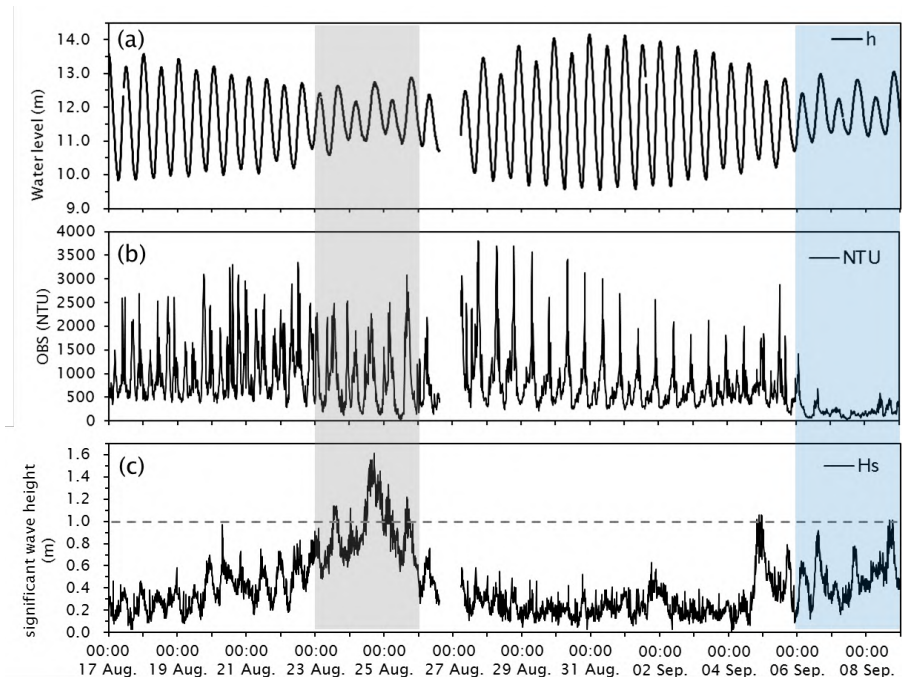


Fig. 2. Time series (23 days of the whole dataset) of water level (a),NTU (b) for OBS-based and significant wave height (c) for ADCP-based. The grey and blue rectangles show the episodic storm and the selected calm conditions.

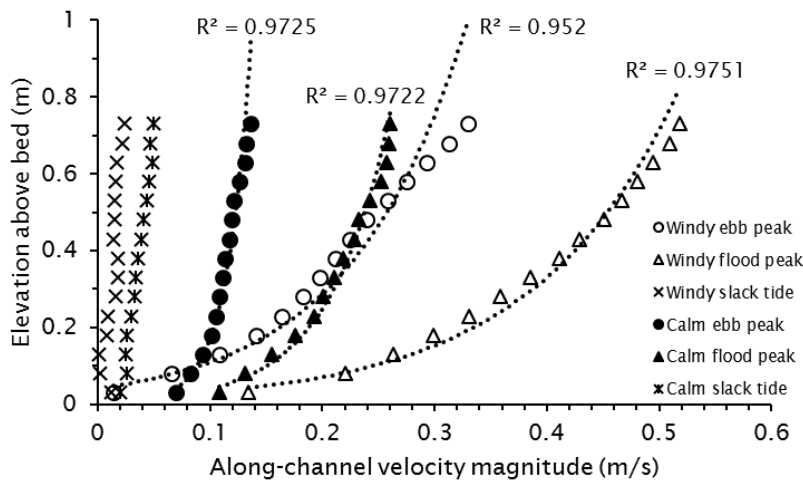


Fig. 3. Near bottom along-channel velocity profiles at particular stages in both windy and calm conditions during a tidal cycle.

Conclusion and outlook

A systematic dataset with a long timescale has been acquired in a deep channel (Changjiang Estuary, China), containing high-resolution hydrodynamic results, wave motion and sediment process within and outside the bottom boundary layer. It reveals wave motion plays a vital role in the mean flow structure as well as an excess shear stress due to waves comparable to current-induced bed shear stress during windy weather. In addition, sediment dynamic is enhanced with increased sediment transport under combined waves and currents. Detailed discussions are in progress and will be given out soon.

References

Klopman, G. (1994). Vertical structure of the flow due to waves and currents - laser-doppler flow measurements for waves following or opposing a current. *Annals of Physical & Rehabilitation Medicine*, 57, e38-e38.

Green, M. O., & Coco, G. (2014). Review of wave-driven sediment resuspension and transport in estuaries. *Reviews of Geophysics*, 52(1), 77–117.

de Jonge, V. N., and J. E. E. van Beusekom(1995), Wind- and tide-induced resuspension of sediment and microphytobenthos from tidal flats in the Ems estuary, *Limnol. Oceanogr.*, 40(4), 788–778.

Carniello, L., A. Defina, S. Fagherazzi, and L. D'Alpaos (2005), A combined wind wave-tidal model for the Venice lagoon, Italy, *J. Geophys. Res.*, 110, F04007, doi:10.1029/2004JF000232.

van Rijn, L.C., 1993. Principles of sediment transport in rivers, estuaries and coastal seas. Aqua Publication, Amsterdam, The Netherlands.

Fine-sediment transfer and accumulation in the Amazon dispersal system: from the beginning of tides to the edge of the shelf

C.A. Nittrouer¹, A.S. Ogston¹, A.T. Fricke¹, D.J. Nowacki^{1,2}, N.E. Asp³, P.W.M. Souza Filho^{4,5}, A.G. Figueiredo⁶, S.A. Kuehl⁷, O.M. Silveira⁴

¹ School of Oceanography, University of Washington, Box 357940, Seattle, WA, 98195, USA
E-mail: nittroue@uw.edu

² present address: United States Geological Survey, Woods Hole, MA, USA

³ Institute for Coastal Studies, Universidade Federal do Pará, Bragança, Pará, Brasil

⁴ Geoscience Institute, Universidade Federal do Pará, Belém, Pará, Brasil

⁵ Instituto Tecnológico Vale, Belém, Pará, Brasil

⁶ Depto. de Geologia, LAGEMAR, Universidade Federal Fluminense, Niteroi, Brasil

⁷ Virginia Institute of Marine Science, College of William & Mary, PO Box 1346, Gloucester Pt., VA 23062, USA

Abstract

The largest point source of particulate material to the global ocean is the Amazon River, and most of this sediment is fine silt and clay. From the first impact of marine processes (tidal modulation of discharge near the village of Obidos) to distal dispersal along the continental shelf of northern South America, the fine sediment passes through a range of environments with differing processes that impact the entrapment or bypassing of sediment. Over the past four decades, progress has been made toward understanding these sequential environments and the mechanisms of transport and accumulation operating within and between them.

Tributary mouths

Two major rivers enter the Amazon main stem within the tidal river (region of tidal modulation, but no salinity). Superimposed seasonal and tidal forcing cause temporally variable differences in water levels, temperature and suspended-sediment signatures of tributary and Amazon waters. The resulting differences cause net flux of Amazon fine sediment into the tributary mouths (~20Mt/y) in addition to trapping sediment supplied by the tributaries themselves.

Tidal floodplain

Tidal modulation begins at Obidos and increases toward to the Amazon mouth (a distance of ~800km) driven by macrotidal conditions (spring tidal range 8+m) seaward of the river mouth. As a result, processes within the river progressively change from fluvial domination to tidal domination. Consequently, the exchange processes for fine sediment between the main stem and the floodplain evolve downstream, resulting in distinct changes for entrapment efficiency and floodplain morphology. Three discrete reaches can be identified along the tidal river. The Upper Reach is strongly impacted by seasonal fluctuations in river level resulting in inundation and drying of the floodplain. The supply of sediment is dominated by inefficient diffusive transport mechanisms, which limit sediment entrapment despite much accommodation space. Although the Lower Reach is impacted by seasonal flooding to a much lesser degree, strong tidal currents provide a regular supply of turbid water throughout the year to and from the floodplain. As a result, the floodplain has built to sea level, and is now nourished by channelized flows that maintain the bed at the elevation of rising sea level. Active accumulation of fine sediment is greatest the Central Reach, where advective flows affected by both seasonal and tidal fluctuations nourish the broad floodplain. In this reach, tidal flows suppress levee building, allowing easy communication between main stem and floodplain, and consequently entrapment and fine-sediment accumulation rates are greatest here.

Marine tidal flats and mangrove shorelines

Both south and north of the Amazon mouth, fine sediment is accumulating in intertidal environments. These deposits of Amazon sediment extend for many hundreds of kilometers northward along the coast of South America. A companion abstract/presentation by Ogston et al. will address these fine-grained deposits and the processes controlling them.

Continental shelf

The primary destination of fine sediment transported by the Amazon dispersal system is the subaqueous delta on the continental shelf (likely the sink for >50% of Amazon sediment). A classic clinoform feature has been created by a complex superposition of baroclinic flows (estuarine circulation on the shelf), tidal currents, surface waves driven by easterly trade winds, and a strong northward western-boundary current. Suspended fine sediment enters an energetic shelf environment, causing transport processes to move much of the sediment northward and seaward. The clinoform topset is characterized by ephemeral deposition, and net accumulation rates that are generally slow (<1 cm/y). Most sediment is displaced seaward to the foreset region, largely by gravity flows of fluid mud, where accumulation can be extremely rapid (>10 cm/y). The pre-existing transgressive sand deposits are being buried by thin bottomset muds.

Summary statement

The Amazon dispersal system comprises an intriguing sequence of environments and mechanisms for transport and accumulation of fine sediment. Most of these processes remain in natural or nearly natural conditions, and provide a valuable contrast to other fluvial dispersal systems that have been intensely altered by humans. The Amazon system of the past four decades also provides a point of comparison for its own future, as local (e.g., land use, damming) and global (e.g., climate change, sea-level rise) human impacts alter the processes and the fate of fine sediment.

The controls on flocculation and suspended sediment concentrations in a muddy subtropical mangrove forest

Iain T. MacDonald¹, Nicola J. Lovett², and Julia C. Mullarney²

¹ NIWA Hamilton, Gate 10 Silverdale Road, Hillcrest, Hamilton, 3216, New Zealand

E-mail: iain.macdonald@niwa.co.nz

² Coastal Marine Group, Faculty of Science and Engineering, University of Waikato, Private Bag 3105, Hamilton, 3240, New Zealand

Introduction

Mangrove forests are some of the world's most productive, but threatened ecosystems, with global coverage declining at rapidly (Valiela *et al.*, 2001). In contrast to the global trend, many mangrove forests in New Zealand are currently expanding. The physical mechanisms underlying sediment transport within these regions are still not fully understood. In particular, there is limited understanding of how the presence of vegetation affects flocculation, owing in part to the difficulty in obtaining reliable measurements of floc properties in these often very muddy environments. Although, previous work has noted that floc properties can widely vary across mangrove and estuarine settings (Wolanski, 1995). This lack of knowledge limits our ability to predict changes in settling velocity and hence deposition rates. The present work aims to explore changes in floc properties in a mangrove forest, and in turn, how these changes may alter suspended sediment concentrations.

Field Site and Measurements

The field site is the Firth of Thames in New Zealand. Owing to relatively recent land-use changes, this location has ample fine sediment supply (average $D_{50}=5-10\mu\text{m}$) and the mangrove forest is expanding (Swales *et al.*, 2015). Data were collected over 6 days, instrumented frames were deployed (with minimal bed disturbance) at 5 sites across the edge of a mangrove forest from the adjacent mud flat to 130m into the forest (Fig. 1a). Each frame incorporated an Acoustic Doppler Current Profiler, an Acoustic Doppler Velocimeter, a Conductivity-Temperature-Depth probe and vertically separated optical backscatter sensors to provide various hydrodynamic properties and suspended sediment concentrations (Fig. 1b). Floc images were taken with a 'FlocCam system' (MacDonald and Mullarney, 2015).

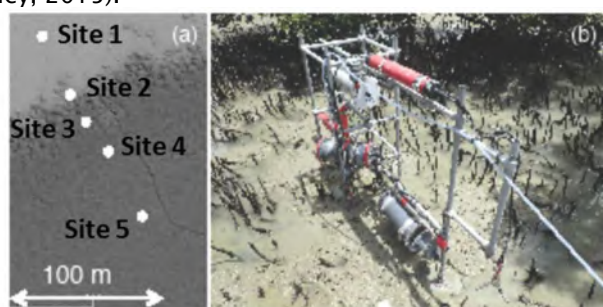


Fig. 1. (a) Instrument deployment sites (circles), (b) Photograph of frames.

Results

Preliminary estimates are shown in Fig. 2. SSCs tended to be higher in low water depths, although a wide range of values over a tidal cycle was observed (200 to 2000 mg/L). Floc image quality was highly variable, with useable images obtained for only a few tidal cycles. Example images (Fig. 3) show that, in general, flocs were small, but nonetheless exhibited substantial variability in shape.

Future work will explore in detail the relationships between floc size, SSC and hydrodynamic conditions.

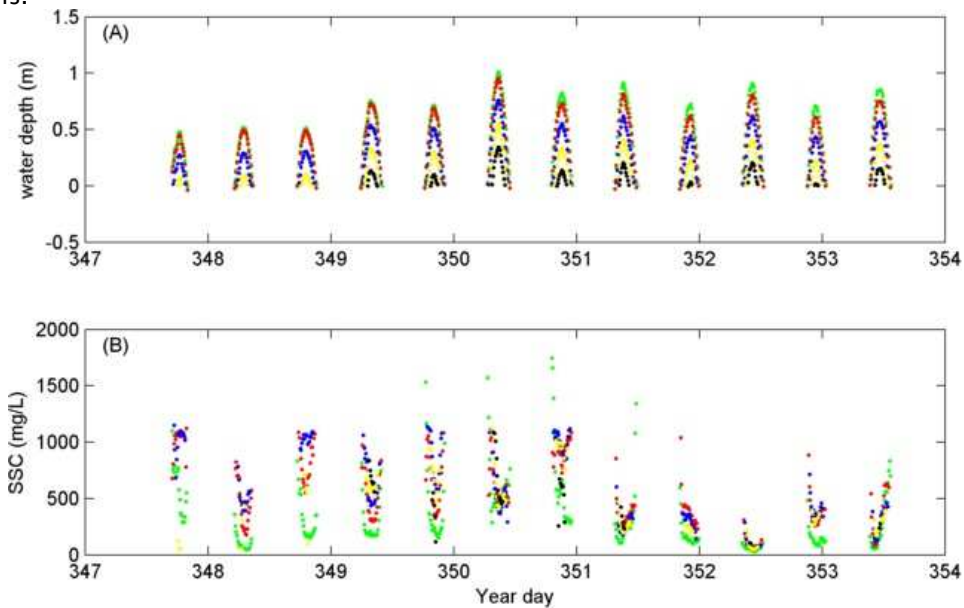


Fig. 2. Water depth and SSC estimates. Panels (A) water depth and (B) SSC. Colours: Green (Site 1), Red (Site 2), Blue (Site 3), Yellow (Site 4) and Black (Site 5)

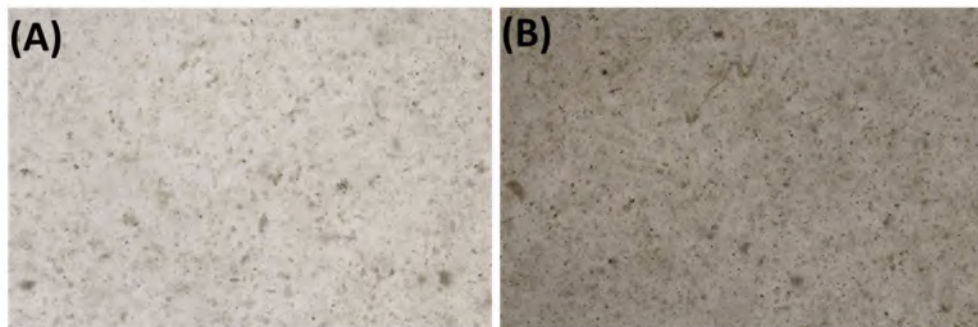


Fig 3. Floc images from (a) mudflat and (b) at mangrove fringe. The field of view is approximately 5 mm x 8 mm.

Acknowledgments

We thank the Waikato Regional Council for student support, Erik Horstman, Chris Eager, Berengere Dejeans, and Rod Budd for assistance with fieldwork.

References

- MacDonald, Iain T and Julia C Mullarney (2015). A Novel FlocDrifter Platform for Observing Flocculation and Turbulence Processes in a Lagrangian Frame of Reference. *JTECH* 32(3): 547–561, doi: 10.1175/JTECH-D-14-00106.1
- Swales, A., S. J. Bentley, and C. E. Lovelock, 2015: Mangrove–forest evolution in a sediment– rich estuarine system: opportunists or agents of geomorphic change? *Earth Surface Processes and Landforms*, 40 (12): 1672–1687, doi:10.1002/esp.3759.
- Valiela, I., Bowen, J.L. and York, J.K., (2001). Mangrove Forests: One of the World's Threatened Major Tropical Environments: At least 35% of the area of mangrove forests has been lost in the past two decades, losses that exceed those for tropical rain forests and coral reefs, two other well-known threatened environments. *Bioscience*, 51(10): 807–815.
- Wolanski, E., 1995. Transport of sediment in mangrove swamps. *Hydrobiologia*. 295: 31–42.

Numerical modeling of cohesive sediment transport along a mud dominated coast

Samor Wongsoredjo^{1,2,3}, Gerben Ruessink¹, Sieuwnath Naipal², Jaak Monbaliu³, Erik Toorman³

¹ Department of Earth Sciences, University of Utrecht
Heidelberglaan 2, NL-3584 CS Utrecht, the Netherlands

² Department of Infrastructure, Anton de Kom University of Suriname
Leysweg, Paramaribo, Suriname

³ Hydraulics Division, Dept. of Civil Engineering, KU Leuven
Kasteelpark Arenberg 40, box 2448, BE-3001 Leuven, Belgium
E-mail: Samor.Wongsoredjo@kuleuven.be

Introduction

Mud banks are a coastal morphological feature along the 1600 km long Amazon–Orinoco coastline. They migrate by (dominantly wave-induced) erosion of their trailing edge (i.e. the eastern side) and deposition on their leading edge (i.e. the western side) at an average rate of the order of 1 km/yr. These mud banks mostly consist of cohesive sediment, that is relatively easy entrained by currents and waves. As a result the suspended cohesive sediment concentration increases above mud banks. Moreover, suspended cohesive sediment concentrations are also determined by residual transport from the sediment discharge from the Amazon river, where all the cohesive material originates from. It is estimated that about 20% of the sediment discharge by the Amazon river is transported along this coastline by the North Brazilian Current and the Guiana Current. Modeling these processes on the scale of the continental shelf requires boundary conditions that differ from the conditions set on a coastal scale. In this research a free surface gradient has been applied in two directions: 1) a gradient in the downstream direction to mimic the Guiana current, and 2) a gradient from the shelf boundary to the coastline. These free surface gradients combined with the tidal database of Le Provost *et al.* (1995) were implemented to model currents for the coast of Suriname in the TELEMAC-2D hydrodynamic modeling software. Waves were also simulated by using TOMAWAC modelling software. The wave simulations were done with the following wave characteristics: peak period of 8 seconds, and a significant wave height of 1.5 meters. The sediment transport modeling software SISYPHE was used together with the TELEMAC-2D and TOMAWAC software to model suspended cohesive sediment transport. The results generated with these free surface gradients produced results that reflect the qualitative descriptions of suspended cohesive sediment transport in literature.

Shore parallel littoral currents and suspended sediment transport

The free surface gradients in both downstream and cross-shore directions were imposed on the model boundary. In particular, the insight of the cross-shore surface gradient was adapted from the study of the North Brazilian rings by Fratantoni *et al.* (2006) and wind driven currents in large oceans (Segar, 2012). Instead of implementing equations to model the North Brazilian rings and wind driven currents, a log-distributed water level gradient, perpendicular to the coast, of on average $1:5 \cdot 10^{-6}$ was imposed on the cross-shore boundaries. In this way the model calculated a shoreward directed current in agreement with computed patterns within the domain and with observations. In addition, the imposed eastward surface gradient was about $1:4 \cdot 10^{-7}$. Implementing both free surface gradients together with the new friction law proposed by Bi and Toorman (2015) in the TELEMAC-2D hydrodynamic modeling software, resulted in a dominant westward flowing littoral current (Figure 1).

The sediment transport modeling software SISYPHE was internally coupled to both the TELEMAC 2D and TOMAWAC modelling software to simulate cohesive sediment transport. An influx of cohesive suspended sediment was imposed on the upstream cross-shore boundary; this influx was set to a concentration of 0.02 g/l for only ten boundary nodes on the upstream cross-shore boundary. Furthermore, mud banks were implemented as erodible layers which could be eroded by bed shear stresses larger than 0.1 N/m^2 . The model result of these implementations is illustrated in Figure 2. The simulated littoral and tidal currents, and waves kept the suspended sediment transport parallel to the coastline.

Implementing these water level gradients on the boundary illustrate one successful way of simulating large scale littoral currents and suspended cohesive sediment transport.

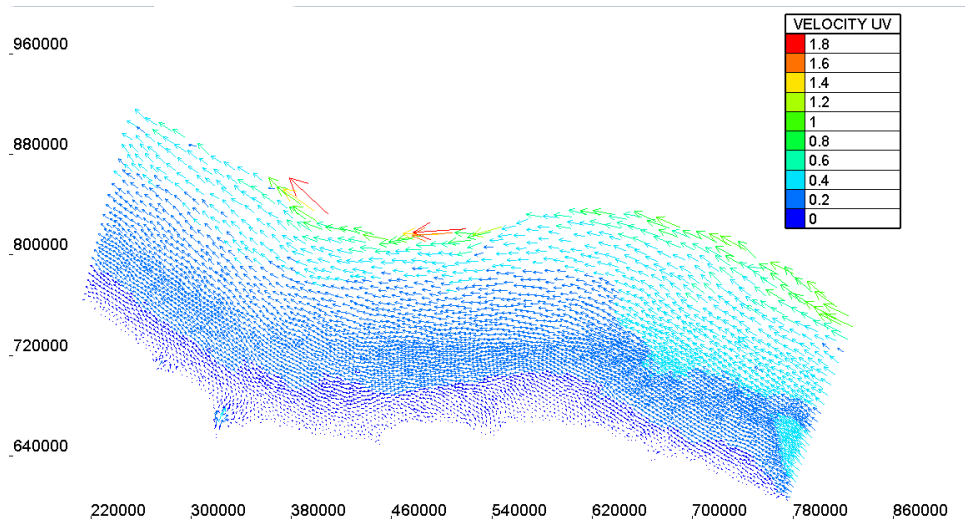


Figure 1: Modeled velocity vectors for large scale coastal model (after 92 simulated days).

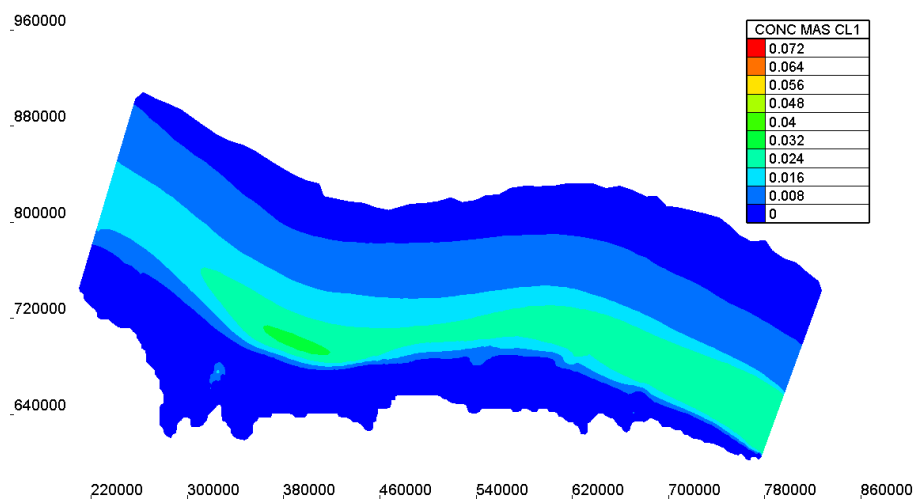


Figure 2: Simulated suspended cohesive sediment concentration (after 92 simulated days).

Acknowledgements

This research has been carried out in the framework of an internship at KU Leuven as part of the MSc program Earth Surface & Water at the University of Utrecht (NL), which study was funded by a scholarship from the Anton de Kom University of Suriname (Paramaribo).

References

- Anthony, E., J., Gardel, A., Gratiot, N., Proisy, C., Allison, M., A., Dolique, and F., Fromard, F. (2010). The Amazon-influenced muddy coast of South America: A review of mud-bank-shoreline interactions. *Earth-Science Reviews*, 103. 99–121. DOI:10.1016/j.earscirev.2010.09.008
- Augustinus, P.G.E.F. (2004). The influence of the trade winds on the coastal development of the Guianas at various scale levels: a synthesis. *Marine Geology*. 208: 145–151. DOI:10.1016/j.margeo.2004.04.007
- Bi, Q. and Toorman, E. (2015). Mixed-sediment transport modeling in Scheldt estuary with a physics-based bottom friction law. *Ocean Dynamics*. 65: 555–587. DOI: 10.1007/s10236-015-0816-z
- Chevalier, C., Froidefond, J., and Devenon, J. (2008). Numerical analysis of the combined action of littoral current, tide and waves on the suspended mud transport and on turbid plumes around French Guiana mudbanks. 28: 545–560. DOI:10.1016/j.csr.2007.09.011
- Fratantoni, D. M. and Richardson, P. L. (2006). The Evolution and Demise of North Brazil Current Rings. *Journal of Physical Oceanography*. 36: 1241–1264. DOI: 10.1175/JPO2907.1
- Segar, D. A. (2012). *Introduction to Ocean Sciences*. Third edition. Open source e-book: <http://www.reefimages.com/oceansci.php>

Investigating Rhone river plume dynamics using innovative metrics: ocean color satellite data Vs 3D sediment transport model results.

Aurélien Gangloff¹, Romaric Verney¹, and Claude Estournel²

¹ Laboratoire DYNECO/DHYSED, IFREMER, ZI pointe du Diable, CS10070, Plouzané, France.

E-mail: aurelien.gangloff@ifremer.fr

² Laboratoire d'Aérodologie, CNRS, Université de Toulouse, 14 avenue Edouard Belin, 31400 Toulouse, France.

Context

In Mediterranean coastal environments, river plumes are a major transport mechanism for particulate matter. Understanding the dynamics of these river turbid plumes is thus essential to have confidence in sediment transport models. Calibration of such models is a challenging issue as suspended solid concentration (SSC) data used to this purpose are generally collected during ship surveys, providing only local and temporary information, or through buoys or mooring lines, providing only one-point information. Another option is to use satellite ocean color imagery, which has proven to be a valuable tool to assess SSC from ocean colour data in coastal environments and which can cover a large area with a high frequency of acquisition (up to 1 image per day), depending on the sensor and the meteorological conditions. Classically, this type of data is used to compare SSC as seen by the satellite to model calculated ones through a pixel-to-pixel value comparison. But this approach can be delicate as algorithms used to retrieve SSC from satellite data can lead to substantial uncertainties. Here, we propose to use these data in another way, both quantitatively and qualitatively, comparing turbid plume metrics extracted from satellite SSC maps to model extracted ones (*e.g.* turbid plume area, centroid, outline, orientation...) in order to investigate if the sediment transport model is able to reproduce turbid plume dynamics. This approach is illustrated here through the example of the Rhône River turbid plume (Gulf of Lions - GoL, France), which is the most impacting tributary of the GoL, providing 95 % of the freshwater inputs in this area.

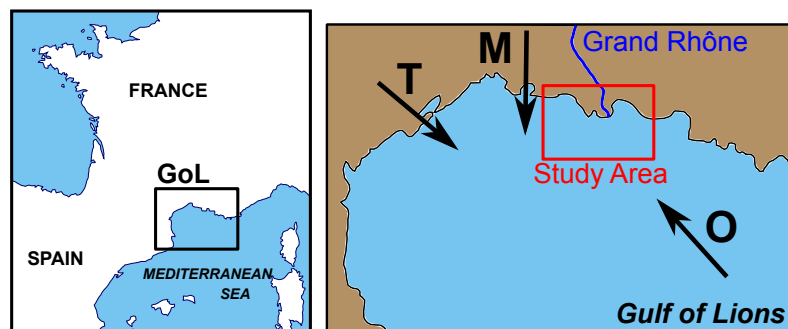


Figure 1: Geolocalisation of the study area. Black arrows represent the dominant winds: Mistral, Tramontane and Onshore winds (M, T & O, respectively).

Methods & results

In this study we used a turbid plume metrics extraction method previously described in (Gangloff et al., submitted) providing turbid plume metrics such as its area of extension (km^2), its outline, its south-east-westernmost points, its skeleton (proxy of its shape) or its centroid (see Fig. 2). This method was applied to SSC maps retrieved from MERIS-300m sensor data with a global coverage every 3 days. The same metrics extraction was applied to MARS3D hydrodynamic model (Lazure and Dumas, 2008) coupled to MUSTANG sediment transport module (Le Hir et al., 2011) outputs. Besides the challenge of calibrating the model with plume metrics, we will investigate the evolution of the Rhône River turbid plume patterns in response to the main forcings acting on the area (winds and river discharge) using both satellite remote sensing data and model outputs. Some results concerning satellite data are shown on Fig. 3. It highlights the flattening of the turbid plume along the coast during onshore wind conditions as centroids are clearly located northern of the study area compared to Mistral and Tramontane winds. However, a limitation of satellite ocean color data is the absence of observation during cloudy periods. For example, it is difficult to collect valuable satellite data during flood events as they are often related to important rainfall, and thus cloudy weather conditions. Model results will provide complementary knowledge on high frequency SSC spatial distributions at the surface, filling the gaps in satellite database and thus contributing to better understand the mechanisms driving sediment fluxes in coastal areas during these critical periods.

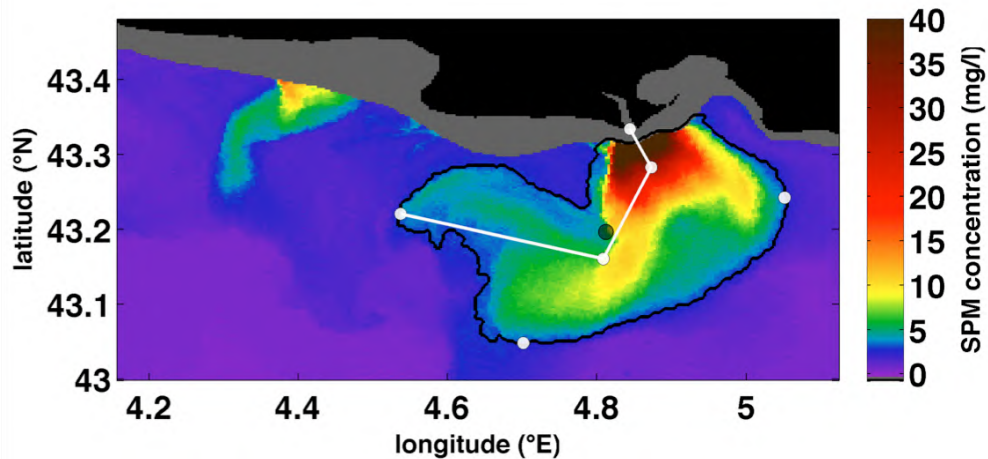


Figure 2: Example of metrics extraction of January 8th 2012. Plume centroid is represented here by a black dot, plume extension by the solid black line (area = 655 km²), southernmost, westernmost and easternmost points are the white dots on the turbid plume's boundary, proximal and distal centroids are represented by the white dots inside the boundary. The skeleton is represented by the white line. To avoid wave-induced resuspension and thus better identify Grand Rhône turbid plume, pixels where water depths are below 20 m are flagged (grey ones).

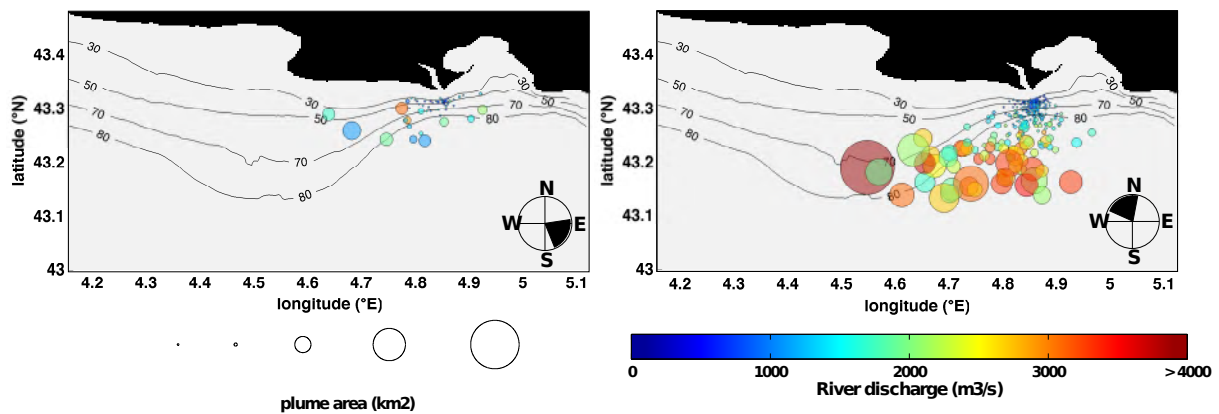


Figure 3: Rhône River turbid plume's centroids for Mistral, Tramontane (NW to N) and Onshore winds (E to SE). The more extended is the plume, the bigger is the circle representing its centroid. Colour is associated to river discharge (m³.s⁻¹). For each illustration, a wind rose reminds the wind orientation associated to the data.

References

Gangloff, A., Verney, R., Doxaran, D., Ody, A., Estournel, C., submitted. Investigating Rhône River plume (Gulf of Lions, France) dynamics using metrics analysis from the MERIS 300m Ocean Color archive (2002 - 2012). *Continental Shelf Research*.

Lazure, P., Dumas, F., 2008. An external-internal mode coupling for a 3D hydrodynamical model for applications at regional scale (MARS). *Advances in Water Resources* 31, 233-250.

Le Hir, P., Cayocca, F., Waeles, B., 2011. Dynamics of sand and mud mixtures: A multiprocess-based modelling strategy. *Continental Shelf Research* 31, S135-S149.

Mississippi River salt wedge estuary: observations of fluid shear and its effect on sedimentary processes

Ramirez, Michael T.¹, and Jarrell Smith¹

¹ U.S. Army Engineer Research and Development Center, 3909 Halls Ferry Rd, Vicksburg, MS, USA
E-mail: michael.t.ramirez@usace.army.mil

Abstract

During the low-water season (late summer–autumn) as the freshwater discharge falls below $\sim 8,000\text{m}^3/\text{s}$, the lowermost Mississippi River is subject to estuary conditions. This estuary takes the form of an upstream–flowing layer of dense saline water (salt wedge) that encroaches up to 100km along the channel bed from the Gulf of Mexico. The high magnitude of freshwater inflow and relatively low tidal forcing lead to highly stratified estuarine conditions with a shear boundary between the two fluid masses. Instability at the boundary generates turbulent mixing which serves to thicken the gradients in temperature and salinity in the downstream direction. Turbulence at this boundary increases the collision rate of fine sediment, and the presence of salinity induces flocculation as these particles come together.

Two surveys were conducted in November 2015 and December 2016 to observe the low-flow conditions in the lowermost 60 km above the Mississippi River outlet at Head of Passes (HOP). Study methods included cross-sectional and stationary acoustic Doppler current profiling (ADCP), sampling of river water and bed materials, vertical profiles of conductivity, temperature (CTD) and laser in-situ scattering and transmissometry (LISST), and photography of the water column with the Particle Imaging Camera System (PICS) to delineate particle diameters and settling velocities.

In November 2015 the head of the salt wedge was between 40 and 60km upstream of the HOP, and in December 2016 the head of the salt wedge was between 25 and 40km upstream of HOP. Survey locations were selected above the head of the salt wedge and in river reaches between tributary outlets along the lowermost river channel. The upstream extent of the saline layer manifests in velocity profiles as a near-bed low velocity zone, while further downstream the salt wedge is a more coherent layer with fully upstream-directed flow. Maximum velocity of the freshwater layer was over 1m/s, while upstream-directed velocities in the saline layer were over 0.5m/s. The mixing zone thickness increases from a few meters near the head of the salt wedge to 10m near HOP. The top of the mixing zone is accompanied by a local maximum in suspended sediment concentration (SSC), suggesting particles are accumulating at this depth.

Work on this project is ongoing and in conjunction with another study in this volume (Smith, J et al) to quantify shear and turbulent mixing at the boundary and how sediment reacts to these forces.

Fine-sediment exchange between fluvial source and Amazon mangrove coastlines

A.S. Ogston¹, N.E. Asp², R.L. McLachlan¹, C.A. Nittrouer¹, P.W.M. Souza Filho³, A.T. Fricke¹

¹ School of Oceanography, University of Washington, PO Box 357940, Seattle, WA 98195 USA
E-mail: ogston@uw.edu

² LAGECO/IECOS Universidade Federal do Pará Campus Bragança, Alameda Leandro Ribeiro, s/n - Aldeia, CEP 68600-000, Bragança, Pará, Brasil

³ Instituto de Geociências Universidade Federal do Pará, Av. Augusto Correa 1 CEP. 66075-110, Belém, Pará, Brasil

Abstract

Mangrove forests depend on sediment supply to keep up with sea-level rise. The coastal mangroves to the north and southeast of the Amazon River mouth have different supply and marine energetics and thus have created different morphologies. Here we focus on recent studies in the mangroves to the southeast of the river mouth, where sediment supply is limited, and compare results to previous studies of regions to the north of the river mouth. Sedimentary processes vary seasonally, and differ in style relative to the history of the filling intertidal surfaces.

Fine sediment and Amazon mangrove coastlines

Mangrove-fringed coastlines are ubiquitous features of tropical deltas around the world. In these environments mangroves exploit extensive low-gradient intertidal zones that are nourished by fine-grained sediments recently discharged from adjacent rivers. Current understanding of the fluvial sediment supply to these coastlines, and to the marine realm in general, is not well constrained. Mangrove forests are extremely valuable marine environments that can protect human habitation against waves and currents, are themselves home to many juvenile marine organisms, and are major repositories for carbon. The mangrove coastlines south and north of the Amazon River mouth are among the most verdant on Earth. The river and coastlines have had little impact from humans, and represent linked systems that can provide valuable insights to help ameliorate conditions in less fortunate fluvial-mangrove systems around the world. Proximity to a fluvial sediment source commonly guarantees a supply of sediment. However, among the many impacts of climate change is accelerated sea-level rise, which will provide opportunity for sediment to be trapped along the lower reaches of rivers that experience tidal fluctuations. The focus of this study is to quantify the range of mechanistic processes that contribute to fine-grained sediment exchange within the Amazon fluvial-mangrove systems, which fits into the overall fine-sediment transfer and accumulation in the Amazon dispersal system discussed in the linked contribution of Nittrouer et al.

The Amazon coastal environment is very energetic, with enormous freshwater discharge, large tidal range, a northward-flowing coastal current (North Brazil Current, NBC), and easterly tradewinds and associated waves. Most sediment discharged by the Amazon moves northward (with the NBC), nourishing the continental shelf and coastline (Nittrouer and DeMaster, 1996; Kuehl et al., 1996). However, active sediment accumulation is patchy, because the energetic physical processes can be very erosive in places.

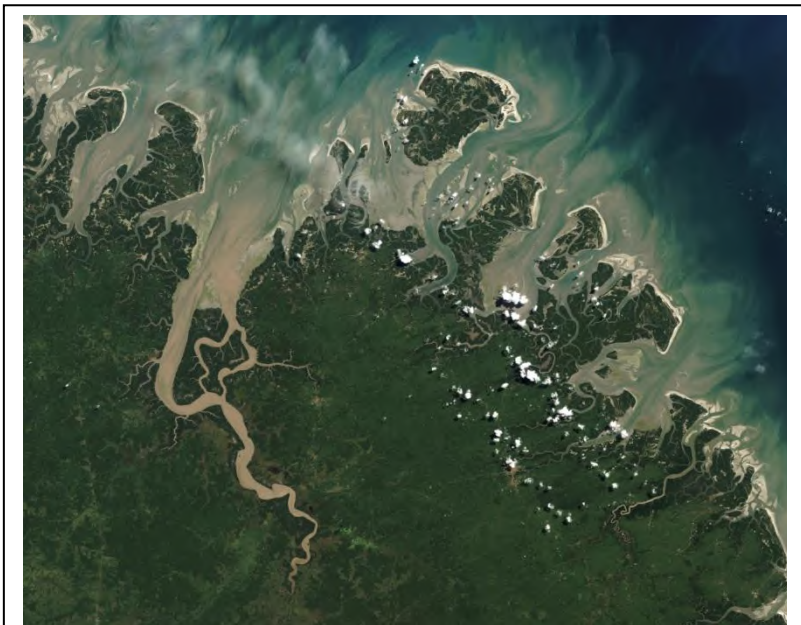


Fig.1. Landsat5 satellite image (<http://earthobservatory.nasa.gov>) of the prograding mangrove shoreline to the southeast of the Amazon River mouth.

Coastal sedimentation, and the progradation of mangrove forests, is observed in some portions of the Brazilian coast north of the river mouth, but other areas are characterized by erosion of the mangrove environments (Allison et al., 1995a; Allison et al., 1999). Ironically, the coast south of the Amazon mouth is not thought to receive much sediment (due to dominantly northwestward transport along the coastline), but the shoreline is actively growing seaward and mangrove forests are healthy (Figure 1) (Souza Filho et al., 2006; Asp et al., 2016). The Amazon River is the most likely source of fine-grained sediment.

Here we focus further into the mangrove environments to the south of the Amazon River mouth, as their coupling with the Amazon fluvial discharge is more constrained, and likely to be a limiting factor in their progradation and mangrove colonization. Additionally, we contrast their sedimentation processes and patterns with those observed in previous studies on the northern shoreline (e.g., Allison et al., 1995a,b; Allison et al., 1999). Seasonal studies of the active processes in a cross-cutting mangrove through-flowing channel and in a dead-end channel illustrate the array of tidal and discharge-related fine-sediment dynamics in these two contrasting study sites that represent different stages within the sedimentation history of a muddy mangrove forest in this region.

References

- Allison, M.A., Nittrouer, C.A., Kineke, G.C., (1995a). Seasonal sediment storage on mudflats adjacent to the Amazon River. *Marine Geology* 125, 303- 328.
- Allison, M.A., Nittrouer, C.A., Faria, L.E.C (1995b) Rates and mechanisms of shoreface progradation and retreat downdrift of the Amazon river mouth, *Marine Geology* 125, 373-392.
- Allison, M.A., M.T. Lee, A.S. Ogston, and R.T. Aller (1999) Origin of Amazon mudbanks along the northeastern coast of South America. *Marine Geology* 163 (1-4): 241-256.
- Asp, N.E., Gomes, V.J.C., Ogston, A.S. et al (2016) Sediment source, turbidity maximum, and implications for mud exchange between channel and mangroves in an Amazonian estuary. *Ocean Dynamics* 66: 285-297.
- Kuehl, S.A., Nittrouer, C.A., Allison, M.A., Faria, L.E.C., Dukat, D.A., Jaeger, J.M., Pacioni, T.D., Figueiredo, A.G., and E.C. Underkoffler (1996). Sediment deposition, accumulation, and seabed dynamics in an energetic, fine-grained coastal environment. *Continental Shelf Research* 16, 787-816.
- Nittrouer, C.A. and D.J. DeMaster (1996). The Amazon shelf setting: tropical, energetic, and influenced by a large river. *Continental Shelf Research* 16, 553-573.
- Souza Filho, P.W.M., Cohen, M.C.L., Lara, R.J., Lessa, G.C., Koch, B., Behling, H. (2006) Holocene coastal evolution and facies model of the Bragança macrotidal flat on the Amazon Mangrove Coast, Northern Brazil. *Journal of Coastal Research* SI 39: 306-310.

Evidence of muddy aggregates as resilient pellets in suspension throughout the water column using traps and a Particle Image Camera System (PICS) in a tidal estuary

Grace M. Massey¹, Kelsey A. Fall^{1,2}, Carl T. Friedrichs¹ and S. Jarrell Smith²

¹ Virginia Institute of Marine Science, College of William and Mary, Gloucester Point, VA 23062, USA
E-mail: Grace.Massey@vims.edu

² U.S. Army Engineer Research and Development Center Coastal and Hydraulics Laboratory, Vicksburg, MS 39180, USA

Biogenic pelletization plays an important role in the packaging of fine sediments to prevent their availability in contributing to the water clarity issues in coastal systems. On the order of 1000 5µm equivalent spherical diameter clay flocculi primary particles can be packaged in a single elliptical-in-shape pellet, 100µm long and 30µm wide. This is a size consistent of those observed in our study area in the Clay Bank Area of the York River, a tributary of the Chesapeake Bay, Virginia, USA. If resuspended, this one pellet will have almost 25 times less surface area and thus have that much less impact on water clarity, than its constituent primary particles. Biogenic pelletization can be significant where there are large numbers of organisms that suspension feed, pump quantities of water into their feeding systems and extract suspended solid particles. It can be even more significant when the pellets are resistant to degradation and breakup under normal tidal stress. For example, one study of *Callinassa major*, a ghost shrimp, estimates it produces 2,480 medium sand size resilient pellets per day, which collect and are transported in the troughs of sand ripples (Pryor, 1975). In the study, Pryor estimates in an area of the Mississippi Sound, where the density of *Callinassa* burrows approach 500/m², they can remove and pelletize nearly 618 metric tons of suspended solids per square kilometer each year. "Enough to cover each square metre of the back island shoreface with 141 mm of fecal pellets each year" (Pryor, 1975).

The resilient pellets in our study have been found to comprise up to 40% of the bottom sediments in the Clay Bank Region of the York River, Virginia, USA (Rodríguez-Calderón and Kuehl, 2013). From video collected by Robert Diaz's WormCam, we believe these resilient pellets are produced by polychaetes. The burrows and fecal pellets, though smaller, are very similar to those described of the polychaete *Nereis diversicolor* in the Kundalika Estuary on the west coast of India (Kulkarni and Panchang, 2015). A nearly continuous series of sediment trap deployments on benthic tripods from September 2012 through March 2015 show a loosely seasonal trend (dotted line in Figure 1) in the pellet concentration of the homogenized sediment collected in each trap with inlet holes 0.4 mab. X-rays of the traps show that the sediment collected, however, is not homogenous. They show thin laminations of coarser material throughout the trap, which we hypothesize to be tidally resuspended pellets, sand and coarse debris.

Two additional sediment traps were deployed on a tower in conjunction with the deployment of the benthic tripod deployed August to November 2016. The surface trap's 1cm diameter inlet holes were within 2m of the surface, and the bottom trap's were at a mid-water depth of ~3.2m above the bed (mab) (referred to as mid-trap). The pellets were separated using a 90µm and a 63µm sieve. The sediment collected in each of the three traps are visually similar in the microscopic photos taken (Figure 2). There was more debris in the mid and tripod traps than in the surface trap and some very large pellets were visible in the mid-depth trap. Each trap contained over 99% mud, and the percentage of mud packaged as pellets in each of the traps was 2.00, 4.05 and 4.89 for the top, mid and tripod traps, respectively. This shows that these pellets are being resuspended and transported throughout the water column. This is consistent with the findings of Haven and Morales-Alamo (1968) during a study in the James River, an adjacent tributary of the Chesapeake Bay, and suggests that sorting during transportation and deposition could result in accumulation in areas of the estuary where fine sediment would not settle out.

Two 4-6 hr profile cruises, one around max flood and the other around max ebb, were conducted early in the deployment of the sediment traps. The instruments mounted on the profiler included a Particle Imaging Camera System (PICS), a LISST 100X, a YSI EXO sonde and a pump for water samples. Future work will include identifying pellets in the PICS video sequences using axis ratios and pixel intensity to differentiate them from like size particles.

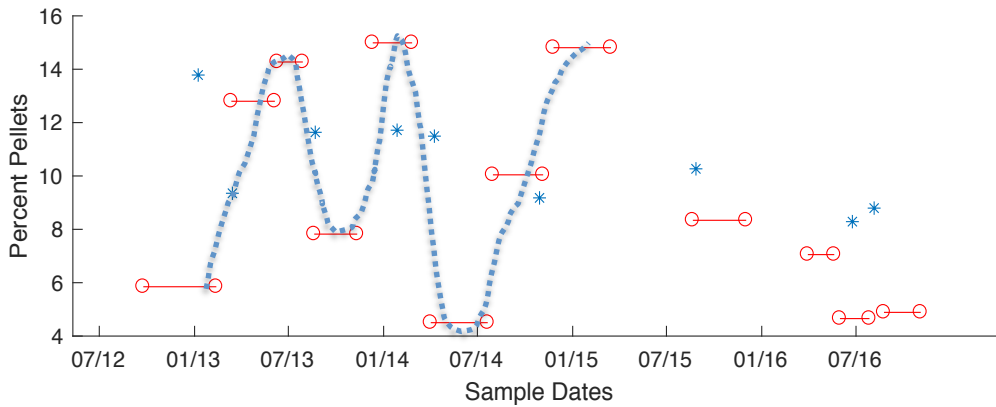


Fig. 1. Red bars are the percentage of mud packaged as resilient pellets captured between the time frame indicated by the red circles. Blue stars are the average of the top 2cm of percent mud packaged as resilient pellets from bottom sediment cores.

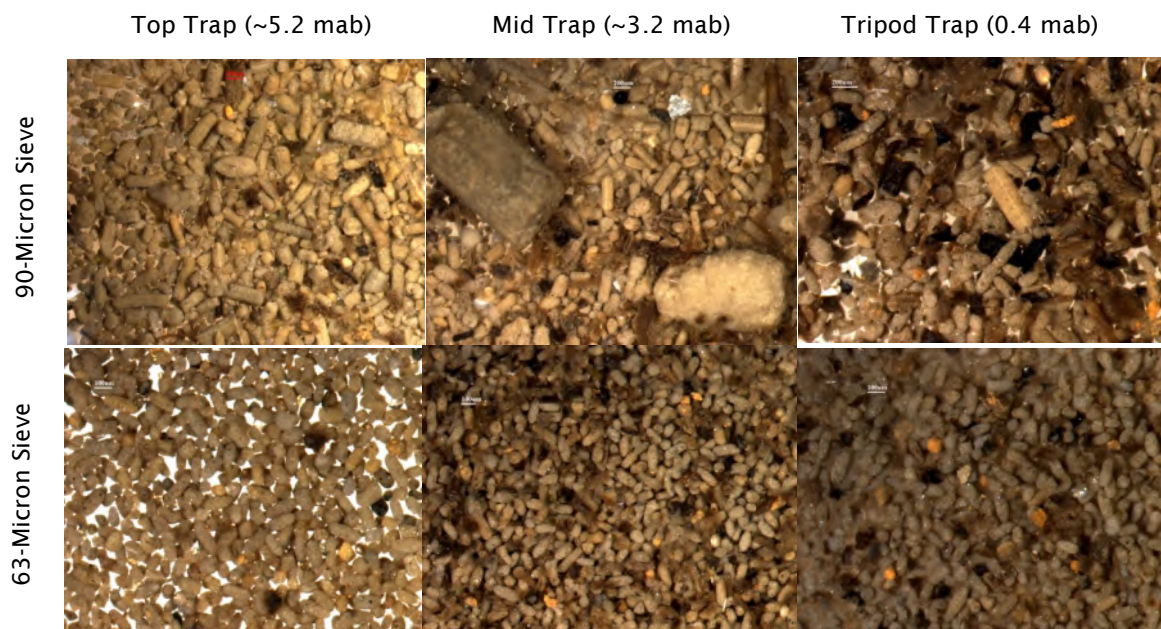


Fig. 2. Pellets sieved from sediment traps deployed August - November, 2016.

References

- Haven D. and Morales-Alamo R. (1968) Occurrence and transport of fecal pellets in suspension in a tidal estuary. *Sedimentary Geology*, 2(2):141-151.
- Kulkarni K.G. and Panchang, R. (2015) New insights into polychaete traces and fecal pellets: another complex Ichnotaxon? *PLoS ONE*, 10(10):e0139933.
- Pryor W.A. (1975) Biogenic sedimentation and alteration of argillaceous sediments in shallow marine environments. *Geological Society of America Bulletin*, 86(9):1244-54.
- Rodríguez-Calderón C. and Kuehl S.A. (2013) Spatial and temporal patterns in erosion and deposition in the York River, Chesapeake Bay, VA. *Estuarine, Coastal and Shelf Science*, 117:148-158.

Fractal floc properties in the surface waters of a partially-mixed estuary: insights from video settling, LISST, and pump sampling

Kelsey Fall^{1,2}, Carl Friedrichs^{*1}, Grace Massey¹, David Bowers³, and Jarrell Smith²

¹ Virginia Institute of Marine Science, College of William and Mary, Gloucester Point, VA, USA

*Corresponding Author, E-mail: Carl.Friedrichs@vims.edu

² U.S. Army Engineer Research and Development Center, Vicksburg, MS, USA

³ School of Ocean Sciences, Bangor University, Menai Bridge, Anglesey, UK

Background

Typical near surface estuarine particles are not isolated, individual sediment grains, but rather are clusters of inorganic and organic components known as flocs. Flocs can be described using fractal geometry such that floc density (ρ_f) exhibits a power-law dependence on floc size (d_f) (Kranenburg, 1994). Due to the fragile nature of flocs, in situ sampling is required to accurately characterize d_f and ρ_f . Two useful approaches for estimating ρ_f in the field are: (i) to use measurements of d_f and settling velocity within an in situ video settling tube (Dyer and Manning, 1999); or (ii) through measuring the ratio of suspended mass concentration to suspended volume concentration as determined by water sampling and laser particle sizing (Mikkelsen and Pejrup, 2001).

The goal of this study is to gain insight into the fractal properties of flocs in estuarine surface waters under conditions of variable floc size, density, concentration, and organic content. The properties of flocculated particles in estuarine surface waters are especially important to the fate of incident light, with direct ramifications for primary production, water quality, and optical remote sensing. Compared with flocs in bottom boundary layers, the in situ fractal nature of flocs in estuarine surface waters has been quantified relatively less. Challenges associated with in situ observation of flocs in estuarine surface waters include the motion of observing platforms, lower particle concentrations, smaller particles, lower settling velocities, and lower contrast in optical imaging.

Methods

This study focuses on observations collected along the York River Estuary, major tidal tributary of the Chesapeake Bay, USA. Although microtidal in terms of tidal range, the partially-mixed York River Estuary experiences near-surface tidal currents of up to 1 m/s at spring tide (Friedrichs, 2009). Observations of particle properties were collected using a profiling system that includes a Laser In-Situ Scattering and Transmissometry (LISST) 100X Type C instrument, a high-definition Particle Imaging Camera System (PICS) incorporating a video settling tube, and a high-speed pump sampler. At each sampling station, the profiler was lowered to a depth of 1-3m below the surface, and kept there while the suite of instruments sampled for 2-5min. With the profiler located above the pycnocline, observed particles were more likely to be dominated by slowly settling flocs, without major influence of heavier non-flocculated particles, such as the compacted mud pellets commonly resuspended in the lower water column of the York River Estuary. Results reported here were collected at a total of 45 samples stations on nine cruises conducted in the York between September and December over the course three years, 2014-2016. Samples were collected in the fall and early winter to avoid phytoplankton blooms, which are most likely to occur during spring and summer in this system. An aim of this study is to examine properties of flocculated particles without observations being significantly confounded by the presence of relatively large, intact algal cells.

The PICS video camera system collected in-situ measurements of particle settling velocity and particle diameter (d_p), which were then combined with standard settling relationships to estimate floc particle excess density, $\Delta\rho$, as a function of d_f (Smith and Friedrichs, 2015). Independent particle size distribution (PSDs) measured by the LISST and PICS were merged to capture a potentially larger size range of particles than could be observed by either instrument alone (2.5-1000 μ m), and to help account for some of the known limitations associated with both instruments. Specifically, LISST results were used for smaller flocs known to be under-represented by the 10 μ m pixel resolution of the PICS, and PICS results were used for larger particles for which erroneous rising distribution tails are commonly produced by the LISST. The LISST scattering property kernel matrix for random shaped particles was used for the inverting the LISST data because the inversion matrix for spherical particles was found to produce unrealistic rising distribution tails toward the

small end of the PSD. Water samples collected by the profiler's high-speed pump were analyzed for total suspended solids (TSS) and organic content via standard gravimetric analysis. Bulk estimates of apparent density ($\rho_{a,bulk}$) for each sample was then estimated by dividing TSS by total volume concentration (VC_T), with VC_T determined from the merged LISST and PICS PSD.

Preliminary Results

Preliminary results suggest that settling velocity (w_s) and excess density as determined by the PICS in surface waters of the York River Estuary are very strongly fractal (Figure 1), with a median fractal dimension of ~ 2.2 . However, fractal dimensions determined by PICS analysis varied significantly among sampling stations as a function of each sample's characteristic floc size, concentration, organic content, and density. Among sampling stations, fractal dimension was found to increase with (i) increased TSS, (ii) increased median d_f , (iii) decreased $\rho_{a,bulk}$, and (iv) decreased organic content. Best-fits of fractal theory to observed PSDs resulted in a median fractal dimension and a sample-to-sample dependence of fractal dimension on other floc properties that was similar to that determined by the PICS settling tube. All PSDs displayed a consistent peak in the number concentration of particles between 5-6 μm , suggesting a stable primary particle size that was largely independent of suspended sediment concentration, organic content or median floc size. In contrast, primary particle density varied significantly among stations, increasing with (i) increased fractal dimension, (ii) increased TSS, (iii) increased median d_f , (iv) decreased $\rho_{a,bulk}$, and (v) decreased organic content.

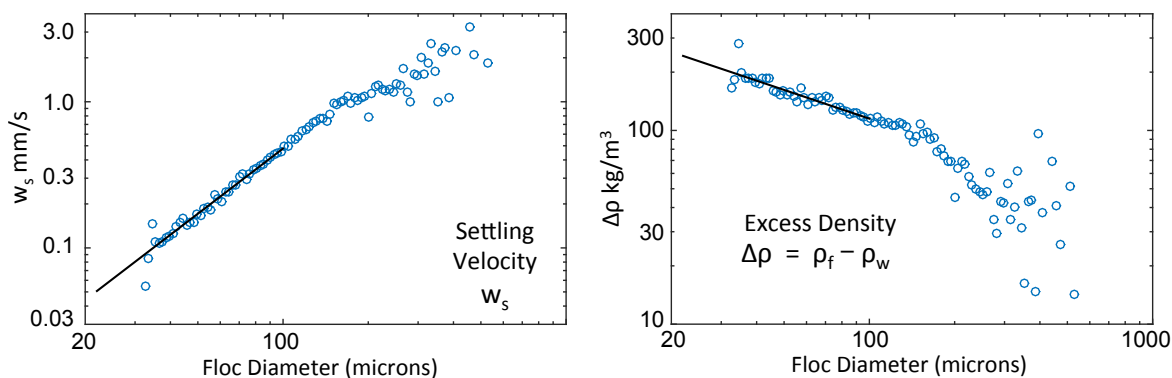


Fig. 1. Example bin-averaged w_s and $\Delta\rho$ measured in York River Estuary surface waters.

References

- Dyer K.R. and Manning A.J. (1999) Observation of the size, settling velocity and effective density of flocs, and their fractal dimensions. *Journal of Sea Research*, 41(1):87-95.
- Friedrichs C.T. (2009) York River physical oceanography and sediment transport. *Journal of Coastal Research*, SI 57:17-22.
- Kranenburg, C. (1994) The fractal structure of cohesive sediment aggregates. *Estuarine, Coastal and Shelf Science*, 39(6):451-460.
- Mikkelsen O. and Pejrup M. (2001) The use of a LISST-100 laser particle sizer for in-situ estimates of floc size, density and settling velocity. *Geo-Marine Letters*, 20(4):187-195.
- Smith S.J. and Friedrichs C.T. (2015) Image processing methods for in situ estimation of cohesive sediment floc size, settling velocity, and density. *Oceanography and Limnology: Methods* 13:250-264.

Trapping and bypassing of SPM, and particulate biogeochemical components, in the river estuary transition zone (RETZ) of a shallow macrotidal estuary.

Colin Jago, Eleanor Howlett, Francis Hassard, Suzanna Jackson, Shelagh Malham, Paulina Rajko-Nenow, Peter Robins

School of Ocean Sciences, Bangor University, Menai Bridge, Anglesey LL59 5AB, UK
Email: c.f.jago@bangor.ac.uk

The River-Estuary Transition Zone (RETZ) is the region where fluvial and tidal modulations of converging fresh water in the tidally influenced river and salt water in the upper estuary give rise to strong gradients in water dynamics and properties that vary significantly on tidal to seasonal time scales. Biogeochemical components (e.g. nutrients) and biological components (e.g. pathogens) from the land must traverse the RETZ in order to progress to the sea; as such the RETZ is a globally significant boundary. Suspended particulate matter (SPM) is potentially a key mediator of biogeochemical and biological fluxes through the RETZ since particles carry carbon and other nutrients and microbial pathogens.

Study region

Our study region is the macrotidal Conwy estuary in North Wales, UK, whose tidal range is large (mean tidal range 5 m), water depths are small (7 m in the RETZ at mean high spring tide), and river discharge is low (average $18.5 \text{ m}^3\text{s}^{-1}$, exceeding $150 \text{ m}^3\text{s}^{-1}$ during river flood events). The estuary empties of salt water during the ebb and at low tide is characterised by mudflats on the margins and extensive sandflats in the centre.

Methodology

Bed frames instrumented with an ADCP, CTD and LISST were deployed at 2 sites in the RETZ. The Tal y Cafn site is in the upper estuary (experiencing salt water on all tides) and the Dolgarrog site is further landward experiencing salt water on spring tides but remaining in the tidally influenced river on neap tides. The bed frames were deployed for 2 weeks in September/October; January/February; March/April; July. Data from the instrumented frames were supplemented with vertical profiles collected from the centre of the channel at each site using LISST and SeaBird CTD, and with surface water samples for nutrients, pathogens, and SPM. Water samples and profiles were collected every 15-30 minutes for up to 12.5 hrs a day over 2 consecutive days on spring tides at each site.

Results

Observations of dynamics and SPM properties made over spring-neap cycles in the RETZ show that turbulence controls both the particle size and flux of SPM. Turbulence dissipation inversely scales on median particle size: high turbulence on flood and ebb breaks up the flocculated particles of SPM while low turbulence at high water gives rise to aggregation of large particles and rapid settling (cf. Jago et al., 2006).

Moreover, at Tal y Cafn in the upper estuary, tidal straining associated with an axial convergent front allows stratification of the water column on the flood tide so that turbulence is reduced; this does not occur on the ebb. So although the upper estuary and RETZ exhibit the velocity-time asymmetry characteristic of tide dominated shallow estuaries, with current velocities much greater on the flood than on the ebb, for turbulence the asymmetry is reversed so that turbulence is greater on the ebb than on the flood (Howlett et al., 2015). The reduced turbulence on the flood leads to reduced mixing of large resuspended flocs upwards from the bed, so the flux of large flocs is also reduced on the flood; however, on the ebb, with increased turbulence for upward mixing there is greater flux of large flocs. The result is that there is a net seaward flux of large flocs. By contrast, in the tidally influenced river at Dolgarrog where stratification does not occur, both velocity and turbulence asymmetries are balanced in favour of increased values on the flood with the result that there is a net landward flux of small flocs. This landward flux of small flocs is an order of magnitude greater than the seaward flux of large flocs.

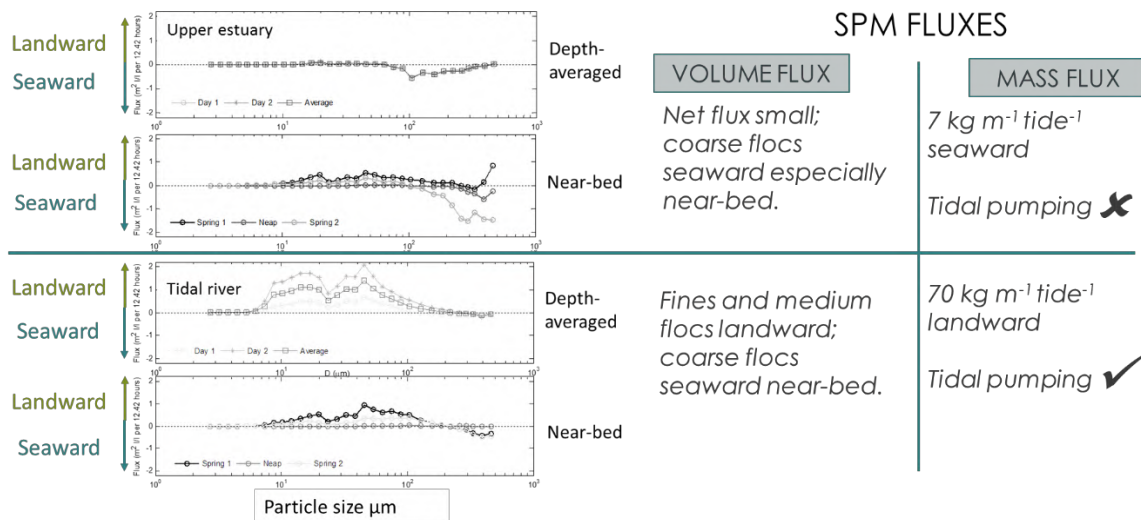


Fig. 1. SPM volume flux per LISST size class and total mass flux averaged over two tidal cycles. Volume flux is by particle size class.

We have examined the distribution of particulate nutrients and FIOs in the particle size spectrum of SPM by determining correlation coefficients (R^2) for the relationships between nutrient and FIO concentrations from filtered samples and the volume concentrations of the 32 particle size classes determined by the LISST for all samples taken through the seasonal campaign at Tal y Cafn.

These analyses produce a consistent trend for all nutrients and pathogens: R^2 values are large and statistically significant for particles sizes in the range 10-200 μm but are not statistically significant for particles <10 μm and >200 μm .

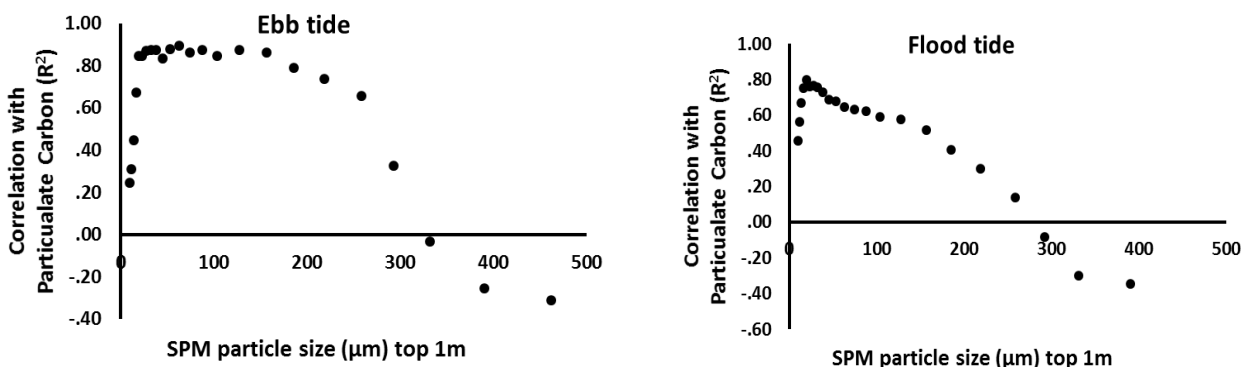


Fig. 2. R^2 values for correlation of particulate carbon concentration with volume concentrations of LISST size classes in near-surface waters at the upper estuary site. Similar results are shown for other nutrients and pathogens.

Thus the nutrient/pathogen components are preferentially concentrated in the 10-200 μm flocs (which are pumped into the tidally influenced river) and not in the large flocs (which are exported to the estuary). The biogeochemical components are therefore pumped landwards into the tidally influenced river which acts as a sink; the seaward export to the estuary is much smaller. So turbulence in the RETZ effectively sorts particles and particulate components and determines whether the RETZ acts as a sink or a bypass zone for different sized flocs.

References

- Howlett E. R., Bowers D. G., Malarkey J. & Jago C. F. (2015). Stratification in the presence of an axial convergent front: Causes and implications. *Estuarine, Coastal and Shelf Science*: 161, 1-10.
- Jago C. F., Jones S. E., Sykes P., Rippeth T. (2006). Temporal variation of suspended particulate matter and turbulence in a high energy, tide-stirred, coastal sea: relative contributions of resuspension and disaggregation. *Continental Shelf Research*, 26: 2019-2028.

Multiple Turbidity Maxima in a Short River Estuary – Why?

David Jay¹, Joseph Jurisa,¹ Saeed Moghimi¹, and Stefan Talke¹

¹ Department of Civil and Environmental Engineering
Portland State University, PO Box 751, Portland, OR 97207, USA, E-mail: djay@pdx.edu

Abstract

This contribution analyses the turbidity maximum dynamics of the Lower Passaic River Estuary or LPR, a narrow, short (length 28km) river–estuary, tributary to Newark Bay, New Jersey USA (Fig. 1). Newark Bay is, in turn, part of the larger New York Harbor complex. The LPR frequently exhibits multiple turbidity maxima, and Newark Bay also exhibits localized high turbidity levels at a channel–depth transition ~5 km seaward of the LPR mouth. The primary question addressed here is the reason or reasons for the occurrence of multiple turbidity maxima in such a short system.

Setting and Background

The LPR has been industrialized since the early 19th century, and it was a center of the American organic chemical industry in the middle 20th century. It has become the subject of a very complex Superfund study, because its sediments are heavily contaminated by organic pollutants and metals, but sewage pollution also remains a major problem. The estuarine turbidity maximum or maxima (ETM) are thought to have played a major role in retaining and re–distributing sediment–bound contaminants (Chant *et al.*, 2011), so ETM dynamics are an important Superfund problem.

New York Harbor, Newark Bay and the LPR are mesotidal (typical range, 1–1.5m), with semidiurnal tides. The LPR is convergent, with depths ranging from 8–10m near its mouth to 4m upstream (Chant *et al.*, 2011). Cross–sectional area decreases from 800m² near Newark Bay to <200m² upriver, the channel is sinuous, and the tidal excursion is typically 5–8 km. In recent years, river inflow at the head of the estuary has varied from 1 to ~600m³s⁻¹; the mean and median and median discharges are 20 and 36 m³s⁻¹, respectively. Despite the low median discharge, the small cross–section usually limits salinity intrusion to between 2 and 18km, so that the head of estuary (at a weir) is always fresh. Bridges are a very important part of system topography – there are 15 bridges within the salinity intruded reach during very low flows, and 25 bridges below the head of the tide. These have blockage factors of up to 20–30% of the flow. Overall, the LPR is near the extreme limit of modified estuaries, with almost 100% loss of wetlands, extensive historical dredging and bulkhead construction, and large pollutant inputs. Also, Chant *et al.* (2011) have argued that over–deepening caused extensive contaminant deposition when dredging ceased.

Possible Mechanisms

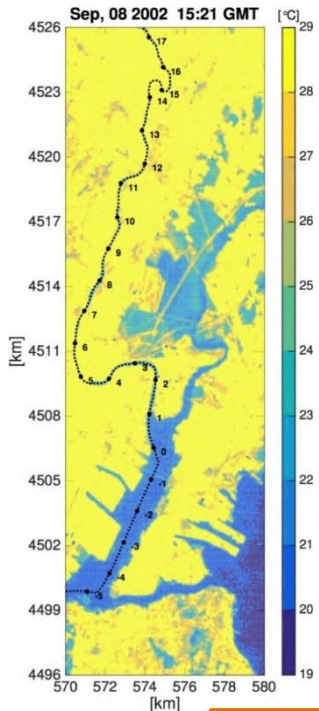
We consider several factors that may lead to the occurrence of an ETM in the system and especially multiple, localized ETM, as seen in Fig. 2:

- Convergent transport near the upstream limit of salinity intrusion: this is the “traditional” ETM trapping mechanism, but does not obviously lead to multiple ETM in a single–channel system.
- Tidal asymmetry landward of salinity intrusion: if one ETM is found at the head of salinity intrusion, then tidal trapping can lead to a second. But these two mechanisms together still do suggest the occurrence of three or more ETM, as is often observed.
- Trapping associated with bathymetric features: elevated turbidity levels are seen at the head of the deep navigation channel in Newark Bay. Shallow crossings between bends may play a similar, if less pronounced, role in the LPR.
- Resuspension at the numerous bridges: these have width constrictions and may cause partial closure of transport cells by vertical mixing, with resultant creation of multiple turbidity maxima.
- Settling lags: while this process is often associated with ETM trapping near the head of salinity intrusion in moderate–energy systems like the LPR, it does not, by itself, create multiple ETM.

Another important factor is the source of resuspension. It appears that width constrictions at bridges and shallow crossings may be sources of localized erosion. Propeller wash is a source of resuspension for the material trapped in Newark Bay, but deep draft navigation is absent in the LPR itself.

Analyses

We have use moored instrument data to relate tidal asymmetry, salinity intrusion length, and SPM fluxes to tidal range, river flow and atmospheric forcing. Vessel transect data are used to provide insight into bridge effects and an intra–tidal view of the system. A conceptual numerical model (implemented in Delft3D) is used to investigate the continuity of alongchannel transport. The Jay *et al.* (2007) approach is used to analyse suspended particulate matter (SPM) fluxes.



Interpretation

Preliminary analyses of data and model results suggest that ETM are related to location-specific processes, and that different ETM locations are likely to be active for different flow levels and salinity intrusion locations. Thus, the ETM upstream of salinity intrusion is likely caused by tidal asymmetry as a landward transport mechanism, but resuspension is probably related to bridge constrictions. Multiple ETMs form within the salinity intruded reach, with two-layer, gravitational circulation and/or internal asymmetry as driving mechanisms. Again, resuspension occurs at bridge constrictions, particularly when bridges are closely spaced, and two layer flow is interrupted at these constrictions (Fig. 3). Thus, the LPR does not appear to conform to the “conveyor belt” paradigm, which posits continuous ETM transport of particles from near the mouth to the head of salinity intrusion. Rather, communication between ETM reaches is limited, and may occur more by tidal dispersion than two-layer flow.

Fig. 1. Newark Bay and its tributary, the Lower Passaic River estuary, with river miles indicated and remotely sensed sea surface temperature (SST, color scale) superimposed. New York Harbor is to the lower right (southeast), and the Kill van Kull connects the harbour to Newark Bay.

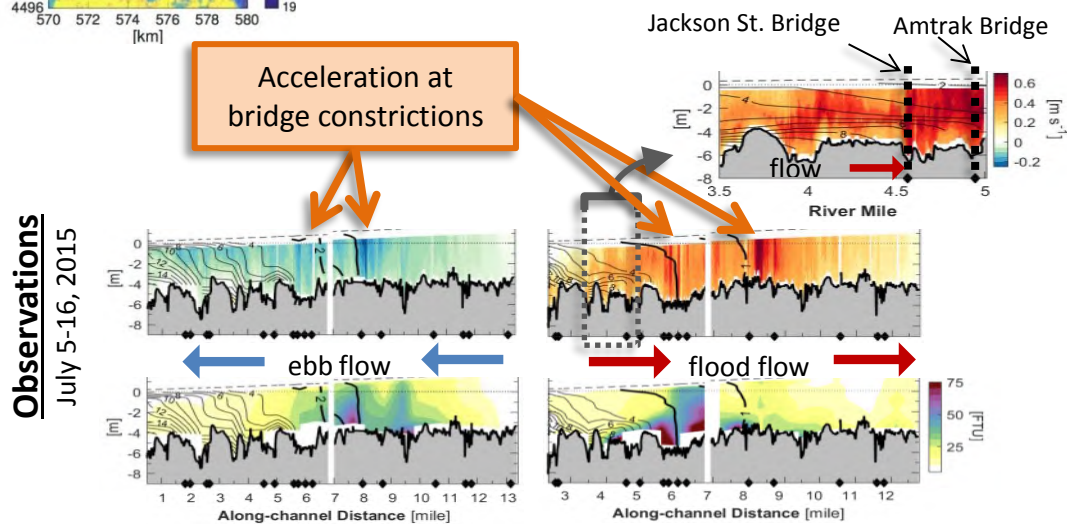


Fig. 2. Observations of velocity and turbidity (colors), and salinity (contours) during ebb and flood transects through the LPR for a moderate flow period, showing multiple ETM and the effects of closely spaced bridges. Diamonds indicate bridges. See Fig. 1 for transect locations.

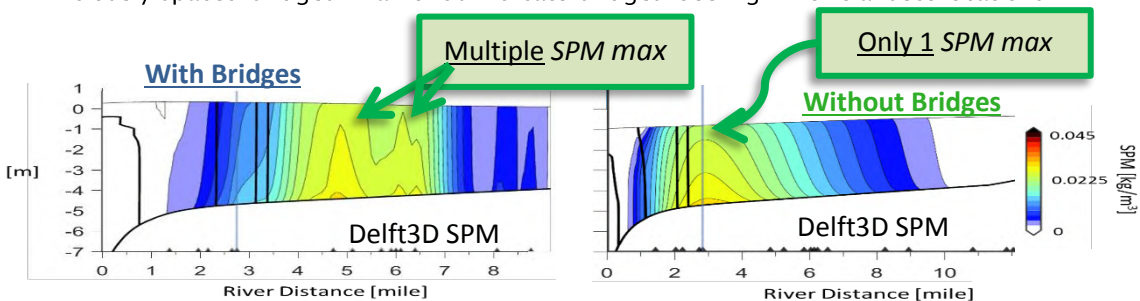


Fig. 3. Delft3D simulation in a conceptual convergent estuary of the distributions of SPM (colors) and salinity (contours), with (left) and without (right) bridges, showing fragmentation of the ETM.

References

Chant, R.J., D. Fugate, and E. Garvey. (2011). The shaping of an estuarine superfund site: Roles of evolving dynamics and geomorphology. *Estuaries and Coasts* 34: 90-105.

Jay, D.A., P.M. Orton, T. Chisholm, D.J. Wilson, and A.M.V. Fain. (2007), Particle trapping in stratified estuaries - I Consequences of Mass Conservation and explorations of a parameter space, *Estuaries and Coasts* 30: 1095-1105.

Laminar, intermittent and turbulent fluid mud flow

Erik A. Toorman¹

¹ Hydraulics Division, Department of Civil Engineering
KU Leuven, Kasteelperk Arenberg 40, box 2448, B-3001 Leuven, Belgium
E-mail: erik.toorman@kuleuven.be

Abstract

Fluid mud is a hyper-concentrated mixture of water and cohesive sediments with a density above its gelling point. The flow of fluid mud is of practical importance for gravity currents on the bottom of aquatic environments (hyper-concentrated rivers, storm-induced density currents, earthquake-induced sediment avalanches, dredged material dumping, ...) or on land (mud slides and debris flows), and for the pumping of slurries (dredged materials, drilling muds, mine tailings, ...).

Many studies have been conducted to study the slow, laminar shear flow of fluid mud and its characterization by rheology. The equilibrium rheology is best described by a visco-plastic model, i.e. a shear-thinning fluid with a yield stress, and its transient behaviour by thixotropy (Toorman *et al.*, 2014). Based on such a rheological model, one can compute the theoretical laminar flow velocity profile for open-channel (or pipe flow), i.e. a linear profile at the bottom (or pipe wall) going over in plug flow at the free surface (or in the center of the pipe).

Checking local Reynolds number values, it can be shown that it is expected that with only a little extra energy, the flows should become turbulent in a shear layer near the wall. Few observations exist that demonstrate this. Probably the most interesting data set is available from the flume experiments by Baas *et al.* (2009), which cover flow ranges from laminar to turbulent.

Because no generally valid modelling framework exists for this type of slurry flow, a new approach is presented based on the low-Reynolds extension of the mixing-length theory. It makes use of an empirical damping function, inspired by the original work of Van Driest (1956) and later followed in most other low-Reynolds turbulence models. However, the chosen damping function is defined in terms of a local Reynolds number, which is independent on the wall distance (unlike Van Driest). Moreover, unlike other damping functions, care is taken that the correct asymptotic behaviour of the solution towards both the turbulent and the laminar regime is fulfilled. This relatively simple model is tested in simple 1DV testcases of steady flow over a flat, sloping bottom for the different flow regimes.

Based on this model, the corresponding friction loss in hydraulic transport can be computed, which enables the calculation of the required pumping capacity. Comparison with measured pressure losses from experiments reported in the literature will be performed.

The same turbulence modelling strategy will be useful for the numerical simulation of water over a fluid mud layer. While the flow in the water layer (usually) is turbulent, the shear with the mud bed may induce some mass transport of the mud, but more likely causes disturbance of its surface, eventually leading to mixing over the interface and entrainment of mud into the water column and dilution of part of the mud layer. Nevertheless, the turbulence model should be able to go from the turbulence in the water down to the laminar non-Newtonian movement of the fluid mud.

Based on the work of Reichardt (1951), an empirical correction for the “wake-effect” at the free surface (or pipe center) can be taken into account. This sheds new light on the discussion on whether the value of the von Karman parameter is constant or not in sediment-laden turbulent flow.

Eventually, this turbulence modelling strategy is combined with a new (“wall-distance free”) low-Reynolds version of the k -epsilon turbulence model. The algebraic model is applied in the wall layer, while the k -epsilon model is solved in the outer layer up to the free surface. Preliminary attempts to test this two-layer strategy to the well-documented case of clear water over a smooth surface has revealed that numerical problems occur when the transient shear layer (between the laminar sublayer and the fully-developed turbulent outer layer) has to be resolved within the numerical domain where the k -epsilon equations are solved. A practical solution to overcome this problem is under investigation.

The results of this research provide new tools to better analyse and understand the energy consumption over the vertical of sediment-laden flows, and is applicable to both cohesive and non-cohesive sediments.

Acknowledgement

This work is part of the internal fundamental research program and has been carried out in the framework of (a.o.) the BRAIN.be project INID67, funded by the Belgian Science Policy Office (BELSPO contract no. BR/143/A2/INDI67).

References

- Baas, J.H., Best, J.L., Peakall, J., Wang, M. (2009). A phase diagram for turbulent, transitional and laminar clay suspension flows *J. Sedimentary Research* 79: 162-183.
- Reichardt, H. (1951). Vollständige Darstellung der turbulenten Geschwindigkeitsverteilung in glatten Leitungen. *Zeitschrift für Angewandte Mathematik und Mechanik*, 31(7), 208-219.
- Toorman, E.A., Liste, M., Heredia, M., Rocabado, I., Vanlede, J., Delefortrie, G., Verwaest, T., Mostaert, F. (2014). CFD Nautical Bottom: Subreport 1: Rheology of Fluid Mud and its Modeling. Version 3_0. WL Rapporten, 00_048. Flanders Hydraulics Research, KU Leuven Hydraulics Laboratory & Antea Group: Antwerp, Belgium.
- Van Driest, E.R. (1956). On turbulent flow near a wall. *J. Aeronautical Science*, 23:1007-1011+1136.

Sediment measures during dredging operations near Montevideo's coast

Rodrigo Mosquera¹, Teresa Sastre², Juliane Castro Carneiro³, Pablo Santoro¹ and Francisco Pedocchi¹

¹ Instituto de Mecánica de los Fluidos e Ingeniería Ambiental, Facultad de Ingeniería, Universidad de la República, PC 11300, Julio Herrera y Reissig 565, Montevideo, Uruguay
E-mail: rmosquer@fing.edu.uy

² Gas Sayago S.A., PC 11200, La Cumparsita 1373, Montevideo, Uruguay

³ Laboratório de Dinâmica de Sedimentos Coesivos, Área de Engenharia Costeira & Oceanográfica, Universidade Federal do Rio de Janeiro, Rio de Janeiro, Brasil

Abstract

This work describes some recent cohesive sediment measurements we performed in front of the Montevideo's coast. The objective of the study was to understand the mechanisms of sediment transport during dredging operations in the area. Sediment concentration profiles were acquired with a turbidimeter and a densimeter, while currents were measured with ADCP, and temperature and salinity profiles were obtained using a CTD. Measurements revealed the existence of a 4 m thick layer with a sediment concentration of 1 kg/m³ laying above a 2 m thick layer with significantly higher concentration of 240 kg/m³. Both layers showed able to behave as fluid mud and to flow near the bed inside the dredged area.

Introduction

The Río de la Plata is a binational, Argentinian and Uruguayan, waterbody that behaves as a large estuary of nearly 300 km long and a width that varies from 30 to 220km covering an area of 3.2×10⁶km² and less than 10 m depth. It has a mean Suspended Sediment Concentration (SSC) of 0.1kg/m³ being mostly clay (Fossati et al., 2014). Previous works in the Río de la Plata showed that in the navigation channels in front of Montevideo, even during calm conditions, there is a transition of a few decimetres from the river SSC to a dense bed material with a density larger than 1300kg/m³ (Groposo et al., 2015).

The implantation of a new offshore Liquefied Natural Gas terminal at 2.5 km from Montevideo's coast involves dredging operation involving the removal and disposal of large quantities of cohesive sediment material. Sediment concentrations generated during dredging works, particularly near the bed, were unknown and an important concern for the environmental and operational aspects of the project.

Methodology and results

A three day measuring campaign was carried on a 13m long and 4.2m beam ship while dredging operations were going on. Velocities were measured with a Teledyne RDI RiverRay, 600 kHz Acoustic Doppler Current Profiler (ADCP) attached with a Global Positioning System (GPS). The Suspended Solid Concentration (SSC) was measured using an Campbell Scientific Inc., Optical Backscatter Sensor, OBS3+, attached to a SeaBird, SBE 19plus V2, Conductivity-Temperature-Depth profiler (CTD). The high concentrated mud layers were measured using a STEMA Survey Systems, tuning fork densimeter, DensiTune. The depth outside the dredged area was 6.5m, with maximum currents of 0.7m/s and a salinity varying from 2 to 9 psu. The dredged area had an extension of 0.25km², 13m depth, with maximum currents of 0.4m/s and the same salinity range than its surroundings.

During the three day campaign measurements focused in capturing the sediment layer generated by the dredge suction arm. Due to security reasons, it was not possible to stay in the dredging area at the same time as the dredge was operating. Therefore, measurements were performed just after the dredge left the area for the damping zone, located 18km away from the dredging area. Once the dredge was gone, the surveying vessel would slowly navigate to the place where the dredge has been working, constantly taking SSC profiles. As the vessel arrived to the last place where the dredge was operating the captain will keep the ship steady with the engines on, and the team will proceed to take several profiles over time in order to observe the dissipation of the soft mud layer. As the tide cycle went on, and currents shifted directions, measurements were performed coming both from upwind and downwind from the dredging area.

Once the field work was finished, the calibration of the instruments in the laboratory was performed. Both the OBS3+ and the DensiTune were calibrated using to different sediment and water mixtures extracted from the study area on the previous days. Particularly care was taken to calibrate the

DensiTune using undiluted high concentrated samples, as it was observed that dilution of the samples particularly affects the calibration process (Groposo et al. 2015).

The calibrated SSC profiles are presented in Fig. 1 . It shows three layers that according to their concentration can be classified as fluid mud. The deepest one, closest to the bed, was a 2m thick mud layer with a density of 1150kg/m³ (equivalent to 240kg/m³ concentration), which looked and flowed like if it was crude oil. The middle layer was a 4 m thick layer with a density of 1010 kg/m³ (equivalent to 1kg/m³ concentration). This intimate layer looked and flowed like dirty water, with not easily noticeable rheology. The top layer, and the thickest one, was a 7m thick layer with a concentration of 0.1kg/m³ and density very close to the clear water.

The sediment flux out of the dredged area during the measuring campaign was limited, and a 1 m thick layer with a SSC of 1kg/m³ was recorded at the edge of the dredging zone in the down current direction.

Conclusions

The presented results together with previous measuring campaigns in front of the Montevideo coast helped to have a deeper understanding of the sediment transport mechanisms during dredging works. Of the three observed layers only the two top ones that have SSC below 1 kg/m³ were able to be transported by currents out of the dredging depression. On the other hand, the lower and higher concentration layer was probably able to form a gravity current and flow into the lower parts of the dredging pit. The reduction of the currents and the characteristics of this layer made unfeasible for it to escape out of the dredged area.

As these measurements were performed after the dredging pit was 6.5 m deep, it reminds unknown if the high concentrated layer would form if no depression was present to protect the dredging plume generated by the cutting head from the currents.

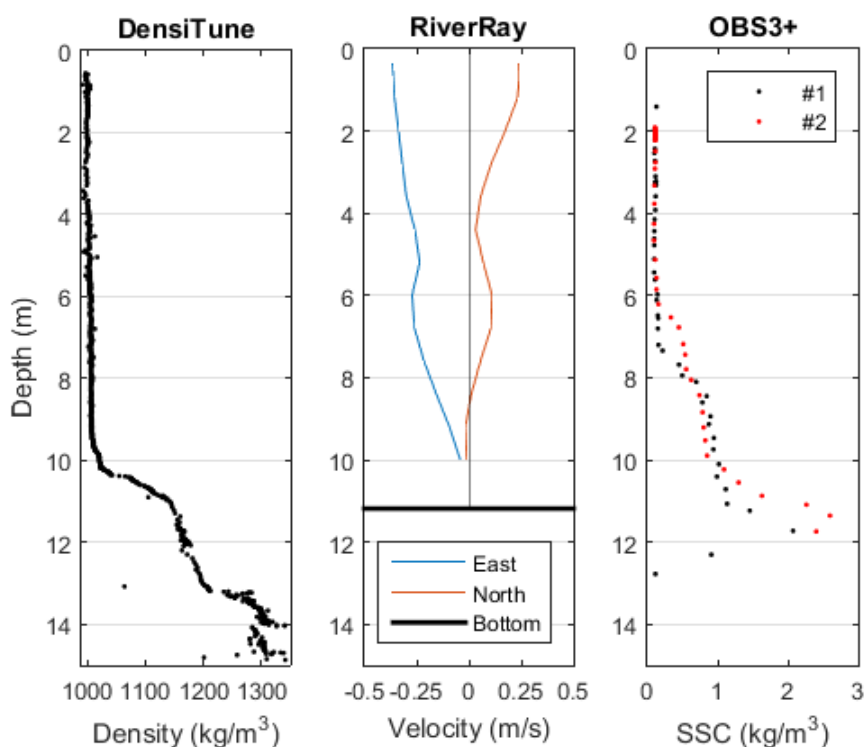


Fig. 1 Profiles of the different instruments in the dredged area.

References

- Groposo V., Mosquera R. Pedocchi F., Vinzón S. and Gallo M. (2015). Mud density prospection using a Turnin Fork, *Journal of Waterway, Port, Coastal, and Ocean Engineering*, ASCE, 141(5) 1-7.
- Fossati M., Cayocca F. and Piedra-Cueva I. (2014). Fine sediment dynamics in the Río de la Plata. *Advances in Geosciences*, 39, 75-80.

Observations of the settling velocity of fine sediment associated with deep sea mining of Fe–Mn crusts

Spearman J¹, Manning A^{1 2 3 4 5}, Crossouard N¹ and Taylor J¹

¹ HR Wallingford

Howbery Park, Wallingford, Oxfordshire, OX10 8BA, UK

² University of Hull, Hull, HU6 7RX, U.

³ Center for Applied Coastal Research, Civil and Environmental Engineering, University of Delaware
Newark, DE 19716, USA

⁴ Engineering School of Sustainable Infrastructure & Environment (ESSIE), 365 Weil Hall,
University of Florida, Gainesville FL 32611, USA

⁵ University of Plymouth

Drake Circus, Plymouth, Devon, PL4 8AA, UK

Abstract

The pressure on resources of rare earth minerals, together with improvements in technology, is leading to increased interest in the mining of deeper waters for polymetallic nodules/crusts and massive sulphides. This increased interest has generated concern about the potential environmental consequences of large scale deep-sea mining and contributing to this concern is the lack of knowledge regarding the behaviour of mine tailings plumes which are likely to arise from such operations. This paper describes some of the ongoing studies associated with the MarineE–tech project into the potential for mining Fe–Mn crusts regarding the flocculation properties of fine sediment associated with the over-burden and crust material that is likely to be disturbed during mining activities. The consequences of the results of the settling velocity measurements for the behaviour of mining plumes are discussed.

Introduction

The pressure on resources of rare earth minerals, together with improvements in technology, is leading to increased interest in the mining of deeper waters for polymetallic nodules/crusts and massive sulphides. As well as raising expectations regarding its viability, this increased interest has generated concern about the potential environmental consequences of large scale deep-sea mining (e.g. Wedding et al, 2015). Contributing to this concern is the lack of knowledge regarding the behaviour of mine tailings plumes which are likely to arise from such operations (Spearman et al, 2016).

The MarineE–tech Project

This paper describes some of the ongoing studies associated with the MarineE–tech project into the potential for mining Fe–Mn crusts. These crusts are particularly rich in elements which are critical for the production of new technologies including clean energy applications. These crusts occur at the interface between the oxygen minimum zone and oxygenated deep-water and so are strongly associated with seamounts. Seamounts in turn are characterised by hydrodynamic features which hinder the mixing of water immediately around the seamount with that of the surrounding ocean and so they can have sensitive and unique ecologies. The MarineE–tech research project concerns all aspects of mining for Fe–Mn crusts but the present paper focuses on the flocculation properties of fine sediment associated with the over-burden and crust material that is likely to be disturbed during mining activities.

Methodology

Laboratory studies are presented measuring the settling properties of samples of Fe–Mn crust and sandy overburden (see Figure below) collected from the Tropic Seamount in the North Eastern Atlantic by the RS James Cook during November and December of 2016. The settling velocity properties of a range of floc and particle sizes, are investigated using the Labs–Floc system developed by Manning (2006). The consequences of the results of the settling velocity measurements for the consequent behaviour of mining plumes are discussed.

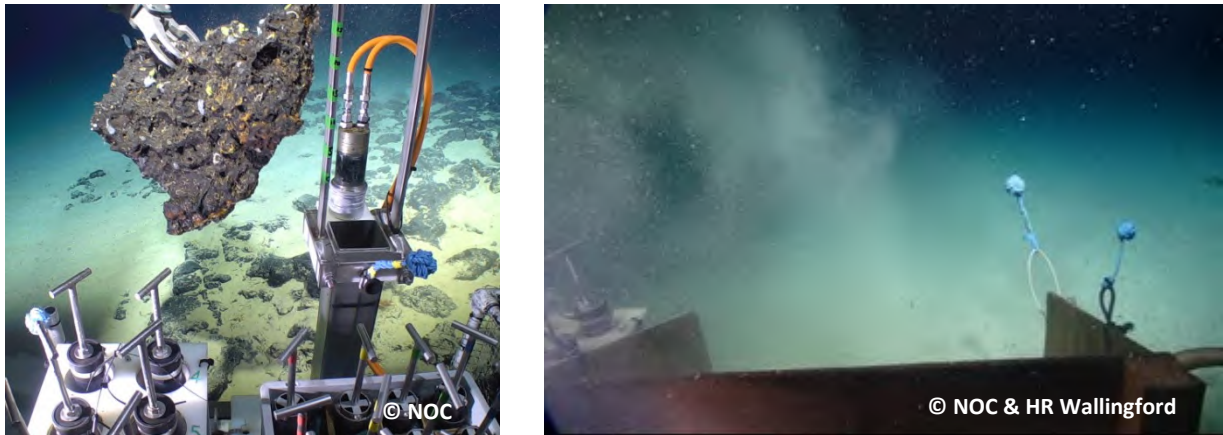


Figure: (*left*) collected sample of a crust pavement. (*right*) sediment plume generated by the ROV.

Manning A J (2006) LabSFLOC – A laboratory system to determine the spectral characteristics of flocculating cohesive sediments. HR Wallingford Technical Report TR 156, 2006.

Spearman J, Lee M, Matthewson T and Newell R (2016) Insights and future research into the impacts of deep sea mining, Proceedings of the World Dredging Congress (WODCON) XXI, Miami, June 13–16, 2016.

Wedding, L.M., Reiter, S.M., Smith, C.R., Gjerde, K.M., Kittinger J.N., Friedlander, A.M., Gaines, S.D., Clark, M.R., Thurnherr, A.M., Hardy, S.M., Crowder, L.B. (2015). “Managing mining of the deep seabed”, *Science*, Vol. 349, no. 6244, 144–145.

Implementation of a high resolution 3D wave-current-sediment transport model for the Río de la Plata and Montevideo Bay

Santoro Pablo¹, Fossati Mónica¹, Tassi Pablo², Huybrechts Nicolas³, Pham Van Bang Damien², Piedra-Cueva Ismael¹

¹ Instituto de Mecánica de los Fluidos e Ingeniería Ambiental, Universidad de la República, Herrera y Reissig 565, CP 11300 Montevideo, Uruguay
E-mail: psantoro@fing.edu

² Saint Venant Laboratory for Hydraulics, EDF R&D, 6 Quai Watier, 78400 Chatou, France

³ Sorbonne Universités, Université de Technologie de Compiègne, CNRS, UMR 7337 Roberval, LHN (joint research unit UTC-CEREMA EMF) Compiègne, France.

Introduction

The hydrodynamics and fine sediment dynamics modelling in estuarine environments is important for coastal engineering design and environmental assessment. Here we present the implementation of a 3D coupled wave-current-sediment transport model with high spatial resolution in a harbor area for a complex estuarine system. The study case is the Río de la Plata (Fig. 1a) focusing on the Montevideo Bay area. In this work we focus on some details about the numerical model implementation and sensitivity analyses especially regarding the fine sediment transport processes.

Methodology

Based on the open source TELEMAC-MASCARET Modelling System (TMS), it was possible to address the simulation of both the tidal and wave hydrodynamics, fine sediment transport and bed evolution with a single code. The modelled domain includes the Río de la Plata and its maritime front zone approximately until the 200 m depth on the continental shelf (Fig. 1a). The TMS is based on the finite elements technique and uses non-structured meshes allowing to cover big domains increasing the resolution on the areas of interest which can have complex geometries e.g. harbor areas.

The circulation module TELEMAC 3D was implemented for the selected domain taking into account the fluvial discharges of Paraná and Uruguay rivers, tides at the oceanic boundary (astronomical and meteorological from a regional model), and wind and sea level pressure from ERA-Interim ReAnalysis. For the wind surface stress an aerodynamic bulk formula is employed. The wind drag coefficient was selected as a calibration parameter. The turbulence model is k-epsilon.

The third generation spectral wave module TOMAWAC is forced with 10m wind from the ERA-Interim Reanalysis. At the oceanic boundary the model is forced by wave statistics from a regional model. The model was configured to take into account the following processes: white capping, bottom friction, depth breaking, and quadruplets interactions.

The sediment transport module SEDI3D considers only one cohesive sediment class. The mean annual SSC is imposed at the two sections corresponding to Uruguay and Paraná. The bed is assumed to be uniform over the domain, however areas where non-cohesive sediments are predominant were set as non-erodables. In order to compute the erosion and deposition fluxes the classical Krone and Partheniades laws were applied. The parameters to be defined in the sediment transport module are the settling velocity (W_s), the Partheniades coefficient (M), and both the critical shear stress for deposition and erosion (τ_{cd} , τ_{ce}). The settling velocity is dependent on the SSC through a linear relationship. The consolidation process was not taken into account.

It was performed a sensitivity analysis to the number of vertical layers, in which we used 10, 16, 20, 30 sigma levels equally spaced along the vertical. Then, it was analyzed the sensitivity of the model results to the wind drag coefficient, and also to the sediment transport model parameters. The latter is divided in two based on the sediment exchange paradigm, exclusive versus simultaneous erosion-deposition paradigms (Ha and Maa, 2009). These two approaches are very different, and so it is the behavior of the model results. For each paradigm it is analyzed the sensitivity to the settling velocity, the Partheniades coefficient, and both the critical shear stress for deposition and erosion.

Results & Conclusions

Regarding the number of vertical layers analysis, we conclude that the number of vertical layers does not have an appreciable effect on the sea surface elevation behavior, and minor differences are observed on the currents and salinity results. Using more than 16 layers produce very similar results. Taking as reference the computation with 10 layers, then the computation time taken by the

simulation with 15 layers was approximately 20% higher, the simulation with 20 layers approximately 55% higher and with 30 layers 360% higher. In this way it was decided to use 16 sigma levels.

A sensitivity analysis to the wind drag coefficient showed that it has a significant impact on the model results. It has a noticeable impact on the SSE especially during the storm surge events. The effect on the currents and salinity distribution are linked and also influenced by the vertical mixing. Higher wind drag coefficient values leads to a location of the salinity front further inside the estuary and less vertical stratification.

We evaluated the sensitivity to the sediment module parameters under two different erosion-deposition paradigms. Using the exclusive erosion-deposition paradigm (EED) high values of settling velocity are needed in order to reproduce observed SSC behavior after the storm events. This leads to low base values for the SSC in calm conditions, which can be compensated by increasing the Partheniades coefficient or decreasing the critical shear stress for erosion threshold. All these actions tends to increase the bottom SSC, which was far too high in all the tested configurations. This was the main problem found with this paradigm, the maximum bottom SSC during storm events were out of the hypothesis of the present model. Increasing the critical shear stress threshold for deposition would help to decrease the high bottom SSC values, however it implies also increasing the critical shear stress for erosion which will not allow us to represent the base SSC values in calm conditions. It was not possible to find a combination of parameters representing properly the general dynamics of the suspended sediment dynamics of the estuary keeping the SSC values under the range of applicability of the present model.

On the other hand with the simultaneous erosion-deposition paradigm (SED) it was possible to find several set of parameters capturing some of the main characteristics of the fine sediment dynamics in the estuary. The Partheniades coefficient showed to have an interesting effect on the SSC signal related to the astronomical tide (Fig. 1d). Different combinations of parameters can give similar SSC results, having however different results on the navigation channel siltation (Fig. 1c). Based on this sensitivity analysis the simultaneous erosion-deposition paradigm was adopted.

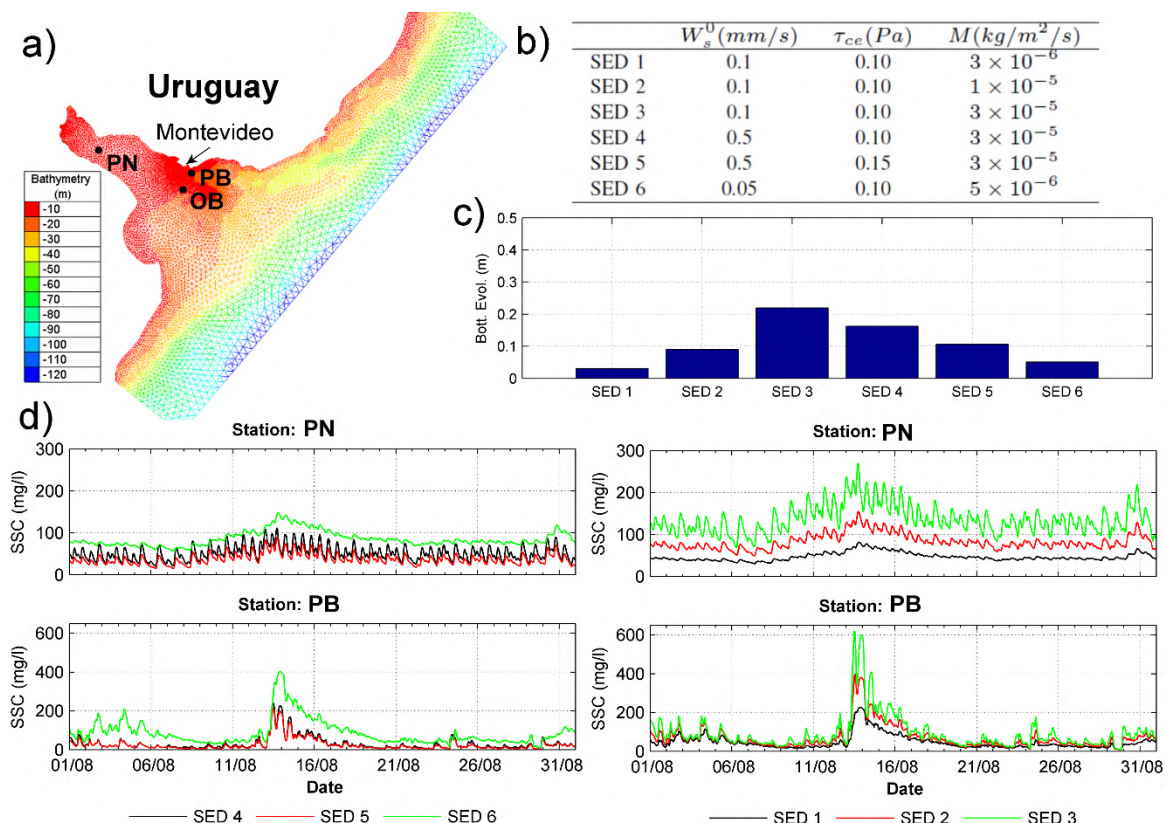


Fig. 1 (a) Río de la Plata mesh and bathymetry, (b) sediment transport module parameters employed in the simultaneous erosion-deposition paradigm simulations (c) bottom evolution at the Montevideo Bay access navigation channel after two months of simulation. (d) Simulated suspended sediment concentration (SSC) at station PN and PB during August 2010.

References

H. Ha and J.-Y. Maa (2009). Evaluation of two conflicting paradigms for cohesive sediment deposition. *Marine Geology*, 265 (3-4): 120-129.

Temporal and spatial changes in floc fraction on a macro-tidal channel-flat complex: Results from Kingsport, Nova Scotia, Bay of Fundy.

B.A. Law^{1,2}, P.S. Hill², T.G. Milligan¹, V. Zions¹

- 1 Fisheries and Oceans Canada, Bedford Institute of Oceanography, Dartmouth, Nova Scotia, Canada, B2Y 4A2, Email: Brent.Law@dfo-mpo.gc.ca
- 2 Department of Oceanography, Dalhousie University, Halifax, Nova Scotia, Canada, B3H 4R2

Abstract

In April 2012, a study was initiated to examine the seasonal change in grain size on a muddy macro-tidal flat and channel complex in Kingsport, N.S., Canada. Surficial sediment samples were collected for disaggregated inorganic grain size (DIGS) analysis every month for 1 year from a tidal flat and from a tidal channel and its banks. The monthly sampling was completed in March 2013. DIGS analysis was used to estimate floc fraction, which is defined as the fraction of the sediment in the seabed that was deposited in flocs. Seasonally, floc fraction was correlated with elevation on the tidal flats, but the sign of the correlation changed. In summer, larger floc fractions were measured lower on the flats, and during winter larger floc fractions were measured at higher elevations. Seasonal changes in wave stress on the tidal flats explain the seasonal change in distribution of floc fractions on the flats.

Introduction

The deposition, transport, and erosion of fine sediment is affected fundamentally by aggregation (McCave, 1984, Kranck and Milligan, 1991). Aggregation is the process whereby particles clump, either by electrochemical attraction or organic bonding, to form “aggregates” or “flocs”. Aggregates sink much faster than the component particles within them (Sternberg et al., 1999). Therefore, settling within aggregates is responsible for the majority of deposition of fine-cohesive sediments (Kranck, 1980, McCave et al., 1995, Curran et al., 2002).

A process-based parameterization of DIGS can be used to quantify the spatial or temporal changes in flocculation in the overlying water column that were responsible for the changes in the texture of fine-grained bottom sediments (Christiansen et al., 2000; Curran et al., 2004; Milligan et al., 2007; Law et al., 2013). On a mesotidal mudflat in Willapa Bay, Washington, Law et al. (2013) showed that the largest floc fractions were found in tidal channels and on channel banks, which were areas of lower elevation. The goal of this research is to apply the process-based parameterization of DIGS to develop an integrated, regional understanding of the role of flocculation in determining the spatial and temporal variations of grain size for mixed-grain-size beds on a muddy, macro-tidal flat in the upper Bay of Fundy.

Methods (Grain-Size Analysis)

The disaggregated inorganic grain size (DIGS) distributions of bottom sediment samples were determined using a Coulter Multisizer III. The DIGS obtained from the Multisizer are expressed as log of equivalent volume fraction versus log of the diameter. Volume fraction is assumed to equal mass fraction, which implies constant particle density across all sizes. For a complete description of the methods, see Kranck and Milligan (1979) and Milligan and Kranck (1991).

Results and Discussion

Floc fraction did not correlate with elevation in the tidal channels in either July or March (Fig 1a & b). In contrast, statistically significant correlations between floc fraction and elevation were evident in July and March, but the sign of the correlations was opposite. In July larger floc fractions were measured at lower elevations on the flats, and in March larger floc fractions were measured at higher elevations on the flats (Fig. 1a & b). The trend of higher floc fraction values at the lower tidal-flat elevations in July also held for August and September, and the trend in March 2013 was also similar in January, February and April. No correlation between floc fraction and elevation was measured in the transition periods of May-June and October-December.

Changes in wave-induced bottom stress likely were responsible for the seasonal change in the correlation between floc fraction and tidal-flat elevation. In late winter and early spring, waves were larger. Following the reasoning of Fagherazzi et al. (2007), larger waves eroded the seabed on deeper parts of the flat and prevented accumulation of sediment there. Flocculated sediment accumulated higher on the tidal flats where small water depths were associated with low wave stresses. In summer, smaller waves did not produce erosive stresses on the deeper parts of the flats, so flocculated sediment accumulated there.

Accumulation of sediment at lower elevations produced lower suspended sediment concentrations higher on the flats. Lower concentrations caused lower floc fractions in the sediment.

In a study by Law et al. (2013) on the muddy meso-tidal channels and flats of Willapa Bay, Washington, USA, floc fraction was inversely correlated with elevation throughout the year. Interestingly, seasonal changes in the wind direction reduced wind fetch in winter, when wind speeds were higher. As a result, seasonal changes in wave stress were minimal. Lack of seasonal variation in wave stresses likely explains the lack of a seasonal change in the relationship between floc fraction and tidal-flat elevation.

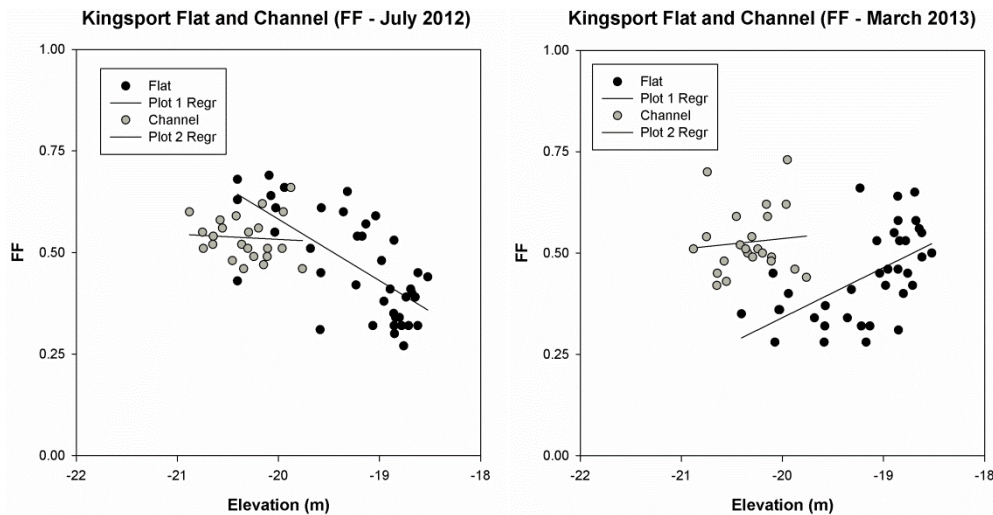


Fig 1(a & b). Floc Fraction (FF) values versus elevation for tidal channel and flat samples from left, July 2012 and right, March 2013.

References

- Christiansen, T., Wiberg, P.L., Milligan, T.G., 2000. Flow and sediment transport on a tidal salt marsh surface. *Estuarine Coastal and Shelf Science* 50, 315-331.
- Curran, K.J., Hill, P.S., Milligan, T.G., 2002. Fine-grained suspended sediment Dynamics in the Eel river flood plume. *Continental Shelf Research* 22, 2537-2550.
- Curran, K.J., Hill, P.S., Schell, T.M., Milligan, T.G. and Piper, D.J.W. 2004. Inferring the mass fraction of floc-deposited mud: application to fine-grained turbidites. *Sedimentology*, 51: 927-944.
- Fagherazzi, S., Palermo, C., Rulli, M. C., Carniello, L. and Defina, A. 2007. Wind waves in shallow microtidal basins and the dynamic equilibrium of tidal flats. *Journal of Geophysical Research*, 112, doi:10.1029/2006JF000572
- Kranck, K., Milligan, T.G., 1979. The use of Coulter Counters in Studies of Particle Size Distributions in aquatic Environments. Report Series/ BI-R-79-7/November, 1979: ii+48p.
- Kranck, K., 1980. Experiments on the significance of flocculation in the settling of fine-grained sediment in still water. *Canadian Journal of Earth Sciences* 17, 1517-1526.
- Kranck, K. and Milligan, T.G. 1991. Grain size in oceanography. In Syvitski, J.P.M.(ed) *Principles, Methods and Application of Particle Size Analysis*, Cambridge University Press, New York, 322-345.
- Law, B.A., Milligan, T.G., Hill, P.S., Newgard, N., Wheatcroft, R.A., Wiberg, P.L., 2013. Flocculation on a muddy intertidal flat in Willapa Bay, Washington, Part I: A regional survey of the grain size of surficial sediments. *Continental Shelf Research*, 60(S), S136 - S144.
- McCave, I.N., 1984. Size spectra and aggregation of suspended particles in the deep ocean. *Deep Sea Research* 31, 329-352.
- McCave, I.N., Manighetti, B., Robinson, S.G., 1995. Sortable silt and fine sediment size/composition slicing: parameters for palaeocurrent speed and palaeoceanography. *Palaeoceanography*, 10(3), 593-610.
- Milligan, T.G., Kranck, K., 1991. Electroresistance particle size analyzers. In: Syvitski, J.P.M. (Ed.), *Principles, Methods, and Application of Particle Size Analysis*. Cambridge University Press, New York, pp. 109-118.
- Milligan, T.G., Hill, P.S. and Law, B.A. 2007. Flocculation and the loss of sediment from the Po River plume. *Continental Shelf Research*, 27: 309-321.
- Sternberg, R.W., Berhane, I., Ogston, A.S., 1999. Measurement of size and settling velocity of suspended aggregates on the Northern California continental shelf. *Marine Geology*, 154, 43-54.

Biological-Physical Interactions In Fine Sediment Environments

Lawrence P. Sanford¹

¹ University of Maryland Center for Environmental Science, Horn Point Laboratory, PO Box 775, Cambridge, Maryland, USA, lsanford@umces.edu

Introduction

In many natural aquatic environments, physical processes control the conditions under which biological systems function, but biological systems exert little return influence on physical processes. Several important exceptions to this rule are found in shallow water environments with fine or mixed bottom sediments. This paper briefly reviews biological-physical interactions in four such environments: tidal marshes, mud flats, underwater grass beds, and underwater filter feeding communities. It explores general themes and identifies common features. It then examines two of these environments, underwater grass beds and bivalve reefs, in greater detail, with examples from recent research in Chesapeake Bay (CB), USA. The perspective adopted is that of a coastal engineer seeking to understand and parameterize important biological influences for sediment transport and morphological modelling.

A general feature of these benthic environments is a threshold of physical disturbance and/or light extinction beyond which no stable benthic ecosystem can exist. Beyond these thresholds either the bottom sediments are disturbed to such an extent that no organisms can become established (Schaffner et al. 2001), or suspended sediment concentrations are so high that benthic primary production is severely limited (Lawson et al. 2007). When local suspended sediment concentrations are maintained by bottom sediment resuspension, these conditions are strongly linked.

Another general feature of these environments is that the threshold between physical and biological dominance may be modified by the environmental history of a site. Thus, for example, a period of relative calm accompanied by favorable conditions for re-establishment of a healthy benthic ecosystem may result in a switch from physical to biological dominance that is maintained by positive feedbacks between the benthos and sediment stability (Gurbisz and Kemp 2014). Positive feedbacks on either side of the threshold can result in significant system hysteresis and/or sudden state changes, or “tipping points” (Van de Koppel et al. 2004, Jordan-Cooley et al. 2011). Marsh grasses, mud flat communities, underwater grasses, and reef-building benthic communities have been described as ecosystem engineers because they use these positive feedbacks to enhance and stabilize their environments.

Underwater Grass Beds

Underwater grass beds, also known as Submerged Aquatic Vegetation (SAV) beds, are an important example of ecosystems with light-based positive feedbacks. The largest SAV bed in CB, the Susquehanna Flats (SF) at the head of the Bay, was destroyed in the mid-1970s by a combination of worsening water quality and a major storm (Gurbisz and Kemp 2014)]. In other words, it crossed a threshold to become a turbid, physically dominated system. This situation was suddenly reversed in the mid-2000s when a combination of improving water quality and three years of favorable growing conditions resulted in the sudden, robust return of the SF SAV bed.

We carried out a series of sediment transport studies in the SF SAV bed to examine changes in fine sediment transport due to the presence of the grasses. The data provide a glimpse of the processes that control sediment delivery, retention, and bypassing near the SF. Our results indicate that the seasonal influence of the SF SAV bed dominates fine sediment transport dynamics. While the shallow depths of the flats tend to focus flow and sediment fluxes into adjacent navigation channels even without SAV, seasonal increases in SAV abundance greatly reinforce this pattern. By late summer, both fine sediment erodibility and water column turbidity are significantly lower inside the bed than outside. The SAV bed also increases sediment retention, most likely due to dissipation of wave and current forcing. The most dramatic example of increased retention was during a high flow event after a tropical storm in 2011, when large amounts of fine sediment were deposited in the beds (Gurbisz et al. 2015). Late spring turbidity levels did not return to normal until the 3rd year after the storm. ⁷Be distributions in the surface sediments of the bed also indicated enhanced sediment retention during the growing season. An idealized flow and sediment transport model of the SF system helps to explain and expand on these observational results.

Bivalve Reefs

Reef-building species such as corals, mussels, and oysters promote access to suspended food resources by increasing their elevation and promoting near-bottom mixing. In fine sediment environments, bivalves also promote water clarity through filtration and rapid biodeposition of

suspended solids (Newell et al. 2005). Like SAV beds, an important part of increased net deposition is likely due to sheltering of fine sediment deposits by the macro-roughness of the reef structure (Pomeroy et al. 2017). This may be parameterized in models by allowing for an increase in overall drag due to macro-roughness, but a decrease in skin friction due to sheltering in the pore spaces of the reef. Exposed shell surface also is swept clean by the increased turbulence, which allows for increased settlement of larvae and faster reef growth (Kennedy and Sanford 1999, Jordan-Cooley et al. 2011). This positive feedback, if allowed to progress, results in reefs that are only limited by water depth and access to suspended food resources. It is thought that extensive oyster reefs in CB prior to European settlement were at least partially responsible for high water clarity and the dominance of benthic primary productivity, a radically different but equally stable ecosystem state compared to the poor water clarity and planktonic dominance of the present estuary (Newell 1988). Preliminary results of a simple numerical model of interactions between fine sediment transport and oyster reefs will be presented and compared to recently collected data over a restored reef in a tributary of the CB for model-data comparison.

Discussion

The examples presented in this paper have emphasized benthic biological-physical interactions that result in stabilization of the benthos and reductions in fine sediment transport. Many studies, however, have identified benthic biological-physical interactions that destabilize bottom sediments and promote enhanced fine sediment suspension, often through bioturbation (Grant and Daborn 1994). There are several characteristics that are common to both stabilizing and destabilizing interactions. First, sufficient densities of benthic organisms can significantly affect fine sediment dynamics, and if present should be accounted for in simulation models. Though many details remain to be explored, biological effects often can be accounted for by modifications of bottom roughness, modification of sediment stability, and changes in particle settling velocity. Second, many successful aquatic benthic populations have evolved to modify their physical environments to their own advantage through positive feedbacks on sediment transport processes. These feedbacks should also be accounted for in long-term simulations. Often the population change rates are sufficiently slower than changes in physical forcing that a separation of time scales is justifiable, treating ecosystem status as a series of quasi-equilibrium states rather than continuously varying dynamical states.

References

- Grant, J. and G. Daborn (1994). "The effects of bioturbation on sediment transport on an intertidal mudflat." Netherlands Journal of Sea Research 32(1): 63-72.
- Gurbisz, C. and W. M. Kemp (2014). "Unexpected resurgence of a large submersed plant bed in Chesapeake Bay: Analysis of time series data." Limnology and Oceanography 59(2): 482-494.
- Gurbisz, C., W. M. Kemp, L. P. Sanford and R. J. Orth (2016). "Mechanisms of Storm-Related Loss and Resilience in a Large Submersed Plant Bed." Estuaries and Coasts 39(4): 951-966.
- Jordan-Cooley, W. C., R. N. Lipcius, L. B. Shaw, J. Shen and J. Shi (2011). "Bistability in a differential equation model of oyster reef height and sediment accumulation." Journal of Theoretical Biology 289: 1-11.
- Kennedy, V. S. and L. P. Sanford (1999). Characteristics of Relatively Unexploited Beds of the Eastern Oyster, *Crassostrea virginica*, and Early Restoration Programs. Oyster Reef Habitat Restoration: A Synopsis and Synthesis of Approaches. M. W. Luckenbach, R. Mann and J. A. Wesson. Williamsburg, Virginia, Virginia Institute of Marine Science: 25-46.
- Lawson, S. E., P. L. Wiberg, K. J. McGlathery and D. C. Fugate (2007). "Wind-driven Sediment Suspension Controls Light Availability in a Shallow Coastal Lagoon." Estuaries and Coasts 30(1): 102-112.
- Newell, R. (1988). Ecological Changes in Chesapeake Bay: Are they the Result of Overharvesting the American Oyster, *Crassostrea virginica*? Understanding the Estuary: Advances in Chesapeake Bay Research. M. P. Lynch and E. C. Krome. Solomons, Maryland, Chesapeake Research Consortium: 536-546.
- Newell, R. I. E., T. R. Fisher, R. R. Holyoke and J. C. Cornwell (2005). Influence of eastern oysters on nitrogen and phosphorus regeneration in Chesapeake Bay, USA. The Comparative Roles of Suspension Feeders In Ecosystems. Netherlands, Springer. 47: 93-120.
- Pomeroy, A. W. M., R. J. Lowe, M. Ghisalberti, C. Storlazzi, G. Symonds and D. Roelvink (2017). "Sediment transport in the presence of large reef bottom roughness." Journal of Geophysical Research: Oceans 122(2): 1347-1368.
- Schaffner, L. C., T. M. Dellapenna, E. K. Hinchey, C. T. Friedrichs, M. T. Neubauer, M. E. Smith and S. A. Kuehl (2001). "Physical energy regimes, seabed dynamics and organism-sediment interactions along an estuarine gradient." Organism-sediment interactions: 159-179.
- Van de Koppel, J., P. M. J. Herman, P. Thoolen and C. H. R. Heip (2001). "DO ALTERNATE STABLE STATES OCCUR IN NATURAL ECOSYSTEMS? EVIDENCE FROM A TIDAL FLAT." Ecological Society of America 82(12): 3449-3461.

Analytical model for the prediction of sedimentation rates in Montevideo navigation channels

Francisco Pedocchi¹, Sebastián Solari¹, and Mónica Fossati¹

¹ Instituto de Mecánica de los Fluidos e Ingeniería Ambiental, Facultad de Ingeniería, Universidad de la República, Julio Herrera y Reissig 565, CP 11300, Montevideo, Uruguay
E-mail: kiko@fing.edu.uy

Abstract

An analytical model for the prediction of the cohesive sediment sedimentation rates in the navigation channels on the coast of Montevideo, Uruguay, is presented. The model assumes that most of the sediment transport takes place as a concentrated layer that forms under storm conditions and is transported near the bed by tidal and meteorological induced currents.

Introduction

The objective of this study was to provide a first approximation to the prediction of the sedimentation rates in the navigations channels that would be dredged associated with the construction of a new Natural Liquid Gas terminal in front of the coast of Montevideo, Uruguay. The information publically available about the sedimentation rates at the nearby port of Montevideo was particularly scarce. However using this information an analytical model was implemented and calibrated to simulate the cohesive sediment transport in the area. The model used information about currents and waves from numerical models already implemented and calibrated.

The cohesive sediment transport can both take place as a dilute suspension covering a large portion of the water column, as well as a high concentrated suspension layer near the bed (Bakker 2009). Previous studies in the Montevideo area (Guarga et al. 1988, Pedocchi 2015), have shown that a layer with a bulk density of 1300kg/m³, and a thickness of order 0.1m, may exist near the bed. On the other hand the highest recorded suspended sediment concentration during storm conditions is of order 1kg/m³. Considering this difference the proposed model focuses on capturing the concentrated layer behavior near the bed.

The model

The transport near the bed is represented by $\mathbf{q}_b = C\delta\mathbf{u}_b$, where \mathbf{q}_b is the sediment transport per unit width, C is the sediment concentration, δ is the layer thickness, \mathbf{u}_b is the nearbed current velocity, which is assumed proportional to the shear velocity. Assuming that both the nearbed concentration and the layer thickness are power functions of the excess shear stress, under equilibrium conditions it is proposed that

$$C\delta = K \left(\frac{\tau - \tau_e}{\tau_e} \right)^\alpha, \quad (1)$$

with τ the total bed shear stress, τ_e the critical bed shear stress for erosion, K a constant [kg/m²] units, and $\alpha=1.5$ a constant.

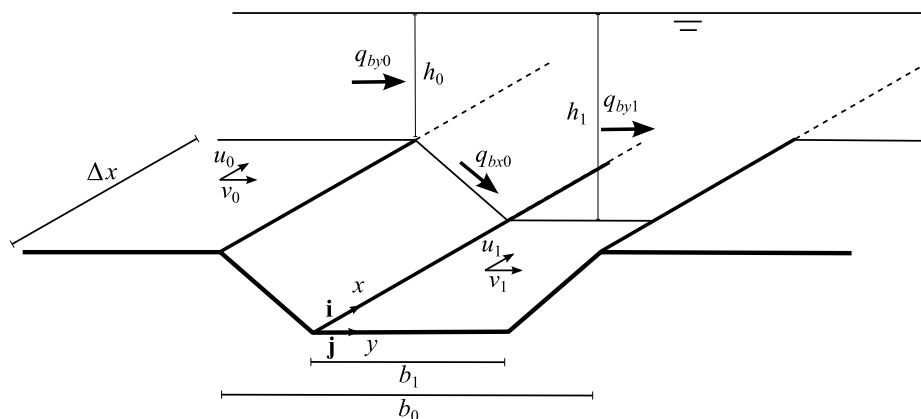


Fig. 1. Sketch of the sediment balance on a channel reach, freely based on the proposals by Rosati and Kraus (2009) and van Rijn (2013).

According to Figure 1 the cross input of sediment is controlled by the sediment transport perpendicular to the channel. The sedimentation rate S due to cross flow is given by

$$\frac{\partial S_y}{\partial t} = q_{by0} - \varepsilon q_{by1} = K_y \left[\left(\frac{\tau_0 - \tau_e}{\tau_e} \right)^\alpha v_{b0} - \varepsilon \left(\frac{\tau_1 - \tau_e}{\tau_e} \right)^\alpha v_{b1} \right], \quad (2)$$

with ε a escape factor and K_y a constant [kg/m²].

Similarly, the sedimentation rate due to the erosion of the channel banks is given by

$$\frac{\partial S_x}{\partial t} = K_x \left(\frac{\tau_1 - \tau_e}{\tau_e} \right)^{3/2\alpha} \left(\frac{h_1 - h_0}{b_0 - b_1} \right)^{1/2}, \quad (3)$$

with K_x a constant [kg/m²], and h and b as defined in Figure 1.

Implementation and results

For each reach of the navigation channel, the velocities and shear stresses inside and outside the channel were computed using a current model implemented in RMA-10 (Santoro et al. 2013), and a wave model based on SWAN. Simulated wave temporal series in intermediate waters were propagated into the coastal area using the non-linear interpolation method of Camus et al. (2011). Currents and waves series were computed for the whole year 2004, with a time resolution of 0.5hrs.

As presented in the previous section, the sediment transport analytical model had four calibration constants K_x , K_y , τ_e , and ε_b , which were calibrated with the average annual sedimentation rates available from the Montevideo Port navigation channels. The observed and predicted sedimentation volumes are presented in Table I.

Table I. Observed and predicted annual sedimentations in four reaches of the existing navigation channel, in millions of m³ a year.

Reach	1	2	3	4
Observed	2,23	1,51	1,29	0,92
Predicted	2,22	1,51	1,29	0,92

Finally, the uniqueness and stability of the set of calibration constants that was found was successfully verified using the DREAM method (DiffeREntial Evolution Adaptive Metropolis) proposed by Laloy and Vrugt (2012), which is based on the Monte Carlo simulation of Markov chains (MCMC).

Conclusions

A simple analytical model based on the assumption of the existence of a concentrated cohesive sediment layer that flows near the bed driven by currents was successfully calibrated against recorded annual sedimentation volumes. The success of the calibration supports the hypothesis of the dominance of this mechanism of cohesive sediment transport in the Montevideo area. Ongoing field measurements would bring new light into this question.

References

- Bakker, S. A. (2009). Uncertainty analysis of the mud infill prediction of the Olokola LNG terminal.
- Camus, P., Méndez, F. J., and Medina, R. (2011). A hybrid efficient method to downscale wave climate to coastal areas. *Coastal Engineering*, 58: 851–862.
- P. Santoro, M. Fossati, and I. Piedra-Cueva (2013) Characterization of Circulation Patterns in Montevideo Bay (Uruguay). *Journal of Coastal Research: Volume 29, Issue 4: pp. 819 – 835.*
- Guarga, R., Borghi, J., Vinzón, S., Piedra Cueva, I., and Kaplan, E. (1988). Control y seguimiento de los estudios hidráulicos del puerto de Montevideo efectuado por INTECSA. Technical Report, IMFIA.
- Laloy, E., and Vrugt, J. A. (2012). High-dimensional posterior exploration of hydrologic models using multiple-try DREAM (ZS) and high-performance computing. *Water Resources Research*, 48(1), 1-18.
- Pedocchi, F. and Mosquera, R. (2015). Medición de la pluma de sedimentos generada durante el dragado de apertura de la Terminal de la Planta Regasificadora. Informe final, Convenio IMFIA – Gas Sayago S.A. Montevideo, Technical Report.

Fine Sediment Dynamics in the ‘Río de la Plata’ river-estuarine-ocean system

Mónica Fossati¹, Pablo Santoro¹, Rodrigo Mosquera¹, Francisco Pedocchi¹, and Ismael Piedra-Cueva¹

¹ Instituto de Mecánica de los Fluidos e Ingeniería Ambiental, Facultad de Ingeniería, Universidad de la República, Julio Herrera y Reissig 565, CP 11300, Montevideo, Uruguay
E-mail: mfossati@fing.edu.uy

Abstract

The paper summarizes and updates the knowledge gained after more than 30 years of research on the main aspects of the fine sediment transport and dynamics in the ‘Río de la Plata’ river-estuarine-ocean system. The analysis tools include field measurements, laboratory experiments and numerical models. Due to the Río de la Plata large geographical extension, the spatial variability of tidal currents and waves is key for understanding the fine sediment dynamics. In spite of the significant progress already achieved, significant questions remain to be answered.

The Río de la Plata system

The Río de la Plata (RP) (Fig1 left panel) is one of the largest estuaries in the world, facing the Atlantic Ocean, bordering Argentina to the South and Uruguay to the North. Albeit its dimensions (280km long and 220km wide at its mouth), its water depth does not exceed 10m, while it exhibits both fluvial and estuarine characteristics. 97% of the continental water input is provided by the Paraná and Uruguay rivers with an annual mean flow of 22 000m³/s, this freshwater mixes with the oceanic water creating a large brackish water zone. Based on the morphology and dynamics of the Río de la Plata it can be divided in two main regions: inner-intermediate and outer (Fig1 left panel). These regions are separated by a shallow area located along the Punta Piedras-Montevideo line. In the inner-intermediate region no stratification is observed, and it is characterized by a fluvial regime with tidal influence. The outer region, where the estuary width increase, shows a complex flow pattern, with waters of variable salinity influenced by the river basing inflow, the tides and winds. The astronomical tidal regime is dominated by the M2 component, followed by the O1 component which is responsible for the diurnal inequality. The tidal amplitude is greater along the Argentinean coast (order of 1 m), while it is about 0.4 m along the Uruguayan coast (Santoro et al., 2013). ADCP data registered near Montevideo city show maximum tidal currents intensities of 0.3 m/s near the bottom and nearly 0.5 m/s at the surface (Fossati and Piedra-Cueva, 2013). An important particularity of the Río de la Plata is that the meteorological tide is of the same order of magnitude as the astronomical tide; meteorological tides are mainly generated in the Argentinean continental shelf and then propagate northward as coastal trapped waves until they reach the estuary (Santoro et al., 2013).

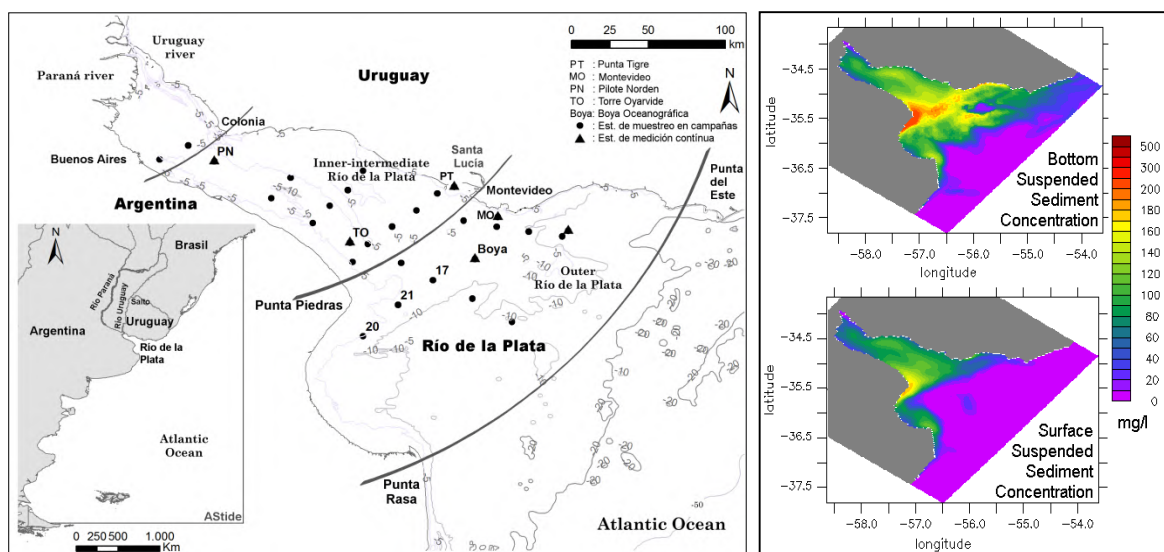


Fig. 1: Río de la Plata location and bathymetry; and measurements stations location (left panel). Numerical modeling example results: suspended sediment concentration during a storm at bottom and surface (right panel).

Measurements

The main available data were collected during the FREPLATA-IFREMER Project founded by the French Fund for the Global Environment (FFEM). The information includes hydrodynamic (temperature, salinity, water level) and turbidity time series over several months in 3 stations (PN, TO, Boya, Figure 1), current profiles and meteorological data at the Boya station. Additionally vertical CTD profiles, turbidity profiles as well as bottom samples were acquired at 26 stations during 5 campaigns spanning 13 months between 2010 and 2011 (Fig1 left panel). More recently, measurements of currents, waves, salinity and turbidity time series in Punta Tigre (PT) and Montevideo (MO) were collected. In this paper this new data is compared with the FREPLATA data project in order to improve the characterization of the Río de la Plata sediment dynamic. Also at Punta Tigre fine sediment were captured several times in a submerged box during 2-3 months. Using the turbidity data and trapped sediment volume different settling velocity laws can be adjusted. Finally, other sediment data available in the Argentinean coast were included in the data analysis (Sathicq et al, 2016).

Numerical Models

Numerical models simplify the real dynamic but allow us to include different models (equations), climate conditions (forcings), and sediments classes in order to analyze spatial and temporal variability. Two hydrodynamic and sediments models with several numerical differences were applied and validated in the RP using the same domain and forcings (fluvial discharge, astronomical and meteorological tides, winds and waves). Between 2010 and 2013 the MARS3D numerical model was implemented using a uniform grid (3 km spatial and 10 vertical sigma levels) for the whole Río de la Plata and two different sediment classes (Fig1 right panel). The TELEMAC-MASCARET Modelling System (TMS) was recently applied using finite elements (unstructured triangular meshes) with more resolution in Montevideo's coastal zone and 16 sigma vertical layers. Both models represent the suspended sediment exchange with the bed, using several parameters to represent the erosion and deposition processes. Different bed-water column sediment exchange paradigms were tested.

Results

Recently collected turbidity time series at Punta Tigre and Montevideo showed the influence of both tides and waves in turbidity variability. The same influence was already identified in the FREPLATA data (Fossati et al, 2014). Nevertheless the relative importance of each forcing showed important spatial variability along the Río de la Plata. Using the turbidity series together with the sediment captured with the sediment box installed at Punta Tigre a constant settling velocity of 0.13 mm/s was adjusted.

The recent numerical implementation using TELEMAC compared the exclusive erosion deposition and the simultaneous erosion deposition paradigms for fine sediment dynamics. Only for the simultaneous erosion deposition paradigm it was possible to find a set of model parameters that would give reasonable suspended sediment results reproducing the main characteristics of the fine sediment dynamics at the RP.

The intermediate zone constantly exhibits high turbidity levels, which increases during storms due to an increase of the resuspension. In the outer zone turbidity levels remain low during fair weather, but they also increase during storms. After the storms, the sediment is redistributed by the currents being also influenced by the salinity horizontal and vertical patterns.

Conclusions and challenges

Based on the analysis of field measurements and hydro sedimentological models we have identified different fine sediment dynamics along the different RP zones. Spatial characterization, using remote sensing and other innovative approaches, is necessary to extend the local information generated by point deployments over space. Regarding the spatial variability on circulation and sediment dynamics, with numerical models further implementations focusing on local processes and parametrization (with properly boundary conditions) appear to be a good way to improve numerical results.

References

- Fossati, M., and Piedra-Cueva, I. (2013). A 3D hydrodynamic numerical model of the Río de la Plata and Montevideo's coastal zone, *Applied Mathematical Modelling*, 37: 1310-1332..
- Fossati, M., Cayocca, F. & Piedra-Cueva, I. (2014). Fine sediment dynamics in the Río de la Plata. *Advances in Geosciences*, 39: 75-80.
- Santoro, P. E., Fossati, M., and Piedra-Cueva, I. (2013). Study of the meteorological tide in the Río de la Plata, *Continental Shelf Research*, 60: 51-63.
- Sathicq, M., Gómez, N., Bauer E., and Donadelli J. (2016). Use of phytoplankton assemblages to assess the quality of coastal waters of a transitional ecosystem: Río de la Plata estuary, *Continental Shelf Research* (In press).

Temporal and Spatial variability of the La Plata and Patos Lagoon Coastal Plumes

Paulo Victor Lisboa¹, Elisa Fernandes¹

¹ Laboratório de Oceanografia Física Costeira e Estuarina (LOCOSTE)

Universidade Federal do Rio Grande, CP 474, CEP: 96201-900, Rio Grande, Brasil

E-mail: paulovictor_fjv@hotmail.com, e.fernandes@furg.br

Introduction

The coastal zones are constantly changing due to the continuous action of winds, waves, currents, tides and river discharges (Rosa et al., 2013). Although their study started decades ago (Blanton, 1981, Zavialov et al., 1998), recent studies still aim to understand these changes, particularly in relation to the sediment transport importance in this process (Marques et al., 2009; 2010). The coastal plumes dynamics play an essential role in the sediment transport of coastal regions, bringing to the coast the continental contributions and redistributing them. This makes riverine and estuarine ecosystems protagonists, due to their importance in enriching coastal waters and consequently increasing productivity. Many estuaries and rivers have a fluvial contribution sufficiently large to perpetuate a coastal plume during long periods and distances. The greater the coastal plume density, the more complex is its interaction with the coastal waters, leading to the formation of fronts and significant horizontal density gradients throughout the depth (Lentz, 1992).

The La Plata coastal plume and its interaction with the coastal zone has been widely studied (Pimenta et al., 2005; Möller et al., 2008). Möller et al. (2008) showed that the intrusion of the La Plata coastal plume in the continental shelf is dependent on high riverine discharges (average of $23,000 \text{ m}^3\text{s}^{-1}$), being strongly modulated by the synoptic action of the wind. For the Patos Lagoon coastal plume, Marques et al. (2009; 2010) studied the physical forcing controlling its dynamics and verified that the interaction of the Patos Lagoon coastal plume with the Coastal Current is controlled by a dominant mode variability associated with a transport towards the south, combined with the effect of river discharge in the region. Although previous studies focused on understanding the physical forcing controlling both plumes, a detailed temporal and spatial variability analysis of the La Plata and Patos Lagoon coastal plumes was not carried out yet. Thus, this is the main objective of this study.

Methodology

The TELEMAC system, developed by the *Laboratoire National d'Hydraulique et Environnement of the Company Electricité de France*, was used for the numerical simulation. The TELEMAC-3D model solves the Navier-Stokes equations by considering local variation on the fluid free surface, ignoring density variations in the mass conservation equation, and considering the hydrostatic pressure and Boussinesq approximations to solve the equations (Hervouet, 2007). The model is based on the characteristic methods and finite-element technique to solve the equations. The suspended sediment concentration was considered as an active tracer for the initial condition, and together with salinity and temperature, can influence the density field fluctuations. Sediment transport rates were calculated based on the classical semi-empirical concepts, which involve the decomposition of sediment transport rates into bed-load and suspended load. The resulting bed evolution is then computed by solving the Exner equation. The model is applicable to cohesive sediment, composed of either uniform grains or multi-grains, characterized by their mean size and density (Villaret et al., 2013). To represent the cohesive effects on sediment transportation, the settling velocity was calculated as a function of the sediment concentration, temperature, salinity, and velocity gradient according to Van Leussen (1994).

The initial and boundary conditions applied to the simulations follow Figure 1. Salinity, temperature and velocity fields were obtained from the HYCOM Project (<https://hycom.org>). Time series of river discharge for the La Plata River and Patos Lagoon main tributaries were prescribed at the continental boundaries. The suspended sediment concentration at the continental boundaries were considered constant. The tidal influence was established at each

nodal point of the oceanic boundary using the amplitude and phase of the five main tidal components in the area (K_1 , M_2 , N_2 , O_1 , S_2), obtained from the Grenoble Model (FES95.2). The surface boundary of the domain was forced with space and time dynamic winds with 6-hours resolution from the ECMWF (<http://ecmwf.int>). The hydrodynamic model was successfully calibrated and validated with field data.

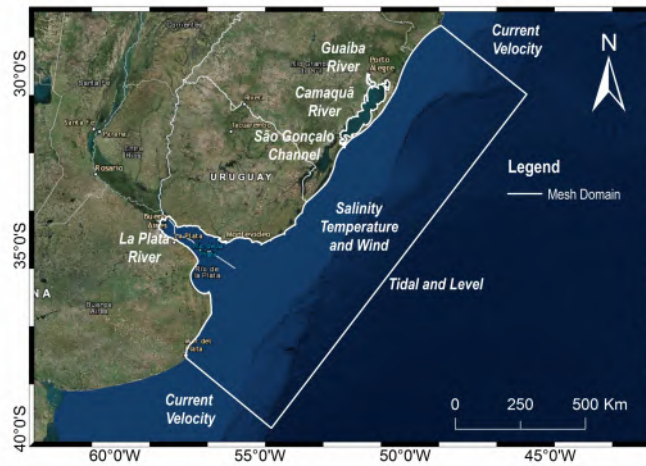


Fig. 1. Model domain with the identification of open boundaries and type of data used.

The calculated suspended sediment concentrations for both La Plata and Patos Lagoon Coastal plumes are being used to perform the Empirical Orthogonal Functions (EOF) analysis. The EOF method has often been used in studies about the spatial and temporal variability of current velocity, salinity and sea surface temperature fields (Zanotta et al., 2010). For the Patos Lagoon coastal plume, Marques et al. (2009) found that the main EOF variability mode of the riverine discharge is controlled by the wind, where north quadrant winds contribute to the southwestward migration pattern of the plume, while south quadrant winds controlling the passage of frontal systems tend to transport the brackish water to the north of the continental shelf. Expected results from this study will focus on the EOF variability modes present on the suspended sediment concentration for both the Patos Lagoon and La Plata river.

References

- Blanton, J. O. (1981). Ocean Currents along a Nearshore Zone on the Continental Shelf of the Southeastern United State. *Journal of Physical Oceanography*, 11, 1627-1637.
- Hervouet, J-M. (2007). *Free surface flows: Modelling with the element methods*. John Wiley & Sons Ltd, Copyright © 2007, England. 356p.
- Marques, W.C.; Fernandes, E.H.; Monteiro, I.O.; Möller, O.O. (2009). Numerical modeling of the Patos Lagoon coastal plume, Brazil. *Continental Shelf Research*, 556-571.
- Marques, W. C., Fernandes, E. H. L., Moraes, B. C., Möller, O. O., and Malcherek, A. (2010). Dynamics of the Patos Lagoon coastal plume and its contribution to the deposition pattern of the Southern Brazilian inner shelf. *Journal of Geophysical Research*, 115(C10):1-22.
- Möller Jr., O.O., Piola, A.R., Freitas, A.C., Campos, E.I.D. (2008). The Effects of river discharge and seasonal winds on the shelf off southeastern South America. *Continental Shelf Research*, 28(13):1607-1624.
- Rosa, F.; Rufini, M.M.; Ferreira, Ó.; Matias, A.; Brito, A.C.; Gaspar, M.B. (2013). The Influence of Coastal Processes on Inner Shelf Sediment Distribution: The Eastern Algarve Shelf (Southern Portugal). *Geologica Acta*, Vol.11, 59-73.
- Van Leussen, W. (1994). *Estuarine macroflocs and their role in fine-grained transport*, These de doctorat, Universiteit Utrecht, Utrecht, Netherlands.
- Villaret, C.; Hervouet, J.M.; Kopmann, R.; Merkel, U.; Davies, A.G. (2013). Morphodynamic modeling using the Telemac finite-element system. *Computers & Geosciences*, Vol. 53, 105-113.
- Zanotta, D. C.; Ducati, J. R.; Gonçalves, G. A. (2010). Surface temperature patterns of Lagoa dos Patos, Brazil, using NOAA-AVHRR data: an annual cycle analysis. *Pesquisas em Geociências (UFRGS. Impreso)*, vol. 37, p. 219-226.
- Zavialov, P., Kostianoy, A.G., Möller, O.O. (2003). Safari Cruise: mapping river discharge effects on southern Brazil. *Geophysical Research Letters* 30, 2126.

Multi-vegetation feedbacks affecting flow routing and sediment distributions in Everglades wetland.

Nardin William^{1,2} and Laurel Larsen²

¹ Horn Point Laboratory, University of Maryland Center for Environmental Science, Cambridge, (MD) USA
E-mail: wnardin@umces.edu

² Department of Geography, University of California – Berkeley, Berkeley, (CA) USA

Abstract

Introduction and background

During recent decades coastal wetlands have experienced unprecedented morphological modifications caused by reduction of water fluxes and sediment supply, subsidence, sea level rise, and extreme events. There is widespread recognition that vegetation can exert strong influence on geomorphology, through flow resistance (Luhar and Nepf, 2013), impacts on erosion (Collins et al., 2004), deposition (D'Alpaos et al., 2007; Nardin and Edmonds, 2014), and organic sedimentation (Mudd et al., 2010).

Most previous modeling studies on flow-vegetation-sediment interactions have focused on one specific vegetated community, but we lack a general understanding of the conditions that lead to the emergence of multiple vegetation species feedbacks. Using a modeling approach, this study generates new understanding of how sediment transport and ecogeomorphic interactions involving water flow, sediment, and multiple species of vegetation influence the hydrodynamic and morphodynamic processes in the Everglades ridge and slough landscape. Diverse studies suggest that the abundance of spikerush (*Eleocharis spp.*) in Everglades sloughs has increased in recent decades. Here we evaluate the sensitivity of the processes sculpting the ridge-slough landscape structure to small changes in the abundance and distribution of multiple morphotypes of slough vegetation.

Methods

We apply numerical modeling (Delft-3D) and subsequent analyses to test hypotheses about how vegetation characteristics on ridge and slough affect shear stress and sediment distribution. Delft3D (Lesser et al., 2004) is a state-of-the-art hydrodynamic model that provides fine-scale (5 × 5m) computations of depth-averaged flow velocity and bed shear stress, which can be linked to sediment deposition and erosion. Vegetation is modeled using the equations of Baptist (2005).

Baptist's approach (Baptist et al., 2005) and is based on the assumption that vegetation can be modeled as rigid cylinders and characterized by vegetation height h , (m), number of stems m , stem diameter D (m) and drag coefficient C_D . In this approach the velocity profile of flow through and above the vegetation are represented in a simplified way and divided in two flow zones when considering submerged vegetation (Fig. 1). The first flow zone is within the vegetation and consists of uniform flow velocity, u_v ($m\ s^{-1}$), whereas the second flow zone is above the vegetated part and is modeled with a logarithmic velocity profile, u_b ($m\ s^{-1}$) (Fig. 1A). For the emergent vegetation this reduces to one flow zone with velocity u_v through the vegetation (Fig. 1B). Those ecological parameter will support to alter the physical vegetation characteristics in the 3 proposed sites (freshwater and salt marshes). Those variations will help to achieve the synthetic understanding. In fact, various combination of vegetation parameters might shows diverse wetland shapes under different water flow conditions.

Here we use values obtained from previous studies for spikerush and sawgrass (*Cladium jamaicense*). Our model domain is a single ridge and slough, 500 m long by 120 – 400 m wide. We evaluate the spatial distribution of bed shear stresses and sediment erosion and deposition for 4 different vegetation scenarios: a) test case with no-vegetation; b) vegetation on ridges; c) vegetation in sloughs and on ridges; d) vegetation on ridges and multiple vegetative species in sloughs. Model scenarios vary the: vegetation height (from 20 to 100cm), density (from 1 to 10m⁻¹), ridge height (10, 20, 40 and 70cm), and representative of historic and current (preserved and degraded) conditions.

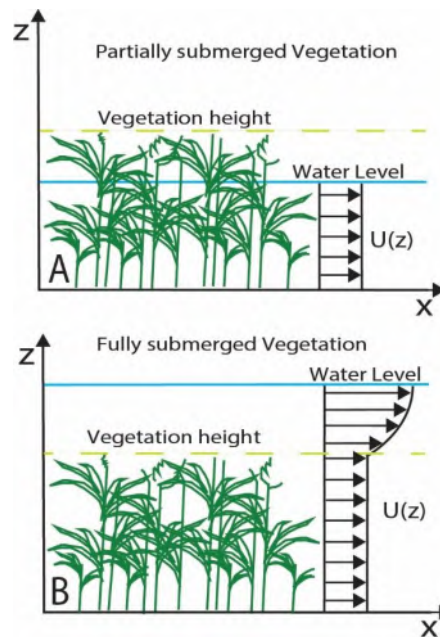


Figure 1: Schematization of the velocity profile in: A) fully submerged vegetation model, and B) partially submerged.

Results and Conclusions

Numerical results show that dense sawgrass on ridges substantially funnels water into sloughs and promotes deposition of sediment at ridge margins. As expected, vegetation within the sloughs decreases velocity and shear stress monotonically with increasing vegetation density. One surprising phenomenon was the emergence of a threshold vegetation density beyond which further increases in vegetation density produce higher velocity in the sloughs with emergent vegetation but lower velocity in sloughs with totally or partially submerged vegetation.

Results are relevant to the conversation about the extent to which spikerush densities in sloughs may need to be reduced in the implement of decompartmentalization. The flipping point behavior suggests that there may be a threshold density of vegetation within sloughs, above which ecogeomorphic feedbacks inevitably lead to further degradation of sloughs.

References

- Baptist, M. Modelling floodplain biogeomorphology Ph.D. thesis, Delft University of Technology, ISBN 90-407-2582-9. (2005).
- Baptist MJ, van den Bosch LV, Dijkstra JT, Kapinga S. Modelling the effects of vegetation on flow and morphology in rivers. *Archiv für Hydrobiologie. Supplement band. Large rivers* 2005;15(1-4):339-57.
- Collins, D. B. G., R. L. Bras, and G. E. Tucker. 2004. Modeling the effects of vegetation-erosion coupling on landscape evolution. *Journal of Geophysical Research: Earth Surface* (2003–2012) 109.
- Deltares (2013), *Delft3D-FLOW: Simulation of Multi-Dimensional Hydrodynamic Flows and Transport Phenomena, Including Sediments—User Manual*, 614 pp., Deltares, Delft, Netherlands.
- D’Alpaos, A., S. Lanzoni, M. Marani, AND A. Rinaldo. 2007. Landscape evolution in tidal embayments: Modeling the interplay of erosion, sedimentation, and vegetation dynamics. *Journal of Geophysical Research* 112:F01008.
- Lesser G, Roelvink J, Van Kester J, Stelling G. Development and validation of a three-dimensional morphological model. *Coast Eng* 2004;51:883-915.
- Luhar, M., AND H. M. Nepf. 2013. From the blade scale to the reach scale: A characterization of aquatic vegetative drag. *Advances in Water Resources* 51:305–316.
- Mudd, S. M., A. D’Alpaos, AND J. T. Morris. 2010. How does vegetation affect sedimentation on tidal marshes? Investigating particle capture and hydrodynamic controls on biologically mediated sedimentation. *Journal of Geophysical Research: Earth Surface* (2003–2012) 115.
- Nardin, W., & Edmonds, D. A. (2014). Optimum vegetation height and density for inorganic sedimentation in deltaic marshes. *Nature Geoscience*, 7(10), 722-726, doi:10.1038/ngeo2233.

Sediment resuspension and flocculation processes in a transverse mudflat-channel

Lee Guan-hong, Steven M. Figueroa, Hyun-Jung Shin, Jongwi Chang, and Adonis Gallentes

Department of Oceanography, Inha University, 100 Inharo, Incheon, 22212, South Korea
E-mail: ghlee@inha.ac.kr

Introduction

To better understand hydrodynamic forcing and sediment response in a mudflat-channel environment, measurements were conducted at five stations transverse to the axis of Asan Bay, Korea for twelve and a half hours on 2016/08/21. Tidal current and wave data were collected by an acoustic profiler deployed in the channel centre while simultaneous vertical profiles of water temperature, salinity, suspended sediment concentration (SSC), and floc size were collected during ten transects by water sampling and instrument casting. The particulate organic matter concentration of filtered water samples was obtained in the lab by the loss on ignition method.

The channel width was 6.5km including a 3km wide mudflat on the northern bank at the transect site. The stations on the transect extended from the lower flat 5km to the opposite bank. The mudflat was subaerial at low tide and the central channel and port on the southern bank had 15m depth at low tide. The tide range was 9m, and the significant wave height varied between 0.1 – 0.25m. Water density was practically constant during the survey indicating that water column stratification was not important.

Results

The transverse sediment responses in Asan Bay were strongly influenced by the draining and submergence of the mudflat. The mudflat influenced the tidal current such that when the mudflat drains, ebb currents resuspended sediment and deflocculated it in a thick bottom boundary layer (BBL) in the adjacent central channel. The mudflat was also susceptible to wind waves, and resulted in further deflocculation to very fine flocs with median size of 40 μ m. In the deeper channels that have been dredged, such as the gravelly port at the opposite bank, the bed sediment type limited resuspension and the development of a concentrated BBL. During flood when currents were relatively faster away from the mudflat, a coarsening upward trend was observed in median floc size. In the central channel when tidal currents generated a thick BBL, median floc sizes were observed to be small and homogenous in the BBL. However, above the BBL the largest flocs were observed of median size 200-300 μ m due to enhanced SSC and relatively gentle turbulent shear that promoted floc growth. This behaviour could have been enhanced in part by suspended particulate organic matter. Evidence for this was that in regions of the channel where sediment supply was limited, such as the surface layer and the gravelly port bank, flocs were observed to have the greatest organic matter content. In contrast, near the mudflat where sediments were abundant, flocs tended to have the least organic matter content.

Detection of fluid mud layers using tuning fork and acoustic measurements

Juliane Castro Carneiro¹, Marcos N. Gallo¹ and Susana B. Vinzon¹

¹ Cohesive Sediments Dynamics Laboratory
Federal University of Rio de Janeiro, CT 203 PO Box 68508 Rio de Janeiro, Brazil
E-mail: julianecastrocarneiro@gmail.com

Many ports around the world suffer from silting and presence of fluid mud layers and this continuous mud deposition can cause reduction in nautical depth. Generally, in its unconsolidated and highly dynamic state, fluid mud cannot be detected adequately by conventional echosounders (Schrottke et al., 2006). The sharp increase in sediment concentration at the top of the fluid mud layer, known as lutocline, can return a false bottom to sonar systems (Carneiro et al., 2017). Acoustic fathometers, the more frequent technology used for waterway depth measurement, yield multiple false bottom echoes when fluid mud lutocline is present (McAnally et al., 2016), which makes water depth determination ambiguous and highly variable.

Kirby and Parker (1983) used the term “lutocline” to describe the sudden increase of suspended sediment concentration (SSC) at some depth in the water column. According Mehta (1989), as a transition zone between the dilute upper suspension layer with relatively low concentrations and the lower dense fluid mud layer with much higher concentrations, the lutocline is governed by the flow-sediment interaction.

The Port of Santos is one the largest in Latin America, with frequent dredging and presence of fluid mud layer. There is still little knowledge about the behaviour of mud in estuaries, navigation channels and port areas. Thus, identification characterization and mapping of these deposits are important for navigation and management of sediments. The objective is compare in situ (e.g. density) with acoustic measurements for detection of fluid mud in the inner of the navigation channel.

30 profiles were selected in the channel and for acoustic measurements with an AIRMAR 28/200 kHz dual frequency bathymetry system, both managed by an ECHOTRAC CV200 control unit, from Odom Hydrographic Systems. In this study, a Meridata Chirp (2–8 kHz) was used, controlled through the Meridata MDCS® package (Marine Data Collection Software). For the processing of the echo and seismic data, were used MDCS software for visualization and Meridata Finland MDPS for treatment and interpretation. In each record, digital filters (high and low pass) were applied, and the gain and vertical scales of each profile were individually configured. For the density characterization along the water column was used the Densitune densimeter (Stema Systems). For each sediment, a frequency/amplitude ratio is obtained which determines the in situ density of the sedimentary material, and calibration was necessary in laboratory. In the example of Figure 1, it is possible to observe two lutoclines levels (1 and 2) (Fig. 1)

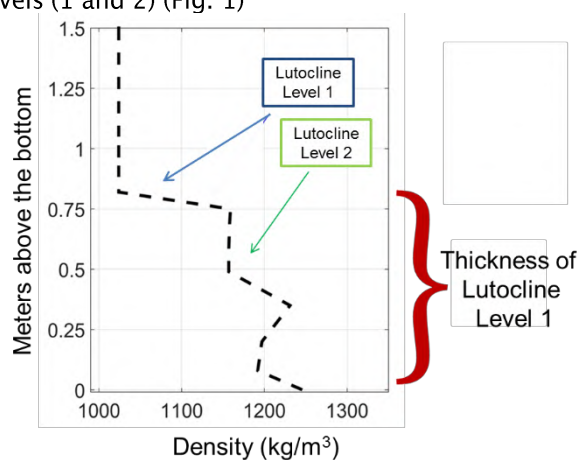


Fig 1. Diagram of definition of Lutoclines level (1 and 2) used in this work.

A multilinear regression was performed between the measured data of density and the data of the echo sounder and Chirp. The Chirp data depth was very similar with the low frequency data of the echo sounder. With the relationships between variables, it was possible to observe that the

frequency of 200 kHz (high frequency) has a coefficient of correlation of 0.99 with the level of the first lutocline found and the lutocline level 2 correlates with the first low frequency reflector (LF1). In the regression between the bottom depth found by the densimeter and low frequency second reflector (LF2), there is a relationship between the variables but the greater intercept (2.18) than the other regressions tested. Regarding the thicknesses, 1100 kg/m³ density is highly correlated with the lutocline level 1, suggesting that, in general, lutocline level1 occurs at the this density (Fig. 2).

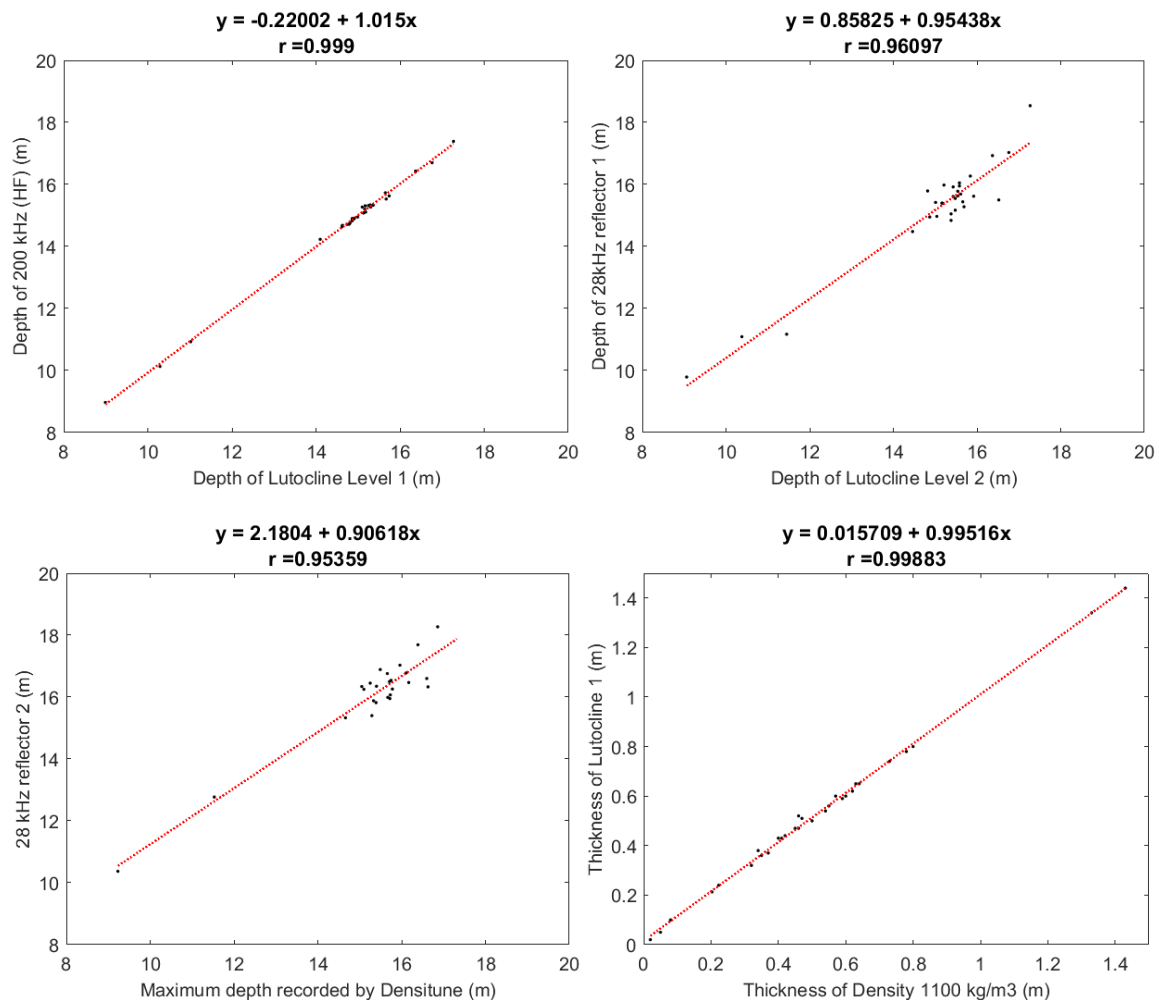


Fig 2. Regressions between the high and low frequency reflectors depths and by the densimeter.

With the correlations it is possible to suggest a methodology for detecting the layers of fluid mud in ports. In the case of the Port of Santos, the difference between the low frequency (28kHz) and high frequency (200kHz) reflector is not a more adequate methodology, but it is possible to infer a respect for the depth of lutoclines found.

References

- Carneiro, J. C.; Fonseca, D. L.; Vinzón, S. B.; Gallo, M. N. (2017). Strategies for Measuring Fluid Mud Layers and Their Rheological Properties in Ports. *Journal of Waterway, Port, Coastal, and Ocean Engineering*, ASCE, 143, 10.1061/(ASCE)WW.1943-5460.0000396
- Kirby, R. and Parker, W. R. (1983). Distribution and Behavior of Fine Sediment in the Severn Estuary and Inner Bristol Channel, U.K. *Canadian Journal of Fisheries and Aquatic Sciences*, 40(S1): s83-s95, 10.1139/f83-271.
- McAnally, W., et al. (2016). Nautical depth for U.S. navigable waterways: A review. *J. Waterway, Port, Coastal, Ocean Eng.*, 10.1061/(ASCE)WW.1943-5460.0000301, 04015014.
- Mehta, A. J. (1989). On estuarine cohesive sediment suspension behavior. *Journal of Geophysical Research*. Vol 94, 14, 303-314.
- Schrottke, K., Becker, M., Bartholomä, A., Flemming, B. W., and Hebbeln, D. (2006). Fluid mud dynamics in the Weser estuary turbidity zone tracked by high-resolution side-scan sonar and parametric sub-bottom profiler. *Geo-Marine Lett.*, 26(3), 185-198.

Modelling Patos Lagoon dredging suspended sediment plume dispersion

Elisa Helena Fernandes¹, Caio E. Stringari², Roberto Valente¹, Pablo Silva¹, Paulo Victor Lisboa¹

¹ Laboratório de Oceanografia Costeira e Estuarina (LOCOSTE)

Universidade Federal do Rio Grande, CP 474, CEP 96201-900, Rio Grande, Brasil

² School of Life and Environmental Sciences, University of Newcastle, University Drive 3018, Callaghan, Australia

E-mail: e.fernandes@furg.br, caio.stringari@gmail.com, robertovalente@furg.br, pdias5@yahoo.com.br, paulovictor_fjv@hotmail.com

Introduction

Previous studies showed that several natural and anthropogenic contributions interact and affect the dynamics of the Patos Lagoon and its coastal zone. Particularly, process occurring at the drainage basin determines the suspended sediment concentration reaching the Patos Lagoon Estuary. Part of this material is exported to the coast and feeds the muddy banks observed off Cassino Beach, and another part deposits in the Rio Grande Harbour navigation channel, demanding more frequent dredging operations. This situation worsens during El Niño periods. But once the dredging operation takes place and the material is deposited offshore, where does the suspended sediment plume go? Does it contribute to the formation of the muddy banks?

Methodology

The Telemac-Mascaret model (<http://www.opentelemac.org>) was used to answer these questions. This model solves the Navier-Stokes equations by considering local variation on the fluid free surface, ignoring density variations in the mass conservation equation, and considering the hydrostatic pressure and Boussinesq approximations (Hervouet, 2007). The model is based on the characteristic methods and uses finite-element discretization. In this study, the suspended sediment concentration was considered as an active tracer, and together with salinity and temperature, can influence the density field fluctuations. Telemac-3D has been calibrated and validated for the Patos Lagoon and its estuary (Marques et al., 2009; 2010). Figure 1 resumes the mesh density, the model open boundaries and illustrates the data used as boundary conditions during the simulation.

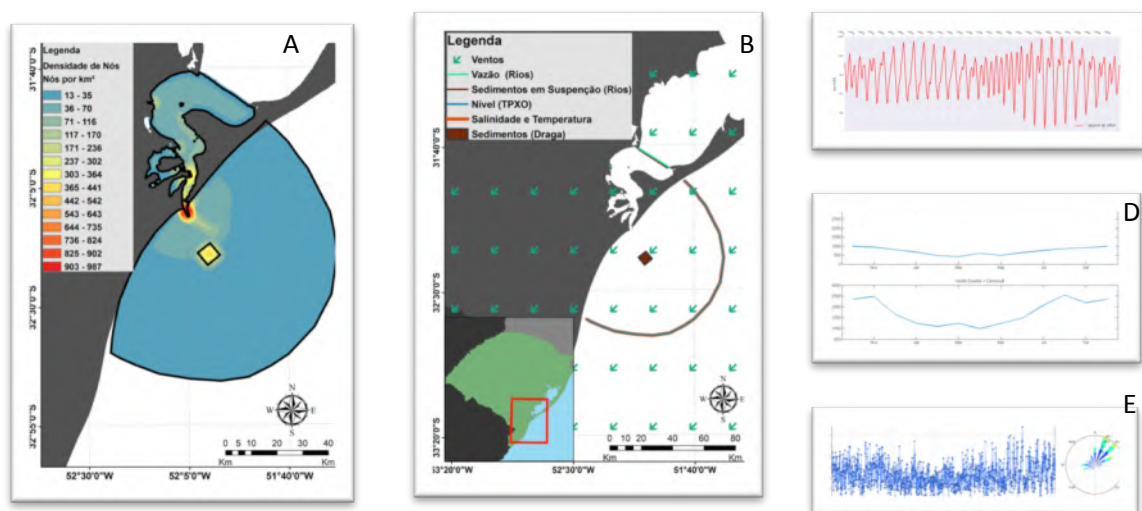


Fig. 1 - A) Mesh density. B) Open boundaries and type of data. C) High frequency data prescribed at the ocean boundary (TOPEX/POSEIDON). D) Freshwater contributions prescribed at the continental boundary (www.ana.gov.br). E) Wind speed and direction time series prescribed at the surface boundary (<http://www.ecmwf.int>).

Results

Figures 2A and 2B present the suspended sediment concentration on the surface during a dredging disposal. The black arrow represents the wind direction. Northeasterly winds are predominant in the region and tend to drive the coastal plume to the south of the Patos Lagoon mouth. Most of the dredging disposal material tend to remain in the disposal site, with small concentrations ($< 0,05\text{g/l}$) being observed at the north of the site and also interacting with the coastal plume at the south of the site. The vertical distribution of suspended sediment concentrations perpendicular to the coast is presented in Figures 2C and 2D, corroborating that most of the dredging material tend to remain in the disposal site distributed throughout the water column. The interaction of small concentrations ($< 0,05\text{g/l}$) from the disposal site and the coastal plume is also evident.

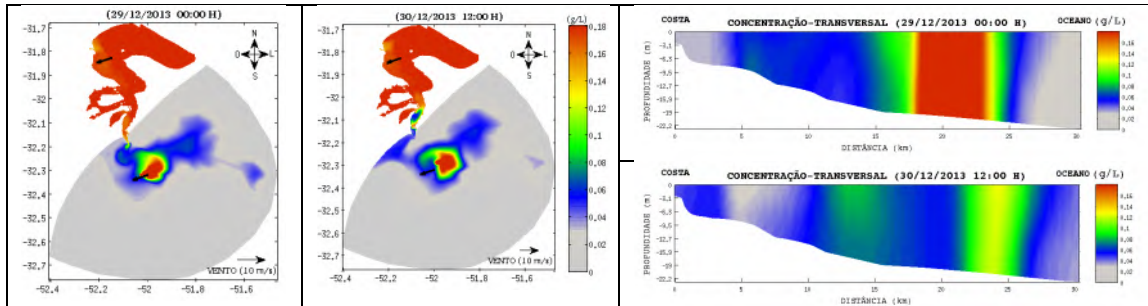


Fig. 2 – A) and B) Suspended sediment concentrations (g/l) on the surface during dredging disposals occurring 29/12/2013 00:00h and 30/12/2013 12:00h. C) and D) Suspended sediment concentrations (g/l) perpendicular to the coast and throughout the depth for the same moments.

Conclusions

The Patos Lagoon coastal plume dynamics is controlled by the wind and freshwater discharge. Northeasterly winds are predominant and form an eddy towards the south at the mouth, which tend to trap the exported fine suspended sediment in front of the Patos Lagoon, feeding the mud banks off Cassino Beach.

The dynamics of the disposal site respond to the wind and to the coastal currents, and the majority of the dredged material tends to remain there. The interaction between fine suspended sediment from the Lagoon and from the disposal site occurs at small concentrations ($< 0,05\text{ g/l}$). During the simulated period the material did not present transport tendency towards the coast.

References

- Hervouet, J-M. (2007). Free surface flows: Modelling with the element methods. John Wiley & Sons Ltd, Copyright © 2007, England. 356p.
- Marques, W.C.; Fernandes, E.H.; Monteiro, I.O.; Möller, O.O. (2009). Numerical modeling of the Patos Lagoon coastal plume, Brazil. *Continental Shelf Research*, 556-571.
- Marques, W. C., Fernandes, E. H. L., Moraes, B. C., Möller, O. O., and Malcherek, A. (2010). Dynamics of the Patos Lagoon coastal plume and its contribution to the deposition pattern of the Southern Brazilian inner shelf. *Journal of Geophysical Research*, 115(C10):1-22.

Fluidization in consolidated mud beds under water waves

Mohsen Soltanpour¹, Mohammad Hadi Jabbari¹, Tomoya Shibayama², Kouroshe Hejazi¹, Shinsaku Nishizaki² and Tomoyuki Takabatake²

¹ Department of Civil Engineering, K. N. Toosi University of Technology, PO Box 19967-15433, No. 1346, Vali-Asr St., Tehran, Iran
E-mail: soltanpour@kntu.ac.ir

² Department of Civil and Environmental Engineering, Waseda University, 169-8555, 3-4-1 Okubo, Shijuku-ku, Tokyo, Japan

Abstract

Fluidization in mud bed under the wave action is investigated through series of laboratory tests. High concentrated mud bed was prepared by mixing the commercial kaolinite and tap water and the mixture was placed between two false beds in the laboratory wave flume. Three micro pore water pressure transducers, equipped with ceramic filters, are employed to trace the variations of pore pressure in mud layer. Different effects of wave characteristics and bed concentrations on the complex fluidization process are investigated.

Introduction

Partially consolidated muddy beds may become as a fluid-like material, so called fluid mud, under the action of the overlying waves. The wave-induced fluidized mud can highly absorb the wave energy, resulting in a considerable wave height attenuation. On the other hand, fluid mud particles oscillate under the waves and the averaged transport of fluid mud layer, i.e. mud mass transport, contributes to the total sediment transport in muddy environments. This might be partially responsible for rapid sedimentation in dredged access channels after storms. Although wave-induced fluidization plays an important role in muddy environments, the mechanism of fluidization of cohesive sediments is not well understood yet.

Ross and Mehta (1990) were first researchers who performed wave flume laboratory tests on the generation of fluid mud. Feng (1992) conducted laboratory experiments to study the rate of bed fluidization by measuring the temporal and spatial changes of effective stress during the wave action. The laboratory experiments of De Wit and Kranenburg (1996) also showed that fluid mud can be generated under overlying wave. They indicated that the pressure-induced shear stresses in the self-weight consolidated bed might become as large as yield strength of the mud, which consequently play an important role on mud fluidization. Their results showed a considerable transient decrease of filtered wave-averaged pore pressure followed by a gradually pressure build-up. Vaisi and Soltanpour (2011) tried to visually estimate the depth of fluidized mud using coloured mud, as a tracer, in their wave-flume laboratory experiments. They injected the dyed mud into soft mud layer, and waited for the self-weight consolidation. After the wave action, the vertical mud profiles were collected to distinguish the motion of the upper part of mud layer, i.e. fluidized mud, from the lower stable mud.

Laboratory experiments

The experiments were conducted in the wave flume of the Coastal Engineering Laboratory of the Department of Civil and Environmental Engineering at Waseda University, Japan (Fig. 1).

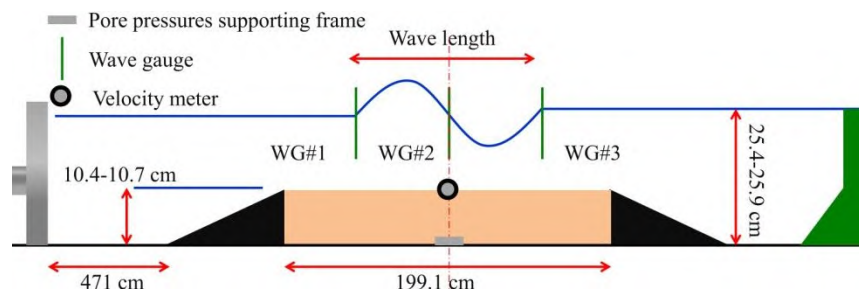


Fig. 1. Sketch of the wave flume experimental setup.

Mud bed was prepared in the form of a so called placed bed by careful mixing of commercial kaolinite with tap water (De Wit, 1995). The prepared fluid mud was placed in the middle part of the flume between two false beds and it was mixed again under drainage condition. The water level was then gradually increased to reach its final elevation (Fig. 1). The flume was equipped with three wave

gauges, an Electromagnetic Current Meter (ECM) and three Pore Pressure Transducers (PPT), fixed at preselected locations (i.e. $z=2.8$ cm, 6.9 cm and 8.9 cm above the bed). Table I. presents a summary of the selected test results.

Table I. Test conditions (wave height=6 cm, water depth=25.5-25.9 cm, mud depth=10.4-10.7 cm).

Test cases	Wave period (s)	Consolidation time (h)	Bed water content (%)
1	1.0	~ 44	~130
2	1.0	~44	~150
3	1.0	~22	~130
4	1.4	~44	~130

Results and discussion

Fig. 2 presents the accumulated measured pore pressures (pressure head, cm) for the selected test cases of Table I. Four distinct stages of rapid/gradual change of pore pressures can be distinguished in all figures during the process of mud fluidization. Choosing a fixed water content ratio of about 130%, test No. 1 represents the threshold wave height of 6 cm for the onset of fluidization. Increasing the water content ratio of prepared mud of test No. 2 to 150% shows a quicker fluidization. Shorter consolidation period of test No. 3 also reduces the necessary time duration of wave action. On the other hand, test No. 4 shows the limited effect of a longer wave period on fluidization process.

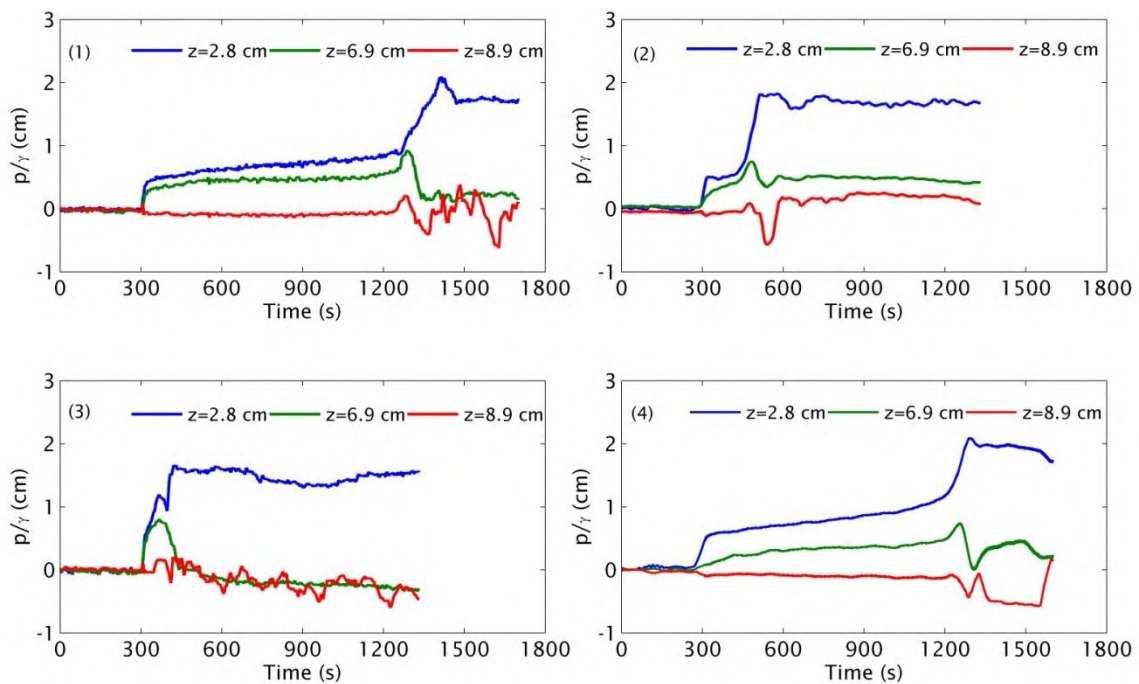


Fig. 2. Samples of pore pressure changes in laboratory tests.

References

- Ross M.A. and Mehta A.J. (1990). Fluidization of soft estuarine mud by waves. p.185-191. In: *The Microstructure of Fine-grained Sediments From Mud to Shale*. Bennett R.H., Bryant W.R. and Bulbert M.H. (Eds.). No.1. Springer Verlag, New York. 589p.
- Feng J. (1992). Laboratory experiments on cohesive soil bed fluidization by water waves. PhD. Dissertation, University of Florida, Gainesville, vi+136p.
- De Wit P.J. (1995). Liquefaction of cohesive sediments caused by waves. PhD. Dissertation, University of Delft, Netherlands, xii+196p.
- De Wit P.J. and Kranenburg C. (1996). On the effects of a liquefied mud bed on wave and flow characteristics. *Journal of Hydraulic Research*, Taylor and Francis, 34(1): 3-18.
- Vaisi H. and Soltanpour M. (2011). Fluidization of muddy beds under water waves. 11th International Conference on Cohesive Sediment Transport, INTERCOH11, Shanghai, book of abstracts: 91-92.

Comparative rheological characterization of fluid mud from different regions in Brazil

Manganeli Caio¹, Diego Fonseca¹, Susana Vinzon¹

¹ Cohesive Sediments Dynamics Laboratory
Federal University of Rio de Janeiro, CT 203 PO Box 68508 Rio de Janeiro, Brazil
E-mail: caio.manganeli@poli.ufrj.br

Several coastal regions present muddy bottoms. For navigation purposes, part of the mud layers may be accounted in the available depth following the nautical bottom concept. At this approach, there is a threshold for the mud rheological properties above which the sediment can adversely affect the ship or its controllability (McBride et al., 2014).

Due to the limitations of in situ rheological surveys, laboratory tests using rheometers are usually employed. However, this is a complex procedure, as different test protocols, rheological models, measuring geometries and types of the employed rheometer may lead to different results (Pang and Ruibo, 2015).

On the other hand, Atterberg Limits are broadly employed and standardized for soil characterization. Employing a simple set of tools and devices, the Atterberg limits indicate the water content above which the sample enters in a liquid state (liquid limit) or below it in a plastic state (plastic limit). These limits can support understanding of the plasticity and cohesive behavior of the sediment and the type of clay mineral involved when associated with grain size analysis (Winterwerp and Van Kesteren, 2004).

Thus, this study aimed to compare rheological properties and Atterberg Limits for several samples, at different densities and from three different locations in Brazil: the Amazon North Bar (at the north of the country), the Port of Santos (southeast) and the Port of Itajaí (south).

Each sample was submitted to grain size analysis (Mastersizer 2000, *Malvern*), Atterberg limits (Liquid and Plastic limits – Casagrande device) and rheological tests, using a bench rheometer (Rheolab-QC, *Anton Paar*). The rheology was assessed following a modification of the protocol proposed by Claeys et al (2015): a pre-shear step (100 s^{-1} for 15s) is followed by an applied rotation speed, where the time trajectory to reach an equilibrium shear stress is recorded. The previous steps are repeated for decreasing rotations (11 different rotations in total from 120 s^{-1} to 0.5 s^{-1}). The equilibrium shear stresses and the shear rates associated with the rotation speeds applied are used to construct the Equilibrium Flow Curve of the sample at a given density. Each sample was tested in the rheometer at several densities obtained by dilution with distilled water, between 1050 kg/m^3 and 1550 kg/m^3 .

The preliminary results for the plasticity-plot (figure 1) indicate that Amazon samples present medium to high plasticity, whereas those from the Port of Santos are considerably more plastic. These differences are also observed for the Bingham Yield Stress, for instance at 1200 kg/m^3 (figure 2). The grain size distribution does not seem to explain the rheological differences observed between these two locations, as both present similar clay contents (around 10%) and total fines content is even higher for Amazon samples (up to 98% fines). Preliminary results comparing the Bingham Yield Stress and the Plasticity Index (PI) show a good correlation, which seems not be site specific. More tests are in progress to corroborate this behavior.

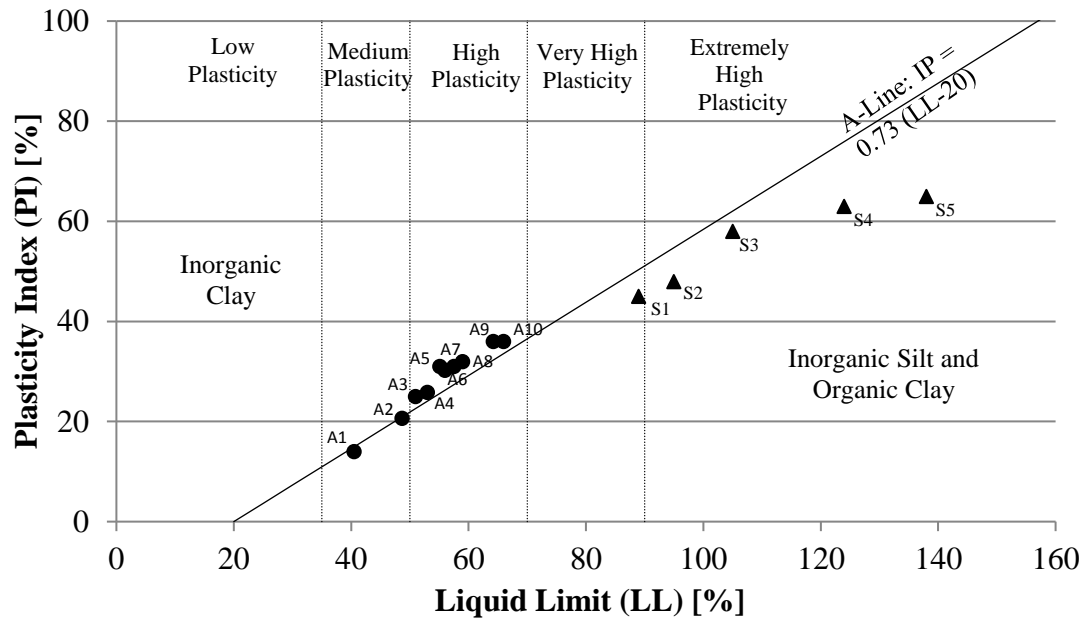


Fig1. Plasticity-plot for mud samples from the Amazon North Bar (● A1-A10) and from the Port of Santos (▲ S1-S5).

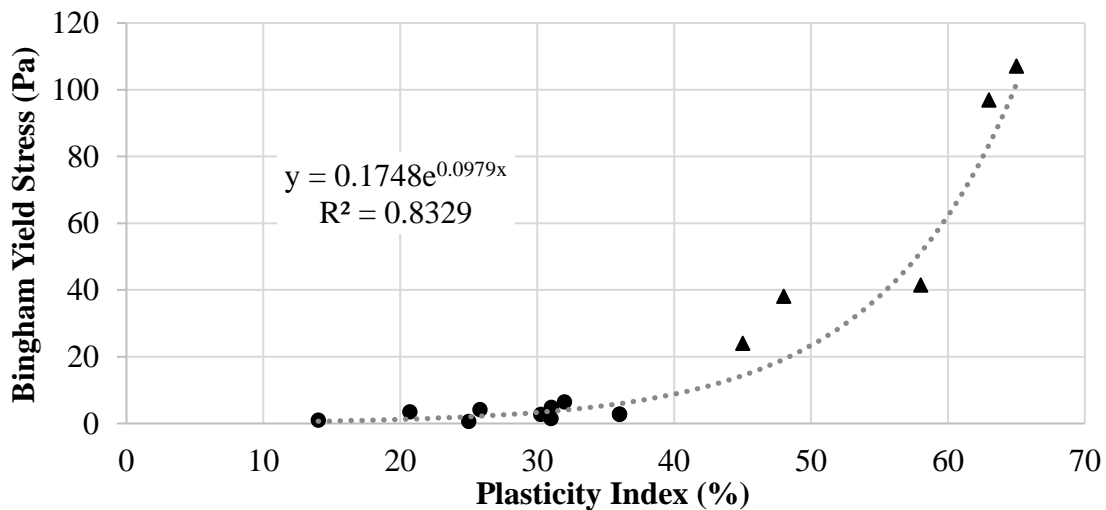


Fig2. Bingham Yield Stress versus Plasticity Index (PI) for mud samples from the Amazon North Bar (●) and from the Port of Santos (▲). Exponential trend adjustment considering all samples.

References

- Claeys, S., Staelens, P., Vanlede, J., Heredia, M., Van Hoestenbergh, T., Van Oyen T. and Toorman, E. (2015). A rheological lab measurement protocol for cohesive sediment. Proc., 13th International Conference on Cohesive Sediments (INTERCOH), Leuven, Belgium, 20–21.
- McBride, M. et al. (2014). Harbor approach channels –Design guidelines. PIANC Report N°. 121. World Association for Waterborne Transport Infrastructure, Brussels, Belgium.
- Pang, Q., and Ruibo, Z. (2015). Factors affecting the rheological characteristics of mud. Proc., 13th Int. Conf. on Cohesive Sediments, E.Toorman, T. Mertens, M. Fettweis, and J. Vanlede, eds., Flanders Marine Institute, Oostende, Belgium, 195–197.
- Winterwerp, J. C. and Van Kesteren, W. G.M. (2004). Introduction to the physics of cohesive sediments in the marine environment. Developments in Sedimentology. Elsevier. ISBN: 0-444-51553-4

Impact of tidal variation in vertical mixing and SPM concentrations on primary production and oxygen concentrations

Tom J.S. Cox¹ and Thijs van Kessel²

¹ Ecosystems Management Research Group
University of Antwerp, Universiteitsplein 1 BE-2610 Wilrijk, Belgium
E-mail: tom.cox@uantwerpen.be

² Deltares, P.O. Box 177
2600 MH Delft, The Netherlands
E-mail: thijs.vankessel@deltares.nl

Abstract

In estuaries suspended particulate matter (SPM) concentrations are typically high, thereby limiting light availability and phytoplankton photosynthesis. SPM concentrations often vary strongly in space and time depending on settling velocity, vertical mixing, erosion and deposition (Figure 1). In estuaries with significant primary production, dissolved oxygen concentrations depend on the balance between primary production, respiration, reaeration, advection and mixing. When light is sufficiently available primary production acts as a source term for oxygen during the day, whereas during the night respiration acts as a sink term for oxygen. From the resulting diurnal variation of the dissolved oxygen concentration, the primary productivity can often be estimated in estuarine and coastal settings with strong imprint of transport processes, even from single depth oxygen recordings. Our recently developed method relates the diurnal harmonic constituent in oxygen time series to time averaged primary production (Cox et al, 2015, 2017).

However, the diurnal biological oxygen variation may be small compared to variation due to physical processes. To determine in which conditions primary production can be feasibly determined from oxygen variations, a 1DV turbulence-closure model has been set up for the coupled simulation of tidal flows, SPM, oxygen concentration and primary production. Numerical experiments with increasing complexity were carried out to generate synthetic oxygen time series. The starting point is a well-mixed water column with a constant SPM level experiencing a truncated sinusoidal incident light. Subsequently, the level of mixing and SPM dynamics is varied by changing the eddy diffusivity and settling velocity. The conditions are chosen to be representative for typical locations along the Scheldt estuary.

These simulations were used to further assess the applicability of our method to estimate phytoplankton primary production. Indeed, this method strongly depends on the assumption that primary production is the only process with a diurnal periodicity. Recently, we demonstrated that even small diurnal tidal constituents can be important when strong longitudinal gradients prevail (Cox et al, 2017). Further, when only single depth oxygen recordings are available, mixing has to be such that oxygen is almost instantaneously mixed over the vertical, although production takes place in the top water layer (Cox et al, 2015). The coupled biological-physical 1DV model allowed us to analyse 1. the impact of tidal variations in vertical mixing, and 2. the impact of M4 constituents in light availability due to vertical redistribution of SPM. Our results further constrain the conditions where primary production estimation from oxygen time series is possible and constrain the uncertainty on those estimates.

References

Tom J. S. Cox, Tom Maris, Karline Soetaert, Jacco C. Kromkamp, Patrick Meire, Filip Meysman (2015). Estimating primary production from oxygen time series: A novel approach in the frequency domain. *Limnol. Oceanogr.: Methods*. doi: 10.1002/lom3.10046.

Cox, T. J. S., van Beusekom, J. E. E., and Soetaert, K.: Tune in on 11.57 μ Hz and listen to primary production, *Biogeosciences Discuss.*, doi:10.5194/bg-2017-81, in review, 2017.

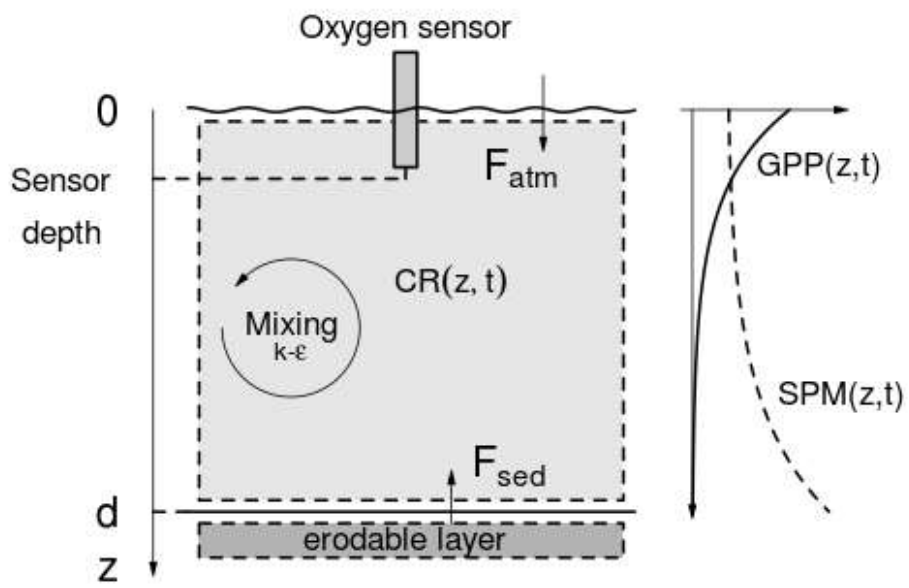


Fig. 1. Schematic representation of water column processes.

Evaluation of the artificial intelligence techniques for estimating suspended sediment concentration in a regularized river

Marcelo Di Lello Jordão¹, Susana Beatriz Vinzon¹ and Marcos Nicolas Gallo¹

¹ Laboratorio de Dinâmica de Sedimentos Coesivos (LDSC)
Universidade Federal do Rio de Janeiro - COPPE/UFRJ, Rio de Janeiro, Brazil
E-mail: dilello@oceanica.ufrj.br; susana@oceanica.ufrj.br; marcosgallo@oceanica.ufrj.br;

Introduction

The modeling and prediction of the fine suspended sediment load involve several dynamic and nonlinear factors, such as climate, pedology, lithology, relief, and soil and water uses (Garcia, 2008). The use of these parameters depends on a large number of records and long-term (decades) responses (Rajaei, 2011). Therefore, many studies have been conducted in order to find models that reduce the complexity of the problem in practical techniques.

Among the most widespread models is the linearized power law model or sediment rating curve (SRC). This is an empirical model, therefore, it has as its starting point, a systematic measurement process. From this set of data conclusions are drawn and an equation is formulated that links to the greatness of interest, without establishing a priori hypotheses. The constraints to the use of this type of model refer more to the characteristics of the data than to attend some physical theory of cause and effect between the quantities involved.

The SRC uses the ratio suspended sediment concentration (SSC) and water discharge (Q). The positive correlation between Q and SSC is explained by the redundancy of the information, while both are effects of the same cause, the runoff after a rainfall event on the basin. Unlike the surface area, which is a process that covers a large area (km²), the river discharge is concentrated in a well-defined section (m²), allowing it to be easily monitored.

Like other linear techniques, the stationarity becomes a critical issue to the time series because it is known that hydrological and environmental phenomena are not stationary. Recently, artificial intelligence techniques have been applied with some success in order to improve their ability to capture non-linearity and non-seasonality of hydrosedimentological data (Kisi, 2005; Rajaei, 2011,). This study aims to evaluate the artificial intelligence techniques to estimated suspended sediment concentration in the regularized section of the Paraíba do Sul River, Rio de Janeiro State, Brazil.

Materials and methods

The time series of SSC and daily rain (R) were extracted from the Instituto Estadual do Ambiente (Inea) and Hidroweb (Agência Nacional de Águas - ANA) databases. Three rain stations were selected considering location and integrity of the time series: Volta Redonda (RVR), Taubaté (RTA) e São Luiz de Paraitinga (RSL). The series of SSC data was supplemented with own daily samplings in the years 2014-2016. The upstream natural discharge (Q) corresponds to the discharge in which the value is corrected of the effect of the operation of the upstream dams and incorporated output water related to the net evaporation of the reservoirs and to the consultative uses of the water in the basin. The time series of daily Q was extracted from Operador Nacional de Sistema Elétrico (ONS). The total data set has 559 daily registers of the SSC, Q, RVR, RTA, RSL.

The intrinsic characteristic of time series is that adjacent observations are dependent. To evaluate these effects, delays were introduced in the 4 input series, considering daily delays ($t-1, \dots, t-i$ where $i=1, \dots, 5$ days) and cumulative effects (a_2, \dots, a_i where $i=2, 3, 4, 5, 7, 15, 30$ accumulated days).

The multivariate analysis identified 3 most correlated variables among the 45 potential input variables: the upstream natural discharge (Q), the upstream natural discharge with 1 day of delay (Q_{t-1}) and the series of the rain fall with 15 accumulated day from Taubaté (RTA_{a15}). This 3 input variables were selected for modeling.

Four typical regression models were selected for estimating suspended sediment concentration: sediment rating curve (SRC), neuro-fuzzy model (NF), neural networks (NN) multi-layer perceptron (MLP) by the conjugate gradient method (CGNN) and neural networks multi-layer perceptron by the Levenberg-Marquardt method (LMNN).

The NF model used explored the three most widely used types of membership function: triangular function (tri), generalized bell function (sin) and gaussian function (gau). The updating and adjustment of the membership functions was done by hybrid method, combining the backpropagated gradient method in the input and least squares methods in the output of the pertinence function. In total, 22 models were tested and evaluated.

The SRC model follows a power law function. The adjustment of the parameters were done by least squares methods after logarithmic transformation of the SSC and Q variables. The NN model used was the MLP with a hidden layer and error backpropagation. The activation function

used in both the hidden layer and the neuron output was the sigmoid function. We used 10 neurons in the hidden layer.

In the modeling with NN and NF the dataset was standardized between 0 and 1 by the maximum and minimum method. The selection of the structured model and optimization was tested and evaluated by the cross-validation method in 5 cycles. The data set was divided into 5 parts (N = 111-112), where 4 formed the training set (N = 448) and 1 formed the test set (N = 111). In each cycle, a new part is selected for testing. At the end, the test outputs of the 5 cycles were concatenated and submitted to evaluation statistics. The evaluation of the model performance was based on the results of the mean squared error (MSE), the root *mean* mean square (RMS), the mean absolute error (MAE), the mean absolute percent error (MAPE), determination coefficient (R^2) and logarithmic determination coefficient (R^2_{log}).

Results and Discussion

All models resulted low determination coefficient values, it means that the model performed worse than the average SSC training set. The best performance in the cross-validation cycles was of the LMNN (Q, Q_{t-1}). This model was the model that best estimated concentrations above 50 mg/l, thus the most suitable model for rainy season. The NF model with generalized bell membership function and 2 pertinence function (2sin:Q) was the model that best estimated SSC between 50 and 100 mg/l.

Tab. I. The three best cross-validation results.

LMNN: Q, Q_{t-1}	1 ^o cycle	2 ^o cycle	3 ^o cycle	4 ^o cycle	5 ^o cycle	Evaluation
MSE	1,372.3	1,085.5	1,012.0	1,326.2	2,225.7	1,401.4
RMS	37.0	33.0	31.8	36.4	47.2	37.4
MAE	23.5	20.5	18.8	23.2	24.7	22.1
MAPE	1.08	1.25	0.83	0.85	0.79	0.96
R^2_{log}	0.1	0.03	0.38	0.36	0.35	0.25
R^2	0.04	0.04	0.44	0.32	0.14	0.22
NF (2sin): Q						
MSE	1,588.9	1,264.5	1,946.1	1,574.7	1,130.7	1,501.5
RMS	39.9	35.6	44.1	39.7	33.6	38.8
MAE	24.0	23.5	26.0	20.5	20.8	23.0
MAPE	1.06	0.95	1.04	0.88	0.93	0.97
R^2_{log}	0.33	0.31	0.21	0.11	0.27	0.26
R^2	0.29	0.26	0.10	0.24	0.36	0.25
SRC: Q						
MSE	1,771.3	1,307.8	2,009.1	1,632.4	1,194.6	1,583.4
RMS	42.1	36.2	44.8	40.4	34.6	39.8
MAE	22.2	21.5	23.8	17.2	18.5	20.6
MAPE	0.71	0.71	0.72	0.57	0.61	0.66
R^2_{log}	0.39	0.38	0.32	0.32	0.42	0.37
R^2	0.21	0.23	0.07	0.21	0.33	0.21

The SRC model obtained the best combination of results both in the final evaluation with the concatenated tests and partially, evaluating each cycle. This behavior is desirable reflecting greater generalization capacity. The SRC model was better than the others in the estimation of lower concentrations (< 50 mg/l), based on the best evaluation in R^2_{log} .

The suspended sediment trapping and regularization discharge in the upstream reservoirs significantly decreased the expected correlation between SSC and Q or R.

Conclusions

In this preliminary study, all models performed poorly. However, comparatively, the LMNN model was the best model for estimating high CSS (>50 mg/l). The SRC model was better than the others in the estimation of lower concentrations (< 50 mg/l). In the future, we are evaluating the combined performance of the three models.

References

- Garcia, M. (2008). Sedimentation engineering: processes, measurements, modeling, and practice. ASCE. 877p.
- Rajae, T. (2011). Wavelet and ANN combination model for prediction of daily suspended sediment load in rivers. Science of the total environment, 409 (15): 2917-2928.
- Kisi, O. (2005). Suspended sediment estimation using neuro-fuzzy and neural network approaches. Hydrological Sciences Journal, 50 (4): 683 - 696.
- Kisi, O. (2010). River suspended sediment concentration modeling using a neural differential evolution approach. Journal of hydrology, 389 (1): 227-235.

